



Marshall, Gillian Elizabeth (2008) *The electrophysiological and molecular effects of chronic beta-adrenoceptor antagonist therapy on human atrium*. PhD thesis.

<http://theses.gla.ac.uk/406/>

Copyright and moral rights for this thesis are retained by the author

A copy can be downloaded for personal non-commercial research or study, without prior permission or charge

This thesis cannot be reproduced or quoted extensively from without first obtaining permission in writing from the Author

The content must not be changed in any way or sold commercially in any format or medium without the formal permission of the Author

When referring to this work, full bibliographic details including the author, title, awarding institution and date of the thesis must be given

# **The electrophysiological and molecular effects of chronic β-adrenoceptor antagonist therapy on human atrium**

A thesis presented by

**Dr Gillian Elizabeth Marshall**

BSc (Hons) MBChB MRCP

for the degree of Doctor of Philosophy at the University of Glasgow

Faculty of Medicine  
University of Glasgow  
Glasgow

September 2008

© Gillian E Marshall, 2008

For my mum and dad, Dorothy and Allan Marshall

## ABSTRACT OF THESIS

The chronic treatment of patients with a  $\beta$ -adrenoceptor antagonist is associated with prolongation of the atrial cell action potential duration (APD), potentially contributing to the ability of these drugs to prevent atrial fibrillation (AF). The mechanisms underlying this APD prolongation are not fully understood but may involve pharmacological remodelling of atrial  $K^+$  currents and underlying ion channel subunits. This project aimed to test the hypothesis that various characteristics of human atrial  $K^+$  currents, including voltage, time and rate dependency, differ between patients treated and not treated with a  $\beta$ -blocker as a result of altered expression of ion channel pore-forming and accessory subunits.

Human atrial myocytes were isolated enzymatically from right atrial appendage tissue obtained from consenting patients, in sinus rhythm, undergoing cardiac surgery. Using whole cell patch clamping,  $K^+$  currents were recorded at physiological temperature. Treatment of patients with  $\beta$ -blockers for a minimum of 4 weeks duration was associated with a significant, 34% reduction in the transient outward  $K^+$  current ( $I_{TO}$ ) density but no change in the sustained outward current ( $I_{KSUS}$ ). There was a reduction in the  $Ba^{2+}$ -sensitive, inwardly rectifying  $K^+$  current ( $I_{K1}$ ) but only at -120 mV and the physiological significance of this is unclear. The reduction in  $I_{TO}$  density was not secondary to changes in the voltage dependency of the current, as determined by Boltzmann curve fits. There was no difference in the time dependent inactivation or re-activation of  $I_{TO}$  between cells from non  $\beta$ -blocked and  $\beta$ -blocked patients, indicating these current characteristics were not contributing to  $\beta$ -blocker induced APD prolongation. The density of  $I_{TO}$  decreased significantly with increasing stimulation rate in cells from both patient groups but remained significantly reduced in  $\beta$ -blocked patients at all rates studied.

To determine a possible mechanism underlying the reduction in  $I_{TO}$  density, the expression of Kv4.3 mRNA, the pore-forming subunit responsible for this current, was compared in right atrial appendage tissue from non  $\beta$ -blocked and  $\beta$ -blocked patients using real-time RT-PCR. mRNA levels were normalised to the expression of both 28S, a marker of total RNA, and the housekeeping gene GAPDH. The levels of mRNA for the accessory subunits KChIP2, KChAP, Kv $\beta$ 1 and 2 and Frequentin, which modify Kv4.3 expression and function, were also measured. No change was found in the relative mRNA levels of any of these ion channel subunits in association with chronic  $\beta$ -blockade. mRNA for the pore-forming subunits Kir 2.1 and 2.2 and Kv1.5 which are responsible for  $I_{K1}$  and  $I_{KSUS}$

respectively, in addition to mRNA for the pore-forming subunits underlying the L-type calcium current and sodium-calcium exchanger were also measured. Again, no significant changes in expression were found in association with chronic  $\beta$ -blockade.

The possibility of ion channel remodelling at a translational level was investigated by measuring Kv4.3 protein levels using Western blotting with a monoclonal anti-Kv4.3 antibody. Kv4.3 protein levels were normalised to GAPDH which was used as a loading control. Chronic  $\beta$ -blockade did not change the ratio of the level of Kv4.3 protein relative to GAPDH.

In conclusion, chronic treatment of patients with a  $\beta$ -blocker is associated with a reduction in atrial  $I_{TO}$  density which may contribute to the APD prolongation reported in cells from these patients. However, this cannot be explained by changes in the expression of Kv4.3 or by changes in the expression of its regulatory accessory subunit genes.

# TABLE OF CONTENTS

## CHAPTER 1: GENERAL INTRODUCTION

1.1	Cardiac electrophysiology.....	2
1.1.1	Normal cardiac conduction.....	2
1.1.2	The cardiac action potential.....	2
1.2	Atrial fibrillation.....	6
1.2.1	Basic mechanisms underlying AF.....	7
1.2.2	AF and electrophysiological remodelling .....	8
1.2.3	Current treatment of AF .....	9
1.2.4	$\beta$ -blockers in AF.....	10
1.2.4.1	Classification of $\beta$ -blockers.....	10
1.2.4.2	Clinical evidence for an anti-arrhythmic action of $\beta$ -blockers in AF.....	11
1.2.4.3	Possible anti-arrhythmic mechanisms of $\beta$ -blockers: pharmacological remodelling .....	11
1.2.4.4	How does chronic $\beta$ -blockade prolong the APD?.....	12
1.3	Potassium currents.....	13
1.3.1	$I_{TO}$ .....	13
1.3.1.1	The role of $I_{TO}$ in determining the action potential duration. ....	14
1.3.1.2	$I_{TO}$ and APD remodelling in cardiac diseases .....	16
1.3.1.3	$I_{TO}$ and chronic $\beta$ -blockade.....	17
1.3.2	$I_{KI}$ .....	18
1.3.2.1	The role of $I_{KI}$ in determining APD. ....	19
1.3.2.2	$I_{KI}$ and APD remodelling in cardiac diseases.....	19
1.3.2.3	Potential modification of $I_{KI}$ by chronic $\beta$ -blockade.....	20
1.3.3	The delayed rectifiers .....	21
1.3.3.1	The contribution of the delayed rectifiers to atrial action potential duration .....	21
1.3.3.2	Remodelling of $I_{KUR}$ in cardiac disease .....	23
1.3.3.3	Potential modification of $I_{KUR}$ by chronic $\beta$ -blockade .....	24
1.4	The structure of $K^+$ channels .....	24
1.4.1	$I_{TO}$ pore-forming protein: Kv4.3.....	24
1.4.1.1	Altered Kv4.3 expression modifies $I_{TO}$ in cardiac disease .....	27
1.4.1.2	Can chronic $\beta$ -blockade modify Kv4.3 expression?.....	28
1.4.2	Modulation of Kv4.3 by accessory proteins.....	28
1.4.2.1	KChIP2 .....	29

1.4.2.2	Kv $\beta$ 1-3 .....	30
1.4.2.3	KChAP .....	31
1.4.2.4	minK and MiRPs .....	31
1.4.2.5	Other accessory proteins.....	32
1.4.3	I <sub>K1</sub> pore-forming proteins .....	33
1.4.4	Kv1.5: the pore forming channel for I <sub>KUR</sub> .....	35
1.5	Hypothesis and Aims.....	36

## **CHAPTER 2: EFFECTS OF CHRONIC $\beta$ -BLOCKADE ON HUMAN ATRIAL REPOLARISING POTASSIUM CURRENTS**

2.1	Introduction .....	39
2.2	Aims .....	39
2.3	Methods .....	40
2.3.1	Principles of whole cell patch clamping.....	40
2.3.2	Obtaining atrial tissue.....	41
2.3.3	Cell isolation.....	44
2.3.4	Measuring currents by whole cell patch clamping .....	44
2.3.4.1	Preparing the patch clamp equipment .....	44
2.3.4.2	Perfusion chamber .....	47
2.3.4.2.1	Microelectrodes .....	47
2.3.4.3	The use of amplifier to record currents and adjust for errors in the voltage clamp mode .....	50
2.3.4.4	Isolating currents .....	52
2.3.4.5	Voltage pulse protocols .....	53
2.3.4.5.1	I <sub>TO</sub> and I <sub>K<sub>SUS</sub></sub> activation, I <sub>TO</sub> voltage dependence and time dependent inactivation .....	53
2.3.4.5.2	I <sub>TO</sub> voltage dependent inactivation .....	54
2.3.4.5.3	I <sub>TO</sub> reactivation .....	54
2.3.4.5.4	I <sub>TO</sub> rate dependence .....	58
2.3.4.5.5	I <sub>K1</sub> voltage dependent activation.....	58
2.3.5	Data analysis.....	58
2.3.5.1	Calculating conductance and the reversal potential .....	58
2.3.5.2	Curve fitting.....	61
2.3.5.3	Other statistical analysis .....	62
2.4	Results .....	63

2.4.1	The effects of chronic $\beta$ blockade on $I_{TO}$ current density.....	63
2.4.2	Effects of patient characteristics on $I_{TO}$ current density .....	67
2.4.2.1	Cell characteristics.....	67
2.4.2.2	Patient characteristics .....	69
2.4.2.3	Effects of heart rate on $I_{TO}$ density .....	69
2.4.2.4	Effects of pre-operative drugs on $I_{TO}$ density .....	69
2.4.2.5	Effects of patient pre-op pathology on $I_{TO}$ density.....	74
2.4.3	Effects of phrixotoxin-2 on $I_{TO}$ density .....	78
2.4.4	Effects of chronic $\beta$ -blockade on time dependent inactivation of $I_{TO}$ .....	78
2.4.5	Effects of chronic $\beta$ -blockade on voltage dependence of $I_{TO}$ .....	81
2.4.6	Effects of chronic $\beta$ -blockade on reactivation of $I_{TO}$ .....	81
2.4.7	Effects of chronic $\beta$ -blockade on rate dependence of $I_{TO}$ .....	84
2.4.8	Effects of chronic $\beta$ -blockade on $I_{KSUS}$ density .....	84
2.4.9	Assessing block of $I_{KSUS}$ by 4-AP.....	87
2.4.10	Effects of chronic $\beta$ -blockade on $I_{K1}$ density.....	87
2.5	Discussion.....	94
2.5.1	Chronic $\beta$ -blockade and reduction in $I_{TO}$ density: comparison with other studies .....	94
2.5.2	Chronic $\beta$ -blockade and reduction in $I_{TO}$ density: a true association? .....	97
2.5.3	Chronic $\beta$ -blockade and other $I_{TO}$ characteristics: a comparison with other studies .....	99
2.5.4	Chronic $\beta$ -blockade and $I_{KSUS}$ : a comparison with other studies.....	100
2.5.5	Chronic $\beta$ -blockade and $I_{K1}$ : a comparison with other studies .....	101
2.5.6	Chronic $\beta$ -blockade and reduction in $I_{K1}$ density: a physiologically significant change? .....	103
2.5.7	Limitations of experiments.....	104
2.5.8	Implications of the effects of chronic $\beta$ -blockade on repolarising potassium currents .....	106
2.5.8.1	Can a reduction in $I_{TO}$ density alone explain chronic $\beta$ -blocker induced APD prolongation?.....	106
2.5.8.2	What can we tell about the mechanisms of $I_{TO}$ reduction by chronic $\beta$ -blockade? .....	108

### **CHAPTER 3: EFFECTS OF CHRONIC $\beta$ -BLOCKADE ON ION CHANNEL EXPRESSION**

3.1	Introduction .....	111
3.2	Aims .....	112
3.3	Methods .....	112
3.3.1	Quantification of mRNA by real time RT-PC.....	112
3.3.1.1	Principles of quantitative polymerase chain reaction (QPCR).....	112
3.3.1.2	Obtaining and Storing Tissue .....	115
3.3.1.3	RNA Extraction .....	115
3.3.1.3.1	Tissue Preparation .....	115
3.3.1.3.2	Protocol for RNA extraction using Quiagen Mini kit .....	115
3.3.1.3.3	RNA quality control and quantifying .....	117
3.3.1.4	Reverse transcriptase .....	118
3.3.1.5	Quantitative Real time PCR .....	119
3.3.1.5.1	Reagents .....	119
3.3.1.5.2	Real time QPCR protocol.....	120
3.3.1.5.3	Melting curves .....	124
3.3.1.6	Analysis .....	124
3.3.2	Quantification of proteins by Western blotting.....	125
3.3.2.1	Obtaining and storing tissue .....	125
3.3.2.2	Measuring protein concentration.....	126
3.3.2.3	Basic Principles of Western blotting .....	127
3.3.2.4	Protein electrophoresis and transfer .....	129
3.3.2.5	Immunodetection of Kv4.3.....	130
3.3.2.5.1	Standard protocol for using a polyclonal anti-Kv4.3 primary antibody.....	130
3.3.2.5.2	Modified protocols for using polyclonal anti-Kv4.3 primary antibody .....	131
3.3.2.5.3	Standard protocol for using a monoclonal anti-Kv4.3 primary antibody.....	132
3.3.2.5.4	Protocol for pre-incubation of primary antibody with antigen.....	132
3.3.2.5.5	Quantification of protein concentration from Western Blots .....	132
3.4	Results .....	133
3.4.1	Effects of chronic $\beta$ -blockade on ion channel mRNA expression .....	133
3.4.1.1	Patient characteristics .....	133
3.4.1.2	Assessing the concentration and quality of extracted RNA .....	133
3.4.1.3	Quantifying the expression of 28S rRNA and GAPDH mRNA .....	138
3.4.1.4	Quantifying the expression of Kv4.3 mRNA and related accessory subunits...	138
3.4.1.5	Quantifying the mRNA expression of other ion channel subunits.....	146
3.4.2	Effects of chronic $\beta$ -blockade on Kv4.3 protein expression .....	146
3.4.2.1	Patient characteristics .....	146

3.4.2.2	Total protein concentration of all human atrial tissue samples .....	146
3.4.2.3	Characterisation of a polyclonal anti-Kv4.3 primary antibody .....	151
3.4.2.4	Characterisation of a monoclonal anti-Kv4.3 primary antibody .....	156
3.4.2.5	Characterisation of a monoclonal anti-GAPDH primary antibody .....	158
3.4.2.6	Establishing a linear relationship between optical density and total protein for GAPDH and Kv4.3 .....	160
3.4.2.7	Comparing the relative amounts of Kv4.3 protein in tissue from non $\beta$ -blocked and $\beta$ -blocked patients. ....	162
3.5	Discussion.....	166
3.5.1	Ion channel mRNA expression in human atrium .....	168
3.5.1.1	A comparison with other studies .....	168
3.5.1.2	RT-PCR compared to Western Blotting.....	170
3.5.2	Kv4.3 protein expression in human atrial tissue.....	170
3.5.2.1	A comparison with other studies .....	172
3.5.3	The role of normalisation in analysis of Western Blots and quantitative RT-PCR. ....	174
3.5.4	What do mRNA and protein expression actually tell us about functional ion channels? .....	175
3.5.5	Can the adrenergic system influence ion channel expression?.....	177

## CHAPTER 4: GENERAL DISCUSSION

4.1	Electrophysiological and molecular effects of chronic $\beta$ -blockade on human atrial potassium currents .....	179
4.2	Do ion current changes always mirror changes in ion channel expression? .....	179
4.3	What is the mechanism underlying $\beta$ -blocker induced $I_{TO}$ reduction?.....	180
4.3.1	Post-translational modification.....	181
4.3.1.1	Phosphorylation .....	182
4.3.1.2	Phosphorylation and $\beta$ -adrenoceptors .....	184
4.3.2	$\beta$ -adrenoceptors, $I_{TO}$ and calcium .....	185
4.4	A clinical perspective .....	185

## LIST OF TABLES

Table 2-1 Composition of solutions for cell isolation.....	45
Table 2-2 Composition of external and internal solutions.....	49
Table 2-3 Electrophysiological characteristics of cells from patients treated (BB Yes) or not treated (BB No) with $\beta$ -blockers.....	68
Table 2-4 Patient characteristics of cells in which $I_{TO}$ was recorded.....	71
Table 2-5 Single (A) and multiple (B) linear regression analysis of $I_{TO}$ current density....	72
Table 2-6 Mean $\pm$ sem peak $I_{TO}$ densities (pA/pF), in non $\beta$ -blocked (BB No) and $\beta$ -blocked patients (BB Yes) when patients were excluded from analysis. .	77
Table 2-7 Patient characteristics of cells in which $I_{KSUS}$ and $I_{KI}$ were measured. ....	89
Table 3-1 Primer details.....	121
Table 3-2 Primer details (Quantitect).....	122
Table 3-3 Characteristics of patients treated or not treated with $\beta$ -blockers prior to cardiac surgery in whom ion channel mRNA expression was measured.....	135
Table 3-4 Concentration of extracted RNA from tissue samples. ....	136
Table 3-5. Mean $\pm$ sem abundance of mRNA of ion channel subunits in tissue from non $\beta$ -blocked (BB No) and $\beta$ -blocked (BB Yes) patients.....	144
Table 3-6 Characteristics of patients treated or not treated with $\beta$ -blockers prior to cardiac surgery in whom Kv4.3 protein expression was measured.....	149
Table 3-7 Total protein concentrations of the tissue samples.....	150

## LIST OF FIGURES

Figure 1-1 The cardiac conducting system..	3
Figure 1-2 The different phases of a human atrial action potential .....	4
Figure 1-3 Schematic representation of Kv4.3 .....	26
Figure 1-4 Schematic diagram of Kir2 channel. ....	34
Figure 2-1 Whole cell patch clamping of an isolated atrial myocyte. ....	42
Figure 2-2 Example of patient consent form for obtaining right atrial tissue.....	43
Figure 2-3 Picture of patch clamp equipment .....	46
Figure 2-4 Diagram of perfusion chamber.....	48
Figure 2-5 Voltage pulse protocol for determining peak $I_{TO}$ and $I_{KSUS}$ activation, $I_{TO}$ voltage dependence and time dependent inactivation.....	55
Figure 2-6 Voltage pulse protocol for $I_{TO}$ voltage dependent inactivation.....	56
Figure 2-7 Two pulse voltage pulse protocol for $I_{TO}$ reactivation. ....	57
Figure 2-8 Voltage pulse protocol for $I_{TO}$ rate dependence. ....	59
Figure 2-9 Voltage pulse protocol for $I_{K1}$ activation. ....	60
Figure 2-10 Current traces showing $I_{TO}$ voltage dependent activation. ....	64
Figure 2-11 Individual voltage current relationships for $I_{TO}$ in all cells.....	65
Figure 2-12 Mean $I_{TO}$ current-voltage relationship and mean peak $I_{TO}$ density .....	66
Figure 2-13 Patient heart rate Vs peak $I_{TO}$ density. ....	73
Figure 2-14 Total daily dose of atenolol given to the $\beta$ -blocked patients Vs peak $I_{TO}$ density .....	75
Figure 2-15 Effects of phrixotoxin 2 on peak $I_{TO}$ current density at +60 mV Vs time.....	79
Figure 2-16 Time dependent inactivation of $I_{TO}$ .....	80
Figure 2-17 Voltage dependence of $I_{TO}$ .....	82
Figure 2-18 $I_{TO}$ reactivation.....	83
Figure 2-19 $I_{TO}$ reactivation .....	85
Figure 2-20 Rate dependence of $I_{TO}$ .....	86
Figure 2-21 Mean peak $I_{KSUS}$ density.....	90
Figure 2-22 Effect of 4-AP on $I_{TO}$ and $I_{KSUS}$ . ....	91
Figure 2-23 Mean current density of $I_{KSUS}$ (A) and $I_{TO}$ (B) at +60 mV after application of varying concentrations of 4-AP. ....	92
Figure 2-24 Effects of chronic $\beta$ -blockade on $I_{K1}$ .....	93
Figure 3-1 Diagram of the reactions in one PCR cycle..	114
Figure 3-2 SYBR green reaction.....	123
Figure 3-3 The basic steps involved in Western Blotting.....	128

Figure 3-4 Electrophoresis of RNA samples .....	137
Figure 3-5 Mean $\pm$ sem abundance of 28S rRNA and GAPDH mRNA.....	139
Figure 3-6 Amplification plots.....	140
Figure 3-7 Melting peaks. ....	141
Figure 3-8. Mean $\pm$ sem relative abundance of mRNA of Kv4.3 and various related ion channel subunits. ....	143
Figure 3-9 Mean $\pm$ sem abundance of mRNA for Kv4.3 and related ion channel subunits. ....	145
Figure 3-10 Mean $\pm$ sem relative abundance of mRNA for Kv1.5, Kir2.1, TWIK1, Cav1.2 and NCX1 .....	147
Figure 3-11 Western blots characterising the polyclonal anti-Kv4.3 antibody (Alomone) in human atrial tissue (HA).. ....	152
Figure 3-12 Western blots characterising the polyclonal anti-Kv4.3 antibody (Alomone) in human atrial tissue (HA) .....	153
Figure 3-13 Western blot comparing the polyclonal anti-Kv4.3 1 <sup>o</sup> Ab (Alomone) in human atrial tissue (HA) with rat (rb) and rabbit brain (RB) and rabbit lung (RL). . ....	155
Figure 3-14 Western blot characterising a monoclonal anti-Kv4.3 1 <sup>o</sup> Ab (Neuromab) in human atrial tissue (HA), rat (rb) and rabbit brain (RB) and rabbit lung (RL). ....	157
Figure 3-15 Western blot characterising the nature of the band detected at just above 60 kDa using with the polyclonal anti-Kv4.3 1 <sup>o</sup> Ab in rat (rb) and rabbit brain (RB) tissue. ....	159
Figure 3-16 Western blot characterising the nature of the bands detected using a monoclonal anti-GAPDH 1 <sup>o</sup> Ab in human atrial tissue (HA). ....	161
Figure 3-17 Establishing the linear range of optical density versus total protein for GAPDH and Kv4.3 primary antibodies. ....	163
Figure 3-18. Western blot of Kv4.3 and GAPDH in human atrial samples from two non $\beta$ -blocked (BBNo) and two $\beta$ -blocked (BBYes) patients.....	164
Figure 3-19 Optical densities of GAPDH (A) and Kv4.3 (B) at three protein loads.....	165
Figure 3-20 Mean $\pm$ sem optical densities of GAPDH (A), Kv4.3 (B) and Kv4.3 normalised to GAPDH (C). ....	167

**ABBREVIATIONS**

$\alpha$ -AR	$\alpha$ -adrenoceptors
Ab	antibody
ACE	angiotensin converting enzyme
AF	atrial fibrillation
ALP	alkaline phosphatase
AODNs	anti-sense oligonucleotides
4-AP	4-aminopyridine
APD	action potential duration
AV	atrioventricular
AVR	aortic valve replacement
$\beta$ -AR	$\beta$ -adrenoceptor
$\beta$ -blockers	$\beta$ -adrenergic receptor antagonists
BSA	bovine serum albumin
CABG	coronary artery bypass graft
CaMKII	calcium calmodulin-dependent protein kinase II
c-AMP	cyclic adenosine monophosphate
CCB	calcium channel blocker
cDNA	complimentary deoxyribonucleic acid
$C_t$	threshold cycle
dNTPs	deoxynucleotide triphosphates
dsDNA	double stranded deoxyribonucleic acid
DTT	dithiothreitol
E	efficiency
ECG	electrocardiogram
$E_K$	potassium equilibrium potential
$E_{Na}$	sodium equilibrium potential
ERK	extracellular signal-related kinase
ERP	effective refractory period
EU	European Union
$F$	Faraday's constant
F	fluorescence
FRP	functional refractory period
g	conductance
GAPDH	glyceraldehyde-3-phosphate dehydrogenase

HA	human atrium
HEPES	N-2-hydroxyethylpiperazine-N'-2-ethanesulfonic acid
HpTx	heteropodotoxin
I	current
$I_{CaL}$	L-type calcium current
$I_K$	delayed rectifier current
$I_{KACH}$	acetylcholine dependent potassium current
$I_{KATP}$	adenosine triphosphate-sensitive potassium current
$I_{K1}$	inward rectifier current
$I_{KR}$	rapid delayed rectifier current
$I_{KS}$	slow delayed rectifier current
$I_{KSUS}$	sustained outward potassium current
$I_{KUR}$	ultra-rapid delayed rectifier current
$I_{Na}$	sodium current
$I_{TO}$	transient outward potassium current
KChAP	Kv channel associated protein
KChIP	Kv channel interacting protein
minK	minimal protein to form potassium channel
MiRP	minK related peptides
MOPS	4-morpholinepropanesulfonic acid
LA	left atrium
LQTS	long QT syndrome
LV	left ventricle
LVSD	left ventricular systolic dysfunction
MAPK	mitogen activated protein kinase
MI	myocardial infarction
mRNA	messenger ribonucleic acid
MVR	mitral valve replacement
NCS	neuronal calcium sensor
NCX	sodium calcium exchanger
PaTx	phrixotoxin
PBS	phosphate buffered saline
PI3K	phosphoinositide 3-kinase
PKA	protein kinase A
PKC	protein kinase C
R	universal gas constant

R	resistance
$R_i$	input resistance
RA	right atrium
Rb	rat brain
RB	rabbit brain
RL	rabbit lung
rRNA	ribosomal ribonucleic acid
RT-PCR	reverse transcriptase polymerase chain reaction
RV	right ventricle
SDS-PAGE	sodium dodecyl sulphate polyacrylamide gel electrophoresis
SERCA	sarcoplasmic reticulum calcium adenosine triphosphate
SR	sinus rhythm
T	absolute temperature
t	time
$\tau$	time constant
TBS	tris buffered saline
V	voltage
$V_{0.5}$	voltage of half maximal activation
$V_t$	test potential
$V_{rev}$	reversal potential

## ACKNOWLEDGEMENTS

I would like to thank my supervisors Tony, Andrew and Kathy. Without their help, enthusiasm, patience and encouragement this thesis would not have been started and certainly not completed. In addition to being fun to work with, Julie Russell taught me to isolate cells, to Western blot and also managed the database. Susan Currie has been my expert witness for all things Western Blotting and James Tellez has been my PCR guru. I would like to thank Mark Boyett and all in his lab, including James, for helping me with my RT-PCR experiments and making me feel welcome while I was in Manchester. Back in Glasgow, I owe a huge debt of thanks to the patients and cardiothoracic surgeons of Glasgow Royal Infirmary for providing me with tissue.

Thanks to all my family, friends and colleagues for their support but, in particular, Laura for “volunteering” to proof read, Pardeep for his help with the stats and Rachel and Ashley for keeping me sane and supplying the laughs, cakes and tunes fundamental for thesis survival.

Finally I would like to thank the British Heart Foundation for funding this work.

## **AUTHOR'S DECLARATION**

Pardeep Jhund performed the single and multiple linear regression analysis of  $I_{T0}$  as indicated in Chapter 2. Real time RT-PCR for KChIP2 was performed by James Tellez and optimisation of all primer reactions was carried out by James and colleagues working with Professor Mark Boyett. Julie Russell calculated the molecular weight of Kv4.3. All other work within this thesis was the author's own.

## **PUBLICATIONS ARISING FROM THESIS**

### **Papers**

Workman AJ, Pau D, Redpath CJ, Marshall GE, Russell JA, Kane KA, Norrie J, Rankin AC. Post-operative atrial fibrillation is influenced by beta-blocker therapy but not by pre-operative atrial cellular electrophysiology. *J Cardiovasc Electrophysiol* 2006;17:1230-38

### **Abstracts**

Marshall GE, Rankin AC, Kane KA, Workman AJ. Pharmacological remodelling of human atrial K<sup>+</sup> currents by chronic beta-blockade. *Heart* 2006; 92: (Suppl 2): A101

Marshall G, Rankin AC, Kane KA, et al. Pharmacological remodelling of human atrial K<sup>+</sup> currents by chronic beta-blockade. *Eur Heart J*; 27: 30-30 Suppl. 1

Marshall GE, Tellez JO, Russell JA, Currie S, Boyett MR, Rankin AC, Kane KA, workman AJ.. Reduction of human atrial I<sub>TO</sub> by chronic beta blockade is not due to changes in ion channel expression. *J Physiol* 2007; Proc Physiol Soc 8, PC20

# **CHAPTER 1**

## **GENERAL INTRODUCTION**

## **1.1 Cardiac electrophysiology**

### **1.1.1 Normal cardiac conduction**

Contraction of cardiac myocytes is triggered by electrical activity within each cell. The organised spread of this electrical current through the heart allows contraction to occur in an effective, co-ordinated fashion, allowing the heart to efficiently pump blood around the body. In the normal heart this electrical activity originates in the sinus node, a specialised area of spontaneously discharging cells located in the right atrium. Electrical impulses are then conducted rapidly through the cardiac myocytes of both atria causing these chambers to contract. These impulses reach the atrio-ventricular (AV) node which lies in the inter-atrial septum and is usually the only site where electrical activity can be transmitted to the ventricles. Electrical conduction is generally slowed through the AV node and then conducted rapidly again through a specialised system of fibres (the Bundle of His and Purkinje fibres) responsible for the spread of electrical impulses through the ventricles. This triggers ventricular contraction. The spread of cardiac excitation in this fashion from the sinus node through the AV node to the ventricles is known as sinus rhythm (SR) (see figure 1-1)

### **1.1.2 The cardiac action potential**

The cardiac action potential represents the brief fluctuation in the membrane potential, or voltage, of a cardiac myocyte that can spontaneously propagate as an electrical wave or impulse through adjacent excitable cardiac tissue. It is caused by the rapid opening and closing of voltage-gated ion channels and can be described in five phases which are illustrated in figure 1-2 (1).

Phase 0 describes the initial rapid depolarisation of the cell membrane and is due to the fast sodium current,  $I_{Na}$ .  $I_{Na}$  is activated at a membrane potential of -60 mV and therefore to initiate this current, the cell has to be partially depolarised from its resting membrane potential of around -90 mV. This can be achieved by a slow intrinsic depolarising current in the context of pacemaker cells, by an external electrical stimulus, or by localised membrane currents generated by a propagating action potential.  $I_{Na}$  is generated by the rapid influx of sodium ions through the open sodium channel in cell membrane and occurs as a result of the  $Na^+$  electrochemical gradient ie  $Na^+$  ions are attracted into the

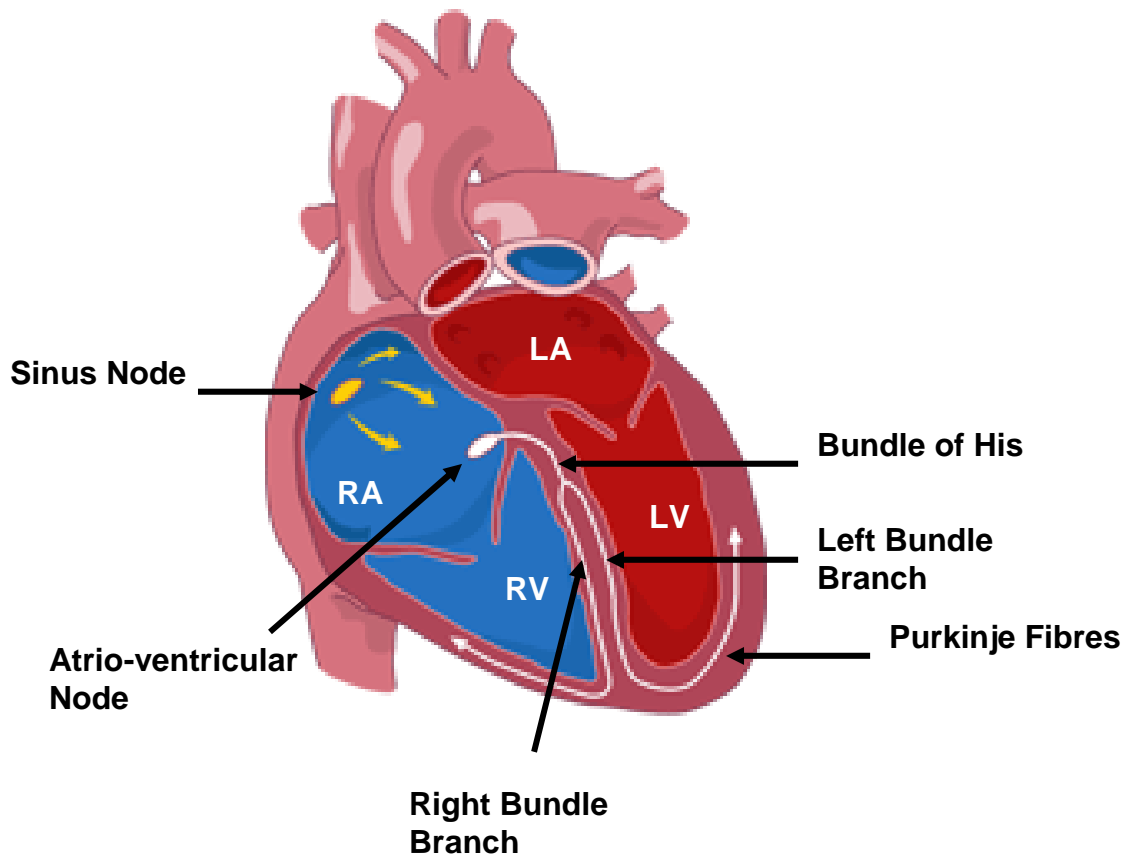


**Figure 1-1** The cardiac conducting system. RA = right atrium, LA = left atrium, RV = right ventricle, LV= left ventricle. Adapted from [images.med.cornell.edu](http://images.med.cornell.edu).

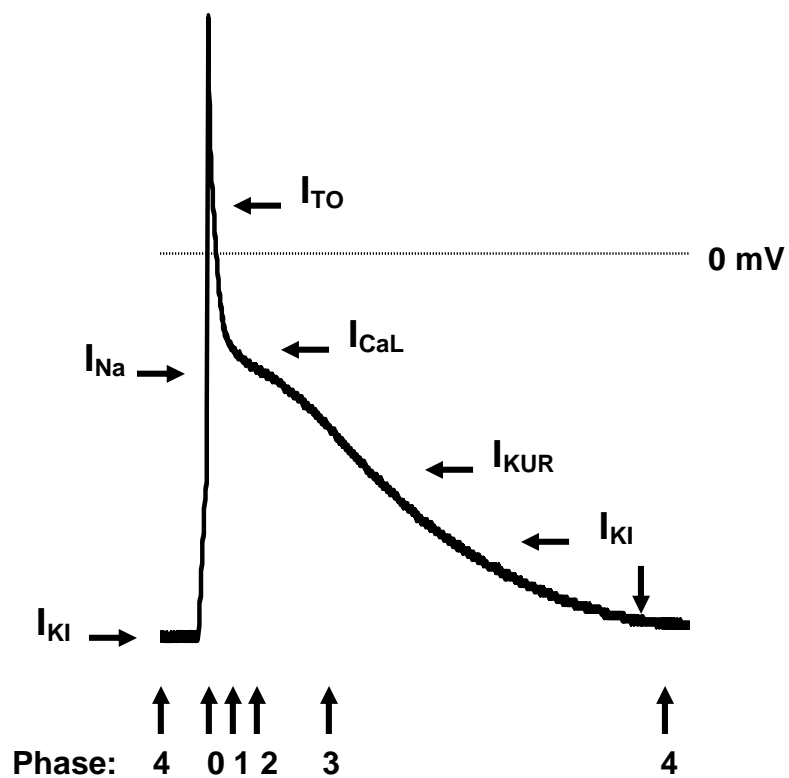


**Figure 1-2** The different phases of a human atrial action potential and the main contributing ion currents. See text for further details. Based on data (2)

cell because of the low intracellular  $\text{Na}^+$  concentration and negatively charged intracellular environment. This depolarises the cell further and also causes more sodium channels to open. The cell membrane potential, therefore, increases rapidly towards the sodium equilibrium potential ( $E_{\text{Na}}$ ) at which point the  $\text{Na}^+$  have equilibrated between the inside and outside of the cell and there is no further  $\text{Na}^+$  flux. The upstroke of the action potential does not fully reach the  $E_{\text{Na}}$ , however, because of the rapid inactivation of the sodium channels and the opposing influence of repolarising currents which are activated by the rising membrane potential. In human atrial cells the upstroke of the action potential can depolarise the cells to around +20 mV.

Phase 1 of the action potential, the first stage of repolarisation preceding the plateau of the action potential, is largely due to the transient outward potassium current  $I_{\text{TO}}$ . This current is activated during the upstroke of the action potential and, once open, allows the efflux of  $\text{K}^+$  along the newly generated electrical gradient in which the inside of the cell has become positively charged relative to the extracellular environment. The normally high concentration of intracellular  $\text{K}^+$  also helps to drive the outward flow of  $\text{K}^+$  and with this current repolarisation is initiated.

During the plateau of the action potential, known as phase 2 repolarisation, the contribution of outward currents to repolarisation are balanced mainly by the inwardly directed L-type calcium current,  $I_{\text{CaL}}$ . This current is activated during membrane depolarisation but is much slower than  $I_{\text{Na}}$ , hence its main effects are not realised until later in the action potential. It is the influx of  $\text{Ca}^{2+}$  during phase 2 repolarisation that triggers calcium release from the sarcoplasmic reticulum within the cell and activation of contractile proteins. Counteracting the depolarising effects of  $I_{\text{CaL}}$  is the delayed rectifying potassium current,  $I_{\text{K}}$ . This is not a single current but three distinct currents.  $I_{\text{KS}}$ , the slow delayed rectifier, activates very slowly following cell depolarisation and also inactivates slowly.  $I_{\text{KR}}$ , the rapid delayed rectifier, has more rapid kinetics and  $I_{\text{KUR}}$ , the ultra-rapid delayed rectifier is activated extremely rapidly.  $I_{\text{TO}}$  contributes minimally to repolarisation during phase 2 of the action potential as the current inactivates rapidly.

By phase 3 of the action potential, also known as terminal repolarisation,  $I_{\text{CaL}}$  has inactivated in a time dependent fashion and the outflow of  $\text{K}^+$  due to the delayed rectifier currents returns the cell to its resting membrane potential. Other currents also contribute to terminal repolarisation, particularly, the inwardly rectifying potassium current,  $I_{\text{K1}}$ . This current is predominantly inward at membrane potentials negative to  $E_{\text{K}}$  or -90 mV but has

a small outward component at potentials more positive than this and so can contribute to repolarisation.

Phase 4 of the action potential refers to the diastolic depolarisation that occurs in spontaneously discharging pacemaker cells but in atrial and ventricular cells the membrane potential usually remains stable during cardiac relaxation or diastole at around -80 to -90 mV. This resting membrane potential sits close to the  $E_K$  and reflects the high intracellular concentration of  $K^+$  relative to extracellular fluid along with an equal and opposite distribution of electrical charge. This is mainly determined by  $I_{K1}$  and the constitutively active Na-K pump which helps to maintain the high levels of intracellular  $K^+$  by pumping out  $Na^+$  in exchange for  $K^+$ .

## 1.2 Atrial fibrillation

Atrial fibrillation (AF) is the most common disorder of cardiac rhythm and is characterised by rapid and chaotic activation of the atria. This results in failure of co-ordinated atrial contraction predisposing to the formation of intra-atrial thrombus and embolic stroke. Rapid conduction through the AV node results in a rapid ventricular rate which, along with the loss of the contribution of atrial contraction to ventricular filling, can result in cardiac failure. The morbidity and mortality associated with AF is considerable with the mortality rate of patients with AF approximately double that of patients in normal sinus rhythm (3). An estimated 4.5 million people in the European Union (EU) have paroxysmal or persistent AF making AF an extremely expensive public health problem costing the EU approximately €13.5 billion per year (3).

There are numerous patient factors that predispose to, or are associated with, the development of AF but by far the most common are other co-existing heart diseases. These include ischaemic, hypertensive, congenital and valvular heart disease, particularly involving the mitral valve. Heart failure can be both a consequence of, and risk factor for, AF. Other risk factors or precipitating causes include drugs, sepsis, endocrine disorders, changes in autonomic tone, and genetic factors. Age is another major risk factor with 8% of people over 80 years having AF compared to 0.4-1% of the general population (3). This may reflect the increasing prevalence of other risk factors with age especially cardiac disease but probably also reflects age-related atrial fibrosis which is thought to be another important predisposing factor to the development of AF. As the population ages the burden of AF is only likely to increase.

### 1.2.1 Basic mechanisms underlying AF

The basis of the abnormal electrical activity and conduction that underlies the initiation and maintenance of AF is complex and not fully understood. Re-entry and abnormal focal activity or ectopics are two key concepts in proposed mechanistic models of AF.

Re-entry describes the situation where abnormal, potentially self-perpetuating, circuits of electrical activity occur across different zones of tissue. After depolarisation or phase 0 of the action potential, the sodium channels remain inactivated and are unable to be opened again until the cell repolarises to around -60 mV. This time period, from the upstroke of the action potential until another action potential can fire, is called the refractory period. If an electrical impulse arrives in an area of tissue which is still refractory it will not be conducted through that area but may find an alternative adjacent pathway through non-refractory tissue. If this electrical impulse arrives back at the refractory area once it has recovered, the impulse will be conducted and may then continue to conduct around this "re-entrant circuit". Re-entry can occur as a result of a single circuit producing regular rapid firing or due to multiple, unstable, co-existing circuits or waves which can produce more irregular activity. The likelihood of re-entry occurring is determined by the conduction velocity and the duration of the refractory period which together define the wavelength or distance travelled by one electrical impulse in one refractory period. Short refractory periods and hence short wavelengths promote re-entry (1;4).

Re-entrant activity is thought to be important in the generation and maintenance of atrial fibrillation and several different models have been proposed. It has been suggested that AF may be caused by a single, rapidly firing, re-entrant circuit which generates irregular activity due to variations in conduction of the electrical impulses through the rest of the atria. Another theory is that AF is due to multiple independent re-entrant wavelets which travel in a randomly distributed fashion through the atria with some colliding and dying out while others self-perpetuate and spawn daughter waves. Re-entrant waves can take the form of spirals or rotors in which the maintenance of re-entry is dependent on the curvature of the spiral wavefront (4-6).

Re-entrant circuits may be triggered by spontaneously active ectopic foci of electrical activity. These can occur in non-pacemaker cells if the normal balance of ion currents is disrupted, resulting in diastolic depolarisation of the membrane potential sufficient to

trigger sodium channels to open and cause a premature action potential to fire. Ectopic foci can be triggered by large after-depolarisations which can occur in calcium overloaded cells. They are caused by sodium-calcium exchanger (NCX) which generates a net inward current as it extrudes the excess free intracellular  $\text{Ca}^{2+}$  in exchange for  $\text{Na}^+$ . It has been suggested that AF may be caused by one or more continuously active, rapidly discharging, ectopic foci which may then be conducted in a non uniform fashion through the atria to produce the characteristic fibrillatory rhythm. It is also possible that the arrhythmia may be triggered by an ectopic focus or foci leading to single or multiple re-entrant circuits which then maintain the arrhythmia (4-6). Some of these ectopic foci originate in and around the pulmonary veins which drain into the left atrium.

It is likely that all of these mechanisms play some role in the initiation and maintenance of AF and hence it is possible to take several different approaches when treating this arrhythmia. Targeting ectopic foci and single re-entrant circuits by catheter ablation has proven to be one successful treatment strategy. Another is to use anti-arrhythmic drugs to prolong the refractory period, which limits the number of functionally re-entrant circuits that can be maintained, so preventing the AF from being sustained.

## **1.2.2 AF and electrophysiological remodelling**

Regardless of the mechanisms underlying the initiation of AF and the mode of electrical conduction, one key finding in both clinical and experimental models is that AF tends to become more persistent with time. In the classic goat model of AF induced by rapid atrial pacing, the duration of AF determines the ability to restore and maintain normal sinus rhythm – “AF begets AF” (7). In this model and others, a number of electrical and structural changes occur following initiation of AF that are thought to contribute to the perpetuation of the arrhythmia. These processes have been termed electrical and structural remodelling (4;8).

The electrical adaptations that occur in AF affect repolarisation at both a tissue and cellular level. AF has been shown to cause shortening of the atrial action potential duration (APD) and effective refractory period (ERP). It also results in an increased spatial heterogeneity of repolarisation and loss of rate adaptation (2;7;8). Shortening of the APD and ERP shortens the minimum wavelength for re-entry thus promoting the occurrence and maintenance of multiple re-entrant circuits. Underlying this shortening in APD and ERP are changes in ion currents which influence repolarisation (8). Studies on isolated human

atrial myocytes have shown reductions  $I_{TO}$ ,  $I_{CaL}$  and  $I_{KUR}$  and an increase  $I_{K1}$ . The net effect of these current changes is APD shortening largely mediated through reduction in  $I_{CaL}$  and increase in  $I_{K1}$ .

Other electrical changes that occur with AF include changes in the proteins that contribute to gap junction formation and facilitate the passage of electrical activity from one myocyte to the next. These proteins are called connexins and several studies have shown alternations in connexin expression along with changes in the pattern of their distribution (14;15).

In addition to the electrical remodelling that occurs in AF, structural remodelling also occurs at both a cellular and organ level. AF can result in the loss of contractile proteins, myocyte death, atrial fibrosis and dilatation (4;16). These changes are likely to increase the heterogeneity of atrial refractoriness thus promoting re-entry, as well as impairing atrial contractile function.

### **1.2.3 Current treatment of AF**

There are currently two main strategies used in the treatment of AF (3;17). The first is to allow the continuation of the arrhythmia but to try to minimise the associated complications by controlling the ventricular rate and anti-coagulating the patient to prevent thromboembolism. The second is to try to restore and maintain sinus rhythm. This can be achieved using either electrical or pharmacological cardioversion followed by drugs which either prolong the refractory period (class III anti-arrhythmic drugs) or block  $Na^+$  channels (class I anti-arrhythmic drugs). Another possible strategy for preventing the recurrence of AF is to burn or ablate any sites of ectopic foci which may be triggering the arrhythmia. These often occur around the origin of the pulmonary veins. Pulmonary vein ablation can also be accompanied by further catheter-based ablation therapy to disrupt possible pathways of abnormal electrical activity through the atria.

Recent large clinical studies have compared these “rate versus rhythm control” strategies and have found that, for many patients, remaining in AF is not an inferior treatment option if they are appropriately managed (18). There are, however, a number of patients for whom a rhythm control strategy is preferable. The major problem for these patients is that both the invasive and pharmacological treatments are not always effective and have the potential for significant complications or side effects. One particular problem with some

of the anti-arrhythmic drugs used in the prevention of AF is that they can cause potentially lethal ventricular arrhythmias.

#### **1.2.4 $\beta$ -blockers in AF**

Recent guidelines for the management of AF have given  $\beta$ -adrenergic receptor antagonists ( $\beta$ -blockers) a prominent role as anti-arrhythmic therapy for the prevention of AF (3;17). Traditionally  $\beta$ -blockers have been used to control the ventricular rate in patients with AF but there is increasing evidence that they can be effective in preventing the recurrence of AF once sinus rhythm is restored. One of the major advantages of  $\beta$ -blockers over many other anti-arrhythmic agents is that they do not have the same dangerous pro-arrhythmic side effects.

$\beta$ -blockers are drugs that bind selectively to  $\beta$ -adrenoceptors ( $\beta$ -ARs) and competitively and reversibly inhibit the effects of  $\beta$ -adrenergic stimulation by endogenous or exogenous catecholamines. Stimulation of  $\beta$ -ARs in the heart principally results in an increased heart rate, increased conduction velocity through the conducting system and increased contractility. However, the effects of  $\beta$ -adrenergic stimulation on the heart and the rest of the cardiovascular system are complex and diverse and blocking these receptors has many potential effects.  $\beta$ -blockers are used to treat a variety of cardiovascular pathologies in addition to arrhythmias, including ischaemic heart disease, heart failure and hypertension. Many of these conditions are themselves risk factors for AF.

##### **1.2.4.1 Classification of $\beta$ -blockers**

$\beta$ -blockers can be categorised into non-selective and selective blockers according to their ability to block both the two main cardiac  $\beta$ -ARs:  $\beta$ -AR<sub>1</sub> and  $\beta$ -AR<sub>2</sub>. Atenolol, bisoprolol, and metoprolol are all examples of  $\beta$ <sub>1</sub>-selective  $\beta$ -blockers. Some  $\beta$ -blockers can also block  $\alpha$ -adrenergic receptors e.g. carvedilol, while some have both weak agonist and antagonistic actions. In addition to its non-selective,  $\beta$ -blocking activity, sotalol is noted to be an atypical  $\beta$ -blocker with well recognised class III, anti-arrhythmic effects, making it useful in the prevention of AF but limiting its uses in other cardiac diseases which benefit from “conventional”  $\beta$ -blockers.

#### **1.2.4.2 Clinical evidence for an anti-arrhythmic action of $\beta$ -blockers in AF**

Several randomised controlled trials have demonstrated a modest benefit of  $\beta$ -blockers in maintaining sinus rhythm after electrical cardioversion of atrial fibrillation (19). Metoprolol has been shown to be more effective than placebo in maintaining sinus rhythm following electrical cardioversion of persistent AF with recurrence rates of 48.7% vs 59.9%,  $p < 0.05$  (20). Treatment with bisoprolol following electrical cardioversion of persistent AF has been shown to be as effective as sotalol at maintaining sinus rhythm at one year (21). In an open label, randomised, cross over study, atenolol was shown to be as effective as sotalol in reducing the frequency of paroxysmal AF (22).  $\beta$ -blockers have also been shown to be effective at preventing AF after cardiac surgery (23).

Heart failure is both a risk factor for, and consequence of, AF and indeed patients with heart failure and AF have a worse prognostic outcome (24). Several studies examining the potential prognostic benefits of  $\beta$ -blockers in the treatment of heart failure have reported a reduction in the incidence of AF in patients receiving either carvedilol or metoprolol when compared to placebo and standard optimal medical therapy (25;26)

#### **1.2.4.3 Possible anti-arrhythmic mechanisms of $\beta$ -blockers: pharmacological remodelling**

The mechanisms by which  $\beta$ -blockers exert their anti-arrhythmic effects are not fully understood and are likely to be multifactorial. Different mechanisms may be more important in different clinical situations. Undoubtedly, blocking excess sympathetic activity and endogenous catecholamines is a major contributing factor. Excessive stimulation of the adrenergic system is known to cause shortening of refractory periods which can promote re-entry, as well as increasing the dispersion of repolarisation and increasing automaticity (27). These drugs also help prevent cardiac ischaemia and improve left ventricular function both of which are likely to contribute to their anti-arrhythmic activity. However there is some evidence that  $\beta$ -blockers may have a direct anti-arrhythmic action rather than just preventing the deleterious effects of factors like ischaemia, cardiac failure and adrenergic over-stimulation.

There are two studies which have shown potentially anti-arrhythmic, adaptive changes in atrial electrophysiology associated with chronic administration of  $\beta$ -blockers, given over a period of weeks to months (28;29). The first study treated rabbits with propranolol, metoprolol or placebo for various periods of time up to 6 weeks (28). After waiting for

approximately 24 hours after the last drug dose, to ensure elimination of the drug, the rabbit hearts underwent electrophysiological studies and those treated with  $\beta$ -blockers were shown to have prolonged repolarisation in both the atria and ventricles, as evidenced by prolonged APDs measured in whole tissue preparations. The animals also had prolonged QT intervals on ECGs, a marker of the duration of ventricular repolarisation. These changes were thought to be an adaptive response to the  $\beta$ -blockers which took almost 10 days to develop and persisted for more than 10 days after cessation of therapy. A more recent study examined the effects of chronic  $\beta$ -blockade with  $\beta_1$ -selective blockers on isolated human atrial myocytes (29). This was a retrospective analysis of ion current and action potential recordings from right atrial appendage tissue obtained from patients undergoing cardiac surgery. It reported an increase in both atrial APD and ERP in cells from patients treated with  $\beta$ -blockers. This effect was thought to occur in the absence of the drug which was presumed to be removed by the cell isolation process. This adaptive and potentially anti-arrhythmic effect was termed “pharmacological remodelling”. This effect has yet to be confirmed in a prospective study of chronic  $\beta$ -blockade and human atrial electrophysiology.

#### **1.2.4.4 How does chronic $\beta$ -blockade prolong the APD?**

As described in section 1.1.2, the duration of the cardiac action potential is determined by the balance of inward and outward ion currents. It is likely therefore that the mechanisms underlying the APD prolongation described in the two studies above involve changes in these ion currents. The mechanism by which chronic treatment with  $\beta$ -blockers prolonged the rabbit atrial APD was not investigated in that study (28). It was noted that the action potentials had a higher plateau and longer phase 2 which might suggest changes in the ion currents are responsible for early repolarisation however, ion currents were not measured. In the isolated human atrial myocytes, APD and ERP prolongation were associated with a reduction in  $I_{TO}$  current density, a possible increase in  $I_{K1}$  but no change in  $I_{CaL}$  or  $I_{KUR}$  current densities (29). These changes were measured in a relatively small group of patients and investigation of the currents was limited to measuring their magnitude. This was the first report of chronic  $\beta$ -blocker therapy affecting ion currents. The lack of effect on  $I_{CaL}$  current density has subsequently been reported in another study by the same group (30)

Given the widespread use of  $\beta$ -blockers it is important to fully understand any electrophysiological effects they may have. If these effects further our understanding of the anti-arrhythmic activity of  $\beta$ -blockers it may allow us to expand their use or even help in the development of new anti-arrhythmic drugs for AF.

## 1.3 Potassium currents

### 1.3.1 $I_{TO}$

The transient outward potassium current,  $I_{TO}$ , was first described in Purkinje fibres as a rapidly activating and inactivating outward current (31;32). It was identified as having two components.  $I_{TO1}$  is a  $K^+$  current, which is not dependent on the presence of calcium for its activation and can be blocked by relatively high doses of the drug 4-aminopyridine (4-AP).  $I_{TO2}$  is now thought to be a  $Cl^-$  current which is calcium dependent and is insensitive to 4-AP (31;31-33). In this thesis “ $I_{TO}$ ” is used to refer to the  $K^+$  selective  $I_{TO1}$ .

One of the original descriptions of  $I_{TO}$  in isolated human atrial cells did describe the presence of two outward currents. One of these was a rapidly activating, rapidly inactivating current which was relatively insensitive to 4-AP (at 3mM), was inhibited by barium, but was not calcium dependent (34). Despite its relative insensitivity to 4-AP, which was not explored at higher doses, it is likely this current was indeed  $I_{TO1}$ . The slow inactivation of the second outward current, along with its sensitivity to 4-AP, suggests this current may actually have been the ultra-rapid delayed rectifier current  $I_{KUR}$  which is discussed in more detail later in this chapter. Other descriptions of the outward currents in atrial myocytes have also identified at least two outward potassium currents, one current consistent with  $I_{TO}$ , an  $I_{KUR}$ -like current and, in one study, a background, uncharacterised, non inactivating current which was not chloride based (35;36). Therefore, in human atrial myocytes, and also in ventricular myocytes, there is only one  $I_{TO}$  current. In contrast to human studies, different types of  $I_{TO}$  do seem to exist in animal models in addition to delayed rectifier currents. Some animals seem to possess two types of rapidly activating potassium currents with similar sensitivities to 4-AP but with different inactivation kinetics. The current which inactivates rapidly is called  $I_{TOf}$  and has the same, or very similar, characteristics to human  $I_{TO}$ . The more slowly inactivating  $I_{TOs}$ , present in rabbit atria and the ventricles of other rodents, has no human correlate and is thought to be due to the expression of different ion conducting proteins in the membrane of the myocytes (see section 1.4.1).

$I_{TO}$  has been characterised in several different species but it is the properties of this current in humans and, particularly, in human atrial myocytes, that are of most interest in this study. Human atrial  $I_{TO}$  is a relatively large current that activates extremely rapidly at physiological temperatures, reaching maximal current in less than five milliseconds

although its activation is slowed considerably at room temperature (37). It activates in a voltage dependent fashion with minimal activation at negative potentials and continues to activate as the cell membrane potential becomes more positive. The inactivation of  $I_{TO}$  is time and temperature dependent and the current characteristically inactivates rapidly. Following inactivation and a return to negative membrane potentials,  $I_{TO}$  can be rapidly reactivated (35;36;38;39).

$I_{TO}$  is also present in the human ventricle but the current characteristics are not identical (35). The density of ventricular  $I_{TO}$  varies across the transmural surface of the left ventricle being larger in epicardial and midmyocardial cells than in endocardial cells (40;41). Ventricular  $I_{TO}$  has been reported as being of a similar size to atrial  $I_{TO}$  but this is clearly dependent on the type of ventricular cells studied and also the presence of other factors such as heart failure which can affect  $I_{TO}$  density (35;42). Ventricular  $I_{TO}$  has been reported to have slightly different kinetics to atrial  $I_{TO}$  with both longer and shorter inactivation reported along with a quicker recovery from inactivation (35;42). Ventricular  $I_{TO}$  is also reported to be more sensitive to 4-AP block (35). Again, it is possible that these changes may reflect the differences between subpopulations of ventricular cells rather than real differences between ventricular and atrial cells.

Following membrane depolarisation,  $I_{TO}$  is activated along with several other ion currents including  $I_{Na}$ ,  $I_{CaL}$  and  $I_{KUR}$ . In order to study the properties of  $I_{TO}$  in isolated atrial myocytes it has to be separated from these other ion currents. This can be done by exploiting the different activation and inactivation properties of these other currents as well as using specific drugs and chemicals to block specific ion currents. As described earlier, one of the characteristics of  $I_{TO}$  is that it can be blocked by 4-AP. Relatively high concentrations of 4-AP, in the region of 10 mM, are required to completely block  $I_{TO}$ , however,  $I_{KUR}$  is blocked by 4-AP at much lower concentrations. Low dose 4-AP has been used to isolate  $I_{TO}$  from  $I_{KUR}$  although the rapid activation of  $I_{TO}$  compared to  $I_{KUR}$  can also be used to separate the currents when they are measured using voltage clamp experiments.

### **1.3.1.1 The role of $I_{TO}$ in determining the action potential duration.**

The rapid activation and inactivation of  $I_{TO}$  means it can only contribute directly to the early phase of action potential repolarisation. A reduction in the magnitude, or current density, of  $I_{TO}$  should, therefore, prolong phase 1 repolarisation. Other changes in the properties of  $I_{TO}$  could also directly affect early repolarisation. The current density could be affected by a change in the voltage dependency of the current. A change in the

inactivation kinetics will influence the “amount” of current available to contribute to early repolarisation. The rapid reactivation or recovery of  $I_{TO}$  implies its contribution to repolarisation is relatively independent of stimulation rate or heart rate. However, this may not be the case at the very rapid atrial rates seen in AF when changes in the reactivation kinetics of  $I_{TO}$  may have the potential to significantly impact on early repolarisation.

However, changes in early repolarisation do not necessarily alter the overall action potential duration. An early study looking at the effects of 4-AP on the action potential in isolated human atrial myocytes showed that, at a dose of 0.5 mM, the plateau of phase 2 repolarisation was elevated suggesting a reduction in the currents underlying phase 1 repolarisation ie the yet uncharacterised  $I_{TO}$  (43). This change was associated with a shortening of the APD measured at 90% repolarisation ( $APD_{90}$ ). At this dose, 4-AP would be expected to reduce  $I_{TO}$  by less than 50% but significantly reduce the yet unidentified  $I_{KUR}$  (33). This in turn might be expected to prolong the  $APD_{90}$  and suggests that the interaction of currents in determining the APD is complex. A subsequent study also reported that 0.5 mM 4-AP appeared to block initial repolarisation with elevation of the plateau height, prolonging early repolarisation but, in this case, shortening the  $APD_{90}$  (39). In isolated atrial and ventricular cells, higher doses of 4-AP, which would be expected to produce greater  $I_{TO}$  block, have been shown to prolong the  $APD_{90}$  in addition to elevating the plateau (2;44).

It would appear that the consequences of  $I_{TO}$  block on APD are complex, particularly, with a non-specific blocker like 4-AP. There are no specific blockers of  $I_{TO}$  in clinical use. Various anti-arrhythmic drugs including quinidine, propafenone and flecainide have been shown to block  $I_{TO}$  and do result in prolongation of atrial APD and atrial refractoriness. However, these drugs have multiple effects on different ion channels and it cannot be assumed that it is the  $I_{TO}$  block which is responsible for the prolonged atrial repolarisation. (33;45). Recently, several new blockers of  $I_{TO}$  have been identified from the toxins of venomous creatures including scorpions, spiders, snakes and sea anemones (46). These toxins can block the cell membrane proteins that are responsible for conducting  $I_{TO}$  and have been used to study this current in cell lines. There is limited evidence of the effects of these blockers in isolated cardiac myocytes. The venom of the Malaysian Heteropoda venatoria spider contains heteropodotoxins (HpTx) which have been shown to block  $I_{TO}$  in isolated rat ventricular myocytes in a voltage dependent manner. HpTx have been shown to shift the voltage dependence of  $I_{TO}$  activation and inactivation, slow the time to peak activation and slow the time constant of inactivation. They also prolong the ventricular  $APD_{90}$  providing further support for the role of  $I_{TO}$  in determining APD (47). The

phrixotoxins (PaTx) were isolated from the venom of the Chile fire tarantula *Phrixotrichus auratus* and have been shown to be specific blockers of  $I_{TO}$ . They also affect the voltage dependency of the current and kinetics of activation and inactivation. When PaTx1 was injected into mice there was a significant increase in QT interval, a marker of ventricular repolarisation on the ECG (48). Neither of these toxins has been used in human cardiac myocytes to investigate the link between  $I_{TO}$  reduction and APD prolongation but, as specific  $I_{TO}$  blockers, they could be very useful tools for confirming the effects of changes in  $I_{TO}$  on late repolarisation.

Computer models have been developed to study the effects of changes in  $I_{TO}$  density on APD in ventricular myocytes. In one study, reducing  $I_{TO}$  had no effect on  $APD_{90}$  (49). In another study, based on canine action potentials, a increase in  $I_{TO}$  could either increase or decrease the APD depending on both the baseline density and degree of change (50), an effect largely modulated by secondary changes in  $I_{CaL}$ .

Therefore, while a reduction in  $I_{TO}$  current density does appear to prolong early repolarisation, its overall effect on APD remains debatable. Any effects of  $I_{TO}$  reduction on late repolarisation may simply represent secondary changes in other ion currents particularly  $I_{CaL}$  and  $I_{KUR}$ . Changes in other properties of  $I_{TO}$  may also affect early and, possibly indirectly, late repolarisation.

### **1.3.1.2 $I_{TO}$ and APD remodelling in cardiac diseases**

Remodelling of  $I_{TO}$  occurs in AF in association with shortening of the atrial APD. Consistently, studies have shown reductions in human atrial  $I_{TO}$  current density of between 44 and 70% in cells from patients with AF (2;9;11;51). This reduction in  $I_{TO}$  has also been reported in animal models of AF and/or atrial tachycardia (52;53). Although this reduction in  $I_{TO}$  could be consistent with shortening in APD as outlined above, there is a theoretical expectation, and evidence to support,  $I_{TO}$  reduction causing prolongation of APD. The contribution of  $I_{TO}$  reduction to AF-induced, APD shortening in AF remodelling is unclear and probably small compared to the effects of  $I_{CaL}$  reduction and increased  $I_{K1}$  (4;54)

In contrast to AF, a reduction in  $I_{TO}$  current density in association with a prolongation of the APD is seen in ventricular myocytes from patients with heart failure (41;44). In general, a prolongation of APD might be expected to be anti-arrhythmic and yet there is a strong link between heart failure and ventricular arrhythmias. This link may well reflect the many other cardiac problems associated heart failure particularly ischaemic heart

disease. However, when APD prolongation is very marked or associated with altered dispersion of repolarisation it may well be pro-arrhythmic. In atrial cells from patients with heart failure secondary to left ventricular dysfunction but with no evidence of atrial dilation or AF,  $I_{TO}$  current density was reported to increase in association with shortening of the atrial APD (55). Why  $I_{TO}$  should be remodelled differently in different cardiac chambers is unclear but these findings may help to explain the increased incidence of AF in patients with heart failure. Changes in the reactivation kinetics of  $I_{TO}$  have also been reported in atrial and ventricular myocytes in these studies.

### 1.3.1.3 $I_{TO}$ and chronic $\beta$ -blockade

As discussed earlier, there is one study that has shown that a significant reduction in human atrial  $I_{TO}$  current density in association with chronic  $\beta$ -blockade (29). This reduction in  $I_{TO}$  was associated with prolongation of atrial  $APD_{90}$ , ERP and slowing of phase 1  $V_{max}$ , the maximum velocity of the downslope of phase 1 of the action potential. This, therefore, provides further support for a reduction in  $I_{TO}$  density causing prolongation of atrial repolarisation. To my knowledge, this is the only study that has examined the effects of chronic  $\beta$ -blockade on  $I_{TO}$  in human cardiac myocytes and there are no similar animal studies. This report did not examine the effects of chronic  $\beta$ -blockade on any other characteristics of  $I_{TO}$  or explore any underlying mechanisms to explain the reduction in current density.

There is some additional evidence to support  $I_{TO}$  modulation by the adrenergic system. The only other study looking at the effects of  $\beta$ -blockers on human  $I_{TO}$  examined the effects of carvedilol on atrial myocytes (56). In this study, acute application of carvedilol also significantly and reversibly inhibited  $I_{TO}$  current density. This was associated with an increase in the activation and inactivation kinetics as measured at room temperature but not with any change in voltage dependency or reactivation. Action potentials were not recorded in this study and there is no description of the drugs the patients were prescribed prior to cardiac surgery and cell isolation. It should be noted that carvedilol is not a  $\beta_1$ -selective blocker as was used in the study by Workman et al 2003. There are no direct reports of the effects of either acute or chronic  $\beta$ -blockade on  $I_{TO}$  in animal cardiac myocytes. There is one report of the effects of propranolol treatment on transgenic mice with dilated cardiomyopathy which showed no change in ventricular  $I_{TO}$  although heart failure itself did significantly affect  $I_{TO}$  current density (57).

Further support for the ability of the adrenergic system to modify  $I_{TO}$  and APD comes from a study of catecholamine depleted rats which have been shown to have reduced ventricular  $I_{TO}$  current density in association with altered voltage dependency of the current and prolonged ventricular APD (58).

$I_{TO}$  can be affected by adrenergic stimulation however, the nature of the response has not been fully determined. Several studies in animals have suggested stimulation with  $\alpha$  - agonists reduces  $I_{TO}$  current density (59). There is very little data examining the effects of  $\beta$ -adrenergic stimulation on  $I_{TO}$ . Cultured canine myocytes have been shown to have reduced  $I_{TO}$  current density compared to freshly isolated cells and this can be restored to normal levels with the addition of the  $\beta$ -adrenoceptor agonist isoproterenol (60). Rats with cardiac hypertrophy secondary to treatment with isoproterenol have decreased ventricular  $I_{TO}$  along with prolonged APDs but it is difficult to separate the effects of hypertrophy from those of direct  $\beta$ -adrenergic agonism in this study (61).

### 1.3.2 $I_{K1}$

An inwardly rectifying current was first identified in cardiac tissue over 50 years ago in sheep Purkinje fibres (62). Inward rectifiers preferentially conduct  $K^+$  inwardly rather than in the outward direction. At voltages negative to  $E_K$  (more negative than -90 mV) the resistance of the  $I_{K1}$  ion channel is essentially independent of voltage and the current-voltage (IV) relationship for  $I_{K1}$  is a straight line, also known as an ohmic relationship. The conductance of the channel (the inverse of the resistance) is high at these hyperpolarised membrane potentials and the channel passes a large inward current. As the voltage rises, however, the conductance of the channel becomes smaller and is no longer independent of voltage. The IV relationship is no longer linear and the amount of outward current that is passed at voltages positive to  $E_K$  is smaller. The activation of  $I_{K1}$  depends on the difference between the membrane potential and  $E_K$ , known as the driving force, rather than just the membrane potential alone.  $I_{K1}$  can, therefore, be controlled by voltage and the extracellular  $K^+$  concentration. It is almost time independent (62-64). Although  $I_{K1}$  has the potential to be a much larger inward than outward current, it is the outward component that is of greatest physiological importance. Normally cells are not hyperpolarised to voltages more negative than  $E_K$  and so the inward current does not occur.

The mechanism by which  $I_{K1}$  can switch from conducting current inwardly to outwardly i.e. the mechanism of inward rectification, is thought to reflect a voltage dependent removal of a positively charged "blocking particle" from the ion channel pore, which

allows  $K^+$  to be conducted out of the cell (62;64). Intracellular divalent cations like  $Mg^{2+}$  and  $Ca^{2+}$  have been shown to facilitate inward rectification but do not fully replicate the inwardly rectifying properties of  $I_{K1}$  (62). Subsequently, it was found that intracellular organic cations called polyamines could cause strong inward rectification similar to that seen with  $I_{K1}$  (65;66) and depletion of these cations could abolish this outward current.(67)

Extracellular ions, particularly barium, have also been shown to be potent selective blockers of both the inward and outward components of  $I_{K1}$  in a voltage dependent fashion. (62;64) Barium is commonly used in experimental studies to dissect out  $I_{K1}$  from other ion currents and also to test the properties of ion currents derived from over-expression of ion channel proteins in cell lines (37;68). It can, however, affect other ion channels such as  $I_{CaL}$  and, therefore, its effect on  $I_{K1}$  is not “clean” (69).

### **1.3.2.1 The role of $I_{K1}$ in determining APD.**

As described earlier, it is the outward component of  $I_{K1}$  that contributes to the repolarisation phase of the action potential. Therefore, if this component of  $I_{K1}$  changes in size it may alter the action potential duration. In atrial cells, both the outward and inward components of  $I_{K1}$  current density are considerably smaller than in ventricular cells and this helps to account for the slower phase 3 repolarisation in atrial cells (64) although it should be noted that the atrial APD remains shorter than the ventricular. Application of barium to block  $I_{K1}$  has been shown to result in prolongation of cardiac APD in a canine ventricular wedge preparation. There are a number of anti-arrhythmic drugs which have been shown to block  $I_{K1}$  along with multiple other ion channels and, although many of these drugs prolong APD, it is difficult to use them to determine the specific effects of  $I_{K1}$  block on APD or the clinical consequences of changing  $I_{K1}$ . (33).

### **1.3.2.2 $I_{K1}$ and APD remodelling in cardiac diseases**

Changes in the current density of  $I_{K1}$  and associated changes in cellular APD have been described in cardiac diseases. Several studies have reported that  $I_{K1}$  is increased in isolated atrial cells from patients with AF (2;9;12;70). This might be expected to increase phase 3 repolarisation and contribute to the shortening of the APD that is seen in these cells. It may also contribute to the more negative resting membrane potential reported in cells from AF patients (70). The importance of  $I_{K1}$  in determining the APD was highlighted by a computer modelling study of human atrial APD remodelling in AF which suggested that upregulation of  $I_{K1}$  had a bigger role to play in APD shortening than changes in  $I_{CaL}$  (54)

Animal models of AF have reported conflicting results with regards to atrial  $I_{K1}$ , showing no change (52) or an increase (53). To my knowledge, there are no studies looking at modification of  $I_{K1}$  as a treatment for AF but several studies have examined its possible anti-fibrillatory effects in context of ventricular fibrillation (VF) using barium, computer models or the selective blocker RP58866 (71-73). Blocking  $I_{K1}$  may be beneficial in terminating or preventing VF by destabilising the high frequency rotors which are thought to help sustain fibrillation (64).

$I_{K1}$  has been reported to be altered in other animal models of cardiac disease. A decrease in ventricular  $I_{K1}$  is reported in some animal models of myocardial infarction (74) and there is also a reduction in ventricular  $I_{K1}$  density, along with prolongation of the APD, in spontaneously hypertensive rats (75). A reduction in ventricular  $I_{K1}$  has been reported in some (76;77) but not all animal models of heart failure (78). In humans, a reduction in ventricular  $I_{K1}$  has also been described in cells from patients with heart failure which also exhibit a prolonged APD (79). In patients with idiopathic dilated cardiomyopathy, ventricular  $I_{K1}$  density is smaller in association with a longer APD and a lower resting membrane potential, when compared to patients with ischaemic cardiomyopathy (80).

### **1.3.2.3 Potential modification of $I_{K1}$ by chronic $\beta$ -blockade**

There is very little evidence regarding any possible effects of chronic  $\beta$ -blockade on  $I_{K1}$ . Workman et al 2003 showed that chronic  $\beta$ -blockade was associated with an increase in the input resistance ( $R_i$ ) of isolated human atrial cells during a clamp protocol which may, in part, be due to a decrease in  $I_{K1}$  (29). Acute application of carvedilol, has been shown to block some  $K^+$  channels including  $I_{TO}$  and  $I_{KR}$  but not  $I_{K1}$  in isolated rabbit cardiac myocytes (81;82). Acute application of another  $\beta$ -blocker, tilisolol, did not affect  $I_{K1}$  in isolated guinea pig ventricular myocytes (83). Adrenergic modulation of  $I_{K1}$  has been further supported by reports demonstrating changes in  $I_{K1}$  density with  $\beta$ -adrenergic stimulation. In isolated human ventricular myocytes, application of isoproterenol, has been shown to reduce both the inward and outward components of  $I_{K1}$ , an effect which was dependent on protein kinase A phosphorylation and reversed by the addition of the  $\beta$ -blocker propranolol. This effect was noted to be reduced in myocytes from failing hearts. Chronic exposure (48 hours) to isoproterenol also reduced the density of  $I_{K1}$  in cultured adult guinea pig ventricular myocytes (84). Another study looking at sympathetic modulation of  $K^+$  currents used antibodies to nerve growth factor in rats to delay sympathetic innervation of heart and showed a reduction in  $I_{K1}$  density compared to hearts with increased sympathetic innervation (85).

It would appear that  $\beta$ -adrenergic modulation can influence  $I_{K1}$  density but the exact nature and magnitude of potential changes are unclear.  $I_{K1}$  does play an important role in repolarisation, with a decrease in the current density being associated with an increase in APD. It is also one of the currents remodelled in AF and other cardiac diseases. It is, therefore, possible that a reduction in the density of  $I_{K1}$  may be responsible, or may contribute to, the prolongation of APD seen with chronic  $\beta$ -blockade. However,  $I_{K1}$  has not been directly measured (by barium subtraction) in human atrial myocytes in a prospective study of the effects of chronic  $\beta$ -blockade.

### **1.3.3 The delayed rectifiers**

The delayed rectifier currents,  $I_K$ , are outward potassium currents which contribute to phase 3 repolarisation. Although the name implies slow activation, the delayed rectifier currents are actually several distinct currents with varying activation and inactivation kinetics.  $I_K$  is made up of a several distinct components with varying inactivation kinetics, the ultra-rapid  $I_{KUR}$ , the rapidly activating  $I_{KR}$  and the slowly activating  $I_{KS}$ . The presence and size of these currents varies in different species and in different anatomical areas of the heart.

#### **1.3.3.1 The contribution of the delayed rectifiers to atrial action potential duration**

$I_{KR}$  was first detected in guinea pig ventricles (86). It activates rapidly, albeit more slowly than  $I_{KUR}$  and  $I_{TO}$ , in a voltage dependent fashion and then inactivates rapidly as the membrane depolarises above 0 mV (86). During an action potential  $I_{KR}$  will start to activate but then quickly inactivate as the membrane depolarises. It, therefore, contributes little, if any, current to early repolarisation. As the membrane potential becomes more negative  $I_{KR}$  can “reactivate” and therefore contribute to late repolarisation. This contribution is also influenced by the time dependent aspect of its activation and, therefore,  $I_{KR}$  is likely to be bigger in cells with longer APDs like ventricular cells. In cardiac myocytes  $I_{KR}$  is generally very small compared to other currents (37). A current with similar, although not identical, properties to the classically described  $I_{KR}$  has been detected in a sub-population of isolated human atrial myocytes in one study (87). In this study, the cells with recordable  $I_{KR}$  had different shaped action potentials with more prominent plateaus and a small proportion did not have  $I_{TO}$  which is thought to be a characteristic feature of atrial myocytes. In a different study,  $I_{KR}$  was also detected in human ventricular cells (88).

$I_{KS}$  is a very slowly activating current which was also identified initially in guinea pig ventricular myocytes. It is also voltage dependent and inactivates with different kinetics in different species (37). It can be separated from  $I_{KR}$  using specific blockers and has been detected in only a very small proportion of isolated human atrial cells (89).

There are currently very few studies that have demonstrated the presence of  $I_{KR}$  and/or  $I_{KS}$  in human atrial cells. Some studies have failed to detect either current in isolated human myocytes of atrial or ventricular origin (35;42) or the presence of significant numbers of the characteristic subpopulations of cells reported to have these currents (2;36). It is possible, that these currents are very sensitive to different experimental techniques making them difficult to measure. There is considerable clinical evidence to suggest these currents do have a significant functional role in determining human atrial APD. Class III anti-arrhythmic drugs like amiodarone and sotalol target  $I_{KR}$  and  $I_{KS}$  and, by blocking these channels, the drugs prolong the atrial APD and can prevent AF. APD prolongation as a result of modifying  $I_{KR}$  and  $I_{KS}$  can have detrimental effects in the ventricle by prolonging the QT interval, a clinical measure of ventricular repolarisation, and predisposing to ventricular arrhythmias. While APD prolongation can be beneficial in preventing re-entrant arrhythmias, excessive prolongation or increased dispersion of repolarisation can be pro-arrhythmic.

$I_{KUR}$  was first described in human atrial myocytes and appears to be atrial specific (90). This makes it an extremely interesting target for anti-arrhythmic drugs with the possibility of prolonging the atrial APD but avoiding ventricular arrhythmias.  $I_{KUR}$  activates in a temperature and voltage dependent fashion. At physiological temperature its activation is almost instantaneous at positive membrane potentials. It, therefore, activates at the same time as  $I_{TO}$  on membrane depolarisation and, unlike the other delayed rectifiers, can contribute to early repolarisation.  $I_{KUR}$  inactivates extremely slowly and complete inactivation can only be appreciated in voltage clamp studies using long depolarising pulses. It takes around 50 seconds for  $I_{KUR}$  to fully inactivate and very little, if any, inactivation occurs during the typical duration of an action potential. As  $I_{TO}$  inactivates rapidly and the contribution of  $I_{KR}$  and  $I_{KS}$  are probably small,  $I_{KUR}$  has its biggest impact on phase 3 repolarisation in human atrial myocytes.

Changes in  $I_{KUR}$ , therefore, have the potential to significantly impact on the atrial APD.  $I_{KUR}$  can be difficult to study in isolation from other currents, particularly,  $I_{TO}$  as both currents activate extremely rapidly upon depolarisation. The different inactivation characteristics of the two currents can be exploited to isolate  $I_{KUR}$  by using prolonged

depolarising pulses or partially depolarising pre-pulses to inactivate  $I_{TO}$ . Blockers of  $I_{KUR}$  are also useful tools to help dissect out the current from others and investigate its role in repolarisation. There are several blockers of  $I_{KUR}$  which have also been shown to prolong atrial APD. 4-AP can be used to separate  $I_{KUR}$  and  $I_{TO}$ . It blocks  $I_{KUR}$  at low concentrations, with 50% block ( $IC_{50}$ ) occurring at 0.001-0.005 mM compared to an  $IC_{50}$  of 1-2 mM for  $I_{TO}$  (33;35;90). Selective inhibition of  $I_{KUR}$  by low dose 4-AP prolongs human atrial APD (90) and has also been shown to prolong atrial refractoriness in canine atria but, unsurprisingly, not in the ventricles (91).  $I_{KUR}$  is relatively insensitive to class III anti-arrhythmics but, along with other ion channels, can be partially blocked by other anti-arrhythmic drugs including calcium channel blockers and class I anti-arrhythmics. Some specific blockers of  $I_{KUR}$  have been developed which have been shown to prolong atrial refractoriness but there is little clinical data on the efficacy of these drugs (33). In contrast, a study of  $I_{KUR}$  block in atrial trabeculae showed that low dose 4-AP shortened the APD in patients in sinus rhythm although it prolonged the APD in AF patients (92). This suggests that the role of  $I_{KUR}$  in determining APD is more complex in the whole heart and may depend on secondary changes in other ion currents.

### 1.3.3.2 Remodelling of $I_{KUR}$ in cardiac disease

As  $I_{KUR}$  is an atrial specific current, its role in AF remodelling has been studied with interest. Several studies have reported a reduction in the sustained outward current,  $I_{KSUS}$ , and  $I_{KUR}$  in cells from patients in AF compared to those in sinus rhythm (11;12).  $I_{KSUS}$  is the outward current measured at the end of a depolarising voltage pulse using the voltage clamp technique. It is often measured as a surrogate of  $I_{KUR}$  as it is composed mainly of  $I_{KUR}$  but is possibly contaminated with other slowly inactivating outward currents. Like  $I_{TO}$ , a reduction in  $I_{KUR}$  or  $I_{KSUS}$  does not initially appear to be consistent with shortening of the atrial APD as is seen in AF. It is probable, therefore, that changes in  $I_{KUR}$  do not play a prominent role in the APD shortening in AF and other currents have a greater impact. Remodelling of  $I_{KUR}$  in AF is not a consistent finding, however, with some studies reporting no change in this current (2;9). Canine models of AF have also reported no remodelling of  $I_{KUR}$  (52).

There is a suggestion that  $I_{KUR}$  may be decreased in atrial cells from patients with heart failure but no direct comparison has been made between patients with normal and abnormal left ventricular function (93).

### 1.3.3.3 Potential modification of $I_{KUR}$ by chronic $\beta$ -blockade

There is evidence to support adrenergic modulation of  $I_{KUR}$ . In isolated human atrial myocytes, acute  $\beta$ -agonist stimulation by isoproterenol increased  $I_{KUR}$  while  $\alpha$ -agonist stimulation with phenylephrine decreased it. In dogs, a similar response was seen to  $\beta$ -agonists but in this case  $\alpha$ -agonists also increased  $I_{KUR}$  (94). These results would perhaps suggest that  $\beta$ -blockers might have the opposite effect and decrease  $I_{KUR}$  which might explain the APD prolongation associated with chronic  $\beta$ -blockade. There is very little data on the effects of  $\beta$ -blockers on  $I_{KUR}$ . In keeping with its known class III anti-arrhythmic action, sotalol does not appear to affect  $I_{KUR}$  (95). Acute application of carvedilol has been shown to reduce  $I_{KUR}$  in isolated human atrial myocytes without affecting the voltage dependency of activation (56). In contrast, chronic  $\beta$ -blockade with  $\beta_1$ -selective blockers was not associated a change in  $I_{KSUS}$  in a small retrospective data analysis (29).

A decrease in  $I_{KUR}$  current density could contribute to atrial APD prolongation. This current does appear to be affected by the adrenergic system and, therefore, it is possible that the APD prolongation associated with chronic  $\beta$ -blockade could at least be partially explained by a decrease in  $I_{KUR}$  current density. At present there is limited evidence to suggest  $I_{KUR}$  may not actually be involved and further work is required to clarify this.

## 1.4 The structure of $K^+$ channels

Voltage gated ion channels carry  $K^+$  currents across the cell membrane. These ion channels usually consist of pore-forming and accessory proteins. The pore-forming proteins are membrane spanning proteins with a central tunnel through which ions can travel down their electrochemical gradients. The structure of the pore-forming proteins determines the specificity of the channel for  $K^+$  and also determines the open and closing properties of the channel. The accessory proteins are proteins of differing structure and function that can associate with the pore-forming proteins and modify their expression as well as altering the properties of the currents they conduct. The different expression and combinations of these pore-forming and accessory proteins underlie the inter-species and intra-cardiac variations in ion currents.

### 1.4.1 $I_{TO}$ pore-forming protein: Kv4.3

The genes for the voltage gated potassium (Kv) pore-forming proteins were originally cloned from the Shaker locus in *Drosophila* and are divided into three homologous

subfamilies according to their structure: Shal, Shaw and Shab. Similar families of pore-forming proteins, or  $\alpha$ -subunits, have subsequently been identified in mammals. The proteins in each family are classified using the nomenclature  $K_{vx.y}$  where x, represents the subfamily and y, the number of genes within the subfamily (96;97)

The  $K_{v\alpha}$ -subunits are proteins consisting of six transmembrane-spanning domains (S1-6) with cytoplasmic amino and carboxyl termini as seen in figure 1-3 (98). These proteins associate as heterozygous or homozygous tetramers to form the structure of the ion channel. Each protein contributes a pore-lining loop (P-loop) to form the central ion conducting pore. The P-loop lies between S5 and S6 and determines the ionic specificity of the pore. The voltage dependency of the channel is controlled by the positively charged S4 domain which moves in response to changes in the membrane potential and mediates channel activation. The cytoplasmic termini play a role in channel inactivation and the tetramerisation domain in the amino terminus helps mediate subunit-subunit interactions. Domains on the cytoplasmic termini help regulate trafficking of the  $\alpha$ -subunits to the cell membrane and are involved with binding to accessory proteins (96;97).

Various techniques have been used to identify the pore-forming proteins responsible for  $I_{TO}$ . Several different  $K_{v\alpha}$ -subunits have been cloned from mammalian cardiac tissue including the Shal-type genes *KCND2* and 3 which encode the pore-forming proteins  $K_{v4.2}$  and 4.3. When these genes are expressed in cell lines they result in potassium currents that activate and inactivate rapidly in a voltage dependent manner, properties that are very suggestive of  $I_{TO}$ . These currents also respond in a similar fashion to  $I_{TO}$  when exposed to pharmacological blocking agents like 4-AP and heteropodotoxins (96;97;99).

Further support for these proteins being the pore-forming proteins for  $I_{TO}$  has come from studies using genetically modified rodents. Anti-sense oligonucleotides (AODNs) against  $K_{v4.2}$  and 4.3 messenger ribonucleic acid (mRNA) have been used in rats to try to block functional expression of the genes. They have suggested a crucial role for  $K_{v4.2}$  in forming atrial  $I_{TO}$  and both proteins in forming ventricular  $I_{TO}$ , possibly by forming heterozygous tetramer ion channels (100;101).  $K_{v4.2}$  also seems to play an important role in murine  $I_{TO}$  as indicated by the lack of ventricular  $I_{TO}$  in transgenic mice that have had the  $K_{v4.2}$  gene replaced by a non-functioning one. These mice also have prolonged ventricular APDs and prolonged QT intervals on ECGs, further supporting the role of  $I_{TO}$  in cardiac repolarisation (102). In rat and ferret ventricles, the expression of mRNA for  $K_{v4.2}$  varies across the ventricle wall with highest expression in the epicardium (96;103). This mirrors the gradient seen in  $I_{TO}$  density.

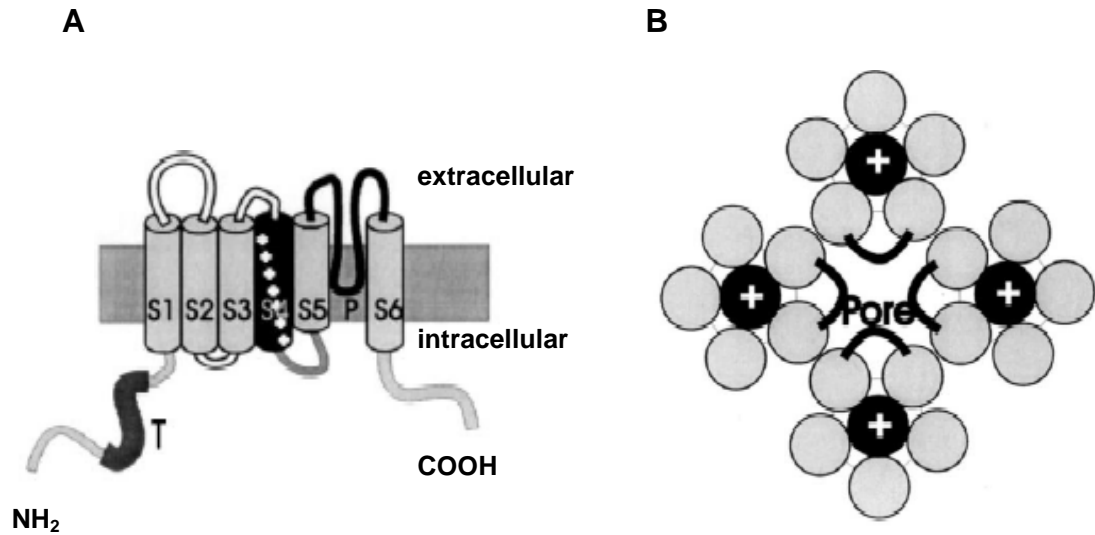


**Figure 1-3** Schematic representation of Kv4.3. **A** shows the six transmembrane domains S1-S6 with positively charged S4 domain and P-loop (P). The functional ion channel with its tetramer structure and central pore is shown in **B**. Modified (98)

Other  $Kv\alpha$ -subunits can also contribute to the formation of  $I_{TO}$  reflecting the inter-species variation in the characteristics of this current.  $Kv1.4$  is expressed in rodents, ferrets and rabbits and appears to mediate the slowly inactivating  $I_{TO}$  current ( $I_{TOs}$ ) found predominantly in the ventricles of these species but also present in rabbit atria (97;104).

In contrast to other species, only one  $Kv\alpha$ -subunit seems to be responsible for human  $I_{TO}$ .  $Kv4.3$  mRNA is highly expressed in human brain and heart tissue and is virtually absent in other tissues like lung and skeletal muscle (105). Two splice variants of  $Kv4.3$  have been identified with the long variant predominantly expressed in the heart (105). In human atrial cells,  $Kv4.3$  mRNA and protein are expressed at high levels but there is no  $Kv4.2$  expression and only  $Kv1.4$  mRNA but not protein has been detected (104;106). The role of  $Kv1.4$  in human atrial tissue is unclear, particularly as several studies have failed to show the presence of  $I_{TO}$  in human atrial myocytes (35;36). This highlights a potential problem with all studies in which mRNA expression is studied, as the presence of mRNA does not necessarily correlate with functional protein expression. Functional evidence for the role of  $Kv4.3$  in mediating human atrial  $I_{TO}$  is further supported by a study showing  $I_{TO}$  attenuation following exposure to  $Kv4.3$  AODNs in human atrial myocytes (104;107).  $Kv4.3$  mRNA and protein, but not  $Kv4.2$ , are also expressed relatively abundantly in human ventricles. (97). There are conflicting reports as to whether  $Kv4.3$  expression varies across the ventricle wall and therefore could be responsible for the transmural gradient in  $I_{TO}$  current density (108-110). These studies have suggested that other proteins (accessory proteins) are important for replicating  $I_{TO}$  in a physiological setting. This is also supported by the fact that the expression of  $Kv4.3$  and other  $Kv\alpha$ -subunits in cell lines do not result in currents which completely replicate all the features of cardiac  $I_{TO}$  (96;97).

#### **1.4.1.1 Altered $Kv4.3$ expression modifies $I_{TO}$ in cardiac disease**

Various disease states and other physiological variables have been shown to result in changes in  $I_{TO}$  density in association with changes in the expression of the  $Kv\alpha$ -subunits responsible for  $I_{TO}$  in the species studied.

Several studies have reported a reduction in both  $Kv4.3$  mRNA and protein in patients with AF which may well explain the reduction in  $I_{TO}$  current density seen in these patients. (111;112). Similar reductions in  $Kv4.3$ , 4.2 and/or 1.4 have been reported in various animal models of AF and atrial tachycardia, again mirroring the reductions in  $I_{TO}$  current density (52;113;114).  $Kv4.3$  expression has also been demonstrated to be reduced, in association with reductions in ventricular  $I_{TO}$ , in patients with heart failure (108;115;116).

In one of these studies the reduction in Kv4.3 protein expression was demonstrated in both epicardial and endocardial myocytes, maintaining the transmural gradient of Kv4.3 expression in the failing heart (108). Cardiac hypertrophy in animal models has also been demonstrated to be associated with parallel reductions in ventricular  $I_{TO}$  and Kv4.3 and 4.2 mRNA however, this is not found in all such models (99).

#### **1.4.1.2 Can chronic $\beta$ -blockade modify Kv4.3 expression?**

There is good evidence to support the link between Kv4.3 expression and  $I_{TO}$  current density. It is possible that any changes in  $I_{TO}$  current density secondary to chronic  $\beta$ -blockade may be explained by changes in Kv4.3 expression. Although there is very little data regarding a possible role for the adrenergic system in modulating Kv4.3 expression, there is one study to support it. In adrenalectomised and catecholamine-depleted rats a reduction in Kv4.2 and 4.3 mRNA expression has been shown in association with a reduction in ventricular  $I_{TO}$  current density (58). No studies have looked at the effects of chronic  $\beta$ -blockade on Kv4.3 expression in animals or humans.

In most of the studies described in the previous section, Kv4.3 expression is determined by examining mRNA and/or protein expression. Detection of mRNA does not necessarily equate to functional protein expression but clearly, one mechanism for altering protein expression would be to increase or decrease gene transcription and translation. Even detection of the protein itself does not necessarily equate to functional ion channel expression as these proteins are subject to post-translational modifications and then have to travel to the cell membrane. If chronic  $\beta$ -blockade alters the expression of functional Kv4.3 it may do so at any of these stages, however, measuring tissue levels of this protein would seem to be a reasonable starting point when looking for potential changes in the functional expression of this ion channel.

#### **1.4.2 Modulation of Kv4.3 by accessory proteins**

Another possibility is that chronic  $\beta$ -blockade may affect  $I_{TO}$  by modifying the expression or function of the accessory proteins which associate with Kv4.3. This may result in changes in  $I_{TO}$  current density but also changes in the kinetics and voltage dependent properties of the current. A number of accessory proteins have been identified in the last few years which have the potential to modify Kv4.3 and hence  $I_{TO}$ .

### 1.4.2.1 KChIP2

The *Kv channel-interacting proteins* (KChIPs) are cytoplasmic proteins belonging to the recoverin-neuronal  $\text{Ca}^{2+}$  sensor (NCS) superfamily. They have a conserved carboxy terminus with calcium binding domains and a unique amino terminus that interacts with the *Kv4.x*  $\alpha$  subunits (96). Four KChIP proteins have been identified, encoded by the genes *KCNIP1-4* but only KChIP2 seems to be expressed in the heart (97). It is expressed in both the atria and ventricles of adult human heart and has multiple splice variants (97;117).

The KChIP proteins are thought to interact specifically with *Kv4*  $\alpha$ -subunits in a 4:4 stoichiometry (97). They were originally described in rat brain tissue where they have been shown to co-localise with *Kv4.2* and *4.3* using immunolocalisation and co-immunoprecipitation studies (118). Subsequent studies expressing KChIPs with *Kv4.2* and *4.3* in cell lines have shown that these accessory proteins increase the cell surface expression of the  $\alpha$ -subunits and so, significantly, increase the current density of  $I_{\text{TO}}$  (96;97). The KChIPs are thought to be important in trafficking *Kv4*  $\alpha$ -subunits to the cell membrane. When COS cells are transfected with *Kv4.2* alone, the protein remains in the endoplasmic reticulum but when the cells are co-transfected with KChIP2, both proteins are present in the Golgi apparatus and at the cell surface (96). KChIP2 has also been shown to affect *Kv4* channel gating and kinetics in expression systems by slowing inactivation, increasing the speed of recovery and shifting the voltage dependency of activation in a hyperpolarising direction. It is thought that different regions of the KChIP proteins may be responsible for the different modulatory effects on the *Kv4* subunits (96;97).

The physiological importance of KChIP2 to cardiac  $I_{\text{TO}}$  has been demonstrated in a number of human and animal studies. Homozygous KChIP2 knock-out mice completely lack  $I_{\text{TO}}$  in isolated ventricular myocytes compared to wild type mice, with the heterozygous knock-outs demonstrating a 50% reduction in  $I_{\text{TO}}$  current density. These mice also have a prolonged ventricular APD and are susceptible to ventricular arrhythmias but have little in the way of ECG changes (119). In both humans and dogs, KChIP2 mRNA and protein expression exists in a gradient across the ventricular wall and is thought to help contribute to the transmural gradient in  $I_{\text{TO}}$  current density.  $I_{\text{TO}}$  is largest in epicardial myocytes but not all studies have demonstrated that *Kv4.3* is expressed more highly in these cells to account for this (108;120). In several, but not all studies, KChIP2 mRNA and protein have been shown to be higher in epicardial cells than in the midmyocardium and endocardium

(108;110;120;121). Remodelling of ventricular KChIP2 mRNA has been described in one study of human heart failure (116) which, along with a reduction in Kv4.3 expression, was thought to contribute to the reduction in  $I_{TO}$  current density. However, this finding was not replicated in another study which looked at KChIP2 mRNA and protein in dogs and KChIP2 protein in humans and found no change in expression associated with heart failure (108). There appears to be only one study which has looked at KChIP2 gene expression in patients with AF and it did not report any change in expression (122).

It would, therefore, appear that alterations in KChIP2 expression can have a physiological impact on  $I_{TO}$  current density although the evidence that it is involved in pathological remodelling of the ion current in cardiac diseases is sparse. It is possible that changing KChIP2 could also have a physiological impact on the other properties of  $I_{TO}$ . There is no evidence to date that KChIP2 expression can be modulated by the adrenergic system and no studies have examined the effects of chronic  $\beta$ -blockade on KChIP2 expression.

#### 1.4.2.2 Kv $\beta$ 1-3

The Kv $\beta$ -subunits are another family of cytosolic accessory proteins which have been shown to interact with Kv4.3 and hence modify  $I_{TO}$ . There are three highly homologous  $\beta$ -subunits that have been identified, Kv $\beta$ 1-3, with a variety of splice variants all encoded by the KCNAB genes. Like the KChIPs, each  $\beta$ -subunit has a conserved carboxy terminus and unique amino terminus (96;123). Both Kv $\beta$ 1 and 3 genes have been demonstrated to be expressed in human hearts with Kv $\beta$ 3 mRNA expression being higher in the ventricles (122;124;125).

The Kv $\beta$  subunits are thought to act as chaperone proteins to promote or stabilise cell surface expression of Kv channels as well as having the potential to alter channel kinetics. When expressed in cell lines with Kv4.3, Kv $\beta$ 1 and 2 have been shown to increase the density of the current conducted by Kv4.3 in association with an increased expression of Kv4.3 protein. These subunits did not affect the voltage dependence or kinetic properties of Kv4.3 (126). Co-expression of Kv $\beta$ 3 and Kv4.3 in a cell line also resulted in an increase in current density in addition to slowing of reactivation and a shift in voltage dependence of inactivation in a hyperpolarising direction (127). The Kv $\beta$ -subunits can also interact with other Kv $\alpha$ -subunits including the Kv1 subunits. (96).

There is very little evidence examining the physiological role of Kv $\beta$ -subunits in the remodelling of  $I_{TO}$  in cardiac disease and none looking at the possible modulation of these

subunits by drugs or the adrenergic system. In one study of gene expression comparing patients with valvular heart disease in AF or SR, Kv $\beta$ 1 was found to be upregulated but Kv4.3 downregulated in the AF patients (122). This study identified significant changes in at least 12 ion channel related genes and there are likely to be complex interactions between these changes, not all of which necessarily have a functional significance. It remains a possibility, however, that changes in the expression of Kv $\beta$  subunits could have a functional impact on I<sub>TO</sub> and altered expression of this subunit may contribute to any change in I<sub>TO</sub> found in association with chronic  $\beta$ -blockade.

#### 1.4.2.3 KChAP

The *Kv channel-associated protein*, KChAP, is another cytoplasmic accessory protein about which there is limited information. It is a member of the protein inhibitor of the activated STAT family of proteins which can interact with a variety of transcription factors and play a role in programmed cell death. (96;97). Originally it was described in rats, with the mRNA detected in a variety of tissues including the heart (128). When expressed in cell lines, KChAP interacts transiently with the amino termini of Kv $\alpha$ -subunits (1.x, 2.1 and 4.3) and increases their expression without changing the channel gating or kinetics, suggesting it is a true chaperone. KChAP has also been shown to interact with Kv $\beta$  subunits (129).

The functional role of KChAP in human hearts is currently unknown but it is possible that it may have a functional role in the modulation of I<sub>TO</sub>.

#### 1.4.2.4 minK and MiRPs

The KCNE1-5 genes encode a group of five small proteins with a single transmembrane domain that associate with various K<sup>+</sup> channels. The first protein to be identified was minK (KCNE1) initially thought to be *minimal* protein to form a K<sup>+</sup> channel which associates with KvLQT1 (to form I<sub>KS</sub>) in expression systems and affects current density and gating kinetics (130). It has also been shown to associate with various other Kv $\alpha$ -subunits in expression systems including hERG1 and Kv4.3 although the functional significance of these interactions is unclear (130). When expressed with Kv4.3 in cell lines there is an increase in Kv4.3 current density with no change in the IV relationship. There is also significant slowing of the current kinetics (127). Different mutations in human KCNE1 result in different types of long QT syndrome (LQTS) including Jervell Lange-Neilson and Romano-Ward syndromes, therefore, it does have a functionally important

role in the human heart (97;130;131). MinK mRNA has also been shown to be upregulated in patients with AF and valvular heart disease (122) although this does not clearly correlate with a change in ion current.

The other proteins encoded by KCNE 2-5 are known as the *minK* related peptides (MiRPs 1-4). Originally thought to form part of a functional hERG channel, MiRP1 has subsequently been shown to associate with various  $Kv\alpha$ -subunits in expression systems and modify their properties and/or cell surface expression (130). Co-expression of MiRP1 with Kv4.3 in a cell line results in increased current density with no change in the IV relationship and modest slowing of rate of inactivation (127). Similarly to KCNE1 (minK), mutations in KCNE2 are also associated with forms of LQTS and, therefore, this gene does appear to have a functionally important role in the human heart (97;130). Mutations in KCNE2 have also been found in cases of familial AF although it is unclear whether the expression of this gene is associated with functional ion current remodelling in AF (131).

The main physiological output of both minK and MiRP1 appears to be to the delayed rectifier currents. Although they have the potential to modify Kv4.3 and hence  $I_{TO}$ , it is unclear whether this has any functional significance.

#### **1.4.2.5 Other accessory proteins**

Frequenin, also known as NCS-1 (neuronal calcium sensor protein-1), belongs to the same superfamily as the KChIP proteins. The protein is expressed in adult mouse ventricles and co-immunoprecipitates with Kv4.3. When expressed with Kv4.2 or 4.3 in an expression system, it increases the current density and decreases the rate of inactivation. It is also associated with increased expression of Kv4.3 at the cell membrane (132). One study has showed very low expression of mRNA in human heart tissue compared to other tissues and, like many of the accessory proteins, its physiological role remains unclear (133).

DPP6, also known as DPPX, belongs to a family of non-classical serine proteases although it has no enzyme activity itself. It is an integral membrane protein which has been detected in the human heart (97;134). When it is expressed in cell lines along with Kv4.3 and KChIP2, it results in a current which resembles human ventricular  $I_{TO}$  more closely than the current generated by any other combination of these proteins. When DPP6 is expressed with Kv4.3, it increases current amplitude but also affects inactivation and reactivation kinetics and voltage dependency (134). DPP6 is thought to enhance

trafficking of Kv4.3 to the cell membrane (135). There is as yet no evidence to link it to changes in  $I_{TO}$  remodelling in cardiac disease.

### 1.4.3 $I_{K1}$ pore-forming proteins

In addition to the  $Kv\alpha$ -subunits family, other  $K^+$  channel, pore-forming proteins have been identified. The  $Kir\alpha$ -subunits are a family of pore-forming proteins encoded by the KCNJ1-15 genes. They have two transmembrane domains which are homologous to the S5 and S6 domains of the Kv channels and one P loop with a signature G-Y-G sequence that confers  $K^+$  selectivity to the channel (see figure 1.4A) (62;64;97). Like  $Kv\alpha$ -subunits,  $Kir\alpha$ -subunits assemble as tetramers to form functional channels.

When the KCNJ genes are expressed in cell lines they are found to conduct strongly inwardly rectifying currents and it is, therefore, thought that this family encode the proteins responsible for  $I_{K1}$ . The properties of the Kir2  $\alpha$ -subunits, in particular Kir2.1 (originally called IRK-1), most closely match the properties of endogenous  $I_{K1}$  (62;97). AODNs against Kir2.1 mRNA have been shown to significantly reduce  $I_{K1}$  in rats but not eliminate it, suggesting that other  $\alpha$ -subunits may contribute to  $I_{K1}$  (136). This has been further supported by a study looking at the barium sensitivity of Kir2 channels which found that heteromeric Kir2 channels more closely resemble native  $I_{K1}$  than homomeric channels (68). The importance of heteromeric complexes to the formation of functional  $I_{K1}$  may contribute to the varying severity of Andersens's syndrome in which Kir2.1 mutations can result in a range of cardiac pathologies ranging from asymptomatic LQTS, through to lethal ventricular arrhythmias (64).

There are three Kir2 channels which are expressed in the human heart (Kir1-3). Kir2.1 is more highly expressed in the ventricles than the atria and Kir2.2 and 2.3 are more highly expressed in the atria (137). This may help explain the variation in  $I_{K1}$  current density between the atria and ventricles although the abundance of these ion channels relative to each other is not known.

There are few studies that have looked for altered expression of Kir2 subunits in non-familial cardiac disease as a possible explanation for altered  $I_{K1}$  current density. In one study of human AF, Kir2.1 mRNA was shown to be upregulated in association with increased  $I_{K1}$  (51). In a rabbit model of heart failure ventricular Kir2.1mRNA was downregulated in conjunction with a decrease in  $I_{K1}$ (138). In contrast, a human study of

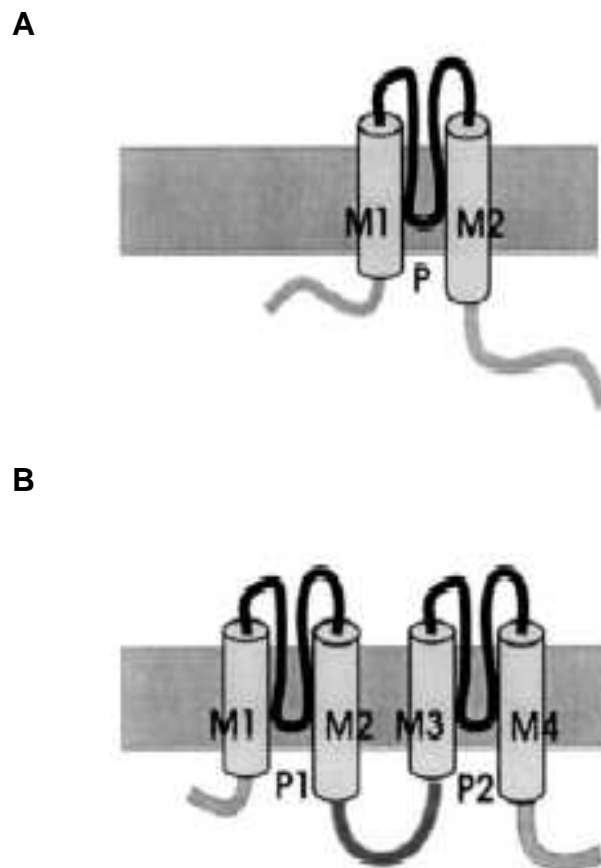


**Figure 1-4** Schematic diagram of Kir2 channel with two transmembrane domains (M1 and 2) and P loop (A). Schematic diagram of TWIK-1 with four transmembrane domains (M1-4) and two P loops is shown in B. Modified (98).

ion channel expression in heart failure did not find any change in ventricular Kir2.1 mRNA expression when they had previously detected a reduction in  $I_{K1}$  current density (115). They did not examine Kir2.1 protein expression or look at the expression of other Kir2.1 subunits. This lack of change in ventricular Kir2.1 mRNA expression in human heart failure was supported by another study which also showed no change in Kir2.2, 2.3 or in TWIK-1 mRNA (137).

Another family of potassium pore-forming subunits has been identified. These proteins have four transmembrane domains and two pore regions and are known as 2P or  $K_{2P}$  channels (see figure 1-4B). TWIK-1 (KCNK1) is a member of a large family of these 2P channels that forms homodimers with four P domains. It is a weak inward rectifier. The TWIK channels have a wide tissue distribution and TWIK-1 is expressed strongly in the heart with higher expression in the ventricles than atria (137;139). When it is expressed in cell lines, TWIK-1 generates a time independent current which is blocked by barium (139). It does not mimic the rectification profile of  $I_{K1}$  and it is unclear whether TWIK-1 does contribute to  $I_{K1}$  or whether it contributes to background  $K^+$  membrane conductance (64;139).

There is evidence that modification of Kir2.1 can influence  $I_{K1}$  current density but whether the adrenergic system can alter the expression of Kir2.1 is unknown. If chronic  $\beta$ -blockade results in a change in atrial  $I_{K1}$ , the altered expression of Kir2.1 and possibly other pore-forming proteins including Kir2.2, 2.3 and perhaps even TWIK-1 could be responsible.

#### **1.4.4 Kv1.5: the pore forming channel for $I_{KUR}$**

The Kv1  $\alpha$ -subunits were the first of the voltage-gated,  $K^+$  channel, pore-forming proteins originally cloned from the Shaker locus in *Drosophila* (97). Ion channels related to the Kv1 Shaker family have been cloned from human and animal hearts and found to conduct currents with similar activation and inactivation profiles to  $I_{KUR}$  when expressed in cell lines (90;94). Of these proteins, Kv1.5 has the most similar pharmacological profile to  $I_{KUR}$ . Further evidence to support Kv1.5 as the molecular correlate of  $I_{KUR}$  comes from the use of AODNs to Kv1.5 which have been shown to attenuate  $I_{KUR}$  in isolated human atrial myocytes (140). Kv1.5 mRNA has also been shown to be very highly expressed in human atria compared to the ventricles, a pattern which fits with the atrial specific nature of  $I_{KUR}$ . In chronic AF, Kv1.5 protein and mRNA has been shown to be reduced, which is thought to explain the reduction in  $I_{KUR}$  current density (12;141). Interestingly, a mutation in

Kv1.5 has been identified in a familial case of AF. Expression of this mutation results in a loss of functional protein and  $I_{KUR}$ , along with prolongation of the APD and potentially pro-arrhythmic, early after-depolarisations (142). It is unclear whether any accessory proteins associate with Kv1.5 and modify  $I_{KUR}$ .

While the other delayed rectifier currents  $I_{KR}$  and  $I_{KS}$  have not been consistently detected in human atrial myocytes, the pore forming proteins thought to be responsible for these currents have been. The KCNH2 gene forms part of an additional subfamily of the Kva genes and encodes hERG1, thought to be the pore-forming protein responsible for  $I_{KR}$  (86;97). The accessory protein MirP1 has been shown to interact with hERG and modify its function (86;97). Although hERG1 mRNA and protein are expressed in human atria their expression is much higher in the ventricles (143). As with KCNQ1, the gene encoding  $I_{KS}$ , mutations in KCNH2 are associated with inherited LQTS in which patients are prone to ventricular arrhythmias (97). The functional roles of  $I_{KR}$  and  $I_{KS}$  in atrial repolarisation remain unclear, however, there are mutations in KCNQ1 which have been linked to familial AF (144). Remodelling of both KCNH2 and KCNQ1 in AF has been reported in some, but not all, studies although the functional significance of this is unclear as there is no corresponding current data (51).

Initial evidence has not suggested that  $I_{KUR}$  is remodelled by chronic  $\beta$ -blockade but this has not been examined in a large prospective study (29). Given the evidence that Kv1.5 expression directly determines the density of  $I_{KUR}$ , if this current were altered by chronic  $\beta$ -blockade, a reduction in Kv1.5 expression would be a possible explanation. No studies have examined the effects of  $\beta$ -adrenergic modulation of Kv1.5. Due to the difficulties in recording atrial  $I_{KR}$  and  $I_{KS}$  the physiological effects of any change in the expression of their pore-forming proteins by chronic  $\beta$ -blockade would be uncertain.

## 1.5 Hypothesis and Aims

The hypothesis of this thesis is that the potentially anti-arrhythmic prolongation of human atrial cell action potentials by  $\beta$ -adrenoceptor antagonist therapy involves altered density, time and voltage dependency of the  $K^+$  currents  $I_{TO}$  and  $I_{K1}$ , associated with changes in atrial tissue levels of the underlying  $K^+$  channel pore-forming and accessory proteins.

The aims of the thesis are:

1. To measure density, time and voltage dependency of  $I_{TO}$  in isolated human atrial myocytes using the whole cell patch clamp technique. These variables would be compared in cells from patients taking or not taking  $\beta$ -blockers, as part of a prospective study.
2. To measure the density of  $I_{KI}$  and  $I_{KUR}$  in isolated human atrial myocytes and compare these variables in cells from patients taking or not taking  $\beta$ -blockers as part of a prospective study.
3. To measure the atrial mRNA levels of pore-forming and accessory ion channel proteins that contribute to the various  $K^+$  current characteristics which are altered in association with chronic  $\beta$ -blockade, by using real time RT-PCR. The levels of ion channel mRNA would be expressed relative to housekeeping genes and compared in tissue from patients taking or not taking  $\beta$ -blockers.
4. To measure the atrial tissue levels of pore-forming and accessory ion channel proteins that contribute to the various  $K^+$  current characteristics which are altered in association with chronic  $\beta$ -blockade, by using Western blotting. The levels of ion channel proteins would be expressed relative to a control protein and compared in tissue from patients taking or not taking  $\beta$ -blockers.

## **CHAPTER 2**

# **EFFECTS OF CHRONIC $\beta$ -BLOCKADE ON HUMAN ATRIAL REPOLARISING POTASSIUM CURRENTS.**

## 2.1 Introduction

The transient outward potassium current  $I_{TO}$  is mainly responsible for early cardiac repolarisation. The atrial specific, ultra-rapid, delayed rectifier current  $I_{KUR}$  and the outward component of the inwardly rectifying current  $I_{K1}$  contribute to late repolarisation. Changes in any or all of these currents therefore have the potential to alter the atrial action potential. Prolongation of atrial APD may in turn have anti-arrhythmic effect in preventing atrial fibrillation, the most common cardiac arrhythmia.

$\beta$ -blockers are amongst the most widely used cardiac drugs for conditions including angina, myocardial infarction, hypertension and heart failure. Although commonly used in atrial fibrillation to control ventricular rate, they are also known to have an anti-arrhythmic action in preventing recurrence of this arrhythmia (19). Several studies have shown that chronic use of  $\beta$ -blockers is associated with prolongation of atrial APD, an effect that may partially explain the anti-arrhythmic action of these drugs (28;29).

The mechanisms underlying the prolongation of atrial APD by chronic  $\beta$ -blockade are unclear. One study has suggested this may be due to a reduction in  $I_{TO}$  density but it is not known whether other properties of the current are affected (29). A reduction in  $I_{TO}$  density at a given voltage and/or stimulation rate may reflect changes in the voltage dependency of the current or its recovery from inactivation. A reduction in the contribution of  $I_{TO}$  to early repolarisation may occur either because the current density is reduced or because it inactivates more rapidly. Determining the effects of chronic  $\beta$ -blockade on the current characteristics of  $I_{TO}$  may help to clarify the contribution of any current change to APD prolongation and may give some insight into the mechanism by which these current changes occur.

The effects of chronic  $\beta$ -blockade on  $I_{KUR}$  and  $I_{K1}$  current densities are unclear. One study has suggested  $I_{KUR}$  may not be affected by chronic  $\beta$ -blockade and  $I_{K1}$  may be reduced but there are very limited data to support this (29).

## 2.2 Aims

The particular aims of the experiments described in this chapter were:

- To compare  $I_{TO}$  density in isolated human atrial myocytes from patients treated or not treated with  $\beta$ -blockers.
- To establish whether any patient characteristics other than chronic  $\beta$ -blockade may be influencing  $I_{TO}$  density.
- To test the potential effects of phrixotoxin block of  $I_{TO}$  in human atrial myocytes with a view to trying to mimic any reduction in  $I_{TO}$  density associated with chronic  $\beta$ -blockade and measure the resulting change in atrial APD in cells from non  $\beta$ -blocked patients.
- To compare the voltage dependency, time dependent inactivation, reactivation and rate dependence of  $I_{TO}$  in cells from patients treated or not treated with  $\beta$ -blockers.
- To assess  $I_{KSUS}$  block by low dose 4-AP to see whether this could be used as a technique for isolating  $I_{TO}$  from  $I_{KSUS}$ .
- To compare  $I_{KSUS}$  density in isolated human atrial myocytes from patients treated or not treated with  $\beta$ -blockers.
- To compare  $I_{K1}$  density using barium subtraction in isolated human atrial myocytes from patients treated or not treated with  $\beta$ -blockers.

## 2.3 Methods

### 2.3.1 Principles of whole cell patch clamping

The whole cell patch clamp technique is an adaptation of technique originally described by Neher and Sakmann to measure ion currents within living cells (145). Using this technique, a glass micropipette containing an “internal” electrolyte solution and silver chloride wire is gently lowered onto the surface of an isolated cardiac myocyte maintained in an “external” electrolyte solution. Using gentle suction, the pipette attaches to the cell and forms a tight, high resistance “seal” with a patch of membrane known as a gigaseal. This allows the flow of ions through channels in the patch of cell

membrane into the interior of the micropipette where they are converted into electrical current at the surface of the electrode wire by the reversible conversion of  $\text{Cl}^- + \text{Ag} \leftrightarrow \text{AgCl} + \text{e}^-$ . The patch of membrane can then be ruptured by further application of gentle suction allowing low resistance access to the whole cell and enables the measurement of ion currents flowing across the whole cell membrane. This is known as the whole cell configuration. Measurements of these ion currents can be made using a single electrode voltage clamp technique. Using this technique, the cell membrane potential is controlled by use of an amplifier which both measures the membrane potential and can change it to a preset command potential by injection of the necessary amount of charge. The magnitude of this charge represents the size of the current that flows at the command potential and is measured using the same electrode. A simplified diagram of this circuit is shown in figure 2-1. The duration and rate at which the cell membrane potential is changed can also be controlled using this technique which allows different properties of ion currents to be studied.

### **2.3.2 Obtaining atrial tissue**

In these experiments ion currents were measured in human, isolated, right atrial appendage cells. These cells were isolated from right atrial appendage tissue obtained from adult patients undergoing cardiac surgery for coronary artery bypass grafting and/or valve replacement. During these operations, the right atrial appendage and aorta are cannulated in order to allow the patients circulating blood volume to be diverted away from the heart via a bypass machine. Tissue can be excised from the right atrial appendage in order to gain access for the bypass cannula without detriment to the patient and it was this tissue that was used in all the experiments described in this thesis. All the procedures followed were approved by the institutional research ethics committee and informed consent was obtained from each patient by either myself, Professor Rankin or Drs Cormack, Jackson, Motherwell, Myles or Nisbet using the form shown in figure 2-2. The investigation conformed to the principles outlined in the Declaration of Helsinki (146).

No patients with a documented history of AF were included in this study. All patients were in sinus rhythm the day before surgery as confirmed by their pre-operative ECG. All the  $\beta$ -blocked patients were taking  $\beta_1$ -selective blockers for  $\geq 4$  weeks prior to surgery unless otherwise stated. All patient characteristics were obtained from case

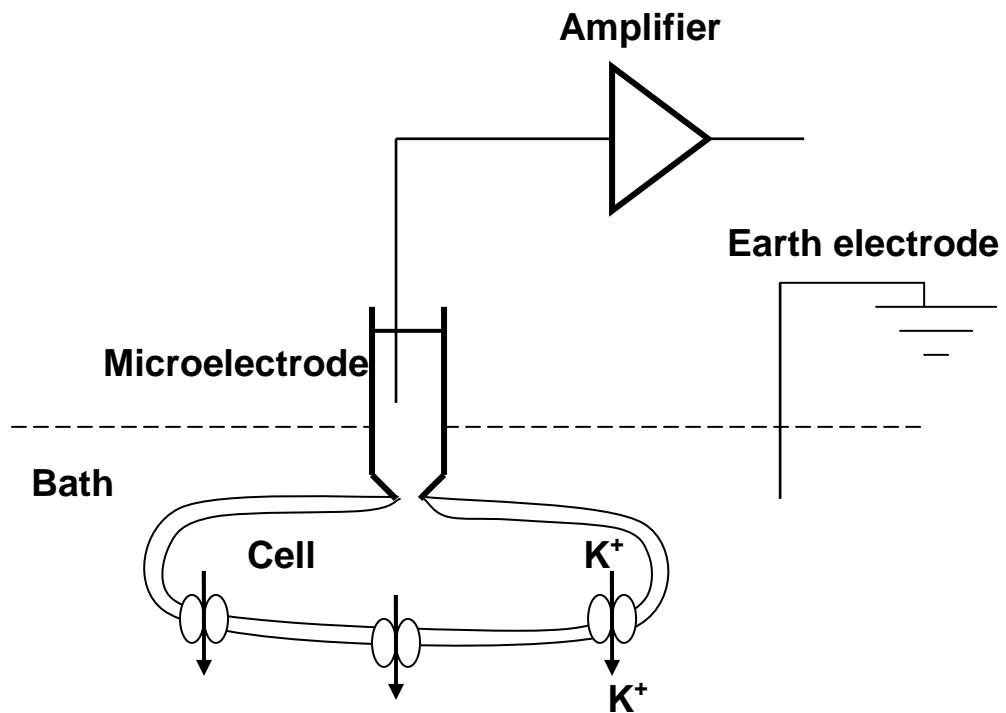


**Figure 2-1** Whole cell patch clamping of an isolated atrial myocyte in a bath of salt solution. The flow of ion currents e.g.  $K^+$  currents through ion channels in the cell membrane can be controlled and detected using a microelectrode and amplifier in contact with the interior of the cell via a ruptured patch in the membrane.

**Right atrial appendage****Glasgow Royal Infirmary University N.H.S. Trust**

## PATIENT INFORMATION AND CONSENT FORM

**Title of Project:** Electrophysiological and molecular properties of isolated human cardiac myocytes.

**Summary:** You are shortly to undergo a heart operation. The reasons for this, and the type of operation to be performed, will have been discussed with you by your cardiologist and by the heart surgeon.

We are undertaking research into why some patients have abnormal heart rhythms and how these cardiac arrhythmias affect the heart cells. In order to understand the biological properties of heart cells we would like to obtain a small sample of your heart muscle.

During the operation, the surgeon routinely makes a small cut in the heart to allow the operation to proceed. Many surgeons perform this by removing a small piece of heart tissue (about the size of a pea), which would normally be discarded. Some surgeons do not routinely remove this piece of tissue, but are willing to do so, since they know that such a procedure would not do you any harm. We are asking for your consent to use this small piece of the heart to obtain heart cells for our study. Part of the tissue will be studied directly for electrical activity and then discarded, and the remainder will be deep-frozen at the hospital for future analysis of molecular activity, after which it will be destroyed. Participation in our study will not change the operation or result in additional risk or discomfort to you.

In addition, we would ask your permission to obtain details of your condition from your medical records. These details will be kept confidential and your identity will be concealed by the use of a coding system. Such information will be retained for comparison with the results of the tissue analysis, and will not be disclosed to anyone outside the hospital.

This research project will not be of direct benefit to you, but the results may help other patients in the future. If you are unwilling to take part, you are entirely at liberty to refuse permission. This would not affect your medical treatment in any way.

**Consent:**

I, (Name) .....

of (Address) .....

agree to take part in the Research Project described above.

Dr ..... has explained to me what is involved, how it might affect me and the purpose of the Research Project.

Signed ..... Date .....

Witness.....Date.....

**Figure 2-2** Example of patient consent form for obtaining right atrial tissue.

notes and stored in a database by Julie Russell and are described in the results section.

### **2.3.3 Cell isolation**

The right atrial appendage tissue was transported to the laboratory for processing within approximately 5 minutes of excision in 50 ml of oxygenated solution A (see table 2-1). Atrial myocytes were isolated enzymatically using a modification of the chunk method (147-149). Excised tissue (0.2 - 1 g) was sliced into approximately 1 mm<sup>3</sup> chunks and washed three times, for 3 minutes per wash, in Ca<sup>2+</sup>-free solution B (see table 2-1). Each wash was performed in an incubation bath at 37°C, under oxygen and shaken at 130 strokes/minutes. After the final wash, the chunks were removed from solution B and incubated in 15 ml of solution C (see table 2-1) containing protease (Type XXIV, Sigma, 4 U/ml). This solution was shaken for a further 45 minutes at 37°C under oxygen. It was then filtered through a nylon gauze filter and the chunks incubated in a similar fashion in 12 ml of solution C containing collagenase (Type 1, Worthington, 400 U/ml). The chunks were incubated for 15 minutes in this collagenase solution and then filtered again through nylon gauze. The partially digested tissue was incubated again in the collagenase solution for 15 and then 20 minutes. The filtrates of isolated atrial myocytes were collected after each of the three incubations and centrifuged at 40 g for 2 minutes. The supernatants were removed and the cells resuspended in 1ml of solution D to wash off residual enzyme. This solution was replaced with a low Ca<sup>2+</sup> solution E following repeat centrifugation (40 g, 2min) and the cell suspension stored in Petri dishes for up to 8 hours at room temperature.

### **2.3.4 Measuring currents by whole cell patch clamping**

#### **2.3.4.1 Preparing the patch clamp equipment**

The arrangement of equipment can be seen in the photograph in figure 2-3. The microscope, perfusion chamber, microelectrodes and micromanipulator were mounted on an air table in order to minimise vibration and were all earthed to eliminate electrical noise. The reservoirs for external solution were mounted above the level of the perfusion chamber on the wire cage. A suction bottle was located on the floor beneath the perfusion chamber to remove external solution. The amplifier, oscilloscope and

	A	B	C	D	E
NaCl	150	120	120		130
KCl	5.4	5.4	5.4	40	4
KOH				70	
KH <sub>2</sub> PO <sub>4</sub>				20	
MgCl <sub>2</sub>	1.2			3	1
MgSO <sub>4</sub>		5	5		
CaCl <sub>2</sub>	1		0.05		0.2
EGTA				0.5	
Glucose	10	20	20	10	10
L-Glutamic acid				50	
HEPES	5	10	10	10	10
Pyruvate		5	5		
Nitrilotriacetic acid		5			
Taurine		20	20	20	
pH with HCl	pH 7.4				
pH with NaOH		pH 6.95	pH 6.95		pH 7.35
pH with KOH				pH 7.2	

**Table 2-1** Composition of solutions for cell isolation. All concentrations are expressed in mM. All chemicals were obtained from Sigma except for MgCl<sub>2</sub>, MgSO<sub>4</sub> and KH<sub>2</sub>PO<sub>4</sub> which were obtained from AnalaR BDH.

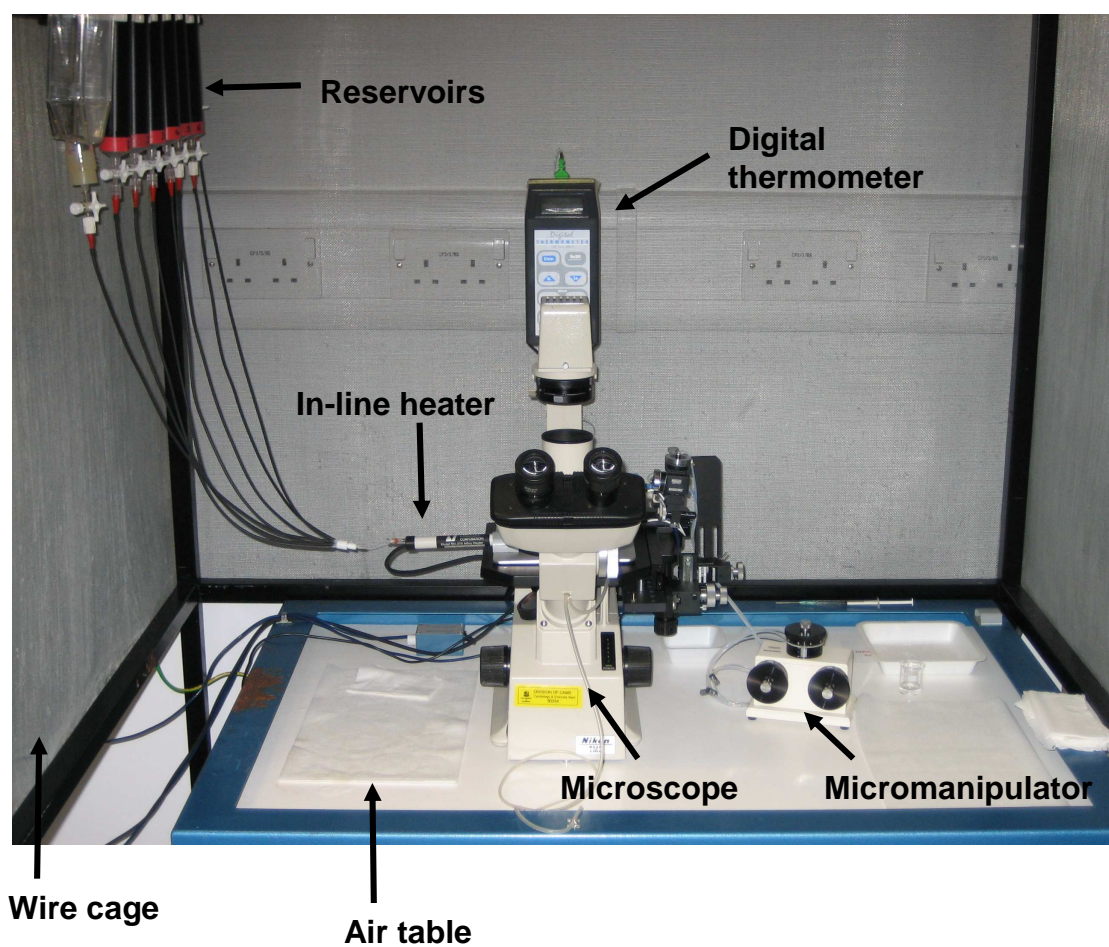


**Figure 2-3** Picture of patch clamp equipment. The perfusion chamber and microelectrodes were located on the microscope stage.

computer, programmed to generate stimulus protocols and acquire data, were all placed in a tower beside the vibration table.

#### **2.3.4.2 Perfusion chamber**

Once the myocytes were isolated, a small aliquot of cell suspension was placed in a 200  $\mu$ l perfusion chamber (RC-24E fast exchange perfusion chamber, Warner) mounted on the stage of a microscope (Nikon TMS). The myocytes were allowed to adhere to a glass coverslip that formed the bottom of well 1 of the perfusion chamber illustrated in figure 2-4. External solution (see table 2-2) flowed into well 1 from a reservoir mounted at a higher level than the perfusion chamber at a rate of approximately 2 ml/minute. Before the external solution entered the well it flowed through an in-line heater (Warner Instrument Corporation Model SH-27A Inline Heater) which heated the solution to 36°C. The temperature was recorded using a temperature probe placed in well 1. Well 1 connected to well 2 by means of a small channel which allowed equalisation of the volumes of solution between the two wells. Well 2 also connected to the suction device that allowed a constant flow of external solution through the perfusion chamber. Well 3 was filled with a 3 M KCl solution into which the earth electrode was placed. The electrical circuit between the earth electrode and the recording electrode in well 1 was completed using an agar bridge linking wells 2 and 3.

The role of the agar bridge was to keep the Cl<sup>-</sup> concentration around the earth electrode constant, as fluctuations in the concentration of Cl<sup>-</sup> between wells 1 and 3 would have resulted in an offset voltage between the earth and recording electrode. The agar bridges were made by heating short lengths of borosilicate glass capillaries without inner filaments (Clark electromedical instruments) into “U” shapes that were filled by emersion in agar solution and then stored in the 3 M KCl solution.

##### **2.3.4.2.1 Microelectrodes**

The micropipettes were made from 15 cm long, 1.5 mm outer diameter x 1.17 mm inner diameter, borosilicate glass capillaries with inner filaments (Clark electromedical instruments). These were cut in two lengths, 7 cm long, using a diamond cutter and each length used to make two microelectrodes using a vertical puller (Narishige PP-83). Each microelectrode was pulled in two steps, the first at 12 A and the second at 9 A.

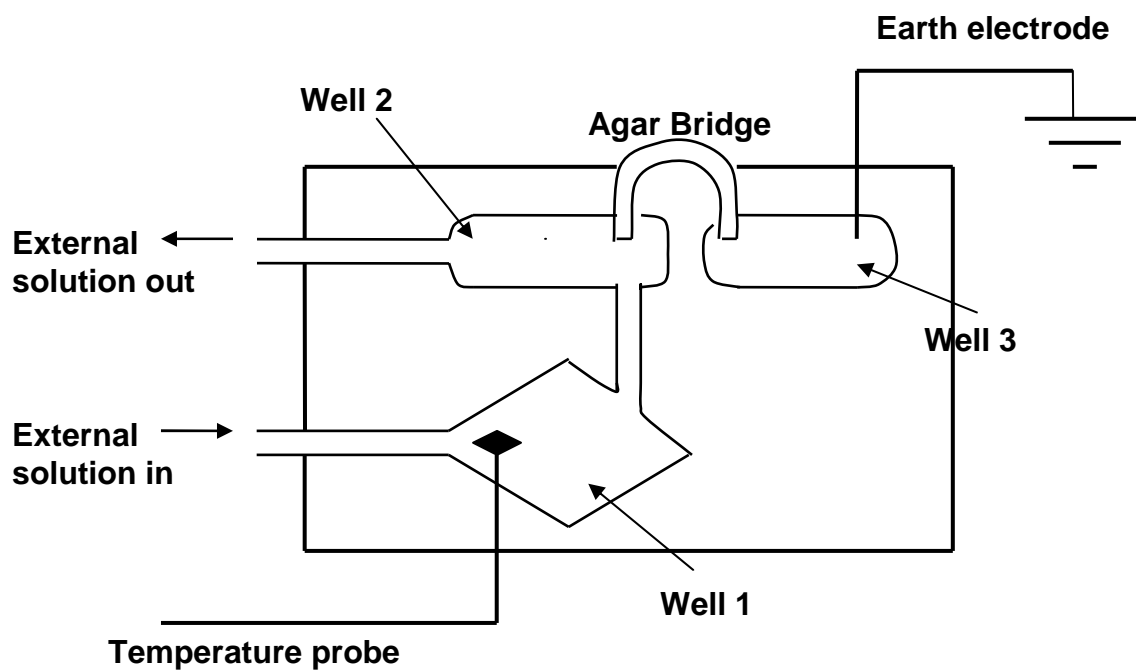


**Figure 2-4** Diagram of perfusion chamber. See text for details of components.

	External Solution	Internal Solution
NaCl	130	
KCl	4	20
MgCl <sub>2</sub>	1	1
CaCl <sub>2</sub>	2	
CdCl <sub>2</sub>	0.2	
Glucose	10	
HEPES	10	5
EGTA		0.15
L-aspartic acid		110
Na <sub>2</sub> ATP		4
Na <sub>2</sub> GTP		0.4
pH with NaOH	pH 7.35	
pH with KOH		pH 7.3

**Table 2-2** Composition of external and internal solutions. All concentrations are expressed in mM. All chemicals were obtained from Sigma except for MgCl<sub>2</sub> which was obtained from AnalaR BDH.

The tip of each microelectrode was then fire polished to remove any imperfections that might damage the cell membrane and prevent the formation of the high resistance seal. The micropipette was then back-filled with an internal electrolyte solution with the same osmolarity as the cytoplasm of the cell (see table 2-2). A silver-chloride wire was placed into the micropipette and connected to the amplifier. Before each experiment, both this wire and the wire used as the earth electrode, were cleaned and chlorinated using electrolysis and a chloride containing solution.

The electrical resistance of a number of microelectrodes was measured to enable adjustments to be made in the pulling process. This enabled the microelectrode resistance to be kept low relative to the cell seal resistance and, therefore, minimise the leakage current when patching the cells. The resistance was measured before patching a cell by applying a 1 mV voltage pulse once the electrode was lowered into the external solution. The current generated across the electrode tip by the voltage step was measured and the resistance calculated using Ohms Law ( $R=V/I$ ). The median microelectrode resistance was 2.8 M $\Omega$  (n=138).

#### **2.3.4.3 The use of amplifier to record currents and adjust for errors in the voltage clamp mode**

An Axopatch-1D amplifier (Axon Instruments) was used in voltage clamp mode in conjunction with the software programme WinWCP (J Dempster, Strathclyde University) to record ion currents. The cell membrane potential was measured and fixed to a preset command by injection of current using a single microelectrode in a whole cell patch clamp configuration. The same microelectrode was used to measure the resulting currents across the cell membrane activated at the preset membrane potential. Using this technique, there are various sources of error which can affect the current recordings and can be compensated for either prior to, or during, recordings using the amplifier.

Once the cells were placed in the perfusion chamber and superfused with heated external solution the microelectrode was lowered carefully into the external solution. At this point various offset potentials occur, including a current which flows between the internal and external solutions, that contain different concentrations of K<sup>+</sup>, known as the liquid junction potential. Adjusting the "junction null" control on the amplifier

compensates for all these effects. However, when the electrode is in contact with the inside of the cell and the cytoplasm has dialysed with the pipette solution, the liquid junction potential no longer exists, as the internal solution of the electrode is the same as the interior of the cell. This means that the voltage measured by the electrode will differ from the true voltage by the size of the liquid junction potential. To correct for this the electrode is nulled "a priori" at a predetermined voltage that is the same size but opposite polarity to that of the liquid junction potential (150). Previous work in our lab has established that the liquid junction potential correction when using the external solution and internal solution was  $-7$  mV.

Following adjustment of the "junction null" a square voltage pulse was applied from a holding potential of zero to  $-1$  mV in order to measure the electrode resistance. The electrode was then lowered onto the cell membrane of a single, elongated, striated myocyte using a micromanipulator (Narishige) and gentle suction applied in order to obtain a gigaseal. At this point, a second voltage pulse was applied, from a holding potential of  $-40$  with a step to  $-50$  mV, in order to visualise the capacity transients of the electrode which could then be nullified with the "fast magnitude" control on the amplifier. Further gentle suction was then applied in order to rupture the patch of cell membrane at the tip of the electrode and gain access to the interior of the cell. This generates further larger currents transients as the voltage pulse charges the cell membrane capacitance. These were compensated for by adjusting the "whole cell capacitance" and "series resistance" controls on the amplitude. The final setting on the whole cell capacitance control is a measure of the capacitance of the cell which is proportional to its surface area and this was recorded for all cells patch clamped. The final setting on the series resistance control is a measure of the combined resistance of the electrode tip and the open patch in the membrane. This resistance was kept to a minimum by ensuring only low resistance electrodes were used and only cells in which a high resistance seal was initially achieved. However, even with low series resistance, large currents can result in a significant voltage error whereby the voltage recorded by the amplifier is different from that actually occurring at the cell membrane. The voltage error was minimised by using series resistance compensation. Series resistance compensation of 64-72% was used in 75% of cells to keep the average voltage error less than 5 mV.

Once the current transients were compensated for, various voltage pulse protocols, designed using the WinWCP software, were applied in order to measure currents.

#### 2.3.4.4 Isolating currents

When the whole cell patch clamp technique is used to record currents it records the net effect of all currents flowing at a particular membrane potential rather than the individual current components. There are several methods that can be used to isolate a particular current of interest. Some voltage dependent currents have different activation and inactivation profiles and this can be exploited in order to separate individual currents. For example,  $I_{Na}$  activates and inactivates rapidly at more negative potentials than  $I_{TO}$  and  $I_{KUR}$  and, by avoiding hyperpolarising the cell to these potentials during recordings of these two currents, the effects of  $I_{Na}$  activation can be prevented. Some currents including  $I_{TO}$ ,  $I_{KUR}$  and  $I_{CaL}$  activate over a similar voltage range and, in this case, other techniques can be used to block the effects of unwanted currents. One method is to add drugs to the external solution to block particular ion currents. In these experiments cadmium chloride was added to the external solution at a concentration of 0.2 mM in order to block  $I_{CaL}$  (33).

Several methods can be used to separate  $I_{TO}$  and  $I_{KUR}$ . One is to exploit the difference in the inactivation profiles of  $I_{TO}$  and  $I_{KUR}$ .  $I_{TO}$  inactivates very quickly and  $I_{KUR}$  extremely slowly in comparison. The current trace obtained using a relatively long voltage pulse to activate both these currents will, therefore, consist of  $I_{KUR}$  at the end of the trace, “the end-pulse current”, while the peak current will consist of both  $I_{TO}$  and  $I_{KUR}$ .  $I_{TO}$  can, therefore, be represented by the peak minus the end pulse current and this was the method used to measure  $I_{TO}$  in the experiments described in this chapter. It should be considered that there are other currents that may also be activated along with  $I_{TO}$  and  $I_{KUR}$  including the other delayed rectifier currents which are more likely to have a greater impact on the end pulse current due to their slow activation. For this reason the end pulse current was labelled as  $I_{KSUS}$  (the sustained outward potassium current) which consists predominantly of  $I_{KUR}$ .

Drugs can also be used to separate  $I_{TO}$  from  $I_{KUR}$ , in particular, 4-AP, which can block both of these currents at different concentrations. The possible use of low dose 4-AP to block  $I_{KUR}$  but not  $I_{TO}$  was investigated in some preliminary experiments, the results of which are described in 2.4.9. External solution was prepared containing no 4-AP, 0.05,

0.1 or 2 mM 4-AP. Patched atrial myocytes were then perfused with these external solutions in turn, starting with the solution without 4-AP. After 90 seconds to allow the drug to equilibrate within the well, a square voltage pulse of 100 ms duration from a holding potential of -50 mV to +60 mV was applied and the resulting currents recorded.  $I_{TO}$  and  $I_{KUR}$  were measured using the end-pulse method and compared with recordings made after exposure to the various concentrations of 4-AP.

The potential use of phrixotoxins to specifically block  $I_{TO}$  in isolated human atrial myocytes was also investigated in preliminary experiments with a view to possibly using this toxin to investigate the effects of  $I_{TO}$  block on APD. Phrixotoxin-2 (PaTx2) was purchased from Calbiochem. The PaTx2 was dissolved in external solution containing 0.1% BSA and used at concentrations of 100 and 200 nM.  $I_{TO}$  was recorded using a series of square voltage pulses of 100 ms duration from -50 to +60 mV repeated at three second intervals.  $I_{TO}$  was initially recorded using external solution without PaTx2. This was then stopped by closing the tap from the reservoir of external solution and replaced with external solution containing PaTx2 from a separate reservoir.  $I_{TO}$  was continually recorded until the cell died, the seal was lost or recordings were electively stopped after a wash out period. In some cells, the PaTx2 containing external solution was replaced with external solution without PaTx2 and further recordings made after 90 seconds of the start of this wash out phase. All the cells used for these experiments were isolated from tissue from non  $\beta$ -blocked patients and experiments were carried out at 36 °C.

$I_{K1}$  was separated from other currents on the basis of its sensitivity to barium. Currents were recorded using external solution and again after 90 seconds exposure to external solution containing 0.5 mM barium chloride.  $I_{K1}$  was determined by subtracting the end pulse current recorded with barium from that recorded without barium.

### **2.3.4.5 Voltage pulse protocols**

#### **2.3.4.5.1 $I_{TO}$ and $I_{KSUS}$ activation, $I_{TO}$ voltage dependence and time dependent inactivation**

A protocol consisting of a series of square voltage pulses of 100ms duration was used to record peak activation, voltage dependent activation and time dependent inactivation of

$I_{TO}$ . This protocol along with an example of the resulting current trace is shown in figure 2-5. There was a three second interval between each pulse when the cell membrane was clamped to the holding potential of -50 mV. The first pulse was a flat pulse at the holding potential of -50 mV. Each subsequent pulse increased in 10 mV increments from -50 to +60 mV, returning to the holding potential of -50 mV at the end of the pulse.

Peak  $I_{TO}$  and peak  $I_{KSUS}$  were measured using only the step from -50 to +60 mV, as was  $I_{TO}$  time dependent inactivation.

#### 2.3.4.5.2 $I_{TO}$ voltage dependent inactivation

A protocol consisting of a series of two square voltage pulses of different durations was used to record the voltage dependence of  $I_{TO}$  inactivation. Part of this protocol is shown in figure 2-6 along with an example of a current trace. Pulse one was 1000 ms long and was immediately followed by pulse two which was 100 ms in duration. Pulse one stepped from the holding potential of -50 mV to -90 mV and pulse two from -90 to +60 mV before returning to the holding potential again. After pulse two, there was a three second interval when the cell membrane was clamped to the holding potential of -50 mV. In subsequent series of pulses, pulse one increased in 10 mV intervals from -90 to +60 mV whereas pulse two remained a constant step to +60 mV from the voltage achieved at the end of pulse one. The holding potential remained at -50 mV throughout.

#### 2.3.4.5.3 $I_{TO}$ reactivation

A protocol consisting of a series of two identical square voltage pulses was used to record reactivation of  $I_{TO}$ . This protocol is shown in figure 2-7 along with an example of a current trace. Each pulse was of 100 ms duration and stepped from -50 to +60 mV. The time interval between the end of pulse one and the start of pulse two (interpulse interval) was varied. The initial interpulse interval was 500 ms. There were then seven subsequent series of pulses in which the interpulse intervals reduced by 50 ms each time until it reached 150 ms. After this, the interpulse interval was sequentially reduced by 10 ms for a further fourteen series of pulses reaching a final interpulse interval of 10 ms. There was a three second interval between each pair of pulses when the cell membrane was clamped to the holding potential of -50 mV.

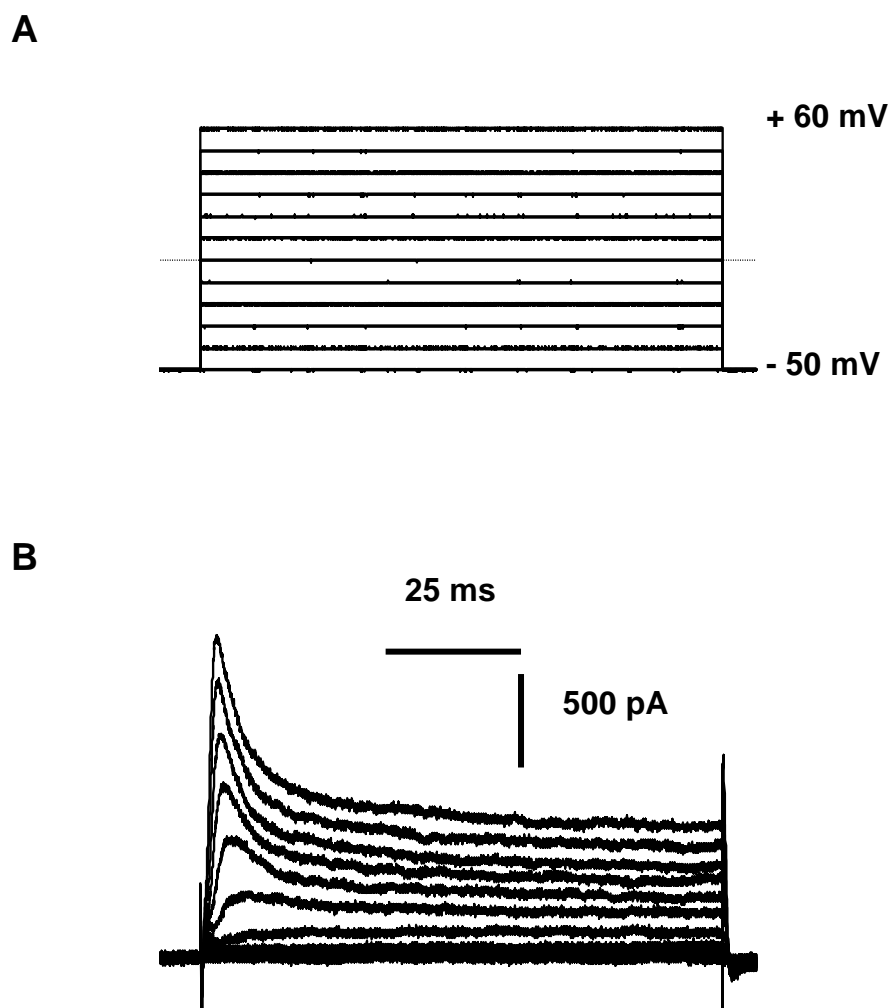


**Figure 2-5** Voltage pulse protocol for determining peak  $I_{TO}$  and  $I_{KSUS}$  activation,  $I_{TO}$  voltage dependence and time dependent inactivation (**A**). An example of the resulting current trace is shown in **B**.

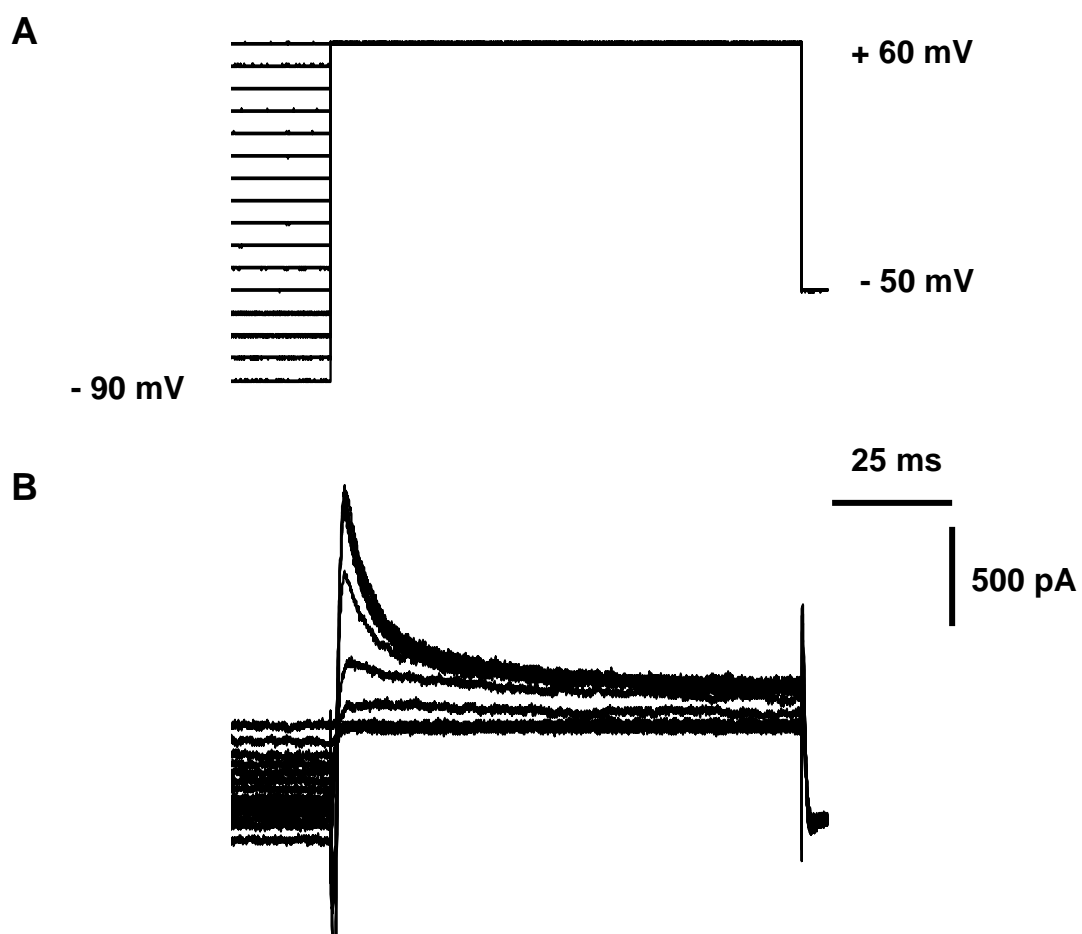


**Figure 2-6** Voltage pulse protocol for  $I_{T0}$  voltage dependent inactivation (A). An example of the resulting current trace is shown in B.

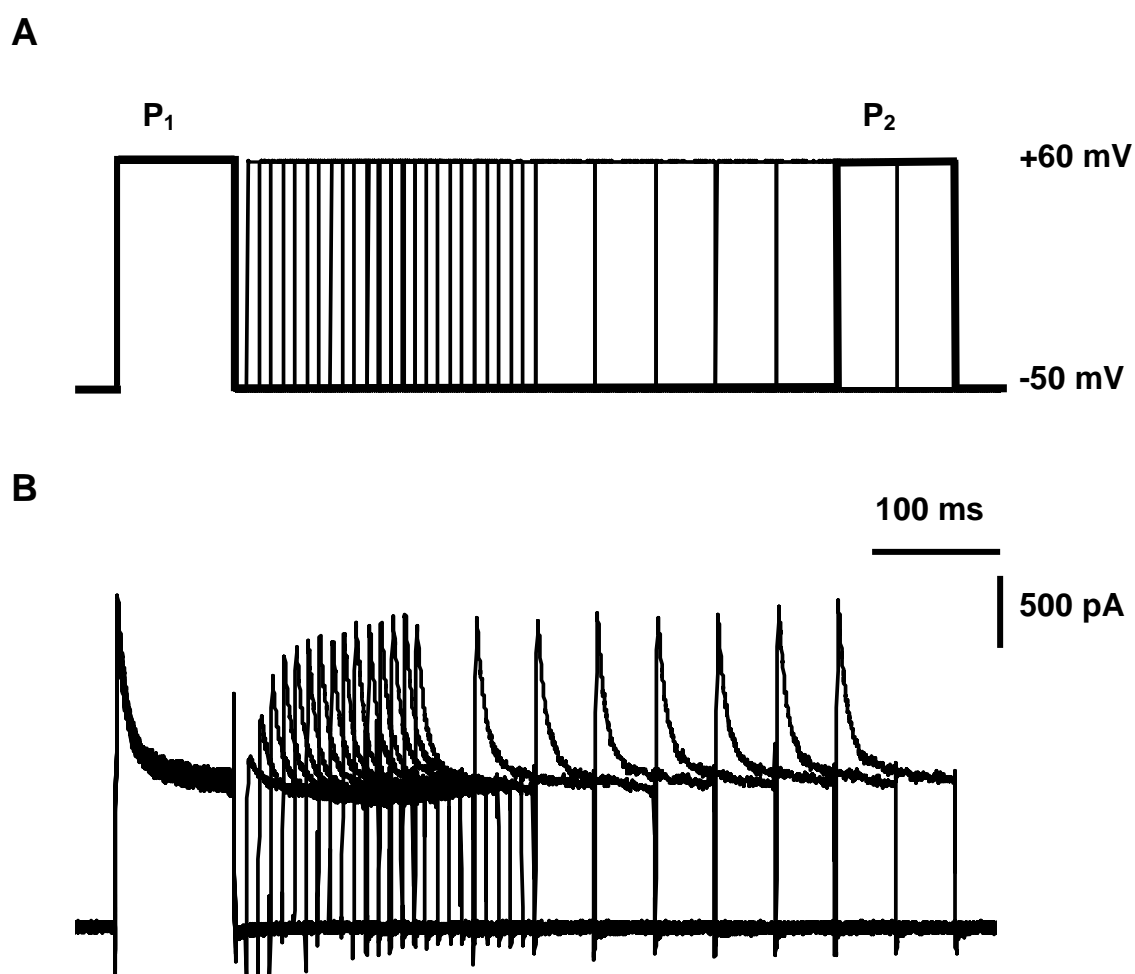


**Figure 2-7** Two pulse voltage pulse protocol for  $I_{T0}$  reactivation (A) with example of resulting current trace (B).

#### 2.3.4.5.4 $I_{TO}$ rate dependence

A protocol consisting of six trains of square voltage pulses with eight identical pulses in each train was used to record  $I_{TO}$  rate dependence. A selection of trains of pulses from this protocol is shown in figure 2-8 along with examples of current traces. Each pulse was of 100 ms duration and stepped from a holding potential of -50 mV to +60 mV before returning to the holding potential again at the end of each pulse. The interpulse intervals varied from one train to the next but, within each train of pulses, the interpulse intervals remained constant. In the first train of eight pulses the interpulse interval was 700 ms, corresponding to a stimulation rate of 75 beats/minute or frequency of 1.25 Hz. The second train of eight pulses had an interpulse interval of 300 ms (150 beats/minute, 2.5 Hz). The interpulse intervals in subsequent trains of pulses were 100, 33 and 20 ms corresponding to stimulation rates of 300, 400 and 500 beats/minute and frequencies of 5, 6.7 and 8.3 Hz respectively. A final train was then repeated at a stimulation rate of 75 beats/minute. There was a three second interval between each train of pulses when the cell membrane was clamped to the holding potential of -50 mV.

#### 2.3.4.5.5 $I_{K1}$ voltage dependent activation

A protocol consisting of a series of square voltage pulses of 500 ms duration was used to record  $I_{K1}$  voltage dependent activation. This protocol is shown in figure 2-9 with an example of the resulting current traces using external solution with and without barium. There was a three second interval between each pulse when the cell membrane was clamped to the holding potential of -50 mV. The first pulse was stepped from the holding potential of -50 mV to -120 mV and then back to the holding potential again. Each subsequent pulse increased in 10 mV increments from -120 to +60 mV returning to the holding potential of -50 mV at the end of each pulse.

### 2.3.5 Data analysis

#### 2.3.5.1 Calculating conductance and the reversal potential

Conductance ( $g$ ) was calculated from the current ( $I$ ) elicited by each voltage pulse using the equation described below.

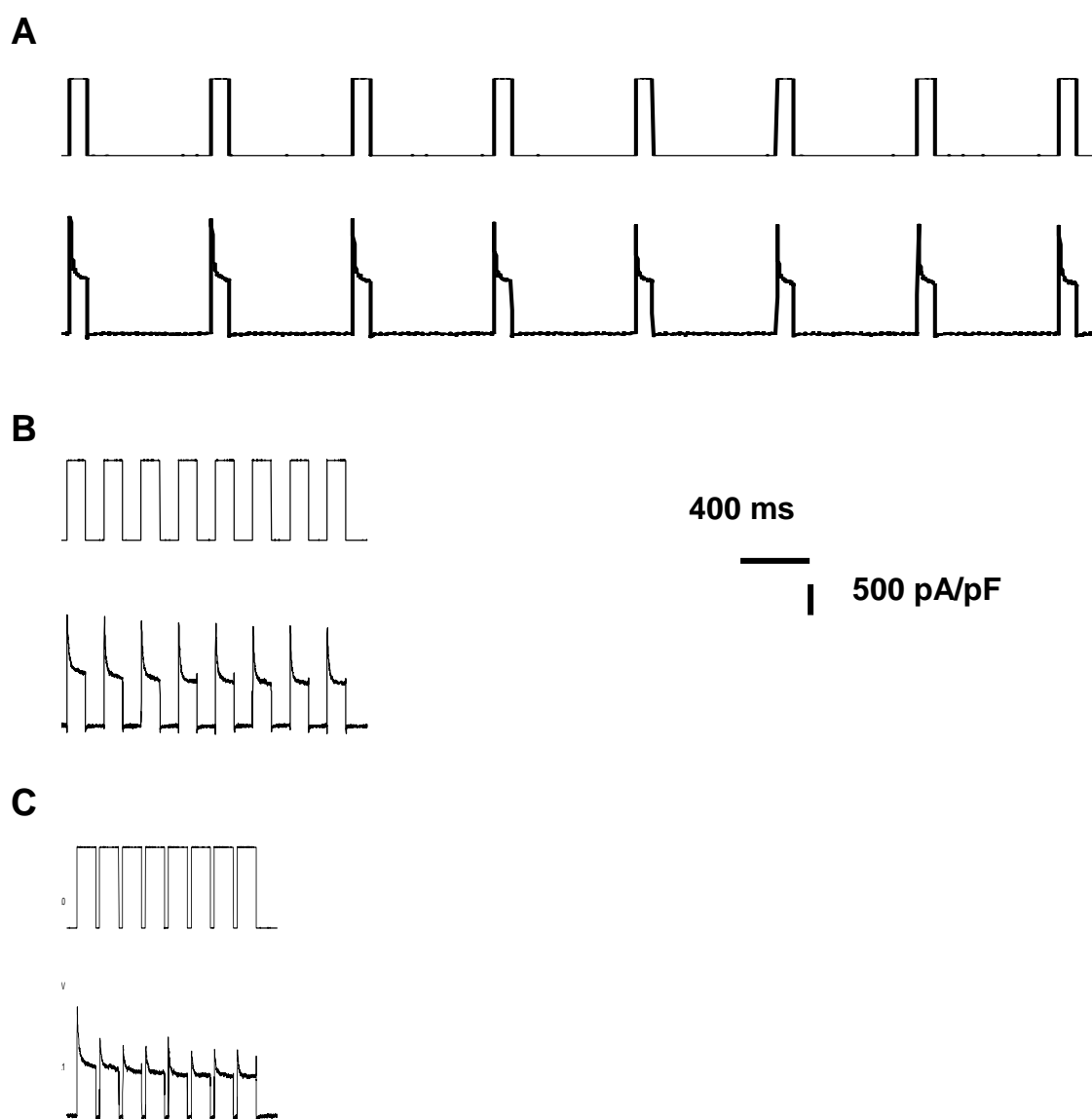


**Figure 2-8** Voltage pulse protocol for  $I_{TO}$  rate dependence at 75 (A), 300 (B) and 500 (C) beats/minute with corresponding current traces.

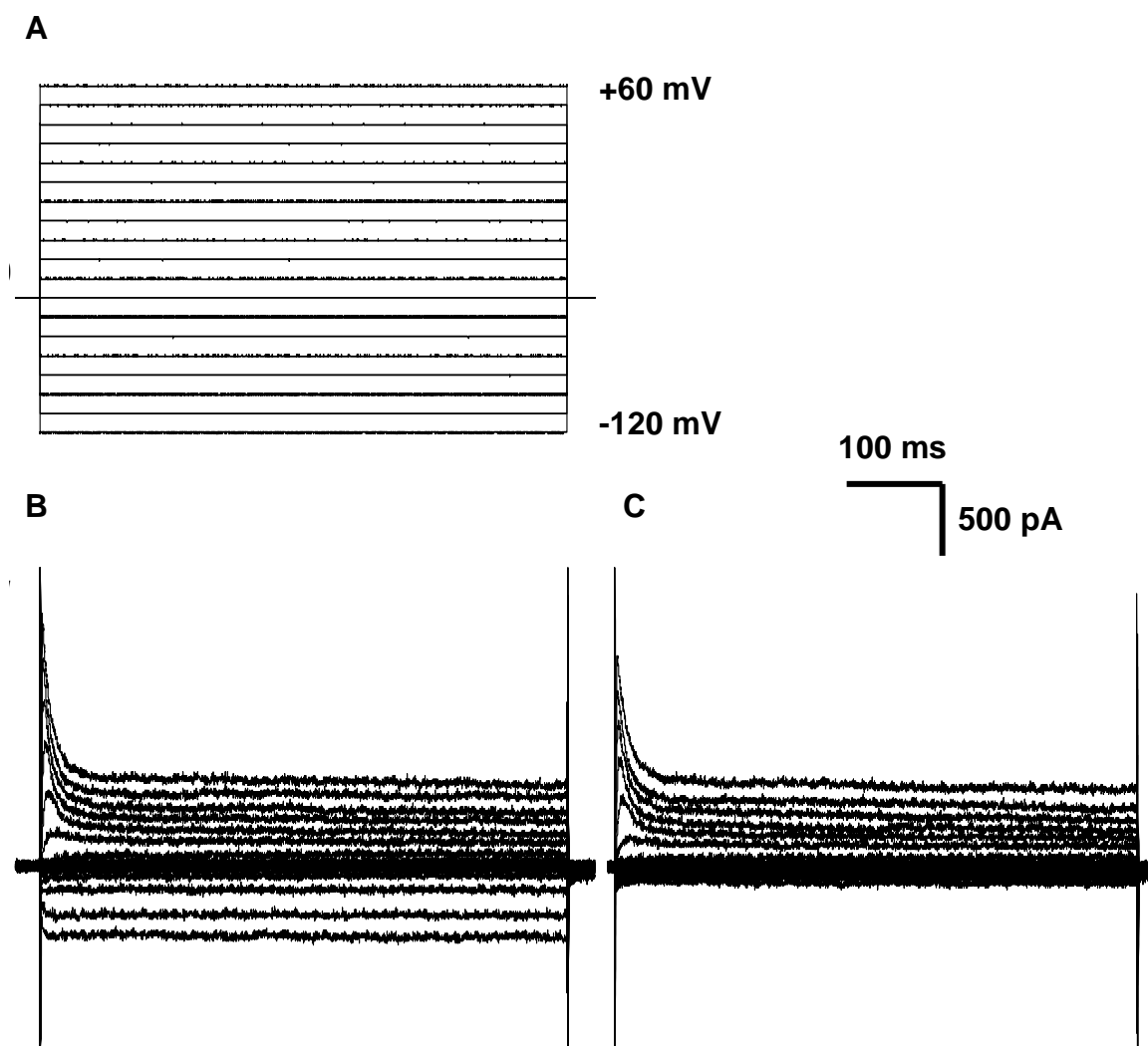


**Figure 2-9** Voltage pulse protocol for  $I_{K1}$  activation (A) with resulting current traces recorded using external solution without (B) and with (C) 0.5 mM barium chloride.

$$g = I/(V_t - V_{rev})$$

where  $V_t$  is the test potential and  $V_{rev}$  is the reversal potential or  $E_K$ .

$E_K$  was not measured but calculated from the Nernst equation using the  $K^+$  concentrations from the internal and external solutions.

$$E_K = RT/F \ln[K^+]_o/[K^+]_i$$

where  $T$  is the absolute temperature of the external solution,  $R$  is the universal gas constant and  $F$  is Faraday's constant.  $E_K$  was calculated as  $-92.7\text{mV}$ .

### 2.3.5.2 Curve fitting

All non linear regression analysis was performed using GraphPad Prism. In order to fit curves to the time course of inactivation of  $I_{TO}$ , all the data from each current trace was exported from WCP into a Microsoft Excel spreadsheet. The  $I_{TO}$  density at every time point was calculated by subtracting the end pulse current from the total outward current. The maximum  $I_{TO}$  density for each cell was termed "the peak  $I_{TO}$  density at time zero" and this data point, along all subsequent data points until the end of the voltage pulse, were exported to GraphPad Prism for curve fitting analysis.

The following equations were used for mono-exponential, bi-exponential associations, mono-exponential decay and Boltzmann curve fits.

Mono-exponential association:  $I(t) = I(1 - \exp^{-t/\tau})$

where  $I$  describes the maximum plateau of the current,  $t$  is recovery period or time and  $\tau$  is the time constant.

Bi-exponential association:  $I(t) = I_1(1 - \exp^{-t/\tau_1}) + I_2(1 - \exp^{-t/\tau_2})$

where  $\tau_1$  and  $\tau_2$  are the fast and slow time constants for the relative amplitudes of the fast and slow current components  $I_1$  and  $I_2$ .

Mono-exponential decay:  $I(t) = I_0 \exp^{-t/\tau}$

where  $I_0$  describes the starting current value,  $t$  the time and  $\tau$  the time constant.

Boltzmann curve fit for activation:  $g(t) = 1 / (1 + \exp [(V_{0.5} - V_t)/k])$

where  $V_t$  is the test potential,  $V_{0.5}$  is the voltage of half-maximal activation and  $k$  is the slope factor.

Boltzmann curve fit for inactivation:  $I(t) = 1 / (1 + \exp [(V_t - V_{0.5})/k])$

where  $V_t$  is the test potential,  $V_{0.5}$  is the voltage of half-maximal inactivation and  $k$  is the slope factor.

The goodness of fit for all curves was assessed by examining several parameters, the most important of which was whether the computer programme was able to converge on a fit. The width of the confidence intervals,  $R^2$  value and runs tests were also examined. The comparison of fits to two different equations was performed as part of the GraphPad Prism analysis programme using an F test. The equation with fewer variables was chosen as the best fitting equation unless  $p < 0.05$ .

### 2.3.5.3 Other statistical analysis

All other statistical analyses were performed using GraphPad Prism unless stated otherwise.

The distribution of  $I_{TO}$  current densities was examined visually but was also tested for the degree of deviation from a Gaussian distribution using the Kolmogorov-Smirnov test. Given the relatively small sizes of the non  $\beta$ -blocked and  $\beta$ -blocked patient groups (<100),  $p > 0.05$  was not taken to be conclusive of a Gaussian distribution but to indicate that the distribution was not inconsistent with a Gaussian distribution.

Comparisons between mean current values in each group of patients or cells were done using a Student's t-test.  $P < 0.05$  was taken to be statistically significant. Comparisons between the numbers of patients with particular characteristics in the  $\beta$ -blocked or non  $\beta$ -

blocked groups were done using a Fisher's exact t-test.  $P < 0.05$  was taken to statistically significant.

The relationship between heart rate and  $I_{TO}$  was assessed using correlation analysis and linear regression analysis was used to investigate the relationship between atenolol dose and  $I_{TO}$ .

Multiple linear regression was used to examine the association of multiple variables with  $I_{TO}$ . This was performed by Pardeep Jhund. Initially  $\beta$ -blocker use was entered into the model as the primary variable of interest and secondly age and sex were also entered to adjust for these variables. Age was entered as a continuous variable while  $\beta$ -blocker use and sex were added as binary variables, where no  $\beta$ -blocker use and female sex were used as the referent categories. Statistical significance was taken at the 5% level ( $P < 0.05$ ). Regression analyses were carried out using Stata Version 10 (Stata Corp., College Stations, Texas, USA).

## 2.4 Results

### 2.4.1 The effects of chronic $\beta$ blockade on $I_{TO}$ current density

$I_{TO}$  was measured in isolated human atrial cells using the voltage clamp protocol described in the methods section of this chapter. An example of the current traces obtained from representative cells from a non  $\beta$ -blocked and a  $\beta$ -blocked patient are shown in figure 2-10. In these traces  $I_{TO}$  (measured as the peak current minus the end pulse current) is represented by the triangular portion of the current trace. In both traces it can be seen that  $I_{TO}$  activates in a voltage dependent fashion, increasing in magnitude as the voltage step increases in magnitude.  $I_{TO}$  is, therefore, largest when activated by the -50 to +60 mV voltage step and is not present with voltage steps of -50 to 0 mV or less. When the two current traces are compared, it can be seen that  $I_{TO}$  is smaller in the cell from the  $\beta$ -blocked patient at each voltage step.

Figure 2-11 shows the  $I_{TO}$  current-voltage relationship for each cell in the two patient groups. Current densities were measured across the voltage range of -50 to +60 mV in 32 cells from 14 non  $\beta$ -blocked patients (BB No) and 30 cells from 15  $\beta$ -blocked patients (BB Yes). These current-voltage relationships show a normally distributed range of current densities for cells in each patient group. Statistical analysis of the current densities at +60

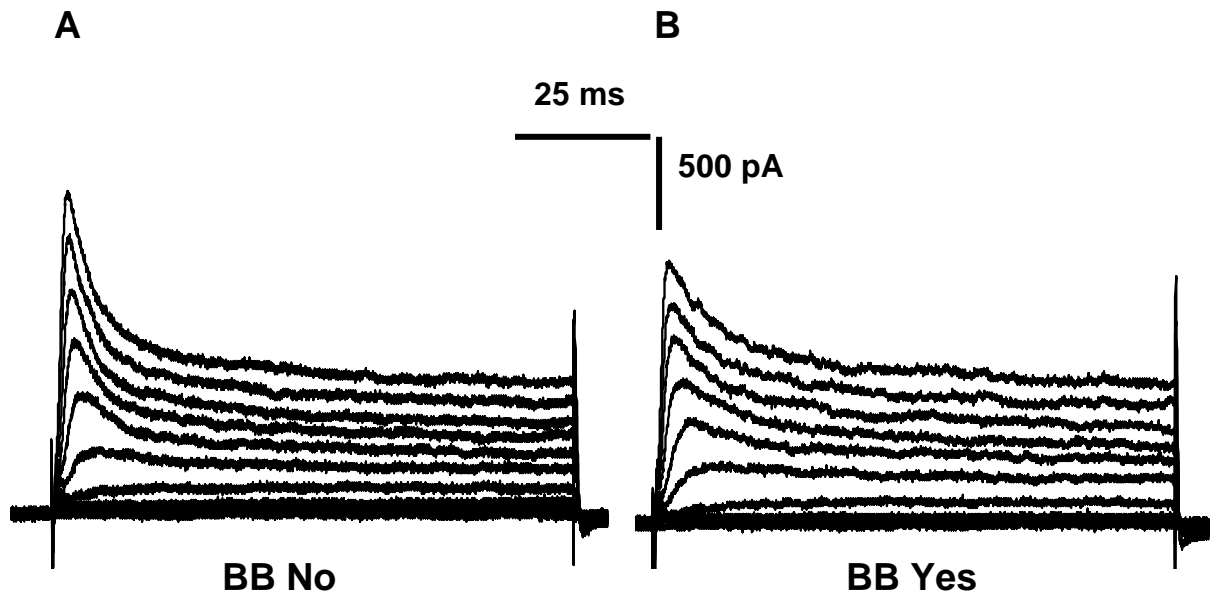


**Figure 2-10** Current traces showing  $I_{T0}$  voltage dependent activation in atrial cells of similar capacitance isolated from a non  $\beta$ -blocked (**A**) and  $\beta$ -blocked (**B**) patient.

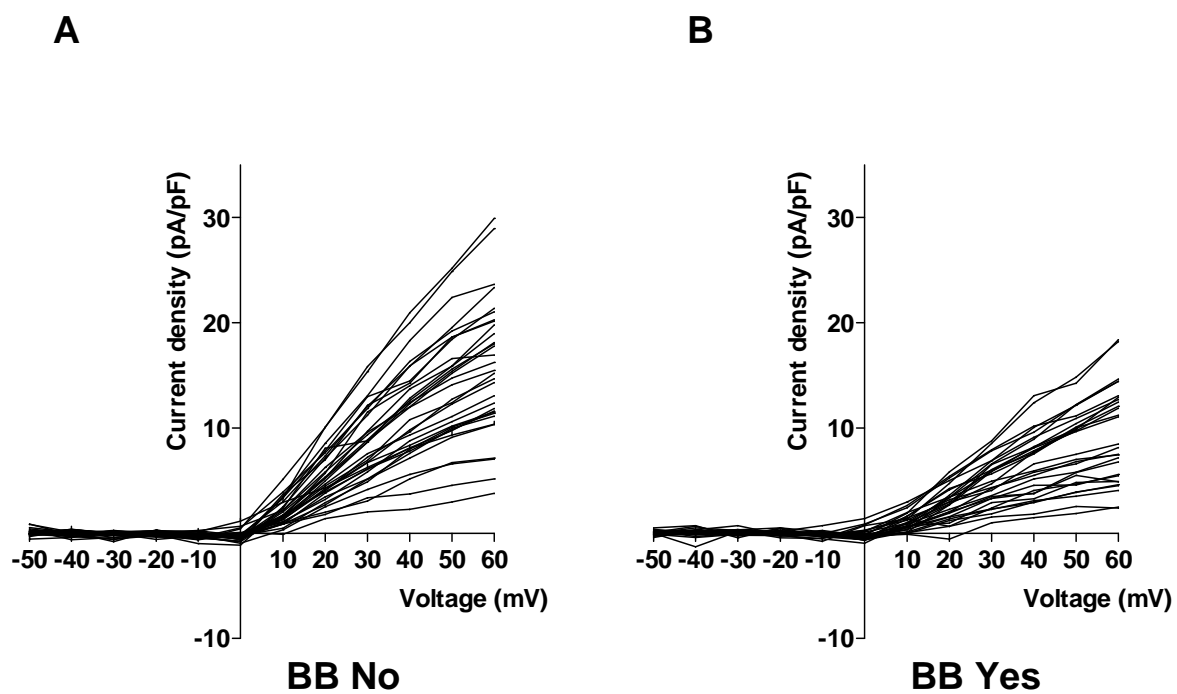
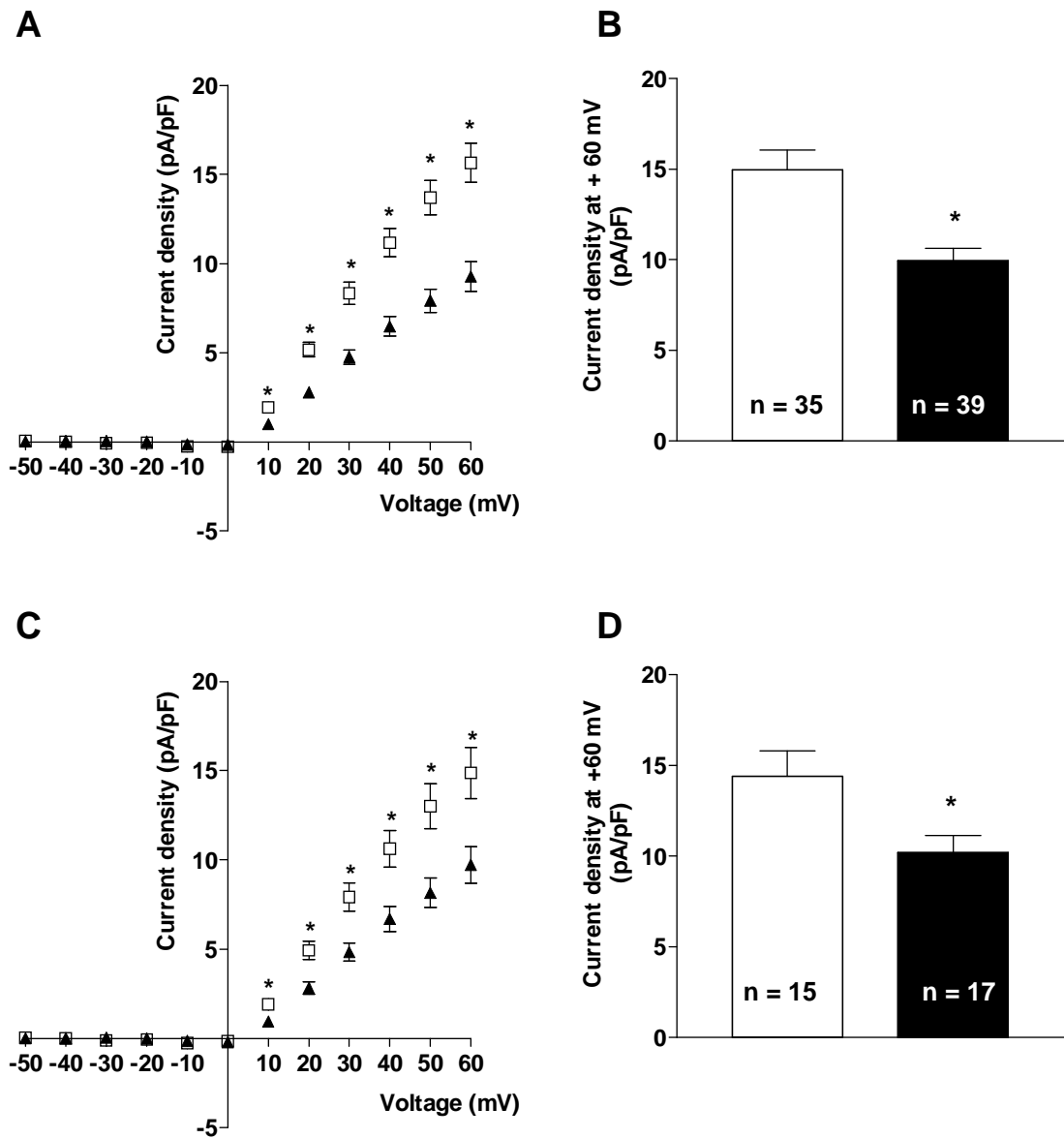


Figure 2-11 Individual voltage current relationships for  $I_{T0}$  in all cells isolated from non  $\beta$ -blocked (A) and  $\beta$ -blocked (B) patients



**Figure 2-12** Mean  $I_{TO}$  current-voltage relationship (A) and mean peak  $I_{TO}$  density at +60 mV (B) for all cells from non  $\beta$ -blocked ( $\square$ ) and  $\beta$ -blocked patients ( $\blacktriangle$ ). Mean patient data are shown in C and D. \* indicates  $p < 0.05$ , Student's t-test.

mV confirms the distribution is not inconsistent with a Gaussian distribution (K-S distances of 0.09 and 0.11,  $p > 0.1$  for BB No and BB Yes cells, respectively). This figure also suggests that the I<sub>TO</sub> current densities in the cells from the  $\beta$ -blocked patients are smaller than those from the non  $\beta$ -blocked patients and this was examined by plotting the mean current-voltage relationships for each group of cells as seen in figure 2-12.

The mean I<sub>TO</sub> current density, at each voltage step to voltages  $\geq +10$  mV, was significantly smaller in the cells from the  $\beta$ -blocked patients (Student's t-test,  $p < 0.05$ ) as shown in figure 2-12A. At peak I<sub>TO</sub> activation, achieved with the voltage step from -50 to +60 mV, chronic  $\beta$ -blockade was associated with a 34% reduction in the I<sub>TO</sub> current density. The mean current densities at +60 mV were  $15.0 \pm 1.1$  pA/pF in the cells from non  $\beta$ -blocked patients and  $9.9 \pm 0.7$  pA/pF in the cells from  $\beta$ -blocked patients as shown in figure 2-12B,  $p = 0.0001$ . This reduction in I<sub>TO</sub> current density was maintained when the data was meaned for patient rather than cell numbers as illustrated in figures 2-12C and D.

## **2.4.2 Effects of patient characteristics on I<sub>TO</sub> current density**

The characteristics of both the cells and patients in the non  $\beta$ -blocked and  $\beta$ -blocked patient groups were examined, to try to determine whether any other factors may be contributing to the difference in I<sub>TO</sub> density demonstrated between these two groups.

### **2.4.2.1 Cell characteristics**

Table 2-3 shows the mean electrophysiological properties of the cells in each patient group. The distribution of each variable was not inconsistent with that of a Gaussian distribution. There was no significant difference in any of the electrophysiological properties of the cells in either group.

Any difference in cell capacity between the two groups of cells which might have contributed to the magnitude of I<sub>TO</sub> had already been corrected for by calculating the current densities. It should be noted that the cells in each group were already depolarised prior to voltage clamping which is not an unusual finding when using human atrial cells isolated in this fashion (151). It might be expected that the voltage error (post series resistance compensation) would be smaller in the BB Yes cells given I<sub>TO</sub> is smaller in these cells. Series resistance compensation was not applied during the first nine experiments in order to avoid additional difficulties when learning the technique of patch clamping. Of

<b>Cell characteristics</b>	<b>BB No cells</b>	<b>BB Yes cells</b>
Capacitance (pF)	74.0 ± 2.8	69.3 ± 3.3
Resting membrane potential (mV)	-20.3 ± 1.8	-23.6 ± 2.2
Series resistance (MΩ) <sup>1</sup>	5.9 ± 0.3	6.3 ± 0.4
Voltage error (mV) <sup>2</sup>	3.7 ± 0.3	4.2 ± 0.5

**Table 2-3** Electrophysiological characteristics of cells from patients treated (BB Yes) or not treated (BB No) with  $\beta$ -blockers prior to cardiac surgery (mean  $\pm$  sem). Series resistance was recorded before series resistance compensation was applied<sup>1</sup>. Voltage error was calculated after series resistance compensation applied<sup>2</sup>

these experiments seven were done using BB Yes cells and this might have resulted in a net increase in the mean voltage error for the entire BB Yes group relative to the BB No group. However, this does not result in any significant difference in mean voltage error (post series resistance compensation) between the two groups and, therefore, is unlikely to have any influence on the difference in  $I_{TO}$  density.

#### **2.4.2.2 Patient characteristics**

Table 2-4 shows the patient characteristics for the cells in which  $I_{TO}$  was recorded. No attempt was made to match patients during the period in which tissue samples were collected. The patients in each group are of a similar age and sex but there are a number of differences including heart rate, pre-operative drugs and pre-operative diseases which may, possibly, contribute to the difference in  $I_{TO}$  density between the groups.

To examine the effects of other patient characteristics on  $I_{TO}$  current density, multiple linear regression analysis was performed by Dr Pardeep Jhund. There were only enough patients in the study to examine the effects of three variables including  $\beta$ -blockade, based on the need to have a minimum of 10 patients per variable studied. An analysis was therefore performed using the standard co-variables of age and sex. The results of this analysis along with single linear regression analysis for chronic  $\beta$ -blockade are shown in table 2-5.

The effects of various patient characteristics on  $I_{TO}$  were then considered individually as described in the following sections.

#### **2.4.2.3 Effects of heart rate on $I_{TO}$ density**

$\beta$ -blockers slow the heart rate. It is possible that heart rate, rather than specifically  $\beta$ -blocker use, determines  $I_{TO}$  current density and that the reduction in  $I_{TO}$  density seen in the  $\beta$ -blocked patient group was due directly to the slower heart rate in that group (see table 2-4). However, within each group of cells there was no correlation between peak  $I_{TO}$  density and heart rate as shown in figure 2-13.

#### **2.4.2.4 Effects of pre-operative drugs on $I_{TO}$ density**

All of the non  $\beta$ -blocked patients in this study were taking  $\beta_1$ -selective blockers with 15 out of 17 patients taking atenolol and the remaining two patients taking bisoprolol (see

Patient Characteristics	Non $\beta$ -blocked patients ( <b>BB No</b> ) n(%)	$\beta$ -blocked patients ( <b>BB Yes</b> ) n(%)	Total patients n(%)
No. of patients	15	17	32
Male patients	13 (86.7)	12 (70.6)	25 (78.1)
Mean age (yrs)	62.0 $\pm$ 2.8	65.7 $\pm$ 2.7	-
Mean heart rate (beats/min)	73.8 $\pm$ 3.5	53.4 $\pm$ 1.4*	-
<b>Surgery:</b>			
CABG	10 (66.7)	17 (100) <sup>T</sup>	27 (84.4)
AVR alone	3 (20)	0 (0)	3 (9.4)
CABG + AVR	1 (6.7)	0 (0)	1 (3.4)
CABG + MVR	1 (6.7)	0 (0)	1 (3.4)
<b>Pre-op drugs:</b>			
$\beta$ -blockers	0 (0)	17 (100)	17 (53.1)
- atenolol	0 (0)	15 (88.2)	15 (46.9)
- bisoprolol	0 (0)	2 (11.8)	2 (6.3)
ACE inhibitors	4 (26.7)	10 (58.8)	14 (43.8)
CCBs	8 (53.3)	3 (17.6)	11 (34.4)
Nicorandil	7 (46.7)	4 (23.5)	11 (34.4)
Statins	11 (73.3)	17 (100) <sup>T</sup>	28 (87.5)
Digoxin	0 (0)	0 (0)	0 (0)
Amiodarone	0 (0)	0 (0)	0 (0)
<b>Pre-op disease:</b>			
MI	1 (6.7)	5 (29.4)	6 (18.8)
Angina	12 (80)	17 (100)	29 (90.6)
LVSD	2 (13.3)	1 (5.9)	3 (9.4)
- mild	2 (13.3)	0 (0)	2 (6.3)
- moderate	0 (0)	1 (5.9)	1 (3.1)
- severe	0 (0)	0 (0)	0 (0)

Hypertension	10 (66.7)	11 (64.7)	21 (65.6)
Diabetes	3 (20)	2 (11.8)	5 (15.6)
Post-op AF	4 (26.7)	4 (23.5)	8 (25)

**Table 2-4** Patient characteristics of cells in which  $I_{TO}$  was recorded

CABG = coronary artery bypass graft, MVR = mitral valve replacement, AVR = aortic valve replacement, Pre-op = before surgery, ACE = angiotensin converting enzyme, CCB = calcium channel blocker, MI= myocardial infarction, LVSD =left ventricular systolic dysfunction. \* indicates a significant difference from BB No ( $p < 0.05$ , Students t-test). <sup>τ</sup> a significant difference from BB No ( $p < 0.05$ , Fishers exact test ).

**A**

<b>Clinical factor</b>	<b>Change in <math>I_{TO}</math> (pA/pF)</b>	<b>95% Confidence Interval</b>	<b>P value</b>
$\beta$ -blockade	-4.14	-7.50 to -0.77	0.02

**B**

<b>Clinical factor</b>	<b>Change in <math>I_{TO}</math> (pA/pF)</b>	<b>95% Confidence Interval</b>	<b>P value</b>
$\beta$ -blockade	-3.57	-6.93 to -0.21	0.04
Age	0.02	-0.15 to 0.19	0.82
Sex	4.00	-0.56 to 8.58	0.08

**Table 2-5** Single (A) and multiple (B) linear regression analysis of  $I_{TO}$  current density for patient co-variables listed. Total number of patients is 32.

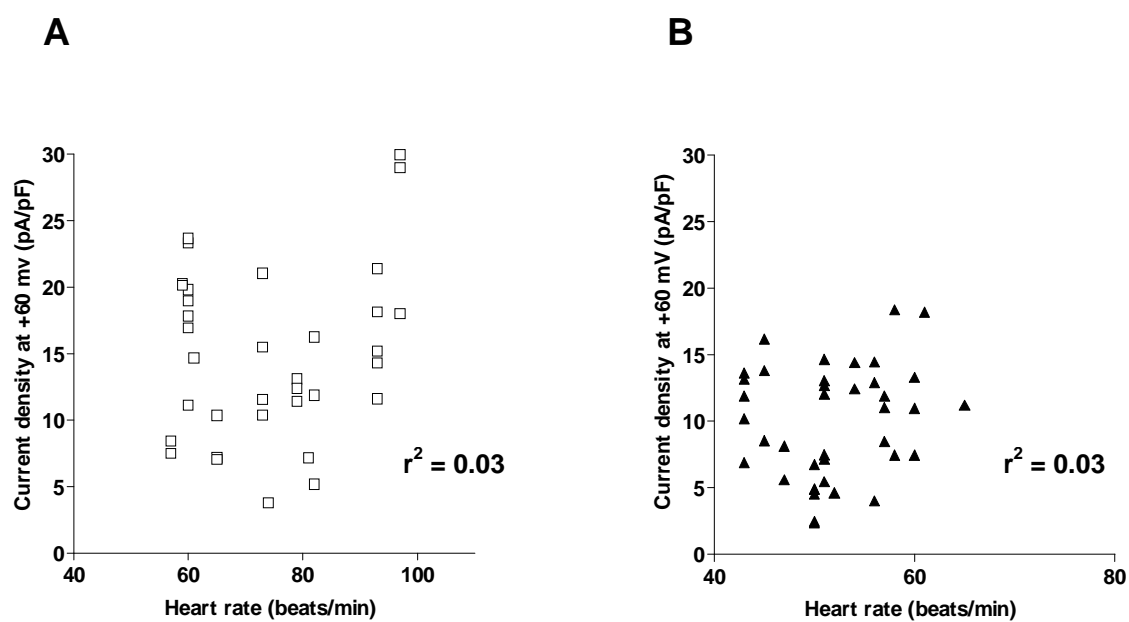


**Figure 2-13** Patient heart rate Vs peak  $I_{TO}$  density in cells from non  $\beta$ -blocked (A) patients and  $\beta$ -blocked (B) patients.  $r^2$  was calculated from the correlation coefficient.

table 2-4). Clearly too few patients were taking  $\beta$ 1-selective blockers other than atenolol to test whether the reduction in  $I_{TO}$  density was a class effect of this type of drug or whether it was specific to atenolol. The inclusion of two patients taking bisoprolol did not have any affect the on the mean  $I_{TO}$  density for the entire  $\beta$ -blocked patient group as shown in table 2-6.

If  $\beta$ -blockers have a direct action on  $I_{TO}$  it might be expected that they would exert a dose dependent effect on  $I_{TO}$  density. Figure 2-14 shows the total daily dose of atenolol each patient was taking and the  $I_{TO}$  densities for all the cells from those patients. Linear regression analysis showed there to be no relationship between these data ( $r^2=0.00$ ).

Many cardiac drugs are known to or have the potential to affect cardiac electrophysiology. Of these drugs, the ones taken prior to cardiac surgery by patients in this study are shown in table 2-4 along with the number of patients taking each drug. Multiple linear regression analysis of the effects of drug therapy on  $I_{TO}$  density could not be performed but the comparison of  $I_{TO}$  densities between the non  $\beta$ -blocked and  $\beta$ -blocked patients was repeated when patients taking different types of cardiac drugs were excluded. Table 2-6 shows both the patient and cell mean  $I_{TO}$  densities when patients taking calcium channel blockers, ACE inhibitors, nicorandil or statins were excluded individually. There remained a significant reduction in  $I_{TO}$  density in the  $\beta$ -blocked patients when those patients taking either nicorandil or statins are excluded. When patients taking calcium channel blockers or ACE inhibitors were excluded, the number of patients in each group was considerably smaller and, perhaps not surprisingly, the difference in the mean patient  $I_{TO}$  was not statistically significant. There remained, however, a significant reduction in  $I_{TO}$  density in the  $\beta$ -blocked patients when the cell means were compared.

#### **2.4.2.5 Effects of patient pre-op pathology on $I_{TO}$ density**

The effects of various pre-operative cardiovascular morbidities on  $I_{TO}$  density were not examined directly but, again, the mean  $I_{TO}$  densities of the non  $\beta$ -blocked and  $\beta$ -blocked patients were compared when various patient groups were excluded from the analysis. The reduction in  $I_{TO}$  density associated with chronic  $\beta$ -blockade was maintained when patients without a previous myocardial infarction, with left ventricular dysfunction or with diabetes were individually excluded (see table 2-6).

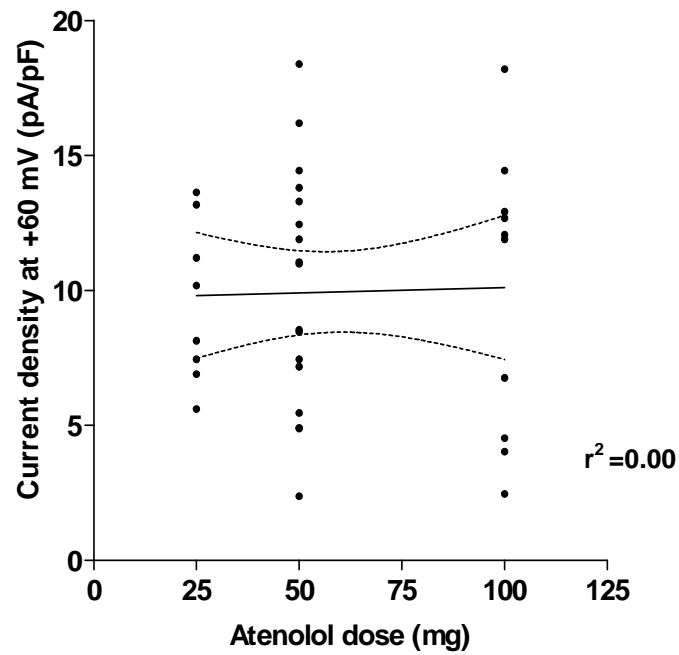


**Figure 2-14** Total daily dose of atenolol given to the  $\beta$ -blocked patients Vs peak  $I_{TO}$  density in cells from those patients with the regression line and 95% confidence intervals.

Patients excluded	BB No I <sub>TO</sub> density mean ± sem	BB Yes I <sub>TO</sub> density mean ± sem
None	14.4 ± 1.4 (n=15 patients) [15.0 ± 1.1 (n=35 cells)]	10.2 ± 0.9 (n=17 patients) * [9.9 ± 0.7 (n=39 cells)] *
Females	15.7 ± 1.3 (13) [16.4 ± 1.0 (30)]	10.5 ± 1.1 (12) * [9.8 ± 0.9 (26)] *
Valve surgery	16.3 ± 1.5 (10) [17.0 ± 1.2 (23)]	10.2 ± 0.9 (17) * [9.9 ± 0.7 (39)] *
<b>Pre-op drugs:</b>		
Bisoprolol	14.4 ± 1.4 (15) [15.0 ± 1.1 (35)]	10.5 ± 1.0 (15) * [9.9 ± 0.7 (35)] *
CCBs	13.7 ± 1.6 (7) [14.7 ± 1.2 (19)]	10.6 ± 1.0 (14) [10.1 ± 0.8 (31)] *
ACE inhibitors	13.0 ± 1.4 (11) [13.2 ± 1.1 (25)]	10.1 ± 1.3 (7) [9.9 ± 1.0 (16)] *
Nicorandil	14.1 ± 1.4 (8) [14.7 ± 1.1 (19)]	10.1 ± 1.0 (13) * [9.9 ± 0.7 (30)] *
Statins	15.2 ± 1.7 (11) [16.0 ± 1.8 (25)]	10.2 ± 0.9 (17) * [9.9 ± 0.7 (39)] *
<b>Pre-op disease:</b>		
No previous MI	14.0 ± 1.5 (14) [14.7 ± 1.1 (33)]	9.8 ± 1.6 (9) * [8.8 ± 1.1 (19)] *
LV dysfunction	14.1 ± 1.6 (13) [14.8 ± 1.2 (31)]	10.6 ± 0.9 (16) * [10.4 ± 0.7 (36)] *

Diabetes	$14.0 \pm 1.4$ (12) $[14.6 \pm 1.0$ (28)]	$10.1 \pm 1.0$ (15) * $[9.7 \pm 0.8$ (32)] *
----------	--	---

**Table 2-6** Mean  $\pm$  sem peak  $I_{TO}$  densities (pA/pF), in non  $\beta$ -blocked (BB No) and  $\beta$ -blocked patients (BB Yes) when patients with characteristics listed in the left column were excluded from analysis. Mean  $I_{TO}$  densities for all remaining cells in each group are shown in square brackets. \* indicates significant difference from non  $\beta$ -blocked patients or cells ( $p < 0.05$ , Student's t-test).

### 2.4.3 Effects of phrixotoxin-2 on $I_{TO}$ density

The results of application of either 100 or 200 nM phrixotoxin 2 on four and two cells respectively are shown in figure 2-15.  $I_{TO}$  density was plotted at approximately twenty seconds intervals for these graphs. The application of either 100 or 200 nM of PaTx2 had no significant effect on the atrial  $I_{TO}$  current density. The two cells with wash recording in figure 2-15A were from the same non  $\beta$ -blocked patient as those in figure 2-15B and, in all four of these cells, the  $I_{TO}$  density is significantly smaller than the mean current density for this patient group. The  $I_{TO}$  densities from the other two cells in figure 2-15A were from a different non  $\beta$ -blocked patient. They have more representative values for this patient group but were also unaffected by PaTx2.

Higher concentrations of PaTx2 were not used due to prohibitive cost and the lack of effect at concentrations previously shown to significantly reduce  $I_{TO}$  in cellular recordings. The use of this blocker of  $I_{TO}$  was not investigated further.

### 2.4.4 Effects of chronic $\beta$ -blockade on time dependent inactivation of $I_{TO}$

The time dependent inactivation of  $I_{TO}$  was found to fit a bi-exponential function. When a comparison was made between mono-exponential and bi-exponential curve fits to the raw data from individual cell, 100 % of the non  $\beta$ -blocked and 93% of the  $\beta$ -blocked cells best fitted a bi-exponential relationship. The mean fast rate constants (the inverse of the fast time constants) were  $0.15 \pm 0.008$  for the non  $\beta$ -blocked cells ( $n = 27$  cells, 15 patients) and  $0.16 \pm 0.012$  for the  $\beta$ -blocked cells ( $n = 22$  cells, 13 patients),  $p = 0.38$ . The slow rate constants were  $0.035 \pm 0.009$  and  $0.033 \pm 0.005$  respectively,  $p = 0.87$ . These data are shown in figure 2-16B. Cells were excluded from the analysis if they did not best fit a bi-exponential function. A few cells (5 non  $\beta$ -blocked and 4  $\beta$ -blocked) also had very small rate constants with very large standard deviations incorporating negative values. These cells were also excluded from analysis on the basis that they did not well fit a bi-exponential function. Bi-exponential curves fits to the mean current densities in both groups of cells are shown in figure 2-16A. It can be seen from these curves that  $I_{TO}$  inactivated rapidly with approximately 80% of the current inactivating within the first 20 ms.

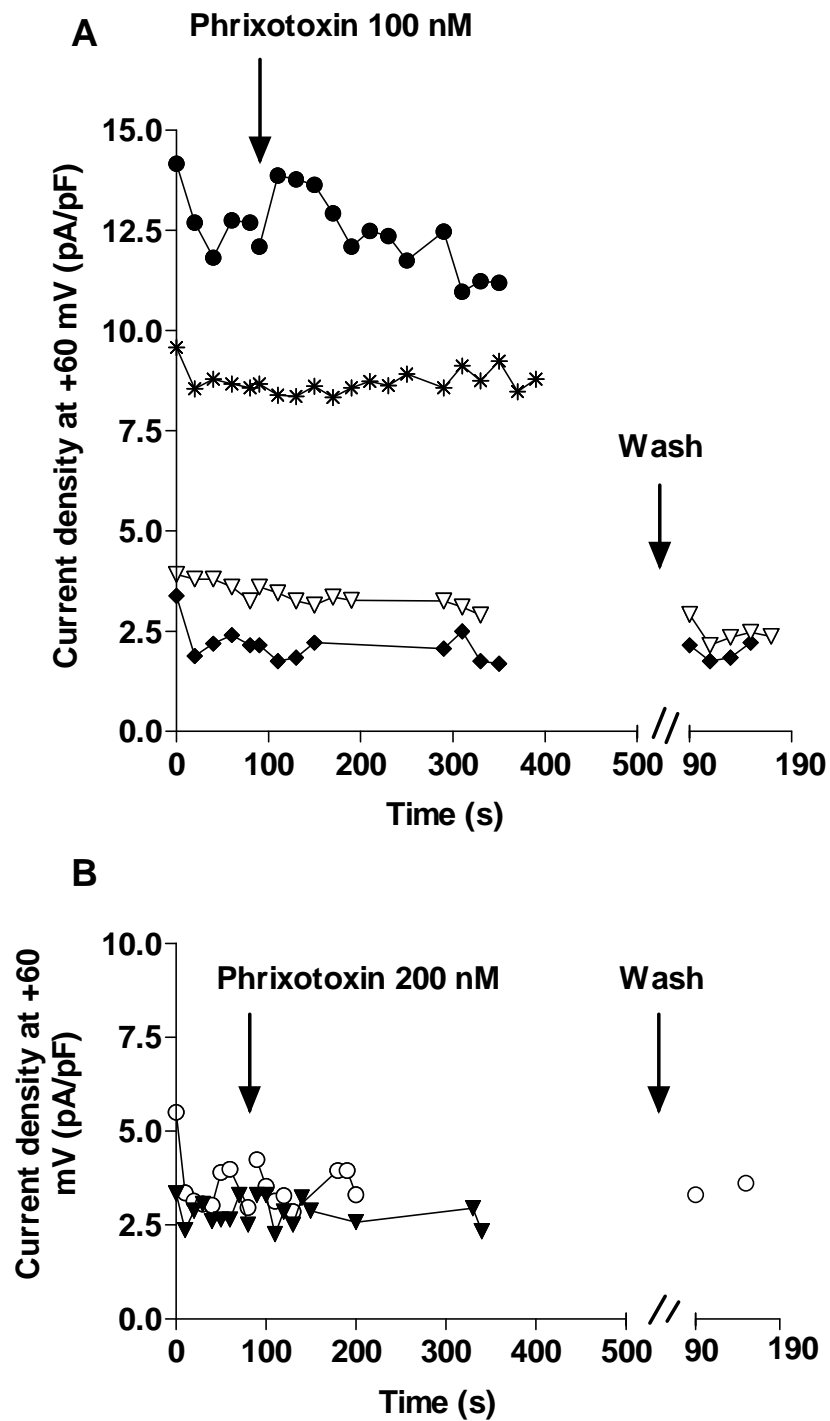


**Figure 2-15** Effects of phrixotoxin 2 on peak  $I_{TO}$  current density at +60 mV Vs time. 100 nM phrixotoxin 2 was applied to four cells represented by the different symbols in **A**. In **B**, 200 nM of phrixotoxin was applied to two different cells.

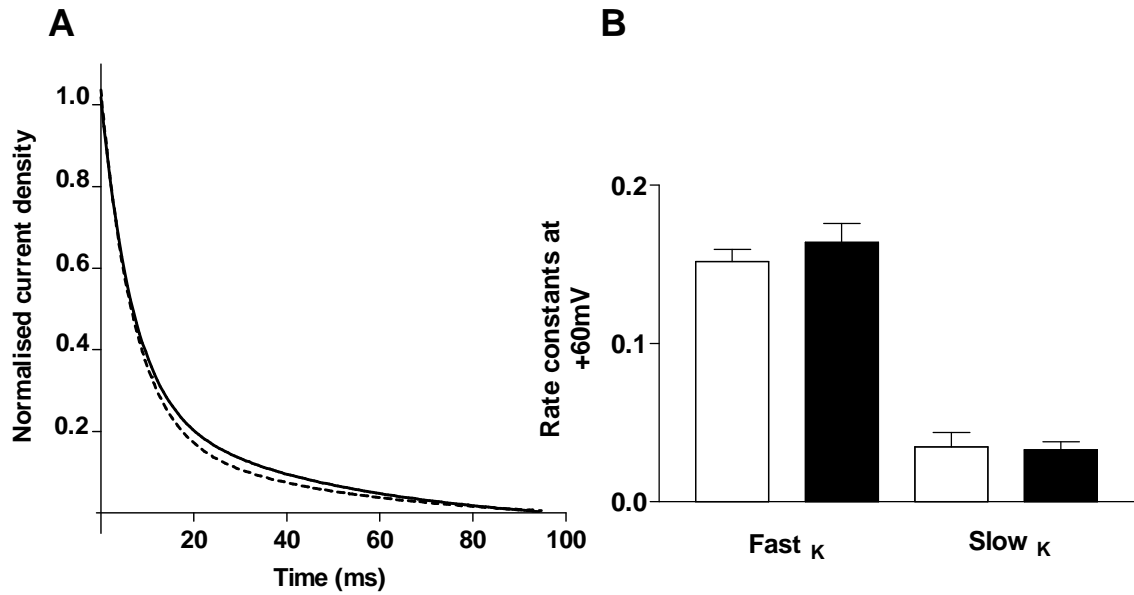


**Figure 2-16** Time dependent inactivation of  $I_{T0}$  at +60mV. **A** shows bi-exponential curve fits to mean  $I_{T0}$  density (pA/pF) normalised to the  $I_{T0}$  density at time zero Vs time, for cells from non  $\beta$ -blocked and  $\beta$ -blocked patients. The mean  $\pm$  sem fast and slow rate constants ( $\kappa$ ) for each group of cells are shown in **B**.

### 2.4.5 Effects of chronic $\beta$ -blockade on voltage dependence of $I_{TO}$

The mean conductance values for voltage dependent activation and the mean current density values for inactivation of  $I_{TO}$  in cells from non  $\beta$ -blocked and  $\beta$ -blocked cells are shown in figure 2-17. The values were normalised to the corresponding maximal conductance/density and Boltzmann curve fits were superimposed on each data set. It can be seen that there was no difference between these curves in either groups of cells for either activation or inactivation. The mean voltage of half maximal activation ( $V_{0.5}$ ), obtained from Boltzmann curve fits to the individual cells, was  $23.8 \pm 0.5$  mV for the non  $\beta$ -blocked cells (32 cells, 14 patients) and  $25.1 \pm 0.7$  mV for the  $\beta$ -blocked cells (29 cells, 15 patients),  $p = 0.15$ . The corresponding slope factors were  $8.6 \pm 0.2$  mV and  $8.5 \pm 0.3$  mV respectively,  $p = 0.78$ . The mean voltage of half maximal inactivation was  $-19.5 \pm 0.6$  mV for the non  $\beta$ -blocked cells (32 cells, 15 patients) and  $-19.0 \pm 1.0$  mV for the  $\beta$ -blocked cells (29 cells, 13 patients),  $p = 0.61$ . The corresponding slope factors were  $4.7 \pm 0.3$  mV and  $5.3 \pm 0.3$  mV respectively,  $p = 0.13$ . Figure 2-17C shows the mean curves for voltage dependent activation and inactivation for the non  $\beta$ -blocked and  $\beta$ -blocked cells. In both groups of cells, inactivation was fully developed at potentials positive to 0 mV and activation did not commence at potentials negative to 0 mV. There was, therefore, no window current.

### 2.4.6 Effects of chronic $\beta$ -blockade on reactivation of $I_{TO}$

The effects of chronic  $\beta$ -blockade on  $I_{TO}$  reactivation are shown in figure 2-18. The mean  $I_{TO}$  densities elicited by the second pulse (P2) of the protocol, which occurred at varying interpulse intervals, are shown in figure 2-18A for the cells from the non  $\beta$ -blocked patients (31 cells, 14 patients) and  $\beta$ -blocked patients (30 cells, 13 patients). Initially, at the longer interpulse pulse intervals ( $\geq 200$  ms)  $I_{TO}$  density remained relatively constant in both groups of cells, albeit smaller in the  $\beta$ -blocked cells, indicating that  $I_{TO}$  recovers quickly from inactivation. At the shorter interpulse intervals ( $<150$  ms),  $I_{TO}$  density was reduced in both groups of cells. This reduction in  $I_{TO}$  density at very short interpulse intervals occurred, to the same extent, in both the non  $\beta$ -blocked and  $\beta$ -blocked cells. This can be seen in figure 2-18B when the mean densities elicited by P2 were normalised to the first, post-rest P1 of the voltage pulse protocol. In this figure the mean data points for both the non  $\beta$ -blocked and  $\beta$ -blocked cells superimpose. The reactivation data best fit mono-exponential curves. A comparison of

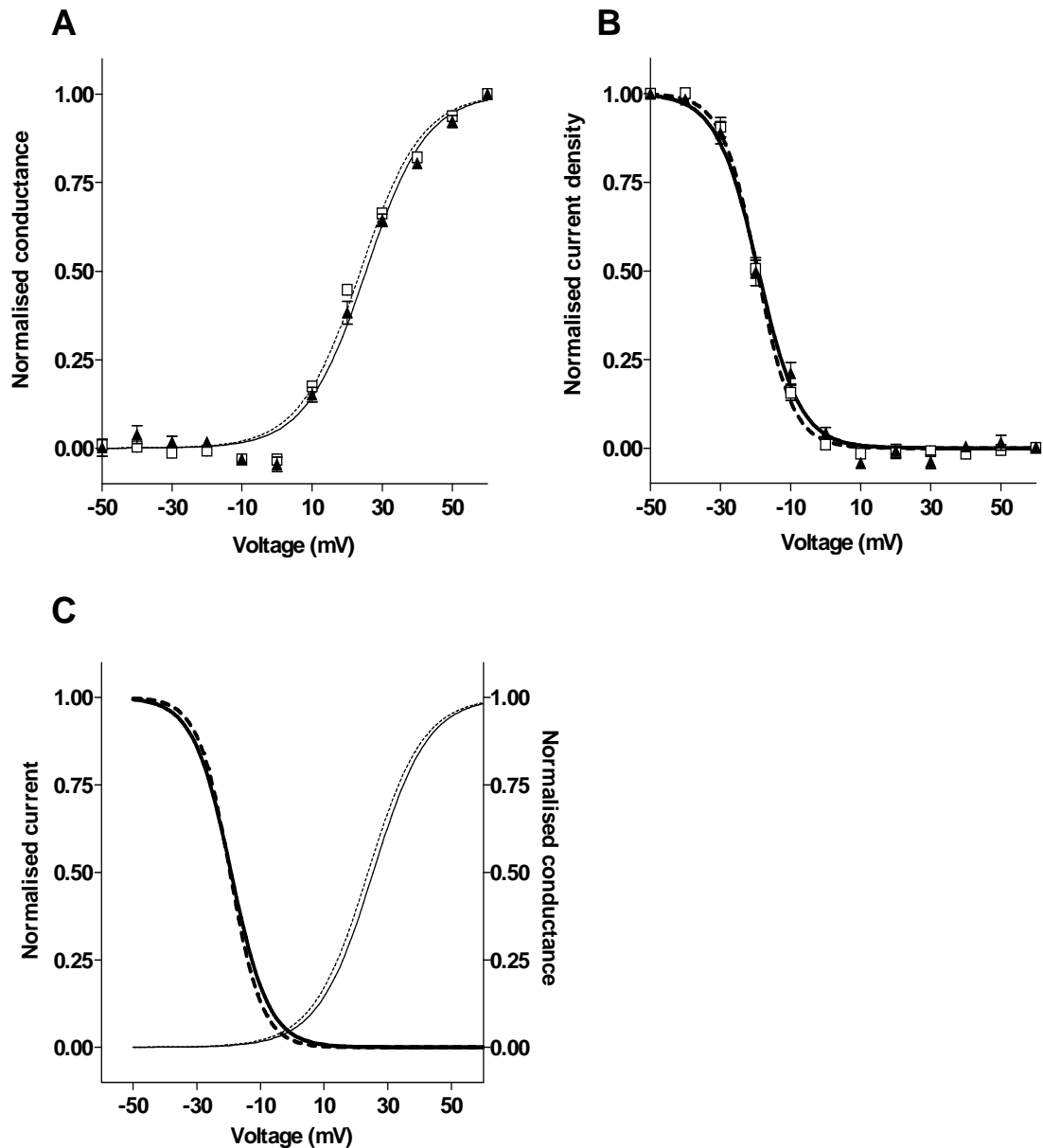


**Figure 2-17** Voltage dependence of  $I_{T0}$ . **A** shows the voltage dependency of activation of  $I_{T0}$  with mean normalised  $I_{T0}$  conductance Vs membrane voltage along with Boltzmann curve fits to cells from non  $\beta$ -blocked ( $\square$  ..... ) and  $\beta$ -blocked ( $\blacktriangle$  — ) patients. **B** shows the voltage dependency of inactivation of  $I_{T0}$  with mean normalised  $I_{T0}$  densities Vs membrane potential for non  $\beta$ -blocked ( $\square$  ..... ) and  $\beta$ -blocked ( $\blacktriangle$  — ) cells and corresponding Boltzmann curve fits. The same activation and inactivation curve fits for both groups of cells are shown in **C**.

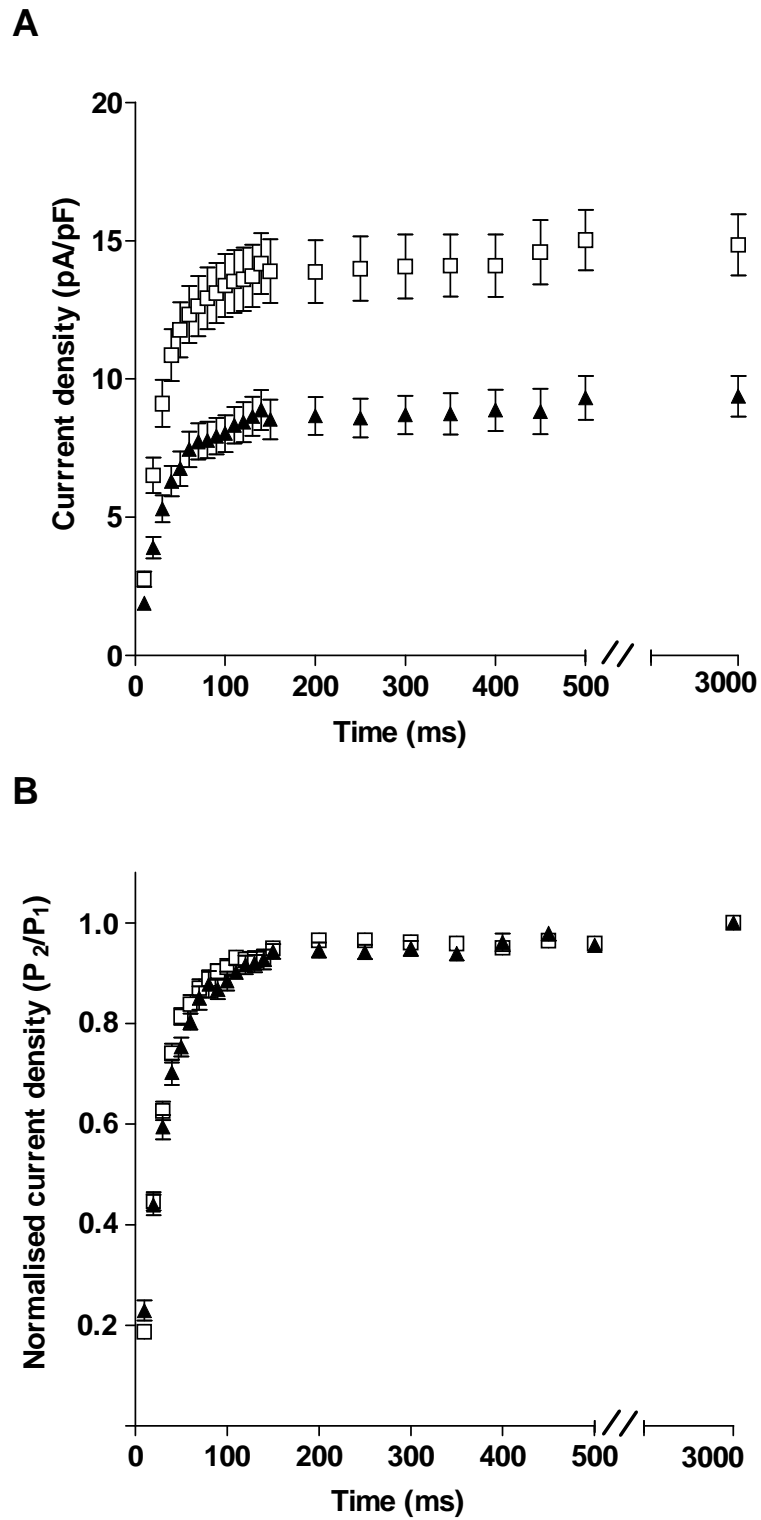


**Figure 2-18**  $I_{TO}$  reactivation. **A** shows the mean  $I_{TO}$  densities elicited by pulse 2 of the protocol Vs the time interval between pulses one and two, in cells from non  $\beta$ -blocked ( $\square$ ) and  $\beta$ -blocked ( $\blacktriangle$ ) patients. In **B** the  $I_{TO}$  densities are normalised to those elicited by the first post-rest pulse one in each group of cells.

mono-exponential and bi-exponential curve fits for each individual cell showed that 93% of the non  $\beta$ -blocked cells (28 cells, 13 patients) and 80% of the  $\beta$ -blocked cells (24 cells, 12 patients) best fitted mono-exponential curves. The mean data for these cells along with their curve fits are shown in figure 2-19. It can be seen that the curve fits for both groups of cells superimpose even at the short interpulse intervals. The mean time constants for reactivation derived from the curve fits to the individual cells were no different in non  $\beta$ -blocked cells at  $31.3 \pm 1.9$  ms compared to  $33.5 \pm 2.6$  ms for the  $\beta$ -blocked cells,  $p = 0.14$ .

#### **2.4.7 Effects of chronic $\beta$ -blockade on rate dependence of $I_{TO}$**

The rapid recovery of  $I_{TO}$  suggests it is relatively rate independent except at extremely rapid stimulation rates. However, the effects of incremental shortening of interpulse intervals, as used to determine  $I_{TO}$  reactivation, do not necessarily replicate the effects of repetitive rapid stimulation. This can be seen using the eight pulse protocols illustrated in figure 2-8 of the methods, in which, at rapid rates, the first, post-rest  $I_{TO}$  recording is larger than the subsequent pulses in the train at rates above 75 bpm. The effects of changing stimulation rate on  $I_{TO}$  ie the rate dependence stimulation of  $I_{TO}$  are shown in figure 2-20.

The mean steady state  $I_{TO}$  densities in cells from non  $\beta$ -blocked (27 cells, 11 patients) and  $\beta$ -blocked (17 cells, 6 patients) patients are shown in figure 2.20A. In both groups of cells  $I_{TO}$  was reduced significantly at rates  $\geq 300$  beats/minute. This reduction was not due to run down of  $I_{TO}$  as it reversed when the stimulation rate returned to 75 beats/minute. Even at the most rapid stimulation rates, the  $I_{TO}$  density in the cells from the  $\beta$ -blocked patients was smaller compared to that of the non  $\beta$ -blocked cells. This reflects the fact that the degree of reduction in  $I_{TO}$  density due to increasing stimulation rate was the same in the  $\beta$ -blocked and non  $\beta$ -blocked cells. This is seen in figure 2.20B when the mean densities for each group of cells superimposed after they were normalised to their respective values at 75 beats/minute.

#### **2.4.8 Effects of chronic $\beta$ -blockade on $I_{KSUS}$ density**

Peak  $I_{KSUS}$  was measured as the end pulse current elicited by the voltage step from -50 to +60 mV.  $I_{KSUS}$  measurements were made from current recordings used to measure

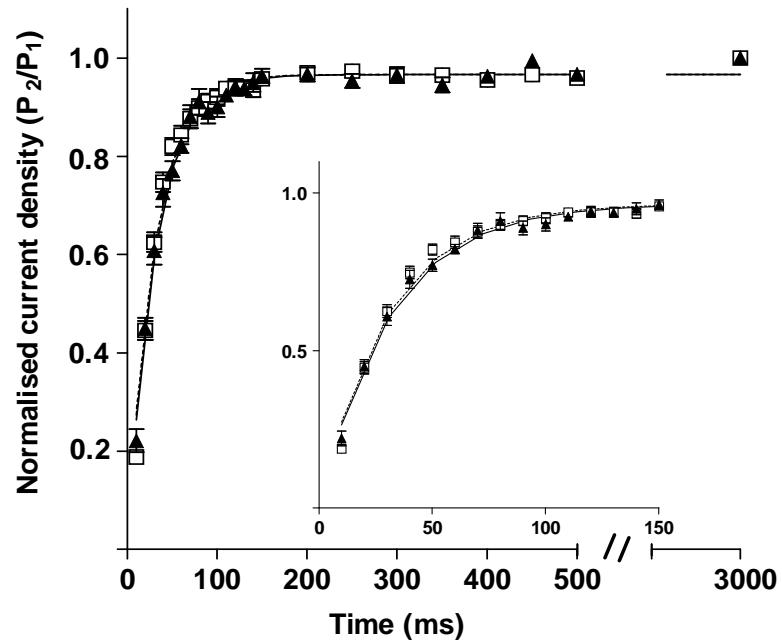


**Figure 2-19**  $I_{TO}$  reactivation. The main graph shows the mean normalised  $I_{TO}$  densities Vs interpulse intervals for all non  $\beta$ -blocked ( $\square$  ..... ) and  $\beta$ -blocked ( $\blacktriangle$  —) cells with the best fitting the mono-exponential curves. The inset graph shows part of the main graph expanded at the shortest interpulse intervals.

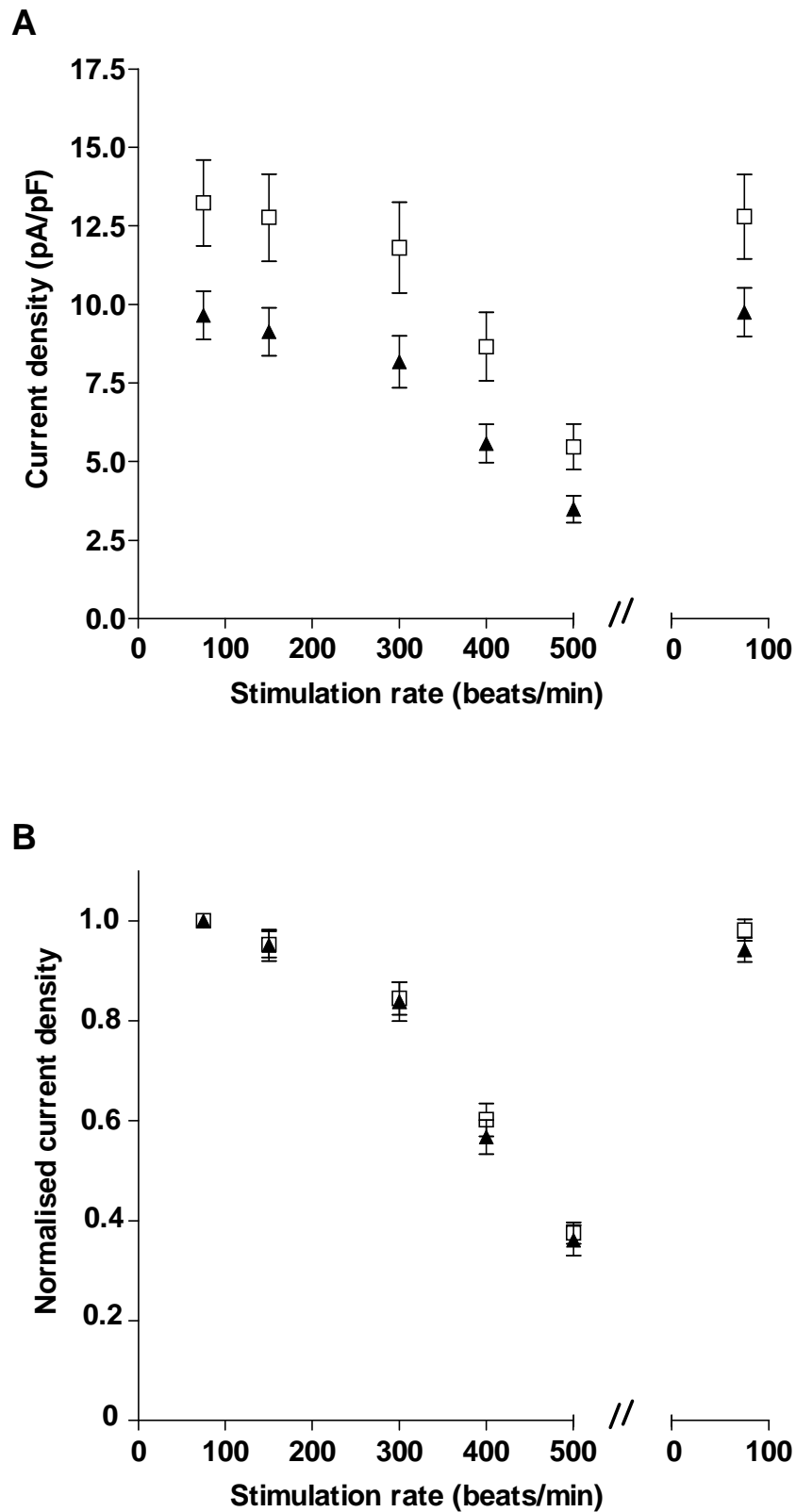


**Figure 2-20** Rate dependence of  $I_{TO}$ . **A** shows the mean, steady state (8<sup>th</sup> pulse)  $I_{TO}$  density Vs stimulation rate for cells from non  $\beta$ -blocked ( $\square$ ) and  $\beta$ -blocked ( $\blacktriangle$ ) patients. The current densities normalised to their respective values at the initial stimulation rate of 75 beats/minute are shown in **B**.

$I_{TO}$  density however,  $I_{KSUS}$  was not measured in every cell in which  $I_{TO}$  was recorded. The patient characteristics for the cells in which  $I_{KSUS}$  was recorded are shown in table 2-7. For each patient group the distribution of the peak  $I_{KSUS}$  densities were not inconsistent with a Gaussian distribution (KS distances of 0.17 and 0.12,  $p > 0.1$  for BB No and Yes cells respectively). The mean peak  $I_{KSUS}$  in cells from non  $\beta$ -blocked patients was  $11.4 \pm 1.1$  pA/pF ( $n = 33$  cells, 13 patients) compared to  $9.7 \pm 0.7$  pA/pF in the cells from  $\beta$ -blocked patients ( $n = 31$  cells, 13 patients). There was no significant difference between mean peak  $I_{KSUS}$  in these two groups as shown in figure 2-21,  $p = 0.21$  Students t-test.  $I_{KSUS}$  density was not formally evaluated at other voltages.

#### **2.4.9 Assessing block of $I_{KSUS}$ by 4-AP**

Preliminary experiments were performed to assess the degree of block of  $I_{KSUS}$  using low dose 4-AP to determine whether this could be used as an alternative method for separating  $I_{TO}$  from  $I_{KSUS}$ . These experiments were performed in cells from non  $\beta$ -blocked patients.  $I_{TO}$  and  $I_{KSUS}$  were measured as the peak minus end pulse current and end pulse current respectively using a voltage step from -50 to +60 mV. The effects of different concentrations of 4-AP on current traces from the same cell can be seen in figure 2-22. It can be seen that, in this cell, there was not complete “wash reversal” of 4-AP. Figure 2-23A shows the effects of varying concentrations of 4-AP on the mean peak  $I_{KSUS}$  current density in all cells exposed to 4-AP. Statistical analysis was not performed on these data as the small numbers of paired data may have led to misleading results however, the graph does suggest that  $I_{KSUS}$  was reduced by all concentrations of 4-AP. The use of 4-AP as a blocker of  $I_{KSUS}$  is only effective if a high level of  $I_{KSUS}$  block can be achieved without affecting  $I_{TO}$  density. At the highest concentration of 4-AP used, 2 mM, approximately 50 % block of  $I_{KSUS}$  did appear to be achieved. However, at this concentration there also appeared to be some block of  $I_{TO}$  when compared to  $I_{TO}$  recorded without 4-AP and after wash out of 4-AP as shown in figure 2-23B. Again, statistical analysis was not performed due to low  $n$ .

#### **2.4.10 Effects of chronic $\beta$ -blockade on $I_{K1}$ density**

The effects of chronic  $\beta$ -blockade on  $I_{K1}$  are shown in figure 2-24. It can be seen that  $I_{K1}$  was significantly reduced at -120 mV with a mean density of  $-2.5 \pm 0.2$  pA/pF in

Patient characteristics	I <sub>ksus</sub>	I <sub>ksus</sub>	I <sub>k1</sub>	I <sub>k1</sub>
	BB No n(%)	BB Yes n(%)	BB No n(%)	BB Yes n(%)
No of patients	13	13	12	11
Male patients	11 (84.6)	8 (61.5)	12 (100)	9 (81.8)
Mean age (yrs)	63.4 ± 3.0	66.9 ± 3.1	61.3 ± 2.2	62.8 ± 3.7
Mean heart rate (beats/min)	74.1 ± 3.9	52.6 ± 1.6*	75.2 ± 4.1	54.4 ± 1.8*
<b>Surgery:</b>				
CABG	9 (69.2)	13 (100)	10 (83.3)	11 (100)
AVR alone	3 (23.1)	0 (0)	2 (16.7)	0 (0)
CABG + AVR	1 (7.7)	0 (0)	0 (0)	0 (0)
CABG + MVR	0 (0)	0 (0)	0 (0)	0 (0)
<b>Pre-op drugs:</b>				
β-blockers	0 (0)	13 (100)	0 (0)	11 (100)
-atenolol	0 (0)	12 (92.3)	0 (0)	10 (90.9)
-bisoprolol	0 (0)	1 (7.7)	0 (0)	1 (9.1)
ACE inhibitors	3 (23.1)	7 (53.8)	3 (25)	5 (45.4)
CCBs	7 (53.8)	2 (15.4)	7 (58.3)	1 (9.1)
Nicorandil	7 (53.8)	4 (30.8)	6 (50)	5 (45.4)
Statins	10 (76.9)	13	10 (83.3)	11 (100)
Digoxin	0 (0)	0 (0)	0 (0)	0 (0)
Amiodarone	0 (0)	0 (0)	0 (0)	0 (0)
<b>Pre-op disease:</b>				
MI	1 (7.7)	3 (23.1)	2 (16.7)	4 (36.4)
Angina	11 (84.6)	13 (100)	11 (91.7)	11 (100)
LVSD	2 (15.4)	1 (7.7)	2 (16.7)	1 (9.1)

-mild	2 (15.4)	0 (0)	2 (16.7)	0 (0)
-moderate	0 (0)	1 (7.7)	0 (0)	1 (9.1)
-severe	0 (0)	0 (0)	0 (0)	0 (0)
Hypertension	8 (61.5)	9 (69.2)	8 (66.7)	5 (45.4)
Diabetes	3 (23.1)	1 (7.7)	3 (25)	0 (0)
Post op AF	3 (23.1)	3 (23.1)	2 (16.7)	1 (9.1)

**Table 2-7** Patient characteristics of cells in which  $I_{K_{SUS}}$  and  $I_{K1}$  were measured.

BB No = non  $\beta$ -blocked patients, BB Yes =  $\beta$ -blocked patients, CABG = coronary artery bypass graft, MVR = mitral valve replacement, AVR = aortic valve replacement, Pre-op = before surgery, ACE = angiotensin converting enzyme, CCB = calcium channel blocker, MI= myocardial infarction, LVSD =left ventricular systolic dysfunction. \* indicates a significant difference from BB No ( $p < 0.05$ , Students t-test).

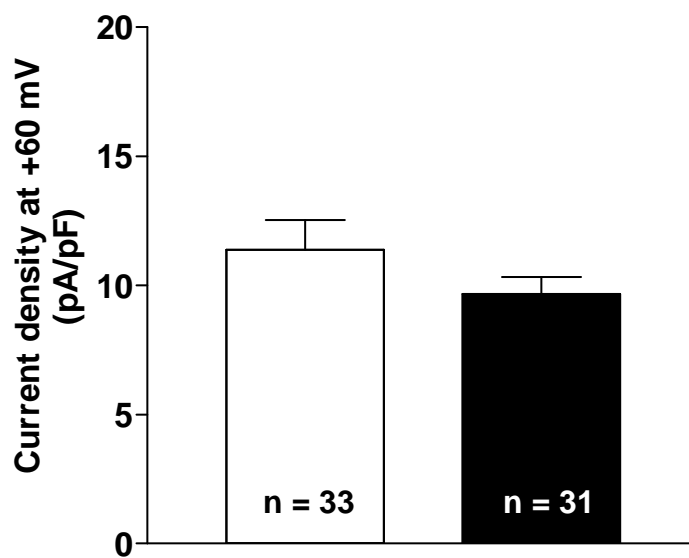


**Figure 2-21** Mean peak  $I_{KSUS}$  density at + 60 mV for cells (n) from non  $\beta$ -blocked ( $\square$ ) and  $\beta$ -blocked patients ( $\blacksquare$ ).

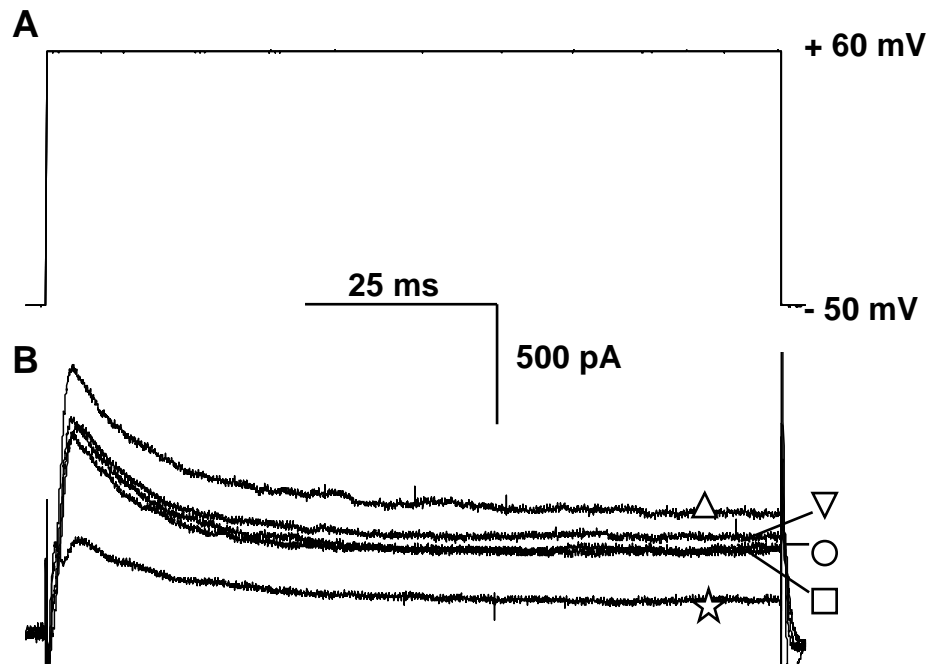


**Figure 2-22** Effect of 4-AP on  $I_{TO}$  and  $I_{KSUS}$ . The voltage pulse is shown in **A** and representative current traces from the same cell exposed to external solution containing varying concentrations of 4-AP. [ $\Delta$  = no 4-AP,  $\circ$  = 0.05 mM 4-AP,  $\square$  = 0.1 mM 4-AP,  $\star$  = 2 mM 4-AP,  $\nabla$  = no 4-AP (wash)] are shown in **B**.

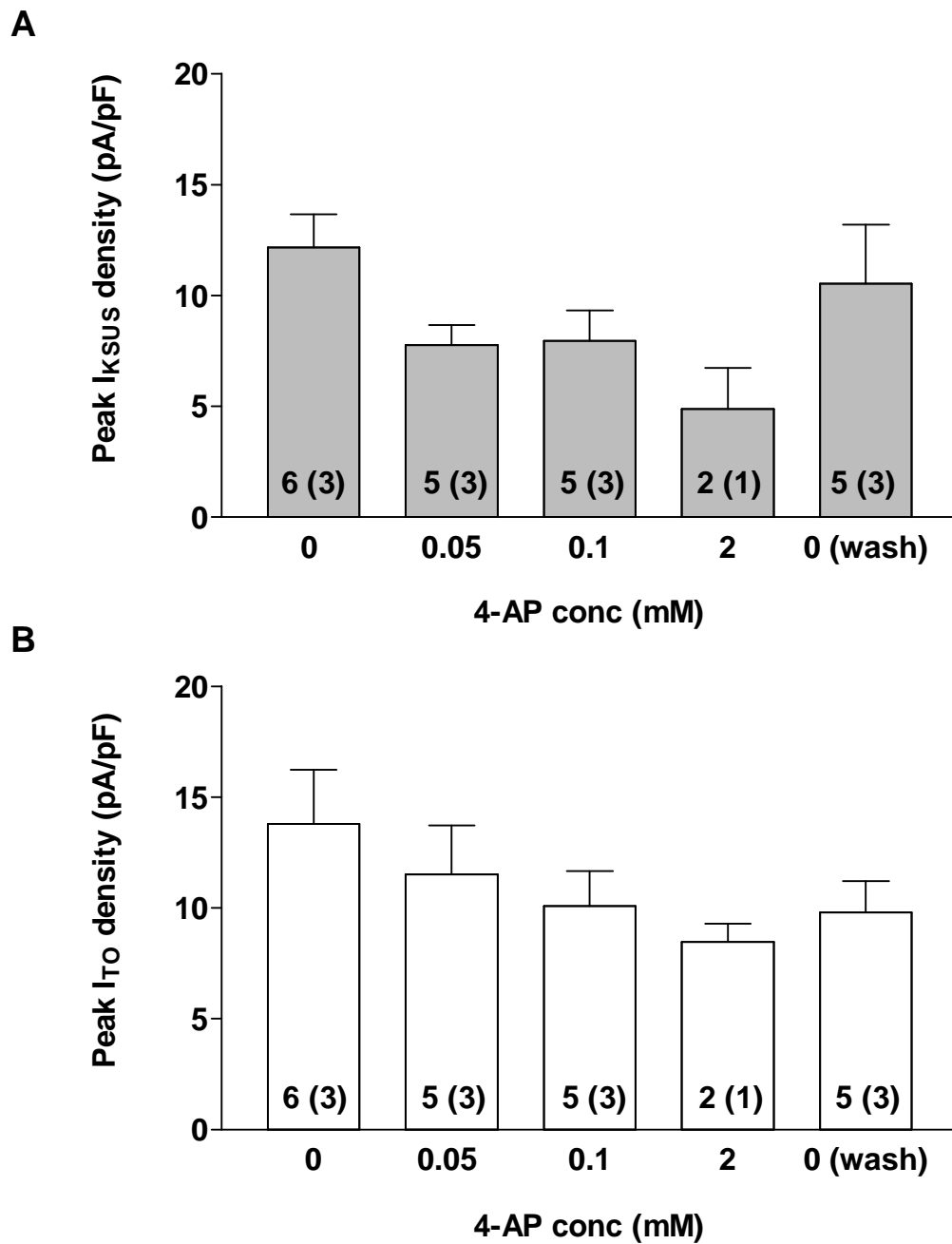


**Figure 2-23** Mean current density of  $I_{KSUS}$  (A) and  $I_{TO}$  (B) at +60 mV after application of varying concentrations of 4-AP. when n(x) indicates the number of cells (n) and patients (x)

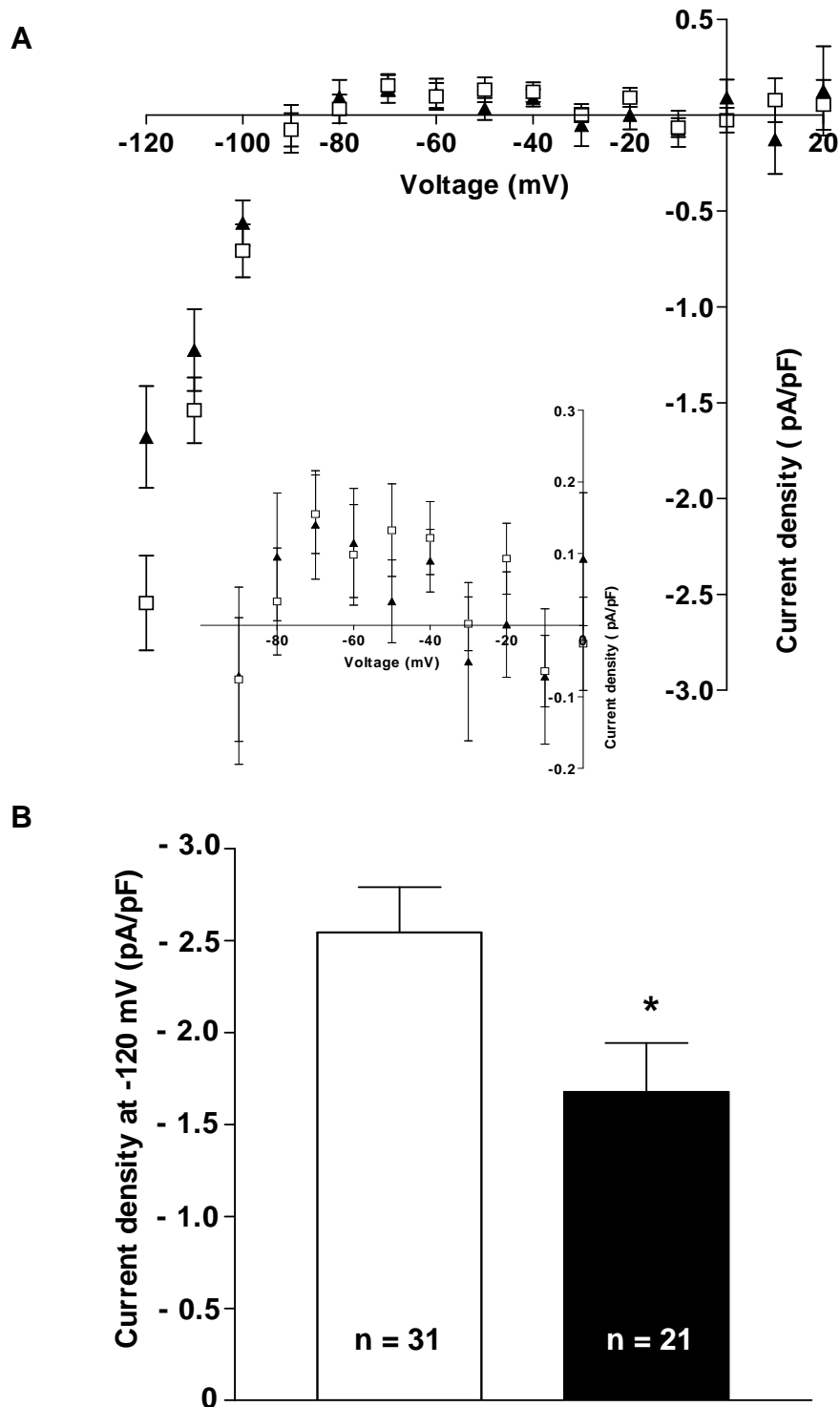


**Figure 2-24** Effects of chronic  $\beta$ -blockade on  $I_{K1}$ . **A** shows the mean current voltage relationship for  $I_{K1}$  in cells from non  $\beta$ -blocked ( $\square$ ) and  $\beta$ -blocked patients ( $\blacksquare$ ). The inset graph shows part of the main graph expanded for small the outward current densities between -80 and -20 mV. Mean peak  $I_{K1}$  density at -120 mV is shown in **B**. \* indicates  $p < 0.05$ , Student's t-test.

cells from non  $\beta$ -blocked patients ( $n = 31$  cells, 12 patients) and  $-1.7 \pm 0.0$  pA/pF in cells from  $\beta$ -blocked patients ( $n = 21$  cells, 11 patients). However, there was no significant difference in current density at voltages less negative than  $-120$  mV in particular, there was no difference in the small outward portion of the current between  $-90$  and  $-30$  mV. This is the portion of the current that would be expected to contribute to terminal repolarisation. There was no current at  $-90$  mV in keeping with the equilibrium potential for  $K^+$ . There was also no net current at around  $-30$  mV as a result of the negative slope conductance of  $I_{K1}$  which may help explain why the cells in this study were depolarised to around this voltage (62).

## 2.5 Discussion

The experiments in this chapter describe the effects of chronic treatment of patients with  $\beta_1$ -selective blockers on repolarising  $K^+$  currents in isolated, right atrial appendage myocytes. There was a significant reduction in the density of  $I_{TO}$  without any change in other properties of the current, specifically its voltage, time or rate dependency. There was also a significant reduction in peak  $I_{K1}$  density but no change in peak  $I_{KSUS}$ .

### 2.5.1 Chronic $\beta$ -blockade and reduction in $I_{TO}$ density: comparison with other studies

This is the first study in which the effects of chronic  $\beta$ -blockade on the characteristics of  $I_{TO}$  have been fully studied. A reduction in  $I_{TO}$  current density in association with chronic  $\beta$ -blockade has already been reported in a smaller retrospective study (29). In that study a 37% reduction in  $I_{TO}$  current density was reported with mean values of  $13.7 \pm 2.1$  and  $8.7 \pm 1.3$  pA/pF in the non  $\beta$ -blocked ( $n = 8$  cells) and  $\beta$ -blocked (10) cells respectively,  $p < 0.05$  (29). In this prospective study, very similar absolute values of  $I_{TO}$  and a similar percentage reduction have been found in larger population of cells and patients.

To my knowledge, no other studies have examined the effects of chronic  $\beta$ -blockade on  $I_{TO}$  in human cardiac myocytes. There are several studies which have examined the effects of either chronic  $\beta$ -blockade or chronic changes in sympathetic innervation in animal hearts. As discussed in chapter 1, the only study to look at the chronic effects of  $\beta$ -blockers on animals showed prolongation of the atrial and ventricular APD in whole tissue after 9 days of treatment with either propranolol or metoprolol (152). That study used microelectrode measurements and did not isolate cardiac myocytes or measure ion currents. In

catecholamine depleted rats, action potentials measured in isolated, perfused left ventricles were prolonged and  $I_{TO}$  density was significantly reduced in isolated ventricular myocytes (153). A reduction in sympathetic innervation of the rat heart, induced by inhibitory antibodies of nerve growth factor during neonatal life, also resulted in a reduction in  $I_{TO}$  density and prolongation of the APD in ventricular cells (85). None of these animal experiments replicate the experimental design of this study but the similarities do provide support for my findings.

Seemingly in contrast to the results of this study, another study looking at transgenic mice with dilated cardiomyopathy showed no change in  $I_{TO}$  following treatment with propranolol for 2 weeks (57). However,  $I_{TO}$  was significantly lower in both the treated and untreated heart failure groups than a non heart failure, untreated control. Perhaps the additional complicating factor of heart failure in these animals is enough to explain the lack of effect of  $\beta$ -blocker on  $I_{TO}$ , particularly, as very few patients in my study had heart failure. Alternatively, the genetic manipulation of the mice may have altered the susceptibility of  $I_{TO}$  to  $\beta$ -blockade.

To further support the role of the adrenergic system as a modulator of  $I_{TO}$ , a number of studies have reported that adrenoceptor agonists can affect  $I_{TO}$ . Cultured, canine, ventricular myocytes have a reduced  $I_{TO}$  density in comparison to freshly isolated cells. Exposure of these cells to isoproterenol, a non selective  $\beta$ -adrenergic agonist, for 24 hrs restored  $I_{TO}$  density to pre-culture levels (60). This perhaps suggests that it may not be the direct effect of  $\beta$ -blockers that reduces  $I_{TO}$  but the unopposed  $\beta$ -adrenergic stimulation that results in a greater  $I_{TO}$  current density in the cells from patients not treated with  $\beta$ -blockers. In contrast to this, another study treated rats with isoproterenol for 7 days, in sufficient doses to induce cardiac hypertrophy, resulting in a reduction of  $I_{TO}$  in isolated ventricular myocytes. (61). However, in this model it is impossible to distinguish between the effects of the  $\beta$ -agonist and the possible synergist or indeed opposing effects of cardiac hypertrophy. It should be noted that both studies looked at the effects of relatively chronic exposure to  $\beta$ -agonists but only ventricular tissue was studied. In contrast,  $\alpha_1$ - adrenergic stimulation appears to reduce  $I_{TO}$  in several animal models as well as humans. This reduction has been shown with both acute and chronic exposure to  $\alpha_1$  agonists in both atrial and ventricular myocytes. However, there does appear to some variation in response between different species and even between different types of cardiac myocytes within the same species (99;154;155).

This study did not examine the effects of either  $\beta$ -agonists or acute application of  $\beta$ -blockers on atrial  $I_{TO}$ . This was partly due to time constraints but primarily reflects an interest in understanding the electrophysiological changes occurring as a result of chronic drug exposure in our patients. Most patients treated with  $\beta$ -blockers tend to continue the drugs for prolonged periods of time and the electrophysiological consequences of chronic drug use are important to establish in their own right, even allowing for any possible anti-arrhythmic actions. The patients in this study were all treated with  $\beta$ -blockers for at least four weeks prior to cardiac surgery. During this time, the exposure to these drugs will have resulted in changes, not only to cardiac tissue, but to the vasculature, the sympathetic nervous system and other organs which, in turn, may further modify the myocardium. Chronic exposure to  $\beta$ -blockers might also be expected to change the responsiveness and or expression of  $\beta$ -adrenoceptors (156;157) which may, in turn, affect how our isolated cells would respond to either acute application of  $\beta$ -blockers or indeed  $\beta$ -agonists. Therefore, acute application of  $\beta$ -blockers on isolated cells would not necessarily be expected to replicate the effects of chronic  $\beta$ -blockade in patients and, what is more, any acute effects on cardiovascular electrophysiology would not necessarily occur via the same mechanisms.

The possibility that chronic  $\beta$ -blockade may have different effects from acute  $\beta$ -blockade has been suggested by several studies. Treatment of patients with oral metoprolol for five weeks was associated with prolongation of the ventricular action potential duration in electrophysiology studies whereas acute, intravenous administration of the drug had no effect on repolarisation (158). The rabbits treated with oral metoprolol or propranolol in Vaughan Williams study did not show any change in atrial or ventricular APD until they had been treated for 9 days. However, studies looking only at the effects of acute  $\beta$ -blockade in humans do report varying results. Intravenous atenolol has been shown to prolong the atrial but not ventricular ERP in a human electrophysiological study (159). Acute intravenous bisoprolol has been shown to increase human atrial FRP and temporarily increase ventricular ERP (160). Low dose intravenous propranolol has been shown to have no significant effect on ventricular repolarisation as assessed by the QT interval (161) whereas, in a different study, higher doses were actually shown to reduce ventricular monophasic APD but have no effect on ventricular ERP (162). The effects on atrial repolarisation were not examined in either study.

The effects of  $\beta$ -blockade on cardiac repolarisation appear to vary considerably. The reasons are likely to be multifactorial, reflecting variations in species, drug dosage, type of  $\beta$ -blocker and methods and site of electrophysiological measurements. None of these

studies describe the effects of either acute or chronic  $\beta$ -blockade on isolated myocytes or the effects on ion currents. It should be noted that two other  $\beta$ -blockers, thought to have additional or possibly different anti-arrhythmic activity compared to “standard”  $\beta$ -blockers, have been reported to affect repolarisation in isolated myocytes with variable effects on ion currents. Sotalol, which has additional class III anti-arrhythmic effects, does prolong the atrial APD acutely but does not affect  $I_{TO}$  (95) and carvedilol, which blocks both  $\alpha_1$  and  $\beta$ -adrenoceptors, prolongs ventricular ADP and reduces rabbit ventricular  $I_{TO}$  in addition to reducing  $I_{CaL}$  and delayed rectifier  $K^+$  currents (33;81).

A number of studies have, therefore, provided support for  $\beta$ -blockers as potential modulators of cardiac repolarisation and  $I_{TO}$ . No other studies are directly comparable with this work and a number of differences have been highlighted between this work and other study designs and results. It would be dangerous to assume that the reduction in  $I_{TO}$  density associated with chronic  $\beta$ -blockade in this study, applies to all human cardiac myocytes, all species or even to  $\beta$ -blockers other than atenolol. The duration of exposure to  $\beta$ -blockade may also be critical. It should be remembered that the behaviour of any isolated cardiac myocyte, even if perfectly unharmed by the removal and isolation process, may not be identical to that in the intact heart within a living human where it is exposed to all manner of other modulating conditions.

### **2.5.2 Chronic $\beta$ -blockade and reduction in $I_{TO}$ density: a true association?**

Does the association between chronic  $\beta$ -blockade and  $I_{TO}$  reduction reflect a direct causal relationship or could there be other factors contributing to the lower  $I_{TO}$  density in the  $\beta$ -blocked patient group? This is a particular problem when dealing with the mixed population of patients within this study as there are numerous patient factors which could not be controlled or matched for and which could potentially affect  $I_{TO}$ . To complicate matters some of these factors are linked to  $\beta$ -blocker use.

Any of the patient characteristics in either group could potentially affect the characteristics of the cells in either group, thereby, affecting  $I_{TO}$ . Alternatively, by chance, the characteristics of the cells could have differed between the two patient groups, skewing the  $I_{TO}$  result. When the cell characteristics were compared, there was no significant difference between the two populations.

When studying the patient characteristics of the two groups the most obvious difference between the  $\beta$ -blocked and non  $\beta$ -blocked patient group is the heart rate. It is possible, therefore, that the reduction in  $I_{TO}$  was due to a reduction in heart rate rather than specifically to  $\beta$ -blocker use. There was no correlation between resting heart rate and  $I_{TO}$  in either group of cells indicating that heart rate alone could not account for the reduction in post-rest  $I_{TO}$  within the  $\beta$ -blocked patient group. This is at least partially supported by evidence from animal models in which pacing induced tachycardia, as opposed to pacing induced bradycardia with atrio-ventricular nodal block, is associated with a reduction in ventricular  $I_{TO}$  (108;114). It should be noted however, that chronic pacing at non physiological rates can have other pathological effects on the heart including causing heart failure which, in itself, is associated with changes in cellular electrophysiology (163).

Age can influence  $I_{TO}$  and this is most marked during neonatal life when  $I_{TO}$  density is significantly smaller than in adults in both animals and humans (164-166). Age was unlikely to play a role in  $I_{TO}$  reduction in this study as all patients were adults and there was no significant difference in mean ages between the non  $\beta$ -blocked and  $\beta$ -blocked patients.

It was not possible within the scope of this study to use multivariate analysis to assess the effects of other patient characteristics on  $I_{TO}$ . I was able to exclude cells from patients with particular characteristics and re-analyse the data to see whether there was still a significant reduction in  $I_{TO}$  in the  $\beta$ -blocked patients. Gender differences and pathological processes like left ventricular dysfunction, myocardial infarction, diabetes and valvular heart disease have all been shown to affect  $I_{TO}$  in human and or animal studies (55;74;99;167-169). Drugs like ACE inhibitors can also influence  $I_{TO}$  (99;167) while others may have the potential to do so. Calcium channel blockers have been shown to affect ventricular  $I_{TO}$  (33) although verapamil does not appear to affect atrial  $I_{TO}$  (170) and nicorandil activates the  $K^+$  channel  $I_{KATP}$  (33). To my knowledge, statins have not been shown to affect  $K^+$  currents but have been reported to have anti-inflammatory actions which may affect cardiac remodelling and have also been shown to reduce the incidence of AF (171;172) However, individually, none of these factors could explain the reduction in  $I_{TO}$  seen in this study. There were, perhaps, insufficient patients once either those taking ACE inhibitors or calcium channel blockers had been excluded from analysis to expect there to still be a significant reduction in  $I_{TO}$  in the  $\beta$ -blocked patients but this reduction was still seen when cell means were analysed.

It would appear that none of the patient characteristics identified in this study, other than chronic  $\beta$ -blockade, were individually responsible for the reduction in  $I_{TO}$  density. It remains possible however, that several linked factors, possibly including chronic  $\beta$ -blockade, could actually be responsible for the reduction in  $I_{TO}$  density rather than  $\beta$ -blocker use alone e.g. the combination of  $\beta$ -blockers, ACE inhibitors and LV dysfunction.

### **2.5.3 Chronic $\beta$ -blockade and other $I_{TO}$ characteristics: a comparison with other studies**

This is the first study to examine the effects of chronic  $\beta$ -blockade on the characteristics of  $I_{TO}$  other than just current density. Chronic  $\beta$ -blockade did not affect the voltage dependency, time dependency of inactivation, reactivation or rate dependency of  $I_{TO}$ . Changes in these characteristics potentially could have contributed to a change in  $I_{TO}$  current density and could have influenced to the “amount” of current available to contribute to repolarisation.

The current characteristics of  $I_{TO}$  vary considerably between species but, even in humans, are affected by numerous factors. These include, the type of cardiac myocytes eg atrial or ventricular, pathology, drugs, cardiac rhythm and experimental conditions including temperature, composition of solutions and methods of isolating and measuring  $I_{TO}$ . This makes it difficult to make any direct comparisons between any absolute values relating to  $I_{TO}$  in this study with others. However, it is possible to compare the current characteristics of  $I_{TO}$  described in this work with the results of other human atrial studies to see if there are any major differences that cannot be easily accounted for and may reflect some other unidentified factor that may affect this current.

Voltage dependent activation of  $I_{TO}$  in human atrial cells can consistently be fitted to single Boltzmann equations with  $V_{0.5}$  values ranging from 1 to 22 mV and slope factors ranging from 8 to 19 mV. Values for voltage dependent inactivation range from -14 to -40 mV for  $V_{0.5}$  and 6 to 15 mV for slope factor (9;35;39;55;164;166). My results are in keeping with these ranges although the  $V_{0.5}$  activation in my study is slightly higher. The variation in these values is likely to reflect different experimental conditions, including temperature, which is certainly known to accelerate  $I_{TO}$  kinetics (35), as well as different mechanisms for separating  $I_{TO}$  from other overlapping currents.

Rapid inactivation is one of the key characteristics of  $I_{TO}$  in all cells. In several studies of human atrial myocytes, time dependent inactivation of  $I_{TO}$  has been described by mono-exponential curve fits with time constants of 12 to 14 ms (9;35;36) at physiological temperature. One other study in addition to this work, has reported a bi-exponential curve fit to  $I_{TO}$  inactivation with fast time constant of 14 to 16ms and slow time constant of around 300 ms (55). The fast inactivation of  $I_{TO}$  reported in all of these studies is in keeping with the results of this study in which the mean fast rate constants approximate to fast time constants of 6 ms. It is possible that the presence and value of a slow time constant is more influenced by differences in the actual process of curve fitting and also the duration of the stimulating voltage pulse.

Reactivation of  $I_{TO}$  has also been reported as being both mono-exponential (38;39;164;166) and bi-exponential (55) in different studies. When mono-exponential reactivation is described, time constants vary from 14 to 17 ms at physiological temperature which is slightly faster than those of this study at around 30 ms. However, this difference is relatively small and may simply reflect differing experimental conditions. One other study has looked at both reactivation and rate dependence of  $I_{TO}$  in human atrial myocytes. It showed no significant change in  $I_{TO}$  density at rates from 0.1-4 Hz but did not examine  $I_{TO}$  at the faster stimulation rates which resulted in reduction in  $I_{TO}$  density in this study (38).

#### **2.5.4 Chronic $\beta$ -blockade and $I_{KSUS}$ : a comparison with other studies**

In this study no change was found in  $I_{KSUS}$  current density between the cells from the  $\beta$ -blocked and non  $\beta$ -blocked patients. This is the first time this has been shown in a large prospective study. This result is supported by the retrospective data analysis of Workman et al who also showed no change in  $I_{KSUS}$  associated with chronic  $\beta$ -blockade in a smaller patient cohort (29). The absolute values for  $I_{KSUS}$  density were similar between that study and this one.

There is limited data to support a role of the  $\beta$ -adrenergic system in modulation of  $I_{KUR}$ . In contrast to the lack of effect of chronic exposure to  $\beta_1$ -selective blockers, acute application of carvedilol has been shown to reduce  $I_{KUR}$  in human atrial myocytes (56). This may represent a distinct difference in the action of carvedilol as compared to other  $\beta$ -blockers or simply the difference in acute versus chronic exposure to the drug. Acute exposure to  $\beta$ -agonists has been shown to increase  $I_{KUR}$  (173). That study was performed at room

temperature although it does not seem likely this would have affected the nature of the current response to isoproterenol although it may have affected the magnitude and/or rate of change. In vivo, particularly in the context of ischaemic heart disease, heart failure and cardiac surgery, there is likely to be considerable activity of both the sympathetic nervous system and endogenous catecholamines. Exposure to  $\beta$ -blockers might be expected block the endogenous  $\beta$ -agonist mediated increase in  $I_{KUR}$  but, under these circumstances,  $I_{KUR}$  would be expected to be higher in the non  $\beta$ -blocked patient group which was not the case. It is possible that this may reflect a combination of the effects of long term exposure to endogenous  $\beta$ -agonists and/or  $\beta$ -blockers with possible associated changes in adrenoceptor receptor expression, in addition to the complicating influence of patient co-morbidities.

In this study  $I_{KSUS}$  was measured as the end pulse current. This current has been shown to be  $K^+$  current distinct from  $I_{TO}$ ,  $I_{K1}$  and  $I_K$  and has properties very similar to the current carried by  $Kv1.5$ , therefore, has been thought to represent  $I_{KUR}$  (90). It remains possible however, that a small proportion of the end pulse current may also consist of a slowly inactivating component of  $I_{TO}$ , other delayed rectifiers and other constitutively active background currents and, it is for this reason, this current was labelled as  $I_{KSUS}$  and not  $I_{KUR}$  in this study. It is possible that this discrepancy between  $I_{KSUS}$  and  $I_{KUR}$  may explain the relative lack of block of the end pulse current using low dose 4-AP although too few cells were studied to accurately establish the degree of  $I_{KSUS}$  block. The lack of full washout also raises the possibility that the current was decaying with time. This was not a feature of later experiments in which relatively long protocols were not associated with significant rundown of either  $I_{KSUS}$  or  $I_{TO}$ . The 4-AP studies were carried out in the early stages of this study and it is possible that suboptimal experimental technique may have resulted in increased current run down. It is also possible however, that the washout phase of 4-AP was simply insufficient for the current to fully recover. Although the differences between  $I_{KSUS}$  and  $I_{KUR}$  are likely to be small, some studies of  $I_{KUR}$  have tried to eliminate these influences by using combinations of long voltage pulses, to eliminate any less slowly inactivating currents and a pre-pulse current, to inactivate  $I_{TO}$ , before measuring the resulting end pulse current (90;93;174). This may result in differences between the results presented here and other studies although the effects of these differences in protocols are likely to be minimal.

### **2.5.5 Chronic $\beta$ -blockade and $I_{K1}$ : a comparison with other studies**

In this study chronic  $\beta$ -blockade was shown to reduce  $I_{K1}$  at -120 mV but, at voltages more positive to this, there was no significant reduction in  $I_{K1}$  density. This is the first study to

examine the effects of chronic  $\beta$ -blockade on human atrial  $I_{K1}$ . An earlier study by Workman et al measured the input resistance of human atrial myocytes as a surrogate of  $I_{K1}$  using a ramp protocol (29). During a ramp protocol only rapidly activating and slowly inactivating currents contribute to the ramp current but, at negative potentials, this could include currents other than  $I_{K1}$  including the so called leak or background currents. Measuring  $I_{K1}$  using a voltage pulse protocol and barium subtraction allows for measurement of a more defined current as well as the ability to directly measure current density at different voltages. Workman et al did detect a reduction in input resistance in cells from patients treated with  $\beta$ -blockers but this could represent either a change predominantly at one particular voltage or across the whole range of the voltage ramp and is not contradictory to the results of this study.

Two studies have examined the effects of carvedilol on  $I_{K1}$  in isolated rabbit ventricular myocytes (81;82). One showed no effect of carvedilol across the voltage range of -100 to + 50 mV using whole cell patch clamping and a square voltage pulse protocol (81). That study did not define the current by using barium subtraction and did not study the current at voltages negative to -100 mV. The other study looked at single  $I_{K1}$  currents from an excised inside-out patch of rabbit ventricular cell membrane, measured at room temperature and without barium. It found no effect of carvedilol on  $I_{K1}$  channel opening (82). These two studies looked at acute application of carvedilol and have suggested a direct blocking action of this drug within the channel pore. This is likely to be a different mode of action than the effect of chronic  $\beta_1$ -selective blockers in this work, as it is unlikely that significant concentrations of the drug remain in my preparations following isolation of the cells. Both of these carvedilol studies differed considerably from this study in terms of experimental technique, protocol and type and species of cardiac myocytes used. Crucially they did not study  $I_{K1}$  at -120 mV and so could not be expected to detect the reduction in  $I_{K1}$  seen in association with chronic  $\beta$ -blockade in this work. In another study, therapeutic concentrations of the non selective  $\beta$ -blocker tilisolol were shown not to affect  $I_{K1}$  current density in isolated, guinea pig myocytes but, again, the maximum negative voltage used was -100 mV (83).

Some experiments have suggested  $\beta$ -adrenergic stimulation may reduce  $I_{K1}$  which would seem to contradict the results of this study (84;175). In one of these studies acute application of isoproterenol significantly inhibited  $I_{K1}$ , not measured by barium subtraction, in isolated human ventricular myocytes, across the whole voltage range from -120 to 0 mV. This effect was prevented by the addition of propranolol (175). That study also showed that the effects of  $\beta$ -adrenergic stimulation on  $I_{K1}$  were reduced in myocytes

from failing hearts. The effects of propranolol alone were not studied. Another study looking at the effects of 48hrs of exposure to isoproterenol in cultured guinea pig ventricular myocytes, demonstrated a reduction in  $I_{K1}$  magnitude across a voltage range of -100 to -70 mV but no change at voltages more positive than -70 mV (84). Again, this effect was reversed by propranolol. Both of these studies show that  $I_{K1}$  can be modulated by the  $\beta$ -adrenergic system. However, the results would suggest that, in my study,  $I_{K1}$  in cells from patients not taking  $\beta$ -blockers might be expected to decrease, reflecting the non antagonised effects of constitutively active sympathetic tone. This is not the case. The relatively low number of patients with heart failure in this study would not explain the difference between this work and the results of these other studies however, it is possible that the influence of other patient characteristics may alter the effects of  $\beta$ -adrenergic modulation of  $I_{K1}$ . A number of other factors including ischaemia, left ventricular hypertrophy and angiotensin II activation, have all been shown to modulate  $I_{K1}$  (74;75;176). Although there is not a marked difference in some of these characteristics between the two patient groups in this study, it is possible that the cumulative effects are enough cause a difference in  $I_{K1}$  density, either by direct effects on the current, or by influencing  $\beta$ -adrenergic modulation. Perhaps more importantly, it should be remembered that there is limited work regarding the effect of  $\beta$ -adrenergic modulation of  $I_{K1}$  and there are marked differences in experimental design between this study and the others described. To my knowledge there are no studies looking at  $\beta$ -adrenergic modulation in atrial myocytes. The potential molecular difference in the composition of  $I_{K1}$  ion channels in atrial and ventricular myocytes may be an important factor in explaining any differences in either the characteristics of the current or its regulation, between these two cardiac chambers (137).

### **2.5.6 Chronic $\beta$ -blockade and reduction in $I_{K1}$ density: a physiologically significant change?**

This study demonstrated a reduction in  $I_{K1}$  current density at -120 mV in association with chronic  $\beta$ -blockade but this effect was not present at more positive voltages. What, if anything, is the physiological significance of this? By convention,  $I_{K1}$  is studied at negative voltages at which a large inward current is generated. However, during an action potential the cell is not hyperpolarised to these voltages. It is possible that even small changes in current density at negative voltages could affect the cell resting membrane potential but no significant difference in  $I_{K1}$  was detected at voltages positive to -100 mV. The resting membrane potential was similar for both groups of cells although the cells

were partially depolarised which prevents any direct comparison of the true resting membrane potential between the non  $\beta$ -blocked and  $\beta$ -blocked patient groups.

If changes in  $I_{K1}$  were to explain the prolongation of the atrial APD in the cells from chronically  $\beta$ -blocked patients it would be expected that the outward component of  $I_{K1}$  would be reduced in cells from these patients. This was not seen in this study and, therefore, it seems unlikely that the reduction in  $I_{K1}$  at -120 mV could have any direct effect on the APD.

Changes in  $I_{K1}$  current density have been reported most frequently in the context of AF. Studies from patients in AF have shown an increase in  $I_{K1}$  that has been postulated to contribute to shortening of the APD, a theory that has been supported by computer modelling (54). One study has suggested an increase in  $I_{K1}$  across a wide negative voltage range using a ramp protocol although only the actual difference at -100 mV was reported (70). Another study, using a series of square voltage pulses but no barium, demonstrated an increase in  $I_{K1}$  but only at -120 mV (2). A significant increase in both the outward and inward components of  $I_{K1}$  in isolated human right atrial appendage cells has only actually been reported in one study (9). The results of these last two studies were used to model the effects of  $I_{K1}$  upregulation on APD duration, however only the maximal change in the inward portion of  $I_{K1}$ , occurring at the most negative voltages in both studies, was applied across the whole voltage range of the AP model (54). This is likely to over represent the true effect of any outward  $I_{K1}$  upregulation on the APD. Interestingly, in another study, an increase in both outward and inward components of  $I_{K1}$  was only detected in isolated left atrial appendage cells in patients with AF with no change seen in right atrial appendage cells (12). These somewhat inconsistent results do raise questions about whether human atrial  $I_{K1}$  is truly remodelled in a disease setting and whether the changes measured  $I_{K1}$  in isolated myocytes are likely to have any real physiological effects.

### **2.5.7 Limitations of experiments**

There are several practical limitations to this work which need to be considered when interpreting the results. Firstly, this was an observational rather than an interventional study and none of the patients from whom tissue was obtained had their treatment altered in any way either as a result of, or specifically for, this study. The major difficulty with this was the number of confounding factors existing for each patient which could potentially mask or contribute to changes in cardiac electrophysiology. The attempt to dissect out the true role of chronic  $\beta$ -blockade has already been discussed. The advantage

of having an observational study is that this patient population should reflect the general population of patients undergoing cardiac surgery in our hospital and, therefore, these results should be representative of a wider “real-life” population. However, it should be noted that selection of patient was not blinded or randomised due to the need to ensure enough non  $\beta$ -blocked patients could be recruited. The very process of agreeing to participate in a study does select out a potentially different population.

The experimental design and protocols themselves have a number of potential problems which need to be considered. All of our tissue was obtained from samples of right atrial appendage as this is a site of access for cardio-pulmonary bypass cannulae. There is evidence to suggest that ventricular  $I_{TO}$  varies across the ventricle wall (40;177) and that there is some variation in  $I_{TO}$  density in different sites of animal atria (178). It is possible that human atrial  $I_{TO}$  may also differ in different parts of the atria and therefore our results may not be applicable to the all cells from both atria.

It is not possible to perfuse the tissue with enzymes, as can be done with animal or whole heart preparations and using the chunk method of cell isolation may result in damage to cells that may affect ion currents. A comparison of these two methods of cell isolation for isolating canine atrial cells did not, however, show a significant effect on  $I_{TO}$  although the delayed rectifier  $I_K$  was affected (179). Unlike animal cell isolations, the yield of healthy, stable and patchable cells in my study was not as high and, those that were patched had less negative resting membrane potentials than would be expected. This may reflect damage to the cells during the isolation process and it is possible that the population of cells that survive are not truly representative of all right atrial appendage myocytes.

In this study attempts were made to isolate  $I_{TO}$  from other, overlapping currents in order to try to accurately record its characteristics. Methods of blocking other ion currents were chosen to try and minimise any detrimental effect on  $I_{TO}$ . It is recognised that cadmium, which was used to block  $I_{CaL}$ , can affect  $I_{TO}$  by altering the voltage dependency of activation and inactivation (180) however, all cells were exposed to cadmium and, therefore, it should not account for the reduction in  $I_{TO}$  density in the  $\beta$ -blocked cells.  $I_{KSUS}$  was not blocked with 4-AP, as preliminary experiments showed doses of 4-AP that did not interfere with  $I_{TO}$  did not even achieve 50% block of  $I_{KSUS}$ . If chronic  $\beta$ -blockade significantly altered the inactivation of  $I_{KSUS}$ , it would impact on the  $I_{TO}$  measurements in these cells however, given the extremely slow inactivation of  $I_{KSUS}$ , the impact of any kinetic changes over the duration of the 100 ms voltage pulse would probably be small.

Other currents including  $Cl^-$  currents and other delayed rectifier currents also contribute to a small degree to the end-pulse current and these currents were neither blocked nor measured. It is possible that chronic  $\beta$ -blockade may have altered any of these currents which, again, would have the potential to affect  $I_{TO}$  measurements in these cells although probably only to a small degree.

In order to measure the voltage dependency of  $I_{TO}$  activation, current was converted into conductance, which involved calculating the reversal potential for  $K^+$  under these experimental conditions. It was assumed that  $I_{TO}$  is carried by a purely  $K^+$  selective channel and, therefore, the reversal potential should be equal to the equilibrium potential for  $K^+$ . It is possible to measure the equilibrium potential by plotting the slope conductance of  $I_{TO}$ . This could be done by using a very brief voltage pulse to fully activate the current and then recording the tail currents as  $I_{TO}$  inactivates to a pre-determined voltages. Some studies have measured the equilibrium potential based on  $I_{TO}$  tail currents and found it to be more positive than my calculated reversal potential between -65 and -70 mV (9;181). This might suggest that the ion channels for  $I_{TO}$  are permeable to other ions but it should be noted that one of these studies was performed in ventricular myocytes and at room temperature which may account for some of the disparity with my results.

When measuring the rate dependency of  $I_{TO}$ , the current was not measured at rates slower than 75 beats/minute. Although this is representative of the mean heart rate of the non  $\beta$ -blocked patients in this study, it is faster than that of the  $\beta$ -blocked patients. It is possible that there is a difference in the rate dependency of  $I_{TO}$  between the two patient groups which is only exists over a narrow range of relatively slow stimulation rates. The physiological significance of such an effect, should it exist, is unclear and it could not account for the reduction in steady state  $I_{TO}$  in the  $\beta$ -blocked cells at higher stimulation rates.

## **2.5.8 Implications of the effects of chronic $\beta$ -blockade on repolarising potassium currents**

### **2.5.8.1 Can a reduction in $I_{TO}$ density alone explain chronic $\beta$ -blocker induced APD prolongation?**

The potential impact of  $I_{TO}$  reduction on APD has already been discussed in chapter 1. A reduction in  $I_{TO}$  may be expected to prolong APD purely by its contribution to early

repolarisation. The reductions in  $I_{TO}$  density in this study were significant across the whole voltage range of activation and not just at +60 mV. This is important when considering the possible impact of this  $I_{TO}$  reduction on APD, as atrial cells usually depolarise to between approximately 20 to 50 mV during the upstroke of the action potential depending on the rate of stimulation (2). The reduction in  $I_{TO}$  demonstrated in this study could therefore be physiologically significant in prolonging early repolarisation.

In the study by Workman et al chronic  $\beta$ -blockade had a greater impact on  $APD_{90}$  than  $ADP_{50}$  which would suggest an additional and, perhaps greater, change in  $K^+$  currents affecting late repolarisation (29). This was not found to be the case in this study, as  $I_{KSUS}$  was not affected by chronic  $\beta$ -blockade and, although  $I_{K1}$  was reduced, its physiological impact on APD is likely to be minimal. Can  $I_{TO}$  reduction alone explain the effect of chronic  $\beta$ -blockade on  $APD_{90}$ ? In addition to its affect on early repolarisation, any reduction in  $I_{TO}$  would be expected to alter the membrane potential at the end of early repolarisation. This would be expected to alter other currents including  $I_{CaL}$  and the delayed rectifiers, even if none of these currents were directly affected by chronic  $\beta$ -blockade.

4-AP has been used to reduce  $I_{TO}$  density by a similar degree to chronic  $\beta$ -blockade resulting in APD prolongation (29). However, 4-AP is not a specific blocker of  $I_{TO}$  and therefore cannot exactly replicate the effects of  $I_{TO}$  reduction on APD. It was hoped that phrixotoxin could be used as a specific blocker of  $I_{TO}$  so it could be applied to cells, when measuring action potentials, in a dose that would mimic the degree of reduction in  $I_{TO}$  seen with chronic  $\beta$ -blockade. However, the lack of effect of phrixotoxin on  $I_{TO}$  in preliminary experiments prevented its use for this purpose. It is unclear why phrixotoxin did not reduce  $I_{TO}$  density. It is possible that the doses of phrixotoxin used were insufficient to cause a reduction in  $I_{TO}$  and these doses only affected  $I_{TO}$  in transfected cells because of the high density of  $Kv4.3$  channels (48). Arguing against this, is a report of similar concentrations of phrixotoxin significantly reducing  $I_{TO}$  in isolated rat ventricular myocytes (48). It is possible that more subtle effects of phrixotoxin on  $I_{TO}$  in atrial myocytes may only have been detected if more cells were studied. Phrixotoxin has been shown to affect  $I_{TO}$  density by altering its voltage dependency of activation and has its greatest effect at voltages of around 20 mV whereas voltage steps to +60 mV were used in my cells. The mechanism by which phrixotoxin has been reported to reduce  $I_{TO}$  does not mimic that of chronic  $\beta$ -blockade which does not affect the voltage dependency of  $I_{TO}$  and, therefore,

phrixotoxin could not have had exactly the same effects on APD even if it had reduced  $I_{TO}$  density.

There are other possible techniques that could be used to test the effects of a reduction in  $I_{TO}$  on APD. Computer modelling could be used to study the impact of  $I_{TO}$  on APD. Some computer modelling has already been done to assess the role of  $I_{TO}$  in determining APD within the ventricle. This has provided conflicting results, showing either no effect on APD (49) or prolongation of APD associated with low densities of  $I_{TO}$  and shortening with high densities (50). Atrial action potentials are different from ventricular action potentials mainly due to the presence of prominent atrial delayed rectifiers like  $I_{KUR}$  (35) and it is possible that changes in  $I_{TO}$  may have a more prominent impact on the atrial action potential due to secondary changes in these currents. If computer modelling were to be used to investigate the consequences of  $I_{TO}$  reduction on APD, the model would have to be representative of a human atrial action potential and, ideally, would be based on an action potential recorded under the same experimental conditions as described here. Computer modelling may also be useful to investigate what, if any, affect  $I_{K1}$  reduction at only negative potentials might have on APD.

The dynamic clamp is another technique which might be useful to further investigate the effects of  $I_{TO}$  reduction on APD. Using this technique the effects of simulated conductances can be tested in living cells. During current clamping the value of the simulated conductance can be calculated by computer, based on the instantaneous membrane potential of the cell and predetermined algorithms describing the conductance. A corresponding current can be injected into the cell and the action potential measured. In order to use this technique to “block” a current, another current of equal magnitude but opposite polarity can be injected into the cell. One such study used this technique to look at  $I_{TO}$  in canine ventricular myocytes and found that “blocking”  $I_{TO}$  reduced the notch in phase 1 repolarisation but did not prolong the APD (182). It would be interesting to use this technique in human atrial cells.

#### **2.5.8.2 What can we tell about the mechanisms of $I_{TO}$ reduction by chronic $\beta$ -blockade?**

It is unclear how chronic  $\beta$ -blockade reduces  $I_{TO}$ . There are a variety of different mechanisms including direct channel block, alteration in ion channel protein or accessory protein expression or alteration in channel protein function. It seems less likely that direct block of the ion pore is the mechanism involved for several reasons. Firstly, one might

expect  $\beta$ -blockade to reduce  $I_{TO}$  in a dose dependent fashion if it were having such a direct action on the channel and this is not the case. Secondly, we believe that the process of cell isolation removes any drugs from the environment of the cells and we would not expect there to be any residual  $\beta$ -blocker present, either bound to our cells or blocking ion channels.

As discussed in chapter 1,  $I_{TO}$  density and other current characteristics have been shown to be linked to expression of both the pore-forming channel protein Kv4.3 and various accessory proteins (97). What is more, the expression of these proteins has been shown to change in association with changes in  $I_{TO}$  under the influence of various cardiac drugs and pathologies including AF (96;99). It is possible therefore, that chronic  $\beta$ -blockade may reduce  $I_{TO}$  by reducing the expression of Kv4.3 or accessory proteins that influence  $I_{TO}$  density and/or Kv4.3 expression. Most accessory proteins, apart from those that are purely involved in Kv4.3 trafficking to the cell membrane like KCHAP, can also modify characteristics of  $I_{TO}$  other than just density. As chronic  $\beta$ -blockade does not alter the voltage, time or rate dependency of  $I_{TO}$ , it suggests that modification of accessory proteins that alter these characteristics is not involved. However, the functions of many accessory proteins have only been studied in expression systems and it may be their functions are different or more limited in a physiological setting, therefore, not ruling out their involvement.

Chronic  $\beta$ -blockade may alter the expression of Kv4.3 or accessory proteins by altering gene expression but may also have effects further downstream, for example, by inducing conformational change in proteins, altering protein phosphorylation or interacting with other signalling pathways which result in altered expression of channel and or accessory proteins. It is also possible that the actual levels of ion channel or accessory protein expression do not change but their functional capacity is altered such that  $I_{TO}$  density is reduced. However, it would seem a reasonable first step to examine the effects of chronic  $\beta$ -blockade on the expression of Kv4.3 and accessory proteins that are known to modify Kv4.3 expression in attempt to explain the reduction in  $I_{TO}$ .

## **CHAPTER 3**

# **EFFECTS OF CHRONIC $\beta$ -BLOCKADE ON ION CHANNEL EXPRESSION**

### 3.1 Introduction

Kv4.3 is the pore-forming protein that forms the ion channel responsible for  $I_{TO}$  in human cardiac tissue (96;97). The cell surface expression of Kv4.3 is an important factor in determining  $I_{TO}$  current density.  $I_{TO}$  current density can also be influenced by a number of accessory proteins including KChIP2, KChAP, Kv $\beta$  subunits and Frequentin (96;97). These proteins can associate with Kv4.3 and regulate its expression and/or function thus potentially modifying, not only the current density, but also other current characteristics including time and voltage dependency. Changes in the expression of Kv4.3 and its accessory proteins have been described in a number of cardiac pathologies including atrial fibrillation and have also been shown to be affected by a number of other factors including cardiac drugs (96;97;99). It is, therefore, possible that the reduction in the  $I_{TO}$  current density associated chronic  $\beta$ -blockade may be explained by changes in the expression of Kv4.3 and/or its accessory proteins.

In this study chronic  $\beta$ -blockade has also been shown to reduce  $I_{K1}$  current density at negative potentials but not to affect  $I_{KUR}$ . There are a number of pore-forming proteins that form the ion channel responsible for human atrial  $I_{K1}$ : Kir2.1; 2.2; 2.3 and possibly TWIK1 (62;97). The pore-forming protein for  $I_{KUR}$  is Kv1.5 (94;97). It is possible that the reduction in  $I_{K1}$  associated with chronic  $\beta$ -blockade may be secondary to a reduction in the expression of some, or all, of its pore-forming subunits whereas the expression of Kv1.5 might be expected to remain unchanged.

A previous study has shown, chronic  $\beta$ -blockade does not affect human atrial  $I_{CaL}$  (29) and therefore would not be expected to change the expression of the pore-forming protein responsible for this current Cav1.2 (97). However, a reduction in  $I_{TO}$  current density and the subsequent slowing of early repolarisation (29) might be expected to influence the calcium entry by prolonging the duration of activation of  $I_{CaL}$ . This may have secondary effects on the cardiac sodium-calcium exchanger (NCX) which utilises the sodium gradient to remove excess calcium from the cell during diastole creating a net inward current (183). It is conceivable chronic  $\beta$ -blockade may affect the expression of NCX1.

Functional changes in ion channels resulting in changes to the currents they carry may occur in a number of ways. Perhaps the most basic, is a change in the absolute amount of one or more protein subunits, pore-forming or accessory. The amount of a particular protein present within a cell can be detected by Western blotting which could be used to compare the abundance of ion channel proteins in tissue from non  $\beta$ -blocked and  $\beta$ -blocked

patients. There are various mechanisms by which the amount of protein within a cell can change and one of these is by altered gene transcription and translation. The abundance of mRNA encoding particular ion channel proteins can be measured as a marker of transcription of the corresponding genes. This can be done using quantitative, real time, reverse transcriptase-PCR (RT-PCR) and, again, compared between tissue from non  $\beta$ -blocked and  $\beta$ -blocked patients.

## **3.2 Aims**

The particular aims of the experiments described in this chapter were:

- To isolate RNA from human atrial tissue
- To use quantitative real time RT-PCR to compare mRNA expression of ion channel pore-forming and accessory subunits in atrial tissue from non  $\beta$ -blocked and  $\beta$ -blocked patients.
- To identify Kv4.3 protein in human atrial tissue samples by Western blotting.
- To use Western blotting to compare Kv4.3 protein expression in atrial tissue from non  $\beta$ -blocked and  $\beta$ -blocked patients.

## **3.3 Methods**

### **3.3.1 Quantification of mRNA by real time RT-PC**

#### **3.3.1.1 Principles of quantitative polymerase chain reaction (QPCR)**

mRNA is transcribed from DNA and encodes the template from which proteins are synthesised or translated. The mRNA within a cell is, therefore, a measure of genetic expression. Quantifying mRNA expression can be technically difficult as it is relatively unstable at room temperature, extremely susceptible to destruction by ribonuclease enzymes and variations in pH. Many cellular proteins are only present in relatively low concentrations and consequently the mRNA encoding these proteins may also be of very low concentration. Techniques to quantify mRNA therefore need to be highly sensitive, if low abundance mRNA is to be detected, highly specific, if only mRNA encoding pre-specified genes is to be quantified and must maintain mRNA stability.

Northern blotting and RNase protection assay are two older techniques for detecting mRNA which can be used to some degree to quantify mRNA expression (184). These techniques have various and different limitations. One of the main problems is that both require the input of relatively large amounts of mRNA and, therefore, are not very useful for quantifying low levels of mRNA expression. They can also be time consuming, prone to RNA degradation and involve the risks of radiation.

Many of these problems were overcome by the development of the polymerase chain reaction (PCR), a highly sensitive technique which allowed the indirect detection of very low levels of mRNA (185). PCR involves the exponential amplification of complementary DNA (cDNA) synthesised from an mRNA template in a reverse transcription reaction (RT). During this amplification process short complementary copies of the cDNA (primers) bind to random or specific parts of single strand cDNA, and are then extended by the polymerase enzyme to make complementary copies of the cDNA using single deoxynucleotide triphosphates (dNTPs). The three steps in a PCR cycle: cDNA separation, primer binding or annealing and elongation occur at different temperatures and by continued cycling through these temperatures the steps can be repeated and the cDNA amplified (see figure 3-1).

Real-time RT-PCR allows for the quantification of mRNA due to the presence of fluorescent reporters which generate fluorescence in direct proportion to the amount of cDNA product in each PCR cycle (186). The amount of fluorescence (or amount relative to background levels:  $\Delta R_n$ ) is monitored during the PCR cycles and, from this, the threshold cycle or  $C_t$  value for the reaction can be determined. This indicates the cycle number at which the fluorescence generated by cDNA copies is detectable above background. Comparing the  $C_t$  values of cDNA copies of different genes allows for the relative comparison of the amount of input cDNA and hence, mRNA expression within a tissue sample. When investigating mRNA expression in different tissue samples, the  $C_t$  values of the cDNA copies have to be normalised to those of housekeeping genes which are expressed to the same degree in all the tissue samples. This ensures the same amount of cDNA for each tissue sample was used at the start of the reaction. Absolute quantification requires reference to a standard curve of fluorescence generated by a known number of cDNA copies.

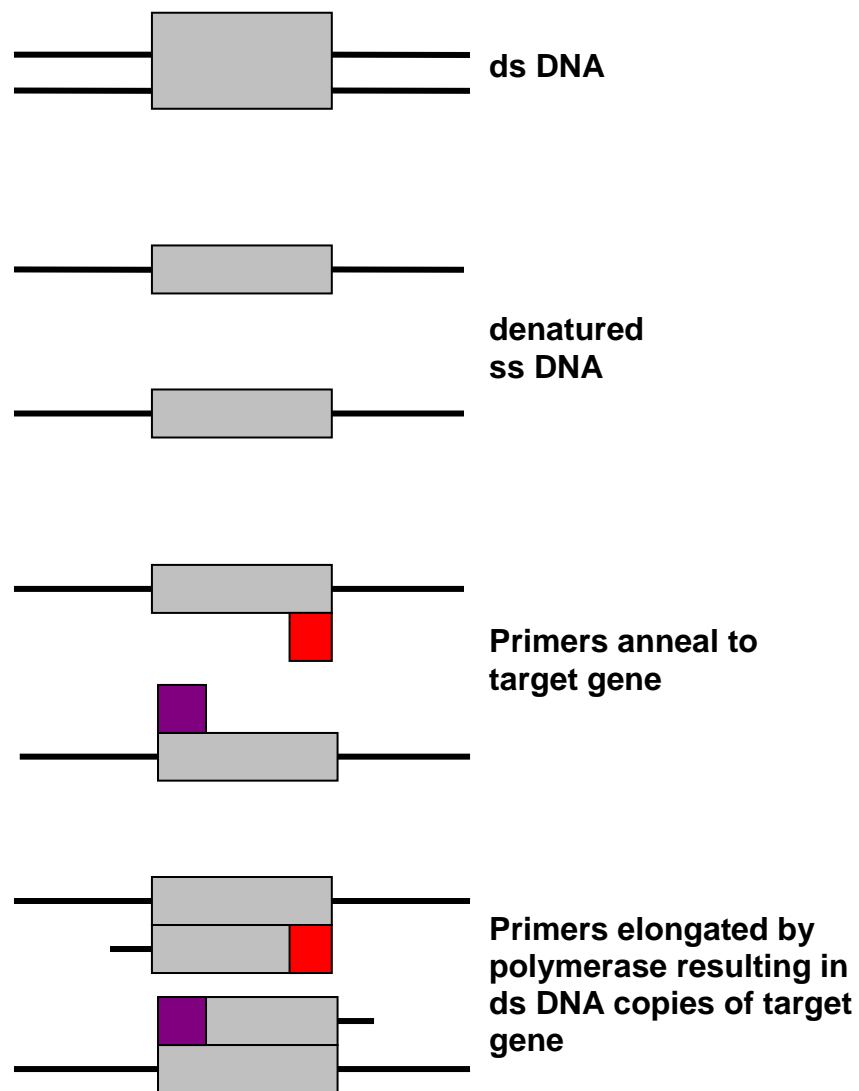


**Figure 3-1** Diagram of the reactions in one PCR cycle. Each cycle can be repeated multiple times resulting in multiple copies of the target gene. ds = double stranded, ss = single stranded, primers represented by red and purple boxes.

The high sensitivity of real time RT-PCR makes this method an ideal tool to study the expression of ion channels in cardiac tissue, where mRNA expression is considered to be low. The methods used to compare the mRNA expression of different ion channel genes in tissues from  $\beta$ -blocked and non  $\beta$ -blocked patients are described in the following sections.

### **3.3.1.2 Obtaining and Storing Tissue**

Right atrial appendage tissue was obtained from 16 consenting patients undergoing coronary artery bypass grafting. All patients were in sinus rhythm at the time of surgery with no documented history of atrial fibrillation. Eight of the patients were treated with  $\beta$ -blockers for at least four weeks before surgery and were compared to eight patients who had not been treated with  $\beta$ -blockers. Tissue was collected in operating theatres at the time of excision, immediately placed in RNAlater solution (Quiagen) and put on ice. The tissue was cut if it exceeded approximately 0.5 cm<sup>3</sup> thick and each section placed in approximately 5 ml of RNAlater. This allowed for stabilisation of the RNA and prevented changes in gene expression due to induction of transcription or degradation of RNA. The tissue was kept at 2°C overnight and then stored at -20°C as per manufacturers recommendations until it was transported on dry ice to the Cardiovascular Research Group in Manchester where the following work was carried out with the help of James Tellez PhD and Professor Mark Boyett.

### **3.3.1.3 RNA Extraction**

#### **3.3.1.3.1 Tissue Preparation**

Each piece of tissue was mounted on a cutting block using OTC Embedding Matrix (CellPath) and dipped in liquid nitrogen to freeze it. The tissue was then sliced into 20  $\mu$ m thick sections using a cryostat (LEICA CM3050S) at -22°C. This method yields a greater amount of high molecular weight RNA than powdering (J. Tellez, personal communication). The cut sections were placed in cryotubes and stored overnight at -80°C. Approximately 30  $\mu$ g of tissue was placed in each tube.

#### **3.3.1.3.2 Protocol for RNA extraction using Quiagen Mini kit**

RNA was extracted from each tissue section using the RNeasy Mini kit (Quiagen) which included pre-prepared buffer solutions. The protocol was a modified version of the manufacturer's instructions (J. Tellez, personal communication). A series of buffers and

mechanical disruption were used to denature cellular proteins, including RNases, and break-up cell membranes in order to release the RNA which could then be extracted using silica columns.

Firstly, the cryotubes of tissue were removed from the freezer and placed on ice. RLT buffer (Quiagen) was heated to 45°C in a waterbath and then 10 µl of β-mercaptoethanol (Sigma) added per 1ml of RLT. Next, 330 µl of RLT+mercaptoethanol were added to each tissue sample which was immediately homogenised for 90 seconds using an Ultraturrax T8 Homogeniser (VWR). Then, 646 µl of molecular grade water (Sigma) was added to each sample followed by 19 µl of proteinase K (Quiagen). Each sample was vortexed and incubated at 45°C for 1hr or until each sample appeared clear.

The contents of each cryotube were then transferred to eppendorfs and centrifuged at 13000 rpm for 15 minutes. The fatty deposit on the surface of each tube was discarded and the remaining supernatant transferred into 15 ml tubes. By this stage the vast majority of proteins including RNases should have been degraded. 1ml of RLT+mercaptoethanol was then added to each tube and vortexed. This increases the salt concentration to favour RNA over DNA precipitation after the addition of alcohol. Next, 1 ml of 100% ethanol (BDH) was added to each tube and vortexed. This promotes binding of the RNA to the silica. 730 µl from each tube was placed onto individual silica columns (Quiagen). Each column was centrifuged at 13000 rpm for 15 seconds, the flow through discarded and a further 730 µl added to each column. This was repeated until all the samples had run through their columns. 700 µl of RW1 buffer (Quiagen) was then added to each column to wash away any remaining proteinase K. The tubes were centrifuged for 15 seconds at 13000 rpm and the flow through discarded. This was repeated once more.

150 µl of DNase (Quiagen) was added to 1050 µl of RDD buffer (Quiagen) and kept on ice. 78 µl of RDD+DNase was added carefully to cover the silica in each column and left for 1 hour. This digested any residual genomic DNA which would contaminate a subsequent PCR reaction. 700 µl of RW1 was added to each column which was then centrifuged for 15 seconds at 13000 rpm and the flow through discarded. 500 µl of RPE buffer (Quiagen) was added to each column which was then centrifuged again for 15 seconds at 13000 rpm and the flow through discarded. Another 500 µl of RPE was added to each column, centrifuged for 2 minutes at 13000 rpm and the flow through discarded. The columns were spun again for 15 seconds at 13000 rpm and any flow through discarded. The columns were then placed in new collecting tubes and 50 µl of molecular

grade water was added to elute the RNA from the silica. This was left for 1 minute before centrifuging for 1 minute at 13000 rpm and the flow through collected. This last step was repeated using another 50  $\mu$ l of water. 9.6  $\mu$ l of 3M sodium acetate (Sigma), pH 5.4, was added to each tube and vortexed. Then 240  $\mu$ l of ethanol and 0.5  $\mu$ l of glycogen (Roche) were added to precipitate the RNA from the water. The tubes were left overnight at -20°C.

Each tube was centrifuged for 30 minutes at 13000rpm at 4°C. The RNA forms a small pellet on the bottom of the tube. The supernatant was removed from each tube and 300 $\mu$ l of 70% ethanol added carefully without disturbing the RNA pellet. Each tube was spun for 5 minutes at 13000 rpm at 4°C. The supernatants were removed, another 300  $\mu$ l of ethanol added to each tube and the tubes centrifuged as before. The supernatants were removed and each pellet left to air dry at room temperature for at least 30 minutes. 15  $\mu$ l of molecular grade water was added to each pellet and the RNA was then stored at -80°C

#### 3.3.1.3.3 RNA quality control and quantifying

In order to achieve reliable quantitative PCR results it is necessary that high quality RNA is used i.e. non degraded RNA, as this will ensure good quality cDNA representative of the extracted RNA. It is also important to measure the concentration of RNA extracted from the tissue so that equal amounts of RNA can be used as templates for generating the cDNA.

Spectrophotometry was used to assess both the quality and quantity of extracted RNA. The concentration of RNA extracted from each sample was measured using a NanoDrop ND-1000 Spectrophotometer (260nm). 1.2  $\mu$ l of each sample was placed in turn onto the sensor after blanking with molecular grade water. The sensor was cleaned between each sample. The quality of the RNA extracted from the tissue was assessed by first ensuring a clean peak absorbance at 260 nm and also by comparing the absorbance at 260 nm versus 280 nm to look for protein impurities.

Eight samples (four from non  $\beta$ -blocked and four from  $\beta$ -blocked patients) were also assessed by looking for 18S and 28S ribosomal RNA bands after electrophoresis on a formaldehyde-agarose gel. Ribosomal RNA (rRNA) is much more abundant than mRNA and can therefore be more easily detected. rRNA consists of two main components 28S and 18S which are 5 and 2 kb respectively. The detection of crisp bands at these molecular weights is considered to be an indication of intact rRNA.

The gel was prepared by first heating 9mls of 10xMOPS buffer, pH7 (Eppendorf) to 55°C in a waterbath. An RNase free gel mould and comb were placed in a cold room. 0.9g of agarose (Nusieve) and 79 mls of deionised water were heated until the agarose dissolved. The solution was then placed in a water bath to cool to 55°C. The warmed 10xMOPS and 1620 µl of deionised 36.5% formaldehyde (Sigma) were then added, the gel poured and left to set in the cold room.

The samples were prepared by making a master mix containing: 100 µl of deionised formamide (Sigma); 33.5 µl of deionised formaldehyde; 32 µl of RNase free water and 25 µl of 10xMOPS+ethidium bromide mix [40 µl of 10xMOPS + 10 µl of 10 mg/ml ethidium bromide (Sigma)]. 19 µl of the master mix were added to 1µl of RNA from each of the eight samples, vortexed and heated to 55°C for 15 minutes. 2 µl of loading buffer (43.5 % glycerol, 2M EDTA, 0.02 % bromophenol blue) were added to each sample, centrifuged at 13000 rpm for 1minute and then loaded into the wells of the gels. One lane of the gel was loaded with a 0.24-9.5kb RNA ladder (Invitrogen).

The gel was covered with a running buffer consisting of 70 ml of 10xMOPS, 617 ml of deionised water and 12.6 ml of deionised formaldehyde. The samples were electrophoresed for 30 minutes at 130 mA. The gel was then removed and the RNA bands visualised using a UV illuminator (BIORAd Gel Doc EQ system). This was possible because the ethidium bromide intercalates with the RNA and emits fluorescence when exposed to UV light. No quantification of the RNA bands was performed.

#### **3.3.1.4 Reverse transcriptase**

The RT reaction produces the first strand of cDNA from the extracted RNA. This is then used as the template for the real time PCR reaction. Errors introduced at this stage will result in inaccurate quantification of the mRNA content of the tissue samples and several steps were taken to try to reduce or eliminate errors. The same amount of RNA from each tissue sample was used for the RT reaction and all samples underwent the RT reaction at the same time using the same master mixes of enzymes and reagents.

All the reagents for the RT reaction were supplied by Invitrogen. A master mix was made containing 17.9 µl of 10mM dNTPs, the building blocks for making the cDNA copy of the input RNA and 17.9 µl of random hexamer primers. These random hexamer primers are short, 6 nucleotide, sequences of cDNA which will bind to different complementary

sequences of RNA and act as the starting point for the reverse transcriptase enzyme to then extend. Random hexamer primers were chosen over gene specific primers as they should result in a copy of all the tissue mRNA which can then be used to look at the expression of multiple different genes. Random hexamer primers were chosen over oligo dT primers which bind to the poly A tail of RNA because of the risk of producing an incomplete mRNA copy due to possible degradation of the poly A tail or disruption of the copy due to secondary structures in the mRNA interfering with the reverse transcriptase reaction. Oligo dT primers would not result in a copy of the rRNA which could not then be used in the analysis of the PCR reaction. A second master mix of RT enzyme and buffers (RT/buffer) was prepared containing: 35.8 µl of 10xRT Buffer; 71.6µl of 25m MgCl<sub>2</sub> (co-factor for the RT polymerase); 35.8 µl of 0.1 M DTT (Dithiothreitol); inhibits RNase activity); 17.9 µl of RNase OUT (an RNase inhibitor) and 17.9 µl of SuperScript III (reverse transcriptase). Superscript III was chosen because it is a mutated version of the M-MLV (Moloney-murine leukaemia virus) enzyme which has less RNase H activity, helping to prevent degradation of the mRNA template and increasing the cDNA yield. It also has a high degree of thermal stability.

Dilutions of each RNA sample were prepared using molecular grade water (2 µg of RNA in 8 µl of solution). 2 µl of the hexamer/dNTPs master mix were added to this, vortexed and briefly spun for 15 seconds at 13000 rpm. The samples were then heated to 65°C using a PCR thermo-cycler (ThermoHybaid PCR Express) in order to denature the RNA. The samples were then immediately put on ice for 3 minutes. While on ice, 10 µl of the RT/buffer master mix was added to each sample. The samples were then incubated at 25°C for 10 minutes in the PCR machine in order for the primers to anneal. The samples were next incubated at 50°C for 50 minutes during which the reverse transcriptase elongated the primers to make the cDNA. A further incubated at 85°C for 15 minutes to stopped the reaction and separated the cDNA from the RNA. The samples were then removed from the PCR machine and a 1:10 dilution made using 3 µl of each sample to use as a working concentration. This was kept at 20°C until required while the remaining neat cDNA was stored at -80°C.

### **3.3.1.5 Quantitative Real time PCR**

#### **3.3.1.5.1 Reagents**

In order to quantify the abundance of mRNA for specific ion channel subunits in each tissue sample, the corresponding cDNA has to identified and amplified. This requires gene

specific primers, a DNA polymerase enzyme, dNTPs and the necessary co-factors. The details for the primers used are shown in tables 3-1 and 3-2. The primers for 28s and Kv4.3 were designed, tested and optimised by J Tellez. All other primers were purchased as part of an optimised assay (QuantiTect) and had previously been used by J Tellez and colleagues. KChIP2 primers [KChIP2 (2)] were also purchased from Applied Biosystems. The DNA polymerase used was AmpliTaq Gold (Applied Biosystems, Power SYBR Green PCR Master Mix). This enzyme is a modified version of the recombinant AmpliTaq enzyme which is based on the naturally occurring Taq (*Thermus aquaticus*) enzyme. One key modification of this enzyme is that it is inactive at relatively low temperatures. This ensures that the elongation phase of the PCR cycle does not begin until the reaction conditions are optimised, resulting in increased yield, increased specificity of end product and allowing the reagents to be assembled at room temperature - "Hot start PCR". In order to quantify the amount of amplified cDNA produced in the PCR reaction, a fluorescent dye called SYBR Green was used. Like ethidium bromide, SYBR green is a non-specific DNA dye which binds to DNA and only fluoresces when it is bound to double stranded (ds) DNA (see figure 3-2). SYBR Green has the advantage of being much less toxic than ethidium bromide. The amount of fluorescence at the end of each cycle is therefore a measure of the amount of ds DNA formed. Because it is a non-specific DNA dye, SYBR green will bind to all newly formed ds DNA and so will measure any DNA that has been amplified by a non-specific primer reaction. This can be minimised by trying to avoid any contamination of the cDNA samples with environmental contaminants and ensuring the primers have been designed to avoid non specific reactions with other genes and cross reactivity with each other to form primer dimers.

#### 3.3.1.5.2 Real time QPCR protocol

A master mix was made up for each new primer containing 252  $\mu$ l of Power SYBR Green PCR Master Mix (Applied Biosystems) which contains AmpliTaq Gold, dNTPS,  $MgCl_2$ , SYBR Green dye and a passive reference dye in an optimised buffer. To this, 50.4  $\mu$ l of one the specific 10x QuantiTect primer assays was added or 20.2  $\mu$ l of the forward primer and reverse primers for either 28S (11.25  $\mu$ M) or Kv4.3 (7.5  $\mu$ M). 453.6  $\mu$ l of molecular grade water was then added to the master mix and vortexed. For each new primer reaction, 1 $\mu$ l of cDNA from each tissue sample and 9  $\mu$ l of the appropriate master mix were placed in three separate wells (i.e. in triplicate) of a MicroAmp optical 96-well reaction plate (Applied Biosystems). For each new primer reaction, 1 $\mu$ l of water and 9  $\mu$ l of master mix were placed in two wells of the plate to act as the negative controls. The plates were then

<b>Target transcript</b>	<b>Accession number</b>	<b>Primer sequence 5'-3'</b>	<b>Fragment length (bp)</b>
28S	AF460236	GTTGTTGCCATGGTAATCCTGCT CAGTACGTCTGACTTAGAGGCGT TCAGTCATAATCCC	133
Kv4.3	NM 004980	TGGCCTTCTACGGCATCCTGCTC GGCGTTCTCCCTCT	84

**Table 3-1** Primer details. Primers designed by J Tellez.

Target transcript	Assay details
hGAPDH	QT01192646
hKChIP2 (1)	QT00016254
hKChIP2 (2)	Hs00752497s1
hKChAP	QT00053158
hKv $\beta$ 1	QT00031136
hKv $\beta$ 2	QT00051961
hKv $\beta$ 3	QT00056931
hFrequenin	QT00038598
hDPP6	QT00080598
hKv4.2	QT00006083
hKv1.5	QT01003177
hKir2.1	QT00001022.
hKir2.2	QT01003296
hTWIK-1	QT00039396
hCav1.2	QT00053480
hNCX1	QT00075376.

**Table 3-2** Primer details. The primers were purchased as part of optimised assays (Quantitect).

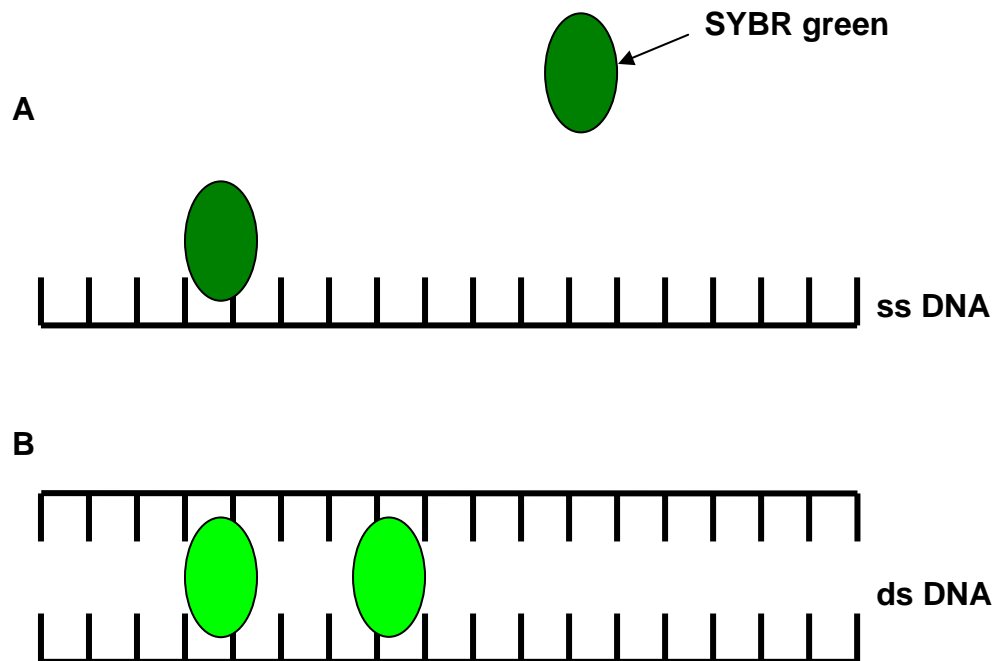


**Figure 3-2** SYBR green reaction. SYBR green does not fluoresce when bound to single stranded DNA or when free (**A**) but does when bound to double stranded DNA (**B**)

spun for a 15 seconds (Multifuge 35 R Heraeus) and covered with an optical adhesive cover (Applied Biosystems).

Each PCR reaction was performed using the 7900HT Fast Real-Time PCR System (Applied Biosystems). Each plate was heated to 95°C for 10 minutes to activate the polymerase followed by 40 cycles of 15 seconds at 95°C and 1 minute at 60°C to denature and anneal/elongate the primers. This was followed by 15 seconds at 60°C and 15 seconds at 95°C to generate melting curves of the reaction products

#### 3.3.1.5.3 Melting curves

SYBR Green will bind to all ds DNA, therefore, potentially, measuring any non specific amplified DNA including primer dimers in addition to the specific amplified target gene. At the end of the PCR cycles the ds DNA products in each well are denatured to generate melting curves and the amount of fluorescence continually measured as the temperature increases. From these curves, melting peaks are automatically calculated by taking the first negative derivative of the melting curve. DNA of different molecular weights and nucleotide compositions will melt at different temperatures. It is possible to compare the melting curve of the actual DNA product with its expected melting point to check the identity of the actual DNA product. However, in this study the presence of one discrete melting peak for each new primer reaction was taken to indicate the formation of a specific amplified DNA product.

#### 3.3.1.6 Analysis

The efficiency (E) of each primer PCR reaction was determined from the fluorescence (F) recorded at the end of each elongation step using the following equation where n is the cycle number.

$$E = \sqrt{F_n/F_{-2n}}$$

This was done for each primer reaction in each tissue sample and used to calculate the mean efficiency for each primer reaction.

The relative abundance of each primer product was calculated by first averaging the  $C_T$  values for each tissue sample from the triplicate reactions. The  $\Delta C_T$  values were then calculated by subtracting the average  $C_T$  value for one of the tissue samples in the same PCR reaction from each of the other mean  $C_T$  values. The same tissue sample was used as the internal control or calibrator for each new primer reaction. The abundance of each primer product including 28S and GAPDH was then calculated using the following equation;

$$\text{Abundance} = E^{\Delta C_T}$$

The abundance of the ion channel subunit in each tissue sample (a) was expressed relative to the abundance of 28S or GAPDH or the mean of the abundance 28S and GAPDH in the same tissue sample (b). This was done using the following equation;

$$\text{Relative abundance} = E^{a \Delta C_{Ta}} / E^{b \Delta C_{Tb}}$$

The mean expression of each ion channel subunit in the tissue samples from the non  $\beta$ -blocked and  $\beta$ -blocked patients was calculated from the  $\Delta \Delta C_T$  values and compared using either a Student's t-test or Mann Whitney test depending on the distribution of the data.

To compare the expression of ion channel subunits relative to each other, the mean  $C_T$  values were not expressed relative to the internal control. The equations were thus modified to:

$$\text{Abundance} = E^{C_T}$$

$$\text{Relative abundance} = E^{b C_{Tb}} / E^{a C_{Ta}}$$

### **3.3.2 Quantification of proteins by Western blotting**

#### **3.3.2.1 Obtaining and storing tissue**

Right atrial appendage tissue was obtained from consenting patients in sinus rhythm undergoing cardiac surgery. The tissue was cut up into small chunks and homogenised using an Ultraturrax T8 Homogeniser (VWR) in 1 ml of protease inhibitor solution containing: 15  $\mu$ l protease inhibitor (Sigma P8340), NaCl 150 mM, KCl 5.4 mM, MgCl<sub>2</sub>

1.2 mM, NaHEPES 5 mM, Glucose 10 mM, CaCl<sub>2</sub> 1.0 mM, pH7.4 with HCl. The tissue was then stored at -80°C.

Rabbit brain and lung tissue was obtained from a New Zealand White rabbit that was being sacrificed for other experiments. The tissue was obtained with the kind assistance of Mr Mike Dunn. Rat brain tissue was kindly provided by Mrs Aileen Rankin from Wistar rats being sacrificed for other experiments. All animal tissue was treated in the same manner as the human tissue.

### **3.3.2.2 Measuring protein concentration**

The concentration of protein in the tissue samples was measured using a modified version of the Bradford Assay. This assay uses Coomassie blue G250 which changes from a red dye with an maximum absorbance of 470 nm to a blue dye with a maximum absorbance of 590 nm when it binds to the arginyl and lysyl residues of proteins. The increase in absorbance at 590 nm can be measured using a spectrophotometer and is a function of the protein concentration. The concentration of protein in an unknown sample can be determined by comparing its absorbance with those of protein standards of known concentrations.

A set of nine dilutions of standard concentrations of a bovine serum albumin (BSA) solution (Pierce) were prepared at 0, 25, 125, 250, 500, 750, 1000, 1500, and 2000 µg/ml using the protease inhibitor solution as the diluent. 10 µl of each solution were then added in triplicate to a 96 well microplate. Dilutions of each tissue sample were prepared using the protease inhibitor solution and added in triplicate to separate wells of the microplate. 300 µl of Coomassie reagent (Coomassie Plus, Pierce) was added to each well starting with the first of every set of triplicates followed by the second and finally the third. The microplate was then placed in the spectrophotometer (Thermo Labsystems Multiskan EX) and mixed for 30 seconds. The absorbance of each BSA standard and the unknown protein dilutions were measured at 595 nm using the well containing the 0 µg/ml BSA solution as a blank. The absorbance of the BSA standards versus concentration was plotted and non linear regression analysis performed using a polynomial fourth order equation (GraphPad PRISM) to generate a standard curve. The concentrations of the tissue dilutions were then determined using the standard curve and a mean concentration for each tissue sample was calculated from the triplicate values.

### 3.3.2.3 Basic Principles of Western blotting

Western blotting, also known as immunoblotting, is a technique which can be used for detection and identification of proteins and can be adapted to allow the relative quantification of proteins (187-189). The technique was first described in 1979 and was developed following methods used to detect DNA (Southern) blotting and RNA (Northern) blotting (190). The basic principles of the Western Blotting are described below and illustrated in figure 3-3 and I am grateful to Julie Russell for teaching me this technique.

Western blotting makes use of sodium dodecyl sulphate polyacrylamide gel electrophoresis (SDS-PAGE) in which a mixture of proteins can be separated strictly on the basis of size. SDS is an anionic detergent which binds to proteins. If proteins are reduced, the same amount of SDS will bind to them per unit of weight regardless of their amino-acid composition. This ensures that all proteins will have the same amount of charge/unit of weight and can be separated on the basis of weight under the influence of an electric current.

The proteins are loaded onto a polyacrylamide gel which is formed from polymerisation of acrylamide and bisacrylamide. These gels consist of two parts, a stacking gel with large pore sizes which allows the proteins to concentrate into sharp bands and a separating gel. The relative amounts of the chemicals within the gel helps determine the size of the pores through which the proteins migrate and the composition of gels can be varied to allow for optimal separation of proteins of different weights. The molecular weight of the proteins loaded onto the gels can be determined by comparison with the migration of calibration proteins of known molecular weights electrophoresed on the same gel.

The separated negatively charged proteins can then be electrophoretically transferred, or blotted, onto nitrocellulose paper. Blotting allows the proteins to be transferred while maintaining their relative positions and resolution and the use of an electric current allows this to be done quickly and efficiently. The purpose of blotting is to allow the subsequent detection of specific proteins using molecular probes or antibodies which is difficult to do while the proteins remain in a gel.

The detection of the proteins bound to the nitrocellulose paper is usually performed using a specific primary antibody which recognises single or multiple epitopes specific to the

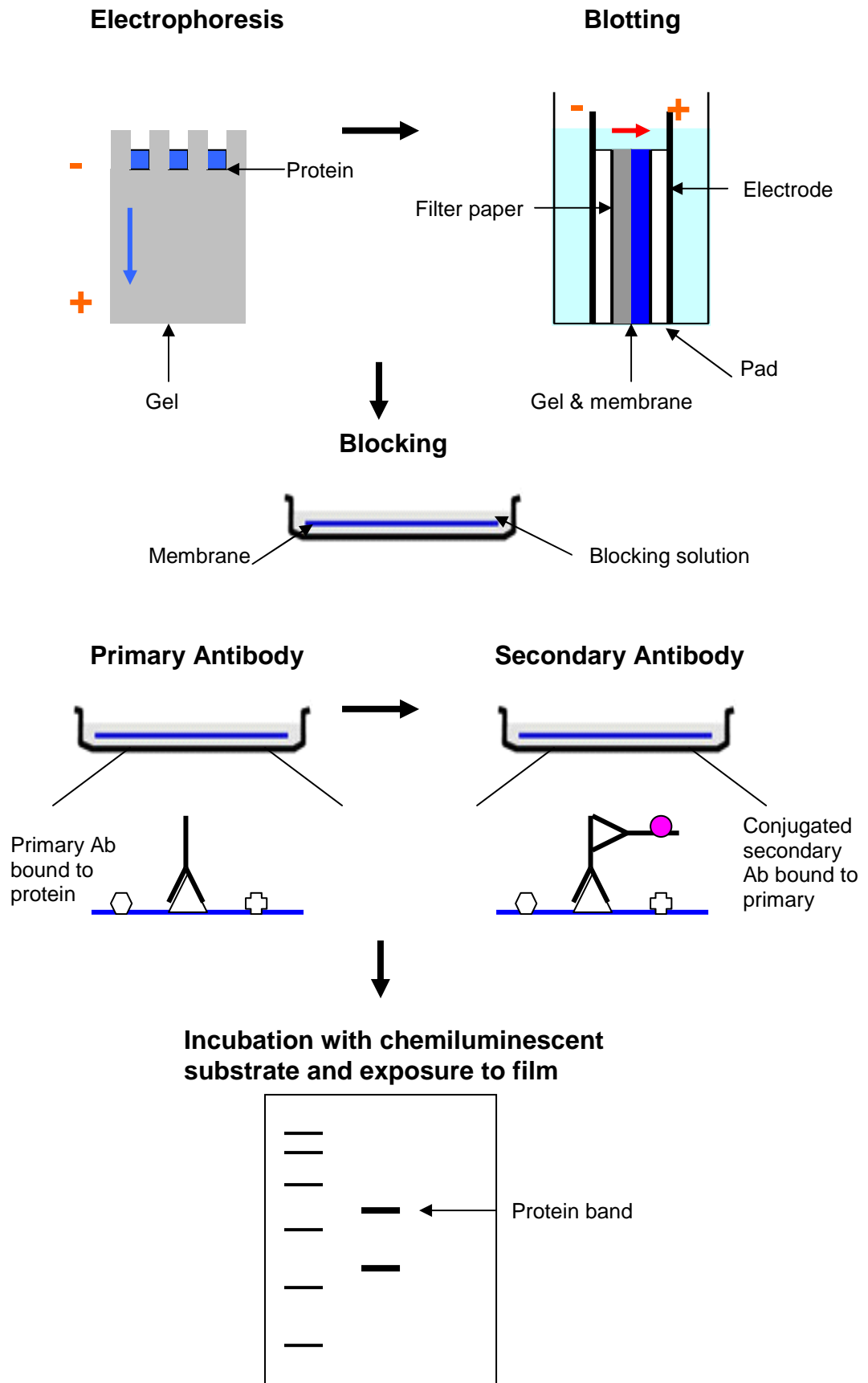


**Figure 3-3** The basic steps involved in Western Blotting.

protein of interest. Before this can be done, it is necessary to block binding sites on the membrane to which the antibody may bind in a non-specific fashion, potentially overwhelming or obscuring the protein-specific reaction. This can be done using a blocking solution containing an inert protein and/or non-ionic detergent.

Once the protein-specific antibody has bound to the protein of interest on the membrane and any excess, unbound antibody removed or washed off, it has to be detected. This can be done in a number of ways, one of which is to use a second antibody which recognises an epitope within the conserved portion of the primary antibody and is conjugated with an enzyme which can be used to indicate the location of the protein. In these experiments any bound secondary antibody was detected using a chemiluminescent substrate which, when catalysed by the enzyme on the bound secondary antibody, emits light that could be detected using film.

#### **3.3.2.4 Protein electrophoresis and transfer**

All solutions and equipment described were purchased from Invitrogen unless otherwise stated.

Tissue samples were thawed and diluted using ultra-filtered water. Various dilutions of the tissue samples were made to allow different amounts of total protein to be loaded onto each gel as specified in the results. Once diluted, 10  $\mu\text{l}$  of each tissue sample were added to 3.75  $\mu\text{l}$  of Nu PAGE LDS Sample Buffer and 1.5  $\mu\text{l}$  of Nu PAGE Sample Reducing Agent, mixed and then heated to 70°C for 10 minutes. The samples were then centrifuged at 1000 rpm for 1 minute to allow all the contents of each eppendorf to collect at the bottom before loading onto either a 12 or 15 well Nu PAGE [gradient (4-12%)] Bis-Tris Gel. Two molecular weight markers, 3  $\mu\text{l}$  of See Blue Plus 2 Pre-stained Standard and 1  $\mu\text{l}$  of Magic Mark Western Standard, were added to 10  $\mu\text{l}$  of sample buffer and, in most experiments, loaded into one or more lanes of the gel. The See Blue marker could be visualised on both the gel and the nitrocellulose membrane and so could be used to help monitor the progress and efficiency of the electrophoresis and transfer. The Magic Mark marker could be visualised on the film after exposure to the chemiluminescent agent and so could be used to measure the molecular weight of any bands detected.

Electrophoresis was performed at 200 V, 200 mA for 50 minutes using XCell Sure lock and PowerEase 500 Supply. The duration of the electrophoresis was initially determined by the time taken for the bromophenol dye in the sample buffer to reach the bottom of the

gel. The running buffer used for the electrophoresis consisted of 50 ml of Nu PAGE SDS MOPS Running Buffer in 950 ml of ultra-filtered water which was used to fill the outer well of the XCell Sure Lock. The central well of the Xcell Sure lock was filled with 200 ml of running buffer containing 0.5 ml of Nu PAGE Antioxidant.

A nitrocellulose membrane (0.45  $\mu\text{m}$  pore) in a filter paper sandwich was prepared by soaking for 2-3 minutes in transfer buffer. The transfer buffer consisted of 100 ml of methanol, 0.5 ml of Nu PAGE Antioxidant, 50 ml of Nu PAGE Transfer Buffer and 850 ml of ultra-filtered water. The membrane was placed on the protein side of the gel with one piece of filter paper placed on top and the other underneath the gel ensuring that there were no air bubbles which would prevent the transfer of the proteins. This sandwich was then placed between transfer pads soaked in transfer buffer and into the XCell II Blot Module. The blot module was placed inside the XCell Sure Lock and then filled with transfer buffer. Water was placed in the XCell Sure Lock around the outside of the blot module. The protein was transferred to the membrane at 30 V, 200 mA for 75 minutes.

The conditions for transfer were optimised by Julie Russell and checked by ensuring the transfer of the See Blue marker. On one occasion, as part of this study, the gel was stained to look for residual proteins to check the efficiency of the transfer. The gel was rinsed three times for 5 minutes each time in approximately 100 ml of ultra-filtered water and then stained by gentle shaking in Simply Blue Safe Stain for one hour at room temperature. The gel was washed again in 100 ml of ultra-filtered water. No protein was detected on the gel.

### **3.3.2.5 Immunodetection of Kv4.3**

#### **3.3.2.5.1 Standard protocol for using a polyclonal anti-Kv4.3 primary antibody**

All solutions and antibodies used were part of the Invitrogen Western Breeze Kit unless otherwise specified. All washes and incubations with blocking solution or secondary antibody were carried out on a rocker (Heidolph Polymax 1040) at room temperature. The membrane was removed from the blot module and placed protein side up in a flat container approximately 10  $\text{cm}^2$  and washed in 20 ml of ultra-filtered water for 5 minutes. The membrane was then blocked for 2 hrs with 10 ml of blocking solution made up of 7 ml of ultra-filtered water, 2 ml of Blocker A and 1 ml of Blocker B. The membrane was washed again in 20 ml water for 5 minutes before being incubated overnight at 4°C in 10 ml of

polyclonal anti-Kv4.3 primary antibody (8 mg/ml, rabbit IgG, Alamone) diluted in blocking solution. Various concentrations of primary antibody were used as detailed in the results section. The membrane was then washed four times in 15 ml of wash solution diluted (1:15) in ultra-filtered water and then incubated for one hour in secondary antibody [anti-rabbit IgG conjugated to alkaline phosphatase (ALP)]. The membrane was then washed again four times in diluted wash solution and three times in ultra-filtered water. The membrane was placed on a transparent plastic sheet and covered with 2.5 ml of chemiluminescent substrate solution made up of 2.375ml of chemiluminescent substrate and 0.125 ml of chemiluminescent substrate enhancer for 5 minutes. After this, excess substrate was blotted off with filter paper and another transparent plastic sheet placed on top of the membrane which was then exposed to X-ray film (Kodak BioMax Light Film, Sigma) in a dark room. The films were developed using a Kodak X-OMAT 1000 processor.

#### 3.3.2.5.2 Modified protocols for using polyclonal anti-Kv4.3 primary antibody

The above protocol was modified in a number of ways to help determine the identity of the bands detected with the primary antibody.

The specificity of the secondary antibody was tested by cutting the membrane in half after the transfer so that half of the lanes could be incubated with both primary and secondary antibody as indicated above and half could be incubated with secondary antibody alone. Each half of the membrane was blocked as described above and, while one half was incubated in the primary antibody diluted in blocking solution, the other half was incubated in fresh blocking solution. Both halves of the membrane were incubated in secondary antibody and developed side by side and at the same time, using the same film.

A different, more sensitive, detection system ECL-advance (Amersham) was also used with this primary antibody. This detection system required the use of a different blocking solution of tris buffered saline (TBS: 140 mM NaCl; 20 mM Tris HCl; pH 7.6; Sigma) containing 0.1% Tween 20 (Sigma) and 2% blocking agent (ECL-advance, Amersham). The secondary antibody used was a horseradish peroxidase-conjugated anti-rabbit IgG (Amersham) diluted in blocking solution as specified in the results. After incubation with both primary and secondary antibodies the membrane was washed once for 15 minutes and then three times for 5 minutes each in TBS with 0.1% Tween 20. 5 ml of the

chemiluminescent substrate solution (ECL-advance, Amersham) was incubated with the membrane for 5 minutes before the membrane was exposed to the X-ray film.

#### 3.3.2.5.3 Standard protocol for using a monoclonal anti-Kv4.3 primary antibody

The monoclonal anti-Kv4.3 primary antibody (Neuromab) was raised in mice and so the only change required to the standard protocol when using this antibody was to change the secondary antibody to an ALP-conjugated anti-mouse IgG (Invitrogen anti-mouse Western Breeze Kit)

#### 3.3.2.5.4 Protocol for pre-incubation of primary antibody with antigen

For these experiments antigenic peptide was obtained from Alomone (0.4 mg/ml). The peptide was added to the primary antibody along with phosphate buffered saline (PBS: 9.1 mM Na<sub>2</sub>HPO<sub>4</sub>; 1.7mM NaH<sub>2</sub>PO<sub>4</sub>; 150 mM NaCl; pH 7.4, Sigma) at concentrations and volumes detailed in the results section. The “antibody alone” solution was made using the same concentration of primary antibody as for the antigenic peptide containing solution and an appropriate volume of PBS so that the total volumes of both solutions were the same. Both solutions were then incubated on the rocker for two hours at room temperature. 10 ml of the blocking solution (Invitrogen Western Breeze kit) was added to each of these solutions. The diluted antigen-antibody solution was then added to one half of a blocked membrane while the diluted antibody alone solution was added to the other half of the blocked membrane and both halves incubated overnight at 4°C. The membrane was then treated according to the standard protocol described in section 3.3.2.5.1.

#### 3.3.2.5.5 Quantification of protein concentration from Western Blots

Once developed the films of the Western Blots were scanned using Fluor-S™ MultiImager (BIO RAD). The digital images were then analysed using Quantity One analysis software (BIO RAD) in order to measure the optical density of the bands. The optical density of each band was normalised to a background optical density of an identical sized area within each lane of the gel where there were no bands. The optical densities for all non β-blocked and β-blocked tissue samples were normally distributed and the mean ± sem were calculated by Student's t-test using GraphPad Prism.

The molecular weights of the bands detected were calculated relative to the molecular weight markers by measuring the distance each band had run using Quantity One, calculating the relative front of each band and then plotted this against the log of molecular

weights of each marker to calculate the values of the unknown bands using Graph Pad Prism. This was done by Julie Russell.

## **3.4 Results**

### **3.4.1 Effects of chronic $\beta$ -blockade on ion channel mRNA expression**

#### **3.4.1.1 Patient characteristics**

The characteristics of all 16 patients from whom tissue samples were obtained and used for mRNA analysis are described in table 3-3. It can be seen that the two patient groups were very similar with the exception of the mean heart rate which, as expected, was lower in the  $\beta$ -blocked patient group although this was not statistically significant. There was one patient in the  $\beta$ -blocked patient group from whom a pre-operative heart rate was not obtained.

#### **3.4.1.2 Assessing the concentration and quality of extracted RNA**

The concentrations of RNA extracted from each tissue sample and measured by spectrophotometry are shown in table 3-4. All the samples had a ratio of  $A_{260}/A_{280} > 1.9$  indicating a satisfactorily pure RNA sample. The concentration of sample 1 is lower in comparison to the others because only the second 50  $\mu$ l containing RNA eluted from the column was collected. The first 50  $\mu$ l was accidentally discarded. Despite this, we felt there was still enough RNA to perform RT-PCR using this tissue sample. Generally the RNA yields were high within the other samples. The mean RNA concentrations for the non  $\beta$ -blocked ( $n = 8$ ) and  $\beta$ -blocked patients ( $n = 8$ ) were  $1268 \pm 195$  ng/ $\mu$ l and  $1602 \pm 145$  ng/ $\mu$ l respectively,  $p=0.19$ .

Eight of the samples of RNA were also assessed by gel electrophoresis to look at the 18S and 28S rRNA bands as shown in figure 3-4. Sample 1 appears very faint partially due to the lower concentration of RNA but also because the gel was thick and was only imaged from one side. Each of the other samples has two distinct bands corresponding to 18S and 28S indicating that the RNA was not degraded.

<b>Patient Characteristics</b>	<b>Non <math>\beta</math>-blocked patients n (%)</b>	<b><math>\beta</math>-blocked patients n (%)</b>	<b>Total patients n (%)</b>
No of patients	8	8	16
Male patients	7 (87.5)	5 (62.5)	12 (75)
Mean age (yrs)	64.8 $\pm$ 2.8	65.5 $\pm$ 1.6.	
Mean heart rate (beats/min)	74.3 $\pm$ 4.0	65.1 $\pm$ 4.1*	
<b>Surgery:</b>			
CABG alone	6 (75)	7 (87.5)	13 (81.3)
AVR alone	2 (25)	1 (12.5)	3 (18.3)
<b>Pre-op Drugs:</b>			
$\beta$ -blockers			
- atenolol	0 (0)	5 (62.5)	5 (31.5)
- bisoprolol	0 (0)	2 (25)	2 (12.5)
- carvedilol	0 (0)	1 (12.5)	1 (6.3)
ACE inhibitors	4 (50)	5 (62.5)	9 (56.3)
CCBs	4 (50)	3 (37.5)	7 (43.8)
Nicorandil	6 (75)	3 (37.5)	9 (56.3)
Statins	7 (87.5)	8 (100)	15 (93.8)
Digoxin	1 (12.5)	0 (0)	1 (6.3)
Amiodarone	0 (0)	0 (0)	0 (0)
<b>Pre-op disease</b>			
MI	2 (25)	2 (25)	4 (25)
Angina	8 (100)	8 (100)	16 (100)
LVSD			
- unknown	1 (12.5)	0 (0)	1 (6.3)
- mild	1 (12.5)	1 (12.5)	2 (12.5)

LVSD (cont)			
- moderate	1 (12.5)	0 (0)	1 (6.3)
- severe	0 (0)	1 (12.5)	1 (6.3)
Hypertension	3 (37.5)	6 (75)	9 (56.3)
Diabetes	2 (25)	2 (25)	4 (25)
Post –op AF	3 (37.5)	0 (0)	3 (18.8)

**Table 3-3** Characteristics of patients treated or not treated with  $\beta$ -blockers prior to cardiac surgery in whom ion channel mRNA expression was measured.

CABG = coronary artery bypass graft, AVR = aortic valve replacement, Pre-op = prior to surgery, ACE = angiotensin converting enzyme, CCB = calcium channel blocker, MI = myocardial infarction, LVSD = left ventricular systolic dysfunction, Post-op = within 1 to 7 days after cardiac surgery.

Sample	RNA concentration (ng/ $\mu$ l)
1	214
2	1805
3	1608
4	1194
5	1059
6	2000
7	1204
8	1063
9	1551
10	1607
11	1439
12	1796
13	1632
14	1303
15	2443
16	1042

**Table 3-4** Concentration of extracted RNA from tissue samples. Samples 1-8 are from non  $\beta$ -blocked patients and samples 9-16 are from  $\beta$ -blocked patients

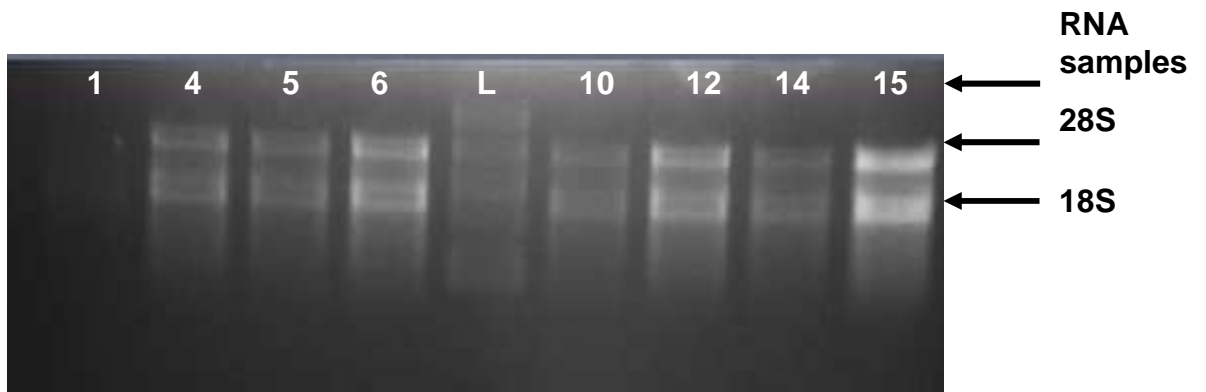


**Figure 3-4** Electrophoresis of RNA samples and a ladder (L) demonstrating the presence of 18S and 28S rRNA band

### 3.4.1.3 Quantifying the expression of 28S rRNA and GAPDH mRNA

The mean abundance of 28S rRNA in the tissue samples from non  $\beta$ -blocked ( $n = 6$ ) and  $\beta$ -blocked ( $n = 8$ ) patients relative to an internal standard is  $0.94 \pm 0.07$  vs  $0.83 \pm 0.10$  respectively,  $p=0.41$ . The mean relative abundance of GAPDH mRNA is  $1.74 \pm 0.19$  vs  $1.85 \pm 0.38$ ,  $p=0.81$ . These results are shown in figure 3-5. 28S was the most abundant of all the primer products measured with lower  $C_t$  values than either GAPDH or any of the ion channel subunits. The change in fluorescence for each PCR cycle for 28S and GAPDH are shown in figure 3-6.

When all eight of the non  $\beta$ -blocked tissue samples are analysed there was much greater variability in  $C_t$  values for 28S than within the  $\beta$ -blocked samples. If the two outlier samples (1 and 6) were included in the analysis of 28S abundance, the data for the non  $\beta$ -blocked samples became non normally distributed with a median value of 0.97 (interquartile range 0.78 to 1.06) compared to a median of 0.80 (0.59 to 0.95) for the  $\beta$ -blocked samples. There remained no significant difference between these groups,  $p=0.23$  (Mann Whitney test). The reason for these outliers is probably due to an error resulting in different concentrations of input cDNA for samples 1 and 6 being used at the start of the PCR reactions. This effect is most obvious for the 28S PCR reaction as this is by far the most abundant primer product tested. If there are significant differences in the amount of cDNA used at the start of PCR reaction the efficiency of the reaction may differ between samples making direct comparisons potentially unreliable. For this reason samples 1 and 6 were excluded from the analysis. It should be noted, however, that for these samples, as for all of the samples there was only a single melting point for 28S and all the other primer products indicating the same, pure PCR DNA product was amplified from each sample (see figure 3-7). Figure 3-7 also shows the melting curves for GAPDH are consistent for all samples but, as expected, are different from those for 28S. In the PCR reaction for GAPDH, no cDNA was detected in the water controls but low levels of cDNA were detected in the PCR reaction for 28S, as seen in both the amplification plots and melting peaks. However, the melting peaks for the water controls are different from those of 28S in the tissue samples and it is likely that the cDNA in the water control is the result of amplified primer-dimers.

### 3.4.1.4 Quantifying the expression of Kv4.3 mRNA and related accessory subunits.

The abundance of mRNA for Kv4.3 and its accessory subunits in each tissue sample was expressed relative to both an internal standard and the mean of the relative abundance of

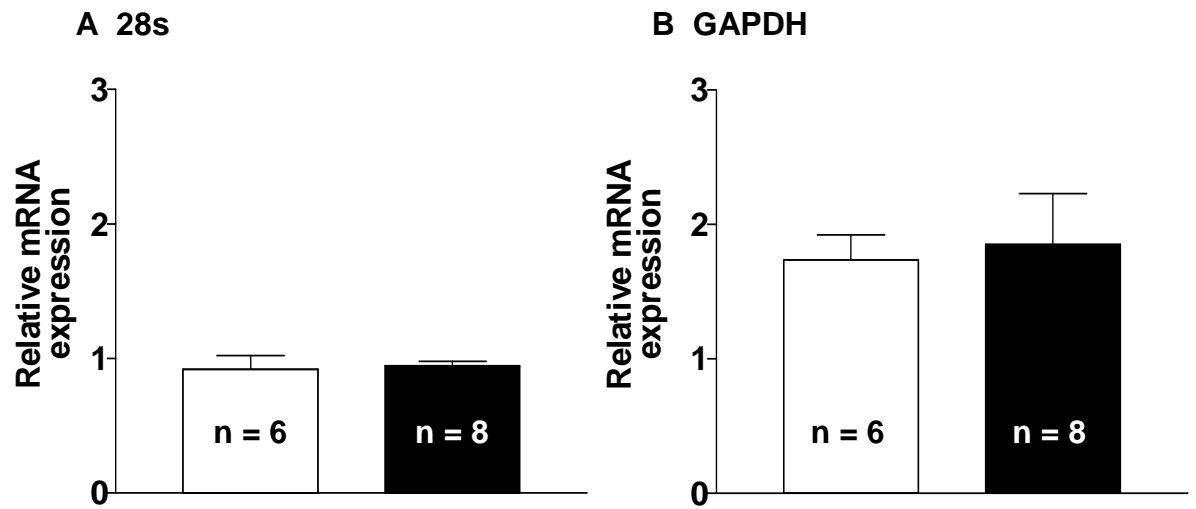


**Figure 3-5** Mean  $\pm$  sem abundance of 28S rRNA and GAPDH mRNA in tissue from non  $\beta$ -blocked ( $\square$ ) and  $\beta$ -blocked ( $\blacksquare$ ) relative to an internal standard in each PCR reaction.  $P > 0.05$

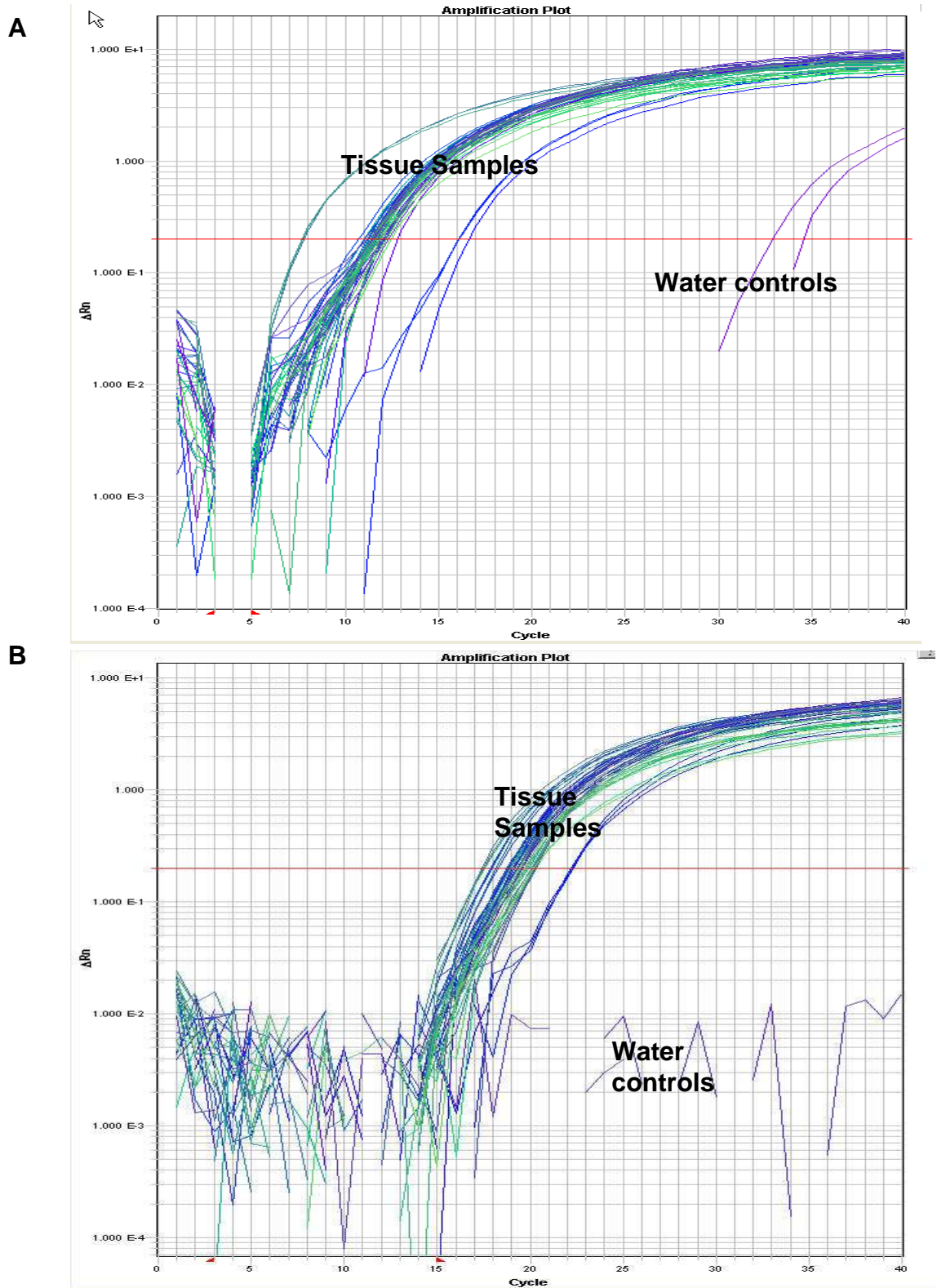


**Figure 3-6** Amplification plots showing the change in fluorescence per PCR cycle for all tissue samples and water controls using 28S (**A**) and GAPDH (**B**) primers. The threshold line is shown in red.

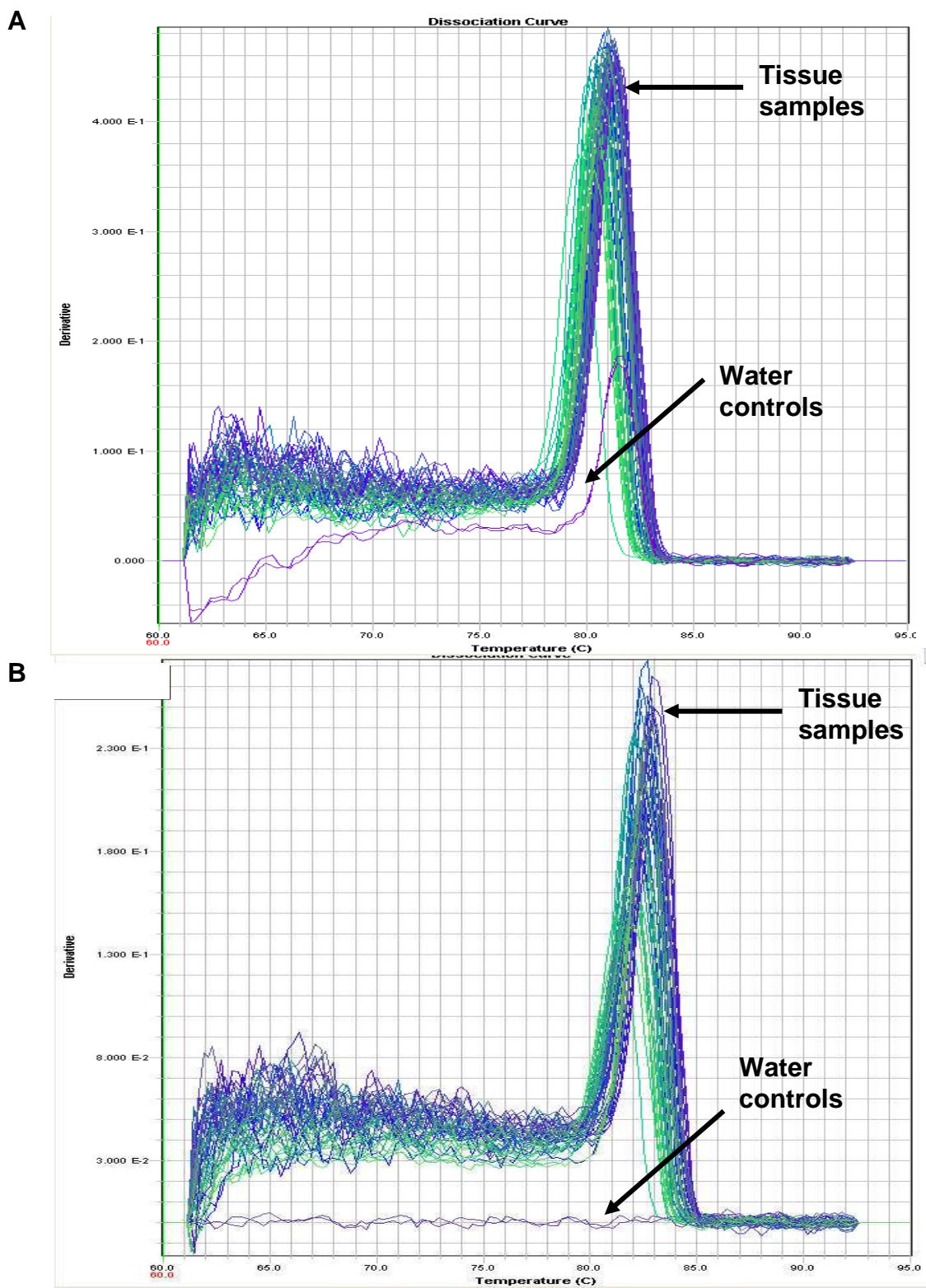


**Figure 3-7** Melting peaks derived from melting curve for cDNA amplified in all tissue samples and two water controls using 28S (A) and GAPDH (B) primers.

28S and GAPDH within the same tissue sample. The mean relative abundances of each ion channel subunit for the tissue samples from non  $\beta$ -blocked ( $n = 6$ ) and  $\beta$ -blocked ( $n = 8$ ) patients are shown in figure 3-8. The mean relative abundance of Kv4.3 mRNA in the tissue from the non  $\beta$ -blocked and  $\beta$ -blocked patients is  $2.09 \pm 0.61$  vs  $1.83 \pm 0.14$  respectively,  $p=0.38$ . If all eight non  $\beta$ -blocked samples are included in the analysis there remains no difference in the median values for relative Kv4.3 abundance at 2.03 (interquartile range 1.63 to 2.25) vs 1.70 (1.57 to 2.01),  $p=0.51$ . There was no difference in the mean relative abundance of mRNA for the accessory subunits associated with Kv4.3: KChIP2 ( $2.23 \pm 0.38$  vs  $2.48 \pm 0.32$ ,  $p=0.69$ ); Kv $\beta$ 1 ( $3.20 \pm 0.53$  vs  $3.75 \pm 0.20$ ,  $p=0.30$ ); Kv $\beta$ 2 ( $1.99 \pm 0.27$  vs  $1.85 \pm 0.15$ ,  $p=0.65$ ); KChAP ( $2.46 \pm 0.32$  vs  $2.46 \pm 0.15$ ,  $p=1.0$ ) and Frequenin ( $2.04 \pm 0.24$  vs  $1.98 \pm 0.15$ ,  $p=0.83$ )  $n = 6$  and  $8$  patients respectively. The mean abundance mRNA for Kv4.3 and the accessory subunits did not differ between the tissue samples from non  $\beta$ -blocked or  $\beta$ -blocked patients when expressed relative to an internal standard and 28S only or an internal standard and GAPDH only as shown in table 3-5

When PCR was first performed using KChIP2 primers from Quantitect the  $C_t$  values were either not identified or too high to be accurate in the majority of the tissue samples. The results shown in this thesis are from a subsequent PCR reaction performed using KChIP2 primers (Applied Biosystems) by James Tellez. PCR was also performed using primers for Kv4.2, Kv $\beta$ 3 and DPP6 but the  $C_t$  values were again not identified or too high to be accurate in the majority of the tissue samples and so further analysis for these primer products was not possible.

The mean abundance of Kv4.3 mRNA and its accessory subunits was also calculated relative to 28S but not an internal control as described in the methods. As no difference was demonstrated in the expression of these ion channel subunits between tissue from non  $\beta$ -blocked and  $\beta$ -blocked patients, the mean abundance of each subunit in all tissue samples was calculated. This allows for a direct comparison between the relative abundance of each ion channel subunit. It can be seen from figure 3-9 that Frequenin, Kv4.3 and KChAP were the most abundant of the ion channel subunits. However, this method of analysis is not as accurate, as the data is not normalised to an internal standard and only limited conclusions should be drawn from this.

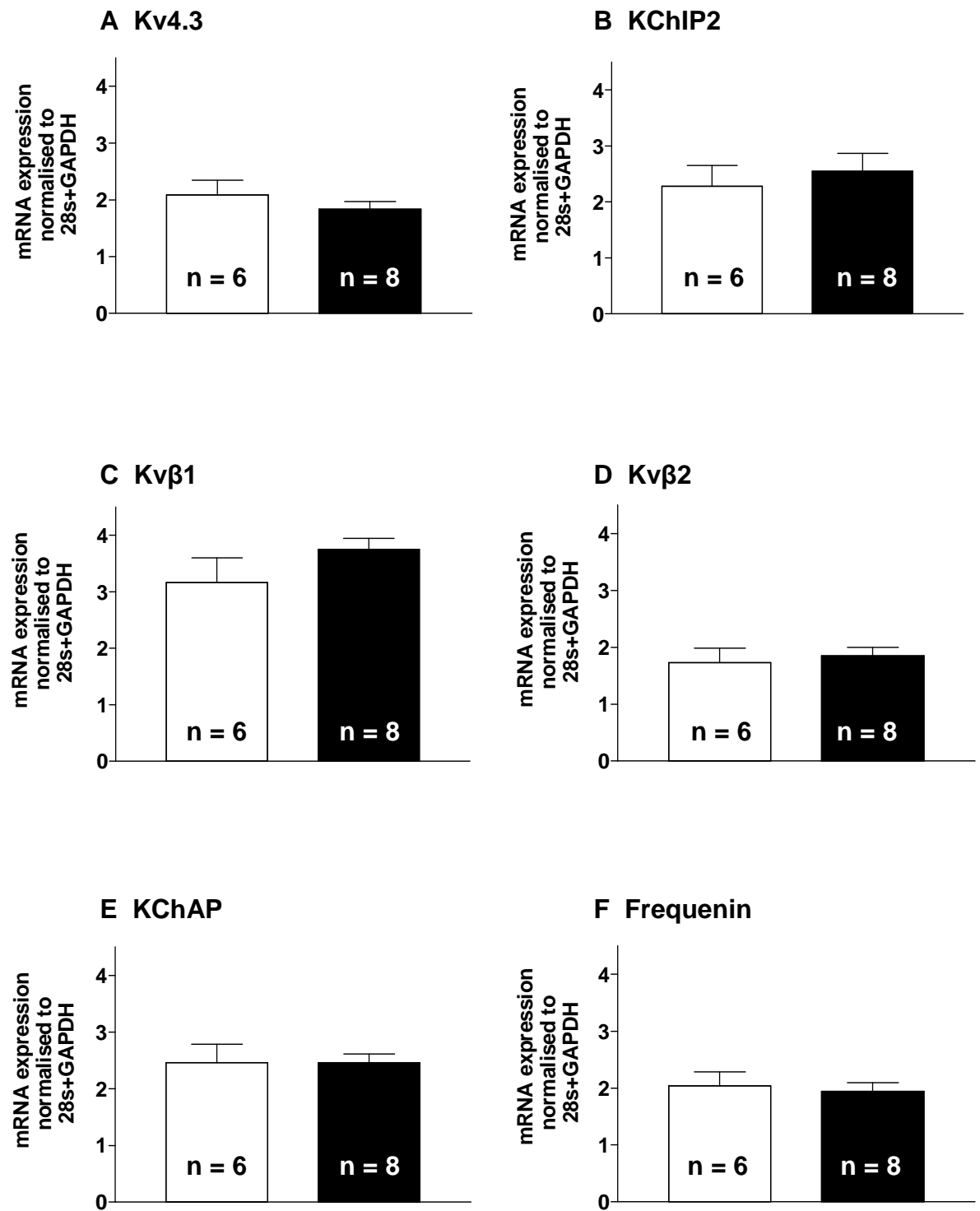


**Figure 3-8.** Mean  $\pm$  sem relative abundance of mRNA of Kv4.3 and various related ion channel subunits in tissue from non  $\beta$ -blocked ( $\square$ ) and  $\beta$ -blocked ( $\blacksquare$ ) patients.

Ion channel subunit	Mean $\pm$ sem abundance relative to 28S (BB No Vs BB Yes)	Mean $\pm$ sem abundance relative to GAPDH (BB No Vs BB Yes)
Kv4.3	2.82 $\pm$ 0.41 vs 2.60 $\pm$ 0.14 p=0.58	1.54 $\pm$ 0.15 vs 1.35 $\pm$ 0.13 p=0.36
KChIP2	3.37 $\pm$ 0.63 vs 3.87 $\pm$ 0.49 p=0.58	1.83 $\pm$ 0.28 vs 1.95 $\pm$ 0.28 p=0.77
KChAP	3.60 $\pm$ 0.52 vs 3.83 $\pm$ 0.37 p=0.79	2.34 $\pm$ 0.54 vs 1.93 $\pm$ 0.13 p=0.84
Kv $\beta$ 1	5.12 $\pm$ 1.10 vs 5.73 $\pm$ 0.34 p=0.31	2.81 $\pm$ 0.43 vs 2.94 $\pm$ 0.19 p=0.33
Kv $\beta$ 2	2.60 $\pm$ 0.43 vs 2.83 $\pm$ 0.26 p=0.85	1.58 $\pm$ 0.24 vs 1.45 $\pm$ 0.12 p=0.50
Frequenin	3.00 $\pm$ 0.57 vs 3.04 $\pm$ 0.25 p=0.96	1.58 $\pm$ 0.14 vs 1.54 $\pm$ 0.12 p=0.66

**Table 3-5.** Mean  $\pm$  sem abundance of mRNA of ion channel subunits in tissue from non  $\beta$ -blocked (BB No) and  $\beta$ -blocked (BB Yes) patients relative to an internal standard and either 28S or GAPDH, n = 6 and 8 respectively..

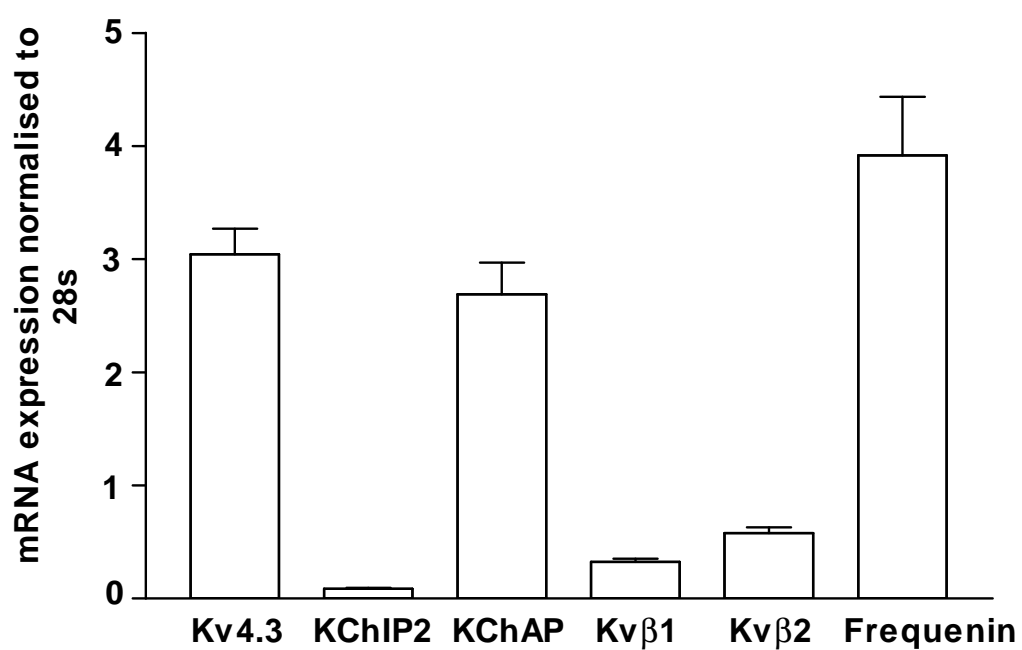


**Figure 3-9** Mean  $\pm$  sem abundance of mRNA for Kv4.3 and related ion channel subunits in all human atrial tissue samples ( $n = 14$  patients) relative to 28S but not an internal standard.

### **3.4.1.5 Quantifying the mRNA expression of other ion channel subunits**

The mean abundance of Kv1.5 mRNA, relative to the mean of the abundance of 28S and GAPDH, in tissue from non  $\beta$ -blocked ( $n = 6$ ) and  $\beta$ -blocked ( $n = 8$ ) patients, was  $1.28 \pm 0.10$  vs  $1.33 \pm 0.13$  respectively,  $p=0.75$ . The relative mean abundance of Kir2.1 was significantly different ( $1.90 \pm 0.21$  vs  $2.56 \pm 0.21$ ,  $p=0.05$ ). However, when the relative abundance of Kir2.1 was expressed relative to 28S ( $2.78 \pm 0.38$  vs  $3.99 \pm 0.45$ ,  $p = 0.07$ ) or GAPDH alone ( $1.54 \pm 0.16$  vs  $2.00 \pm 0.17$ ,  $p=0.08$ ) the difference between the two groups just lost statistical significance. The relative mean abundance of TWIK1 was not different ( $2.04 \pm 0.29$  vs  $2.31 \pm 0.22$ ,  $p=0.47$ ) nor were the relative mean abundances for Cav1.2 ( $2.34 \pm 0.38$  vs  $2.03 \pm 0.26$ ,  $p=0.50$ ) or NCX1 ( $2.30 \pm 0.31$  vs  $2.0 \pm 0.18$ ,  $p=0.40$ ) when all were expressed relative to 28S and GAPDH. These results are shown in figure 3-10. With the exception of Kir2.1, none of the results for the other ion channels changed when the abundance was expressed relative to 28S or GAPDH alone. Quantitative real time PCR was also performed to look at the abundance of Kir2.2 but the Ct values in five of the samples (three from non  $\beta$ -blocked and two from  $\beta$ -blocked patients) were too high to be accurate, suggesting low expression of this subunit.

## **3.4.2 Effects of chronic $\beta$ -blockade on Kv4.3 protein expression**

### **3.4.2.1 Patient characteristics**

The characteristics of all 20 patients from whom tissue samples were obtained for protein analysis are described in table 3-6. It can be seen that there is a significantly lower heart rate in the  $\beta$ -blocked patient group as would be expected.

### **3.4.2.2 Total protein concentration of all human atrial tissue samples**

The concentrations of total protein in the 20 samples of right atrial appendage tissue, as measured using a modified Bradford's assay, are shown in table 3-7. The mean protein concentration for the tissue from the non  $\beta$ -blocked patients ( $n = 10$ ) was  $4.25 \pm 0.56$  mg/ml compared to  $4.65 \pm 0.37$  mg/ml for the tissue from  $\beta$ -blocked patients ( $n = 10$ ),  $p = 0.56$ .

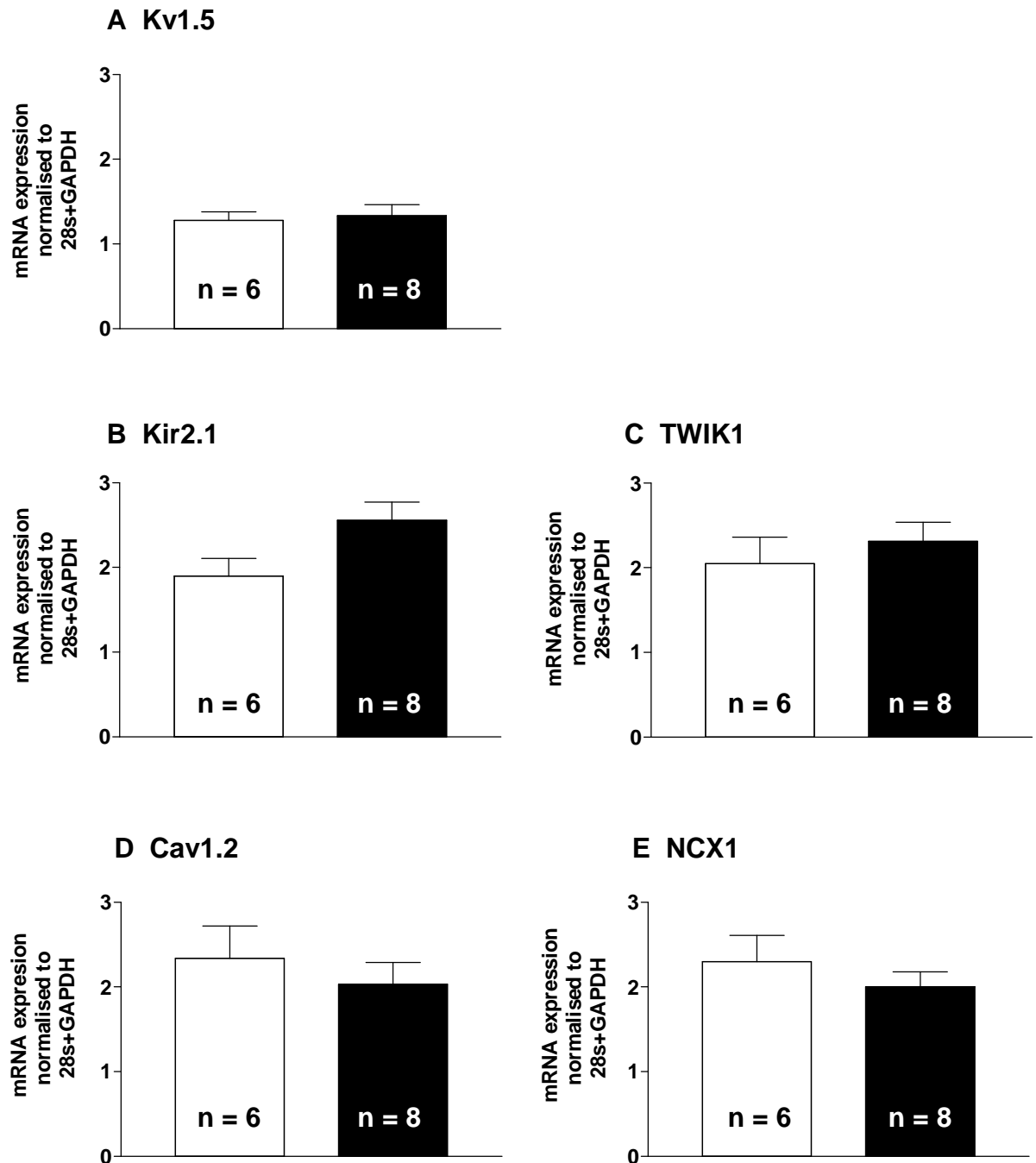


**Figure 3-10** Mean  $\pm$  sem relative abundance of mRNA for Kv1.5, Kir2.1, TWIK1, Cav1.2 and NCX1 in tissue from non  $\beta$ -blocked ( $\square$ ) and  $\beta$ -blocked ( $\blacksquare$ ) patients.  $P > 0.05$  for all except Kir2.1 when  $p = 0.05$ .

<b>Patient Characteristics</b>	<b>Non <math>\beta</math>-blocked patients n (%)</b>	<b><math>\beta</math>-blocked patients n (%)</b>	<b>Total patients n (%)</b>
No of patients	10	10	20
Male patients	6 (60)	6 (60)	12 (60)
Mean age (yrs)	66.7 $\pm$ 3.2	66.3 $\pm$ 2.1	
Mean heart rate (beats/min)	74.3 $\pm$ 3.6	52.9 $\pm$ 2.7*	
<b>Surgery:</b>			
CABG alone	9 (90)	10 (100)	19 (95)
AVR alone	1 (10)	0	1(5)
<b>Pre-op Drugs:</b>			
Beta-blockers			
- atenolol	0 (0)	10 (100)	10 (50)
ACE inhibitors	5 (50)	5 (50)	10 (50)
CCBs	6 (60)	4 (40)	10 (50)
Nicorandil	5 (50)	7 (70)	12 (60)
Statins	10 (100)	10 (100)	20 (100)
Digoxin	0 (0)	0 (0)	0 (0)
Amiodarone	0 (0)	0 (0)	0 (0)
<b>Pre-op disease</b>			
MI	8 (80)	4 (40)	12 (60)
Angina	9 (90)	9 (90)	18 (90)
LVSD			
- unknown	0 (0)	1 (10)	1 (10)
- mild	4 (40)	1 (10)	5 (50)
- moderate	1 (10)	2 (20)	3 (30)
- severe	0 (0)	0 (0)	0 (0)

Hypertension	5 (50)	7 (70)	12 (60)
Diabetes	5 (50)	1 (10)	6 (30)
Post -op AF	1 (10)	4 (40)	5 (25)

**Table 3-6** Characteristics of patients treated or not treated with  $\beta$ -blockers prior to cardiac surgery in whom Kv4.3 protein expression was measured.

CABG = coronary artery bypass graft, AVR = aortic valve replacement, Pre-op = prior to surgery, ACE = angiotensin converting enzyme, CCB = calcium channel blocker, MI = myocardial infarction, LVSD = left ventricular systolic dysfunction, Post-op = within 1 to 7 days after cardiac surgery. \* indicates a significant different from non  $\beta$ -blocked patients ( $p < 0.05$ , Students t-test)

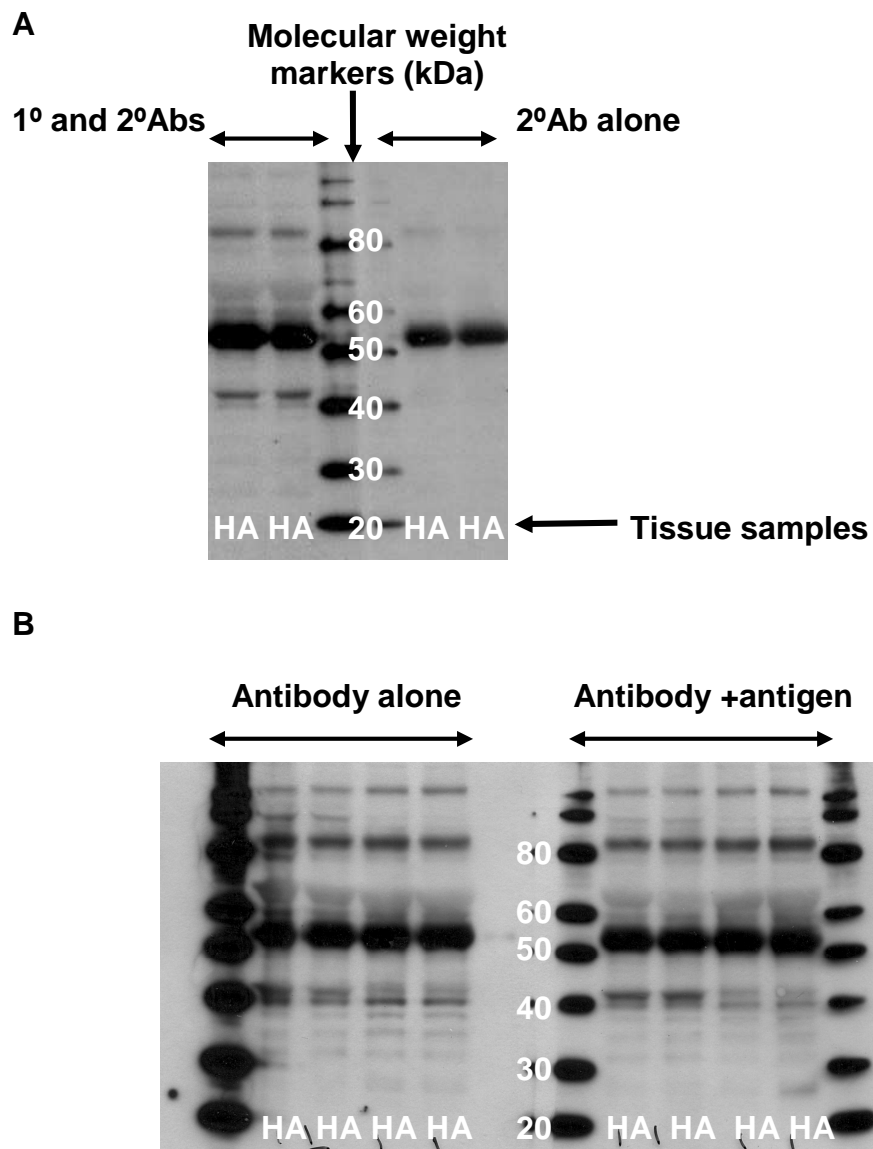
Sample number	Total protein concentration (mg/ml)
1	3.3
2	6.8
3	3.0
4	3.4
5	5.0
6	4.2
7	3.7
8	4.0
9	7.5
10	1.6
11	3.0
12	3.4
13	6.1
14	6.0
15	6.1
16	5.0
17	3.9
18	5.0
19	4.5
20	3.5

**Table 3-7** Total protein concentrations of the tissue samples in which Kv4.3 was measured. Samples 1-10 are from non  $\beta$ -blocked patients and samples 11-20 from  $\beta$ -blocked patients

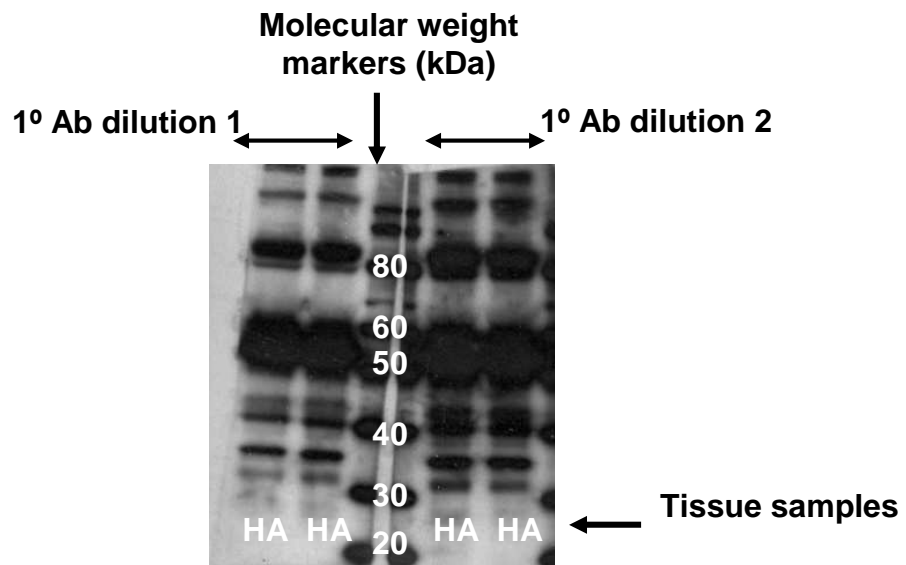
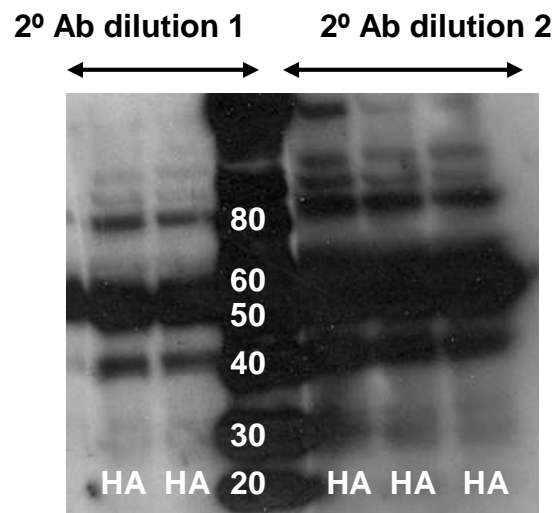
### 3.4.2.3 Characterisation of a polyclonal anti-Kv4.3 primary antibody

Western blotting was performed on a human atrial tissue sample using the standard protocol for the polyclonal anti-Kv4.3 antibody (Alomone) on one half of a membrane and compared with secondary antibody alone on the other half of the membrane (see protocols in methods sections). Approximately 7  $\mu\text{g}$  of total protein was loaded into the four marked wells of the gel and the primary antibody was used at a dilution of 1:800. The resulting film is shown in figure 3-11A. It can be seen that the combination of primary and secondary antibodies detected a dense band between 50 and 60 kDa along with two other distinct bands, one just above 80 kDa and another just above 40 kDa. The band between 50 and 60 kDa was also detected with the secondary antibody alone indicating that some, if not all, of this band was the result of non-specific, secondary antibody binding i.e. the secondary antibody was binding to something other than the primary antibody. There are also several other very faint bands detected between 50 and 80 kDa. In an attempt to help clarify the nature of these bands, a pre-incubation experiment was performed. One half of the membrane was treated with primary antibody which had been incubated in 1ml of blocking solution. The other half of the membrane was treated with primary antibody that had been pre-incubated in antigenic peptide made up to 1ml in blocking solution. The final dilution of primary antibody used to treat both halves of the membrane was 1:533 (a slightly higher concentration than in figure 3-11A) and the ratio of antigen to antibody was 10:1 (further details in the modified protocols section of methods). 10  $\mu\text{g}$  of total protein from the same human atrial sample was loaded into each of the wells of the gel although this was a different tissue sample than used in figure 3-11A. The results of this experiment are shown in figure 3-11B and it can be seen that pre-incubation with antigen does not cause any change in the bands at 80 or 50-60 kDa. There may be a slight decrease in the intensity of in the bands around 40 kDa in the outer lanes of the pre-incubated half of the gel but it is far from convincing.

A number of other experiments were performed in an attempt to clarify the nature of the bands detected with this primary antibody and to see whether any bands representing Kv4.3 were being missed from these early results due to the low concentration of this protein in the tissue samples. Different concentrations of primary antibody and a different, more sensitive, detection system incorporating a different secondary antibody and blocker were used. Figure 3-12A shows the result of using two higher concentrations of primary antibody to see whether any new bands could be detected. It can be seen that there is clearly a double band around 40 kDa which was faintly seen on the previous films and a further two bands between 30 and 40kDa. All the other bands detected on previous films



**Figure 3-11** Western blots characterising the polyclonal anti-Kv4.3 antibody (Alomone) in human atrial tissue (HA). In **A**, the left half of the membrane was treated with both primary (1°Ab) and secondary (2°Ab) antibodies and the right half with only 2°Ab (Invitrogen). In **B**, the left half of the membrane was treated with primary antibody and the right half with primary antibody pre-incubated with antigenic peptide (Alomone).

**A****B**

**Figure 3-12** Western blots characterising the polyclonal anti-Kv4.3 antibody (Alomone) in human atrial tissue (HA). In **A**, the membrane was incubated with high concentrations of 1°Ab, 1 = 1:160 dilution, 2 = 1:100 dilution. In **B**, the 1°Ab was detected using two dilutions of a different 2°Ab, 1 = 1:20000 and 2 = 1:10000, (Amersham) and the bands detected using the more sensitive chemiluminescent detection system (ECL advance, Amersham)

appear darker in this film. Because of the high intensity of the bands in this film the development time was reduced to one minute. Even at this short exposure time the bands still appear very intense.

Other experiments were performed to test the effectiveness of different blocking agents including BSA and Blotto A. These experiments were performed by Julie Russell prior to the work presented in this thesis and are not described here. The most effective blockers for the antibodies used in this work are the ones described in the methods ie Invitrogen Western Breeze blockers.

The results of using the same polyclonal primary anti Kv4.3 antibody at a 1:800 dilution, the more sensitive ECL-advance detection system along with two different concentrations of secondary antibody are shown in figure 3-12B. Three distinct bands were detected for each antibody concentration, one at just above 40 kDa, one large band between 50 and 60 kDa and one band just above 80 kDa. Additional bands above 80 kDa were also clearly visible when using the highest concentration of secondary antibody, although, at this concentration, the other bands started to blur together indicating that the concentration of antibody was too high. Several other concentrations of primary and secondary antibody were used with this detection system the results of which are not shown but this detection system did not seem to offer any benefits compared to the standard Invitrogen Western breeze system.

In an attempt to establish the nature of the bands detected with this polyclonal primary antibody, particularly the bands around 80 and 40 kDa, a positive control was required. It was not possible to purchase a pure source of recombinant Kv4.3 protein to use as a positive control. Attempts to obtain a plasmid containing the cDNA for Kv4.3 in order to transfect cells and isolate Kv4.3 protein also proved unsuccessful. Kv4.3 is known to be highly expressed in brain and its expression in lung tissue is thought to be minimal (105;191). Rat and rabbit brain tissue along with rabbit lung tissue brain tissue were obtained and Western blots performed using these tissue and human atrial tissue and the resulting bands compared. The polyclonal primary antibody was reported to recognise Kv4.3 in these species as well as in humans (Alomone, product information).

An example of Western blot of using these tissue samples is shown in figure 3-13. One half of the membrane was treated with the polyclonal primary antibody (1:800 dilution) according to the standard protocol and the other half treated with secondary antibody alone

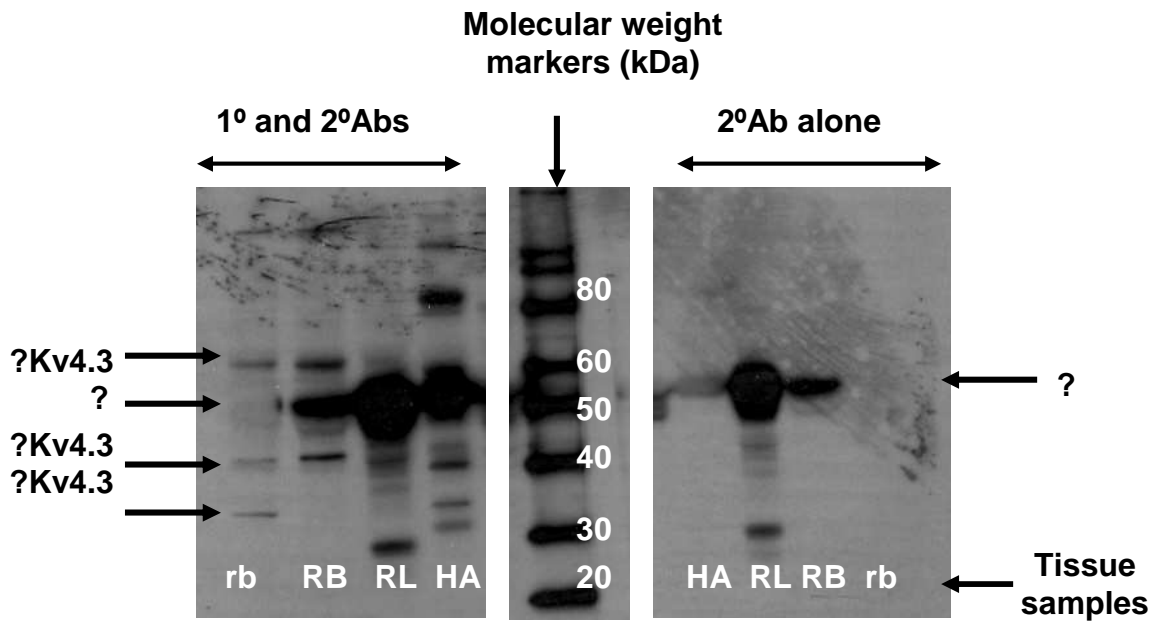


**Figure 3-13** Western blot comparing the polyclonal anti-Kv4.3 1°Ab (Alomone) in human atrial tissue (HA) with rat (rb) and rabbit brain (RB) and rabbit lung (RL). Non specific bands (?) due to 2°Ab binding were demonstrated by treating half of the membrane with 2°Ab alone (Invitrogen). Potential bands representing Kv4.3 are labelled “?Kv4.3”.

(Invitrogen Western Breeze kit). Approximately 10  $\mu$ g of total protein was loaded onto the gel for each tissue sample. Distinct bands can be seen in both brain samples at just above 60 and 40 kDa which were not detected by specific primary antibody binding in the rabbit lung tissue. This would suggest these bands represent Kv4.3. However, no identical bands were detected in the human atrial sample. There was a band detected around 40 kDa in a similar, although not identical, position to that in the positive controls which may represent Kv4.3. No clear band was clearly detected around 60 kDa in the human tissue, although a band at this position was detected faintly in some Westerns using this antibody. In rat brain tissue, another band was detected between 30 and 40 kDa which was not present in the rabbit brain. In the human tissue, two bands were detected between 30 and 40 kDa, the darker of which is at a very similar position to the band in rat brain. This raises the possibility that these bands may also represent Kv4.3. A further band at around 80 kDa was detected in the human tissue which did not correspond to any band detected in the animal samples and the nature of this is unclear. In rabbit brain, lung and human atrium there is a dense band between 50 and 60 kDa which is also present with the secondary antibody alone. The identity of this band is not clear but it is unlikely that it consists only of Kv4.3 protein given the non-specific interaction with the secondary antibody. There are numerous bands detected below 50kDa in the rabbit lung all of which are present with the secondary antibody alone. In summary, the bands most likely to represent Kv4.3 in the brain tissue are those at 40 and just above 60 kDa and possibly one between 30 and 40 kDa. Of these, only the band at 40 kDa is comparable with a band detected in the human atrial tissue

#### **3.4.2.4 Characterisation of a monoclonal anti-Kv4.3 primary antibody**

A monoclonal antibody against Kv4.3 was obtained from Neuromab. Figure 3-14 shows a Western blot of human, rat and rabbit brain and rabbit lung tissue (10  $\mu$ g of total protein was loaded for each sample) using this primary antibody at a 1:100 dilution and compared to secondary antibody alone. Using this primary antibody two very dark bands were detected in the human tissue, one between 50 and 60 kDa and another between 20 and 30 kDa, both of which are detected with the secondary antibody alone. This secondary antibody is different from that used with polyclonal primary antibody being anti-mouse IgG (Invitrogen). In the human atrial tissue, there is also a distinct band just above 60 kDa which corresponds to a much darker band seen at the same molecular weight in the rat and rabbit brain tissue. This band is barely visible in the rabbit lung tissue and not detected by the secondary antibody alone. This monoclonal primary antibody also detects a very faint

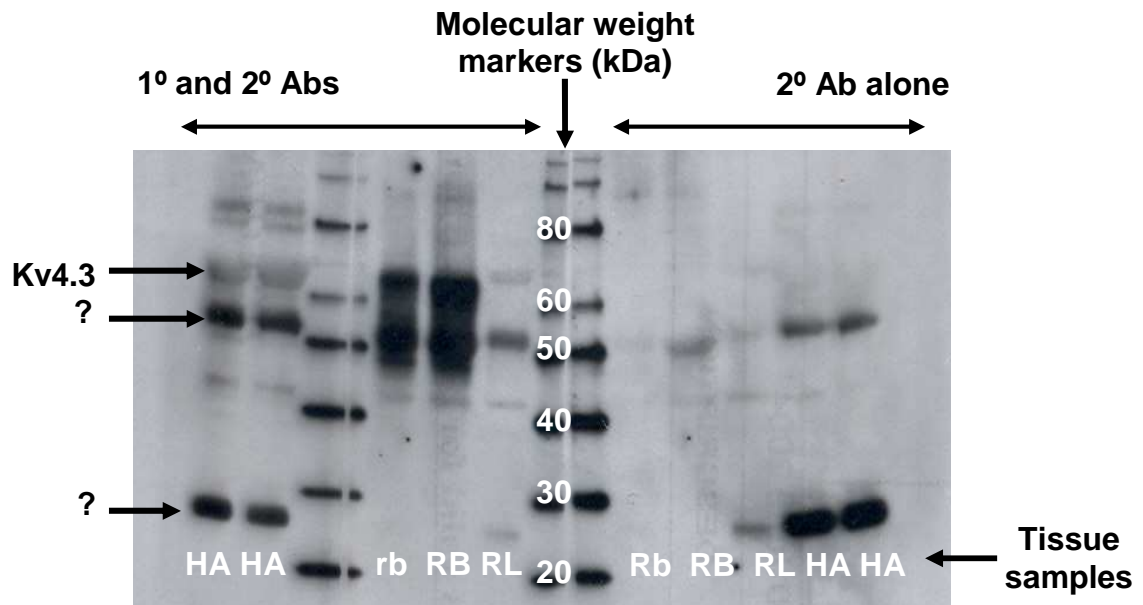


**Figure 3-14** Western blot characterising a monoclonal anti-Kv4.3 1°Ab (Neuromab) in human atrial tissue (HA), rat (rb) and rabbit brain (RB) and rabbit lung (RL). The left half of the membrane was treated with both 1°Ab and an anti-mouse IgG 2°Ab (Invitrogen) while the right half was treated with 2°Ab alone to identify bands due to non-specific 2°Ab binding labelled "?".

band around 40 kDa in the human atrial and animal brain tissue in addition to two very faint bands around 80 kDa in the human atrial tissue.

If figures 3-13 and 3-14 are compared, it can be seen that both the polyclonal and monoclonal anti-Kv4.3 primary antibodies detect a band at the same position just above 60 kDa in the animal brain tissue. In an attempt to further characterise the nature of this band a pre-incubation experiment was planned in which the specificity of the primary antibody would be assessed by pre-incubation with antigenic peptide. If a saturating concentration is used, the antigen should bind all of the primary antibody and, therefore, prevent the primary antibody from binding to any Kv4.3 on the membrane. Unfortunately, the only antigenic peptide that could be obtained was from the company from which the polyclonal primary antibody was purchased (Alomone). This did not contain the same epitope recognised by the monoclonal antibody and, unsurprisingly, an experiment in which this antigenic peptide was pre-incubated with the monoclonal primary antibody (Neuromab) at a ratio of 100:1 did not show any difference in the of the bands detected (results not shown). A pre-incubation experiment was also performed using the polyclonal antibody and antigen in animal brain tissue. 10 µg of total protein was loaded into each well of the gel with duplicates for each sample. One half of the membrane was treated with the polyclonal primary antibody which had been pre-incubated in 0.5ml of PBS and the other, treated with primary antibody that had been pre-incubated with antigenic peptide made up to 0.5ml in PBS. The final dilution of primary antibody used to treat both halves of the membrane was 1:1600 and the ratio of antigen to antibody was 10:1. Both halves of the membrane were treated identically thereafter. The resulting film is shown in figure 3-15. It can be seen that pre-incubation with antigenic peptide prevented the primary antibody from binding to protein at 60 and also 40 kDa in the brain tissue from both the rat and rabbit.

Based on these experiments, the band just above 60 kDa detected with the Neuromab monoclonal primary antibody in human atrial tissue is likely to be Kv4.3 and, when its position was compared to the molecular weight markers, its molecular weight was confirmed as being 65kDa.

#### **3.4.2.5 Characterisation of a monoclonal anti-GAPDH primary antibody**

A preliminary Western blot of varying protein loads of human atrial tissue (30, 25, 20, 15,

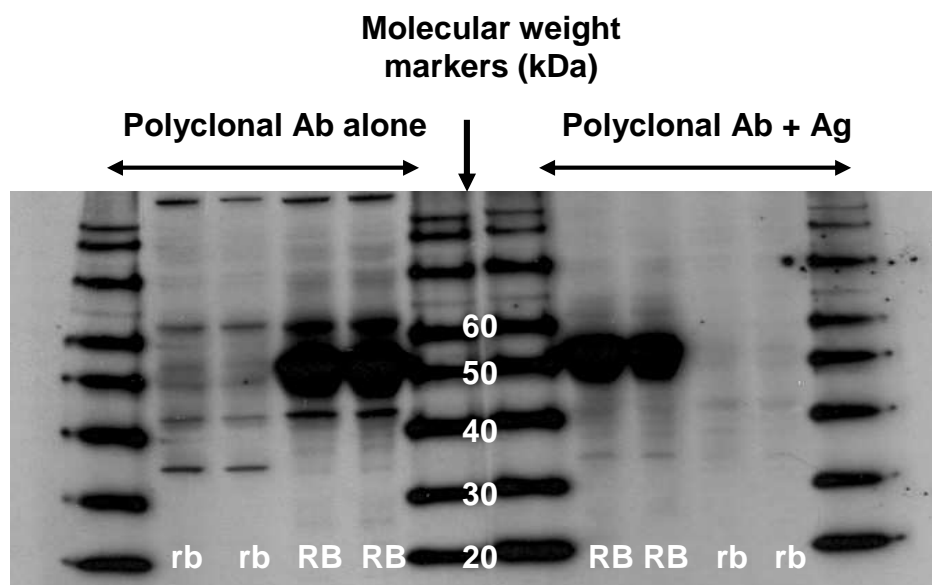


**Figure 3-15** Western blot characterising the nature of the band detected at just above 60 kDa using with the polyclonal anti-Kv4.3 1°Ab in rat (rb) and rabbit brain (RB) tissue. The left side of the membrane was treated with both polyclonal 1°Ab and 2°Ab whereas the right side was treated with an identical concentration of polyclonal 1°Ab pre-incubated with antigen (Ag) in addition to 2°Ab.

10, 8 and 7  $\mu\text{g}$ ) treated with a monoclonal anti-GAPDH primary antibody (1:1000 dilution) was performed in order to confirm the position of the band(s) detected with this primary antibody. This was compared with a previous Western blot of the same human atrial tissue sample (10  $\mu\text{g}$  total protein loaded in two lanes of the gel), in addition to animal tissue, treated with the same secondary antibody but no primary antibody. This allowed the identification of any bands detected as a result of a non specific secondary antibody reaction. Films of these blots are shown in figure 3-16. It can be seen that the combination of primary and secondary antibodies resulted in the detection of three bands; one between 50 and 60 kDa, one just below 40 kDa and one between 20 and 30 kDa. There are additional very faint bands at 30, 40 and several around 80 kDa. The secondary antibody alone detected similar bands between 50 and 60 kDa and between 20 and 30 kDa, suggesting the only band detected as a result of a specific primary antibody reaction is the band just below 40 kDa

#### **3.4.2.6 Establishing a linear relationship between optical density and total protein for GAPDH and Kv4.3**

In order to compare the relative amounts of Kv4.3 protein between tissue samples from non  $\beta$ -blocked and  $\beta$ -blocked patients, the conditions for Western blotting had to be optimised such that the relationship between the total protein load and optical density of the bands of interest was linear. The main variables that determine band intensity are the amount of protein, concentration of antibodies and film exposure time. Preliminary experiments comparing different films developed after different exposure times established that the optimum exposure was 10 minutes (results not shown) and this was used for all films unless stated otherwise. The concentration of the secondary antibody remained constant as this antibody was supplied pre-diluted as part of the anti-mouse Invitrogen Western Breeze Kit.

Preliminary experiments using wide ranges of total protein loads (2 - 50  $\mu\text{g}$ ) and different primary antibody dilutions helped to establish the conditions at which, either no bands were detected, or at which, complete saturation occurred i.e. no change in optical density in relation to changes in protein load (results not shown). Based on these initial experiments, further Western blots were performed to establish the range of protein load and primary antibody dilution at which a linear relationship between protein load and optical density occurred. Four Western blots were performed using the same range of total protein loads from tissue from two non  $\beta$ -blocked and two  $\beta$ -blocked patients. After blocking, each

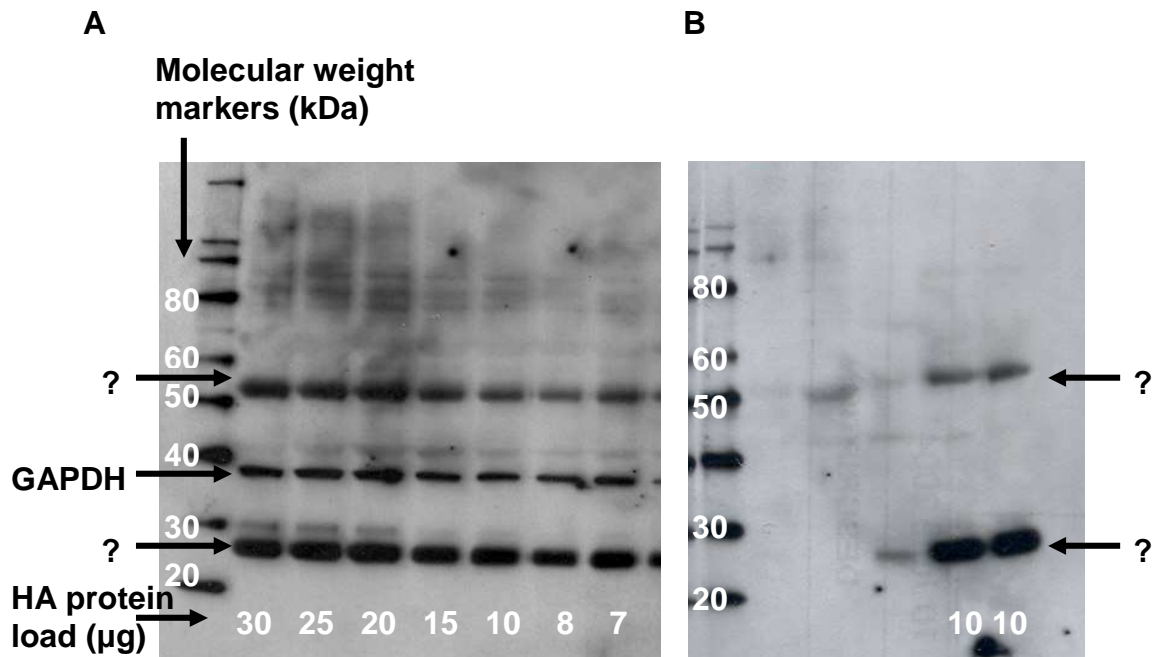


**Figure 3-16** Western blot characterising the nature of the bands detected using a monoclonal anti-GAPDH 1°Ab in human atrial tissue (HA). In **A**, different total loads of protein were treated with monoclonal anti-GAPDH antibody (Abcam) and 2°Ab (anti-mouse IgG Invitrogen). In **B**, 2°Ab alone was used to identify non specific bands labelled “?”.

membrane was cut vertically into three sections so that the same range of protein loads could be incubated with three different dilutions of primary antibody as detailed in the legend of figure 3-17. The three sections of each membrane were then treated identically and developed at the same time. The optical densities of the bands just above 60 kDa and just below 40 kDa were measured in the membranes treated with either anti-Kv4.3 or anti-GAPDH antibodies respectively. The results of these experiments are shown in figure 3-17. It can be seen from figures A and B that a linear relationship between optical density and protein load for the GAPDH antibody only exists in loads <10 µg of total protein and, for both tissues, the optimal antibody dilution appears to be 1:20000. Figures C and D demonstrate that a linear relationship exists over the same range of protein loads for Kv4.3 in both tissues for all the antibody concentrations. The exception was the 1:200 primary antibody dilution using tissue from the β-blocked patient, in which the bands were partially obscured by damage to the membrane and the optical densities could not be reliably measured.

#### **3.4.2.7 Comparing the relative amounts of Kv4.3 protein in tissue from non β-blocked and β-blocked patients.**

All the tissue samples were pre-diluted to a concentration of 1 mg/ml, blinded and randomised so that two samples from non β-blocked and β-blocked patients were loaded in a random order on each gel. Five Western blots were then performed using three protein loads for each tissue sample of 10, 7.5 and 5 µg and a dilution of 1:20000 for the anti-GAPDH antibody and 1:133 for the monoclonal anti-Kv4.3 antibody. Each membrane was cut in half horizontally between the 40 and 50 kDa markers after the blocking stage so the lower half could be incubated in the anti-GAPDH antibody and the upper half in the anti-Kv4.3 antibody. Both halves of the membrane were then treated identically thereafter. The identity of each tissue sample was not known until after the optical densities of the bands had been measured.

The film of one of these Western blots is shown in figure 3-18. It can be seen that the density of the bands for both the Kv4.3 and GAPDH bands decreased as protein load decreased. There is no marked visual difference in the intensity of the bands of corresponding protein loads for GAPDH or Kv4.3 between the non β-blocked and β-blocked tissue samples. The optical densities of each of the bands in this figure are shown in figure 3-19 along with the ratio of the optical densities of Kv4.3 protein relative to GAPDH in each sample. It can be seen from figures A and B that, in each of the samples

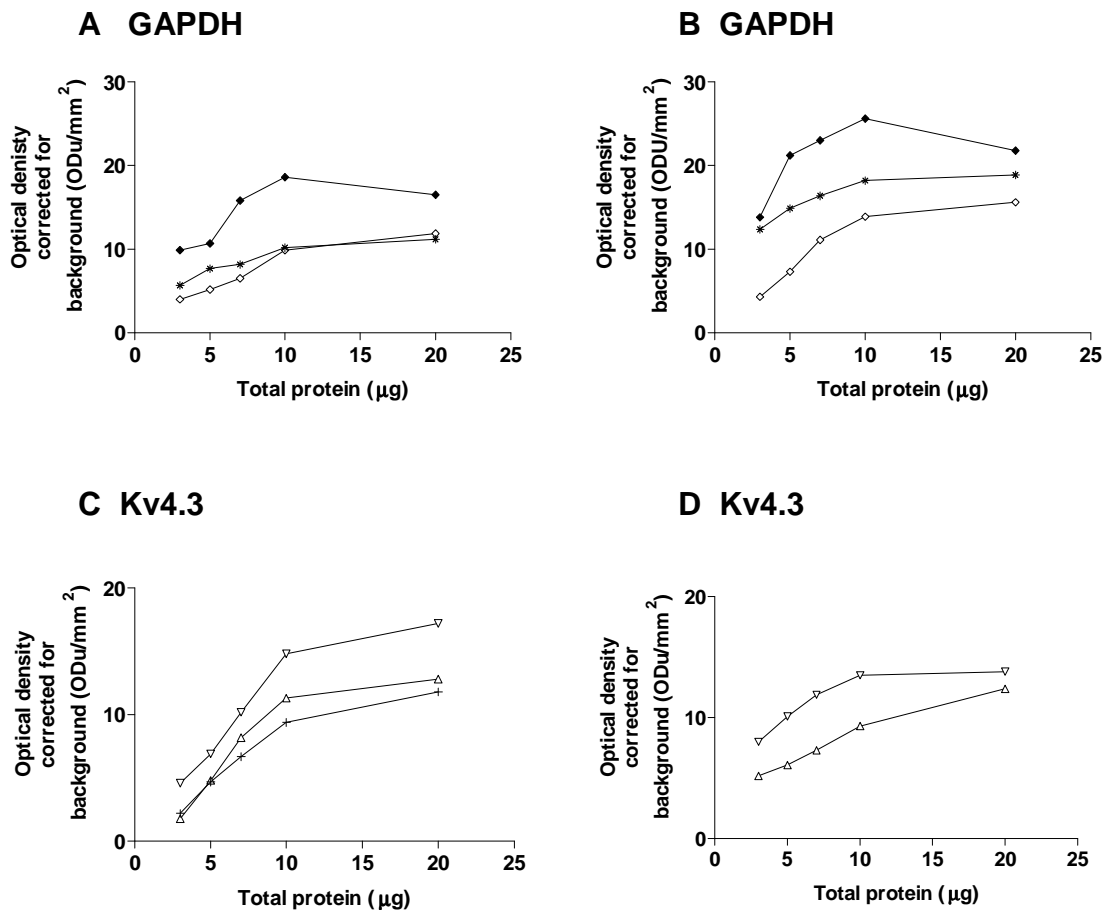


**Figure 3-17** Establishing the linear range of optical density versus total protein for GAPDH and Kv4.3 primary antibodies. Figures A and B show the relationship between optical density and total protein in tissue from a non  $\beta$ -blocked (A) and  $\beta$ -blocked (B) patient using different dilutions of GAPDH primary antibody ( $\blacklozenge = 1:5000$ ,  $*$  = 1:10000  $\diamond = 1:20000$ ). Figures C and D show the relationship between optical density and total protein in tissue from a non  $\beta$ -blocked (C) and  $\beta$ -blocked (D) patient using different dilutions of Kv4.3 primary antibody ( $\nabla = 1:100$ ,  $\triangle = 1:133$ ,  $+$  = 1:200).

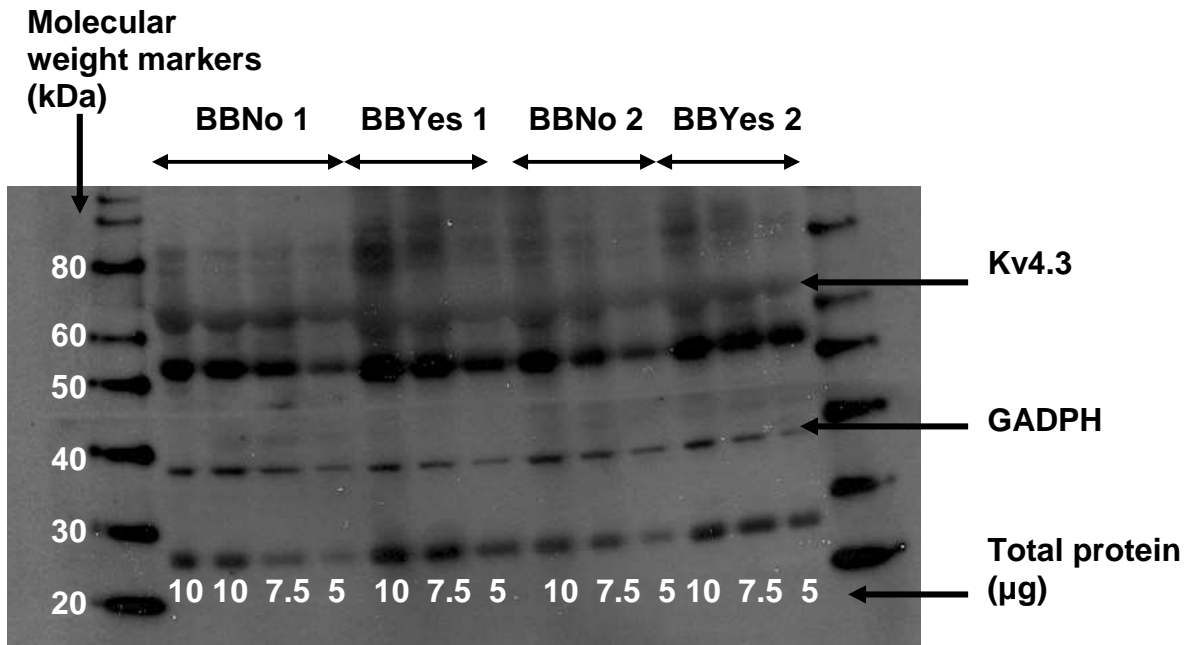


**Figure 3-18.** Western blot of Kv4.3 and GAPDH in human atrial samples from two non  $\beta$ -blocked (BBNo) and two  $\beta$ -blocked (BBYes) patients.

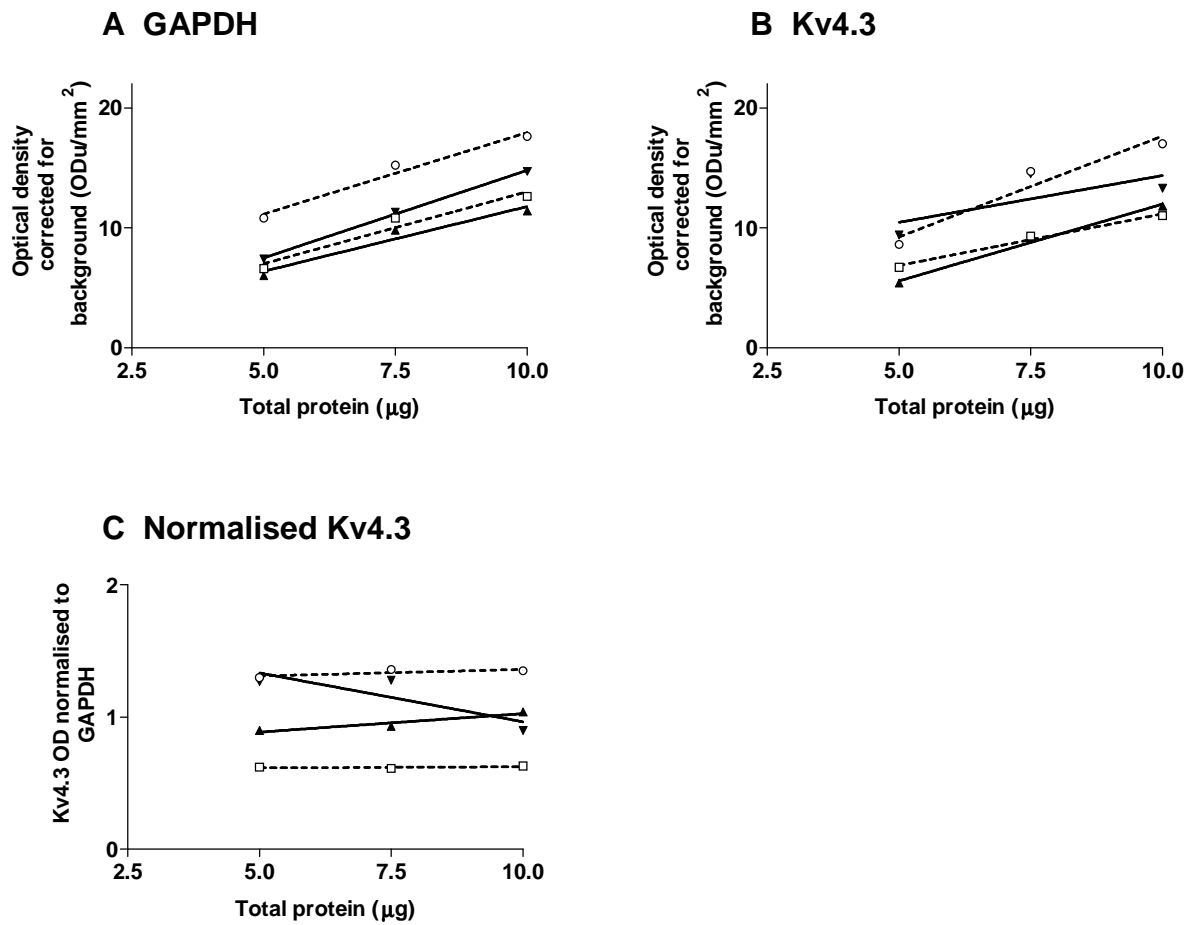


**Figure 3-19** Optical densities of GAPDH (A) and Kv4.3 (B) at three protein loads 5, 7.5 and 10 µg. A best fitting straight line has been fitted to the results from two non β-blocked samples 1 ( ..... □ ) and 2 ( ..... ○ ) and two β-blocked samples 1 ( ..... ▲ ) and 2 ( ..... ▼ ). In C, the optical densities for the Kv4.3 bands in each sample are normalised to the respective GAPDH optical densities.

for both GAPDH and Kv4.3, the optical density decreased with decreasing protein load in a linear fashion with the exception of Kv4.3 in  $\beta$ -blocked sample 2, where the optical density is slightly lower at the 10  $\mu\text{g}$  protein load than at 7.5. When the expression of Kv4.3 is normalised to that of GAPDH in figure C, the relationship between optical density and protein load is reversed for this one  $\beta$ -blocked tissue sample and the relationship is no longer logical. This sample was, therefore, excluded from further analysis.

The optical density versus protein load was plotted for both GAPDH and Kv4.3 in all the remaining tissue samples. In one other  $\beta$ -blocked sample the bands for both GAPDH and Kv4.3 were too faint to analyse and, therefore, this sample also had to be excluded from further analysis. There was no difference in the actual mean optical densities of GAPDH as measured at a protein load of 7.5  $\mu\text{g}$  in the tissue from non  $\beta$ -blocked ( $n = 10$ ) compared to the tissue from the  $\beta$ -blocked ( $n = 8$ ) patients ( $10.66 \pm 1.61$  vs  $9.56 \pm 0.70$  ODu/ $\text{mm}^2$ ,  $p=0.57$ ). These results are shown in figure 3-20A. The data was also analysed to compare the mean gradients of the best fitting straight lines for GAPDH optical density versus total protein load in each patient group and, again, there was no difference ( $0.78 \pm 0.15$  vs  $0.7 \pm 0.10$ ,  $p=0.80$ ). When then optical densities of the Kv4.3 bands were measured, there was no difference demonstrated in the mean optical densities at a total protein load of 7.5  $\mu\text{g}$  in the tissue samples from non  $\beta$ -blocked ( $n = 10$ ) and  $\beta$ -blocked ( $n = 8$ ) patients ( $11.57 \pm 1.31$  vs  $11.44 \pm 1.03$ ,  $p=0.94$ ) (see figure 3-20B). Again, there was no difference when the mean gradients were analysed ( $0.99 \pm 1.15$  vs  $1.18 \pm 0.14$ ,  $p=0.38$ ). When the optical density of Kv4.3 was normalised to that of GAPDH at each of the three protein loads, the mean optical densities at a total protein load of 7.5  $\mu\text{g}$  were  $1.30 \pm 0.27$  vs  $1.24 \pm 0.13$ ,  $p=0.86$  in the tissue samples from non  $\beta$ -blocked ( $n = 10$ ) and  $\beta$ -blocked ( $n = 8$ ) patients respectively. These results are shown in figure 3-20C. The normalised mean gradients were no different ( $0.02 \pm 0.006$  Vs  $0.03 \pm 0.01$ ,  $p=0.34$ ).

### 3.5 Discussion

The experiments in this chapter describe the effects of chronic treatment of patients with  $\beta$ -blockers on the expression of  $\text{K}^+$  ion channel pore-forming and accessory subunits. Despite the reduction in the current density of  $I_{\text{TO}}$  seen in association with chronic  $\beta$ -blockade, there was no change in the level of mRNA for Kv4.3, the pore-forming ion channel subunit responsible for conducting this current. Nor was there any change in the

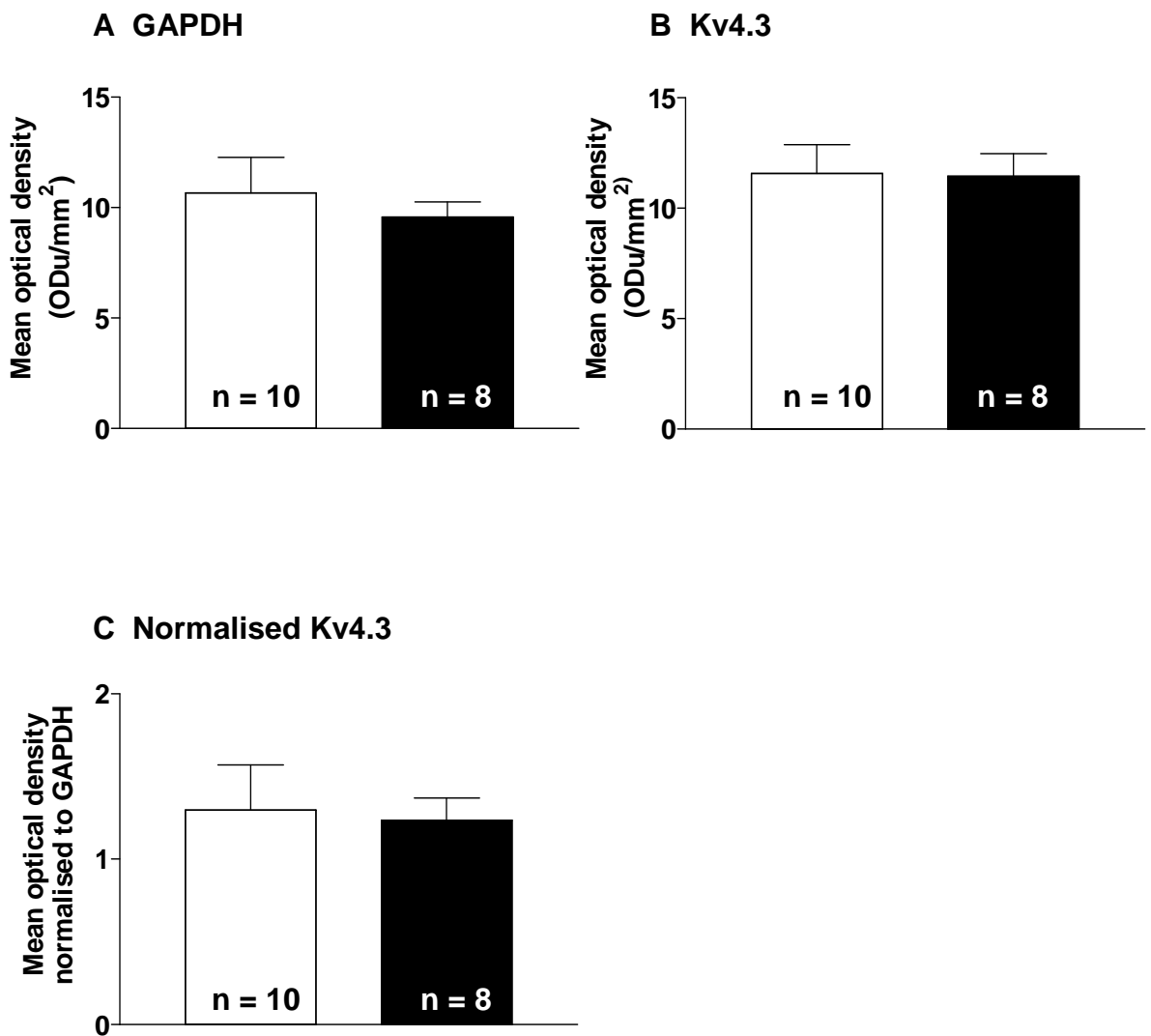


**Figure 3-20** Mean  $\pm$  sem optical densities of GAPDH (A), Kv4.3 (B) and Kv4.3 normalised to GAPDH (C) at a protein load of 7.5 $\mu$ g and corrected for background, for the tissue samples from the non  $\beta$ -blocked ( $\square$ ) and  $\beta$ -blocked ( $\blacksquare$ ) patients,  $p < 0.05$ .

level of mRNA expression for the accessory subunits KChIP2, KChAP, Kv $\beta$ 1-3, or Frequentin, all of which can affect Kv4.3 function and/or expression. This indicates that ion current remodelling in this situation is not the result of altered ion channel gene expression. As expected, given the lack of change in  $I_{KSUS}$ , there was no change in the mRNA expression for the pore-forming subunit for this channel, Kv1.5. There was an increase in the mRNA expression for Kir2.1, one of the pore-forming ion channels responsible for  $I_{K1}$ , in contrast to the reduction seen in this current associated with chronic  $\beta$ -blockade. This reduction persisted, but was not statistically significant, in all when normalised to individual “housekeepers” raising some concerns about the strength of this result although the relatively small number of samples may partially account for this. Chronic  $\beta$ -blockade was not associated with any change in the level of Kv4.3 protein expression indicating that ion current remodelling was not the result of a reduction in translation.

### **3.5.1 Ion channel mRNA expression in human atrium**

#### **3.5.1.1 A comparison with other studies**

This study is the first to examine the effects of chronic  $\beta$ -blockade on ion channel expression in human atrial tissue. Many of the studies looking at ion channel expression in human atrial tissue have been performed to look for changes in mRNA levels associated with cardiac disease or other patient characteristics and, therefore, it is very difficult to make any direct comparisons with this study. The end product of a RT-PCR reaction is often not representative of the entire mRNA sequence of a gene and therefore the size or melting peaks of the products are not comparable between studies. One possible area of comparison between this study and others, is the relative abundance of ion channel subunits in atrial tissue although this measurement is often not the primary aim of many studies including this one. It should be remembered that the analysis of relative abundance of each ion channel subunit does not incorporate normalisation to an internal standard and, therefore, does not take into account any differences in polymerase efficiency between different tissue samples.

In this study the abundance of Kv4.3, KChAP, and Frequentin mRNA were more highly than Kv $\beta$ 2, Kv $\beta$ 1 and KChIP2 which were all expressed at relatively low levels. These results would appear to conflict with one study that used RT-PCR along with a slightly different method of analysis, specifically to look at the relative abundance of groups of ion channel subunits in left atrial tissue samples from donor hearts (192). It showed found that

KChIP2 was highly expressed in atrial tissue and was significantly more abundant than either Kv $\beta$ 1 or Kv $\beta$ 2 with Kv $\beta$ 1 being the more abundant of these  $\beta$  subunits. It did not directly compare the abundance of Kv4.3 with these subunits. There are several possible explanations for this difference. Firstly, the methods of analysis were different and all samples in the study by Ordog et al were normalised to  $\beta$ -actin. In that study, data was collected from left as opposed to right atrial appendage tissue and the clinical characteristics of the patients were not identical to those in this study which may result in different ion channel and housekeeping gene expression. The difference in KChIP2 expression is however quite striking and several other studies have suggested KChIP2 expression is relatively highly expressed. KChIP2 mRNA has been detected in human cardiac tissue using less sensitive techniques than quantitative RT-PCR and there is sufficient protein expressed to be detectable by Western Blotting (108;110;116;117). KChIP2 has at least 18 splice variants (97;117;130;192). The Quantitect primer that was first tested in this study detected extremely low levels of KChIP2 and, when it was compared to the genomic sequence of KChIP2 and that of its major splice variants, this primer was found not to detect the ones reported to be most abundant in human atrial tissue (117). A different primer was designed (Applied Biosystems) and targeted to recognise regions common to the most abundant splice variants. Higher levels of KChIP2 were detected with this primer and these are the results shown in figures 3-8 and 3-9 but the overall abundance remained low. It is possible that some splice variants were not detected and the abundance of KChIP2 was underestimated. It is, therefore, also possible that any possible effects of chronic  $\beta$ -blockade on KChIP2 expression could have been underestimated.

Interestingly, this study suggests Frequentin is relatively highly expressed in human atrial tissue suggesting it may have quite a significant functional role. There is very little information about the role or expression of Frequentin in cardiac tissue. It has been shown to interact with Kv4.3 in expression systems and is structurally related to the KChIP family but other studies have suggested its role is not limited to modulation of ion channel function or expression. It is likely to be involved in a number of signalling and regulatory intracellular pathways via involvement with cAMP and phosphoinositide production (193).

There is very little information regarding the relative expressions of KChAP and the Kv $\beta$  subunits in human cardiac tissue. In this study, several other ion channel subunits including Kv $\beta$ 3, DPP6 and Kir2.2, either could not be detected at all, or were not detected at a high enough level to yield reliable results. For these subunits, this was the case within all the tissue samples. There are reports of the mRNA for these subunits being detected in

human cardiac tissue (124;134;137;192;194) although expression of Kir2.2 has been shown to be relatively weak in comparison to Kir2.1(137). The reasons for these discrepancies may include different methods of RNA extraction and quantification, the use of different primers, variable expression in different cardiac chambers, and variable expression according to different patient characteristics.

### **3.5.1.2 RT-PCR compared to Western Blotting**

Various techniques can be used to study ion channel expression, including, microarrays to look at large number of genes and RT-PCR, northern blots and ribonuclease protection assays to look at mRNA of individual genes. A technique like real time RT-PCR has a significant advantage over Western blotting in that it is much more sensitive and better able to measure ion channels which are often expressed at a much lower level than many structural or regulatory genes. The reaction between primer and mRNA/cDNA in an RT-PCR reaction can be manipulated to be dependent on a unique piece of genetic code, whereas, the reaction between antibody and protein in a Western reaction is dependent on a number of features including conformation shape and charge therefore, controlling specificity is more difficult. The use of microplates, the speed of the PCR reaction and the help of Mark Boyett's research group, who had already tested the different primers, allowed RT-PCR to be used to look at many more ion channel subunits than just Kv4.3. However, it should be remembered that Western blotting and RT-PCR are techniques that look at different aspects of ion channel expression. By examining protein expression Western blotting comes closer to studying the functional impact.

### **3.5.2 Kv4.3 protein expression in human atrial tissue**

In this study Kv4.3 protein was detected at 65 kDa in human atrial tissue using a monoclonal primary antibody. To my knowledge, this is the first report of Western blotting using this antibody in human atrial tissue and, therefore, a number of control experiments were performed to confirm the nature of the bands detected by this antibody. The band at 65 kDa was of similar molecular weight to a band detected at a high intensity in rat and rabbit brain tissue which were used as positive controls because of the high levels of expression of Kv4.3 in these tissues (105;191). This band was virtually absent in rabbit lung tissue which has minimal Kv4.3 expression and was, therefore, used as a negative control (105;191). Although the structure of Kv4.3 is highly homologous between species and, therefore, should be of identical molecular weight in different tissues and species this is not necessarily the case and is a potential weakness of using these types

of control. Different splice variants of Kv4.3 exist, although reports suggest that the two currently identified are expressed in both brain and cardiac tissue (105;191). It is possible that other variations in Kv4.3 may exist between species and tissues e.g. in tertiary structure, glycosylation etc which may alter the molecular weight of the Kv4.3 protein. Non or partially reduced forms of the protein along with partially degraded forms may also result in different bands being detected in different species or tissues by Western Blotting all of which may still represent Kv4.3 protein. The bands at 65 kDa, detected in animal brain tissue using the monoclonal antibody, were comparable to bands detected with the polyclonal antibody (Alomone) in this tissue. Pre-incubation with antigenic peptide prevented the binding of the polyclonal antibody to the band at 65 kDa in animal brain tissue helping to confirm the specificity of the antibody-protein interaction resulting in the detection of this band. This experiment could not be performed using the monoclonal antibody as no antigenic peptide for this antibody was available. Ideally, a further positive control the monoclonal antibody and a pure source of Kv4.3 protein e.g. recombinant Kv4.3 would have been performed for comparison with the human atrial tissue, however, it was not possible to obtain any recombinant Kv4.3.

The band detected at 65 kDa was demonstrated to be detected as a direct result of monoclonal primary antibody binding and was not due to non-specific secondary antibody binding which seemed to be responsible for two other bands detected in human atrial tissue, one between 50 and 60 kDa and one between 20 and 30 kDa. The secondary antibody used with the monoclonal anti-Kv4.3 recognised mouse IgG and it is possible that it is cross-reacted with human IgG in blood within in the cardiac tissue samples. The molecular weight of IgG heavy chains is 50 kDa and light chains are 25kDa, consistent with the bands detected by the secondary antibody alone. It remains possible these bands could contain some variant of Kv4.3, in addition to IgG, and, by not including the optical density of these bands in the analysis, information on the expression of Kv4.3 protein may have been missed.

As discussed above, it is possible to detect multiple variants of Kv4.3 by Western blotting. In addition to the band at 65 kDa, the monoclonal primary antibody also detected a much fainter band just above 40 kDa which was present in brain tissue and was not due to non-specific secondary antibody binding. It is possible, therefore, that this band also represented another variant of Kv4.3. However, this band was not detected when Western Blotting was performed using all the human atrial samples because each membrane was cut around this position in order to detect Kv4.3 at 65 kDa and GAPDH in each tissue

sample. Therefore, it is possible that some additional information on Kv4.3 expression could have been missed.

### **3.5.2.1 A comparison with other studies**

There are very few reports of Western Blotting for Kv4.3 in human atrial tissue. This may reflect the difficulty in obtaining human tissue for experimental work but may also reflect difficulties in actually detecting this protein using this technique, particularly, with relatively small amounts of tissue. There are several reports of Kv4.3 protein being detected around 70 kDa in Western blots of human atrial tissue. In one study Kv4.3 was detected in explanted human hearts using a custom made primary antibody at 74 kDa (104). Under experimental conditions of that study, the position of the Kv4.3 band in human atrium was consistent with a band detected in rabbit atrium and rat brain and disappeared with pre-incubation with antigen. That study also reported bands around 45 kDa in both human and rabbit atrial samples when using the anti-Kv4.3 primary antibody. Other studies have successfully used a polyclonal primary antibody from Alomone to detect Kv4.3 in human cardiac tissue. One study using this antibody describes Kv4.3 in human atrial tissue as a band at 72 kDa (111). However, this study did not show whole membranes of the Western blots or molecular weight markers and did not mention the presence of any other bands detected. What is more, they showed no evidence of positive or negative controls to help confirm the identity of the band they had detected with this antibody and no further information was provided about the primary antibody to confirm it was the same antibody as was used here. Another study reported a band at 79 kDa using a polyclonal anti-Kv4.3 primary (Alomone) in human atrial tissue although, again, only partial membranes were shown with no controls and no further details about the primary antibody were provided (195).

Kv4.3 protein has also been detected in human ventricular tissue by Western blotting. In one study using tissue from explanted hearts, Kv4.3 was detected as a very faint band around 75 kD using a polyclonal primary antibody (Alomone) (108). This band was not present when the antibody was pre-incubated with antigen and was comparable in molecular weight to a band detected using recombinant Kv4.3 isolated from transfected CHO cells. Interestingly, in this positive control, a band was also detected around 43 kDa. Another study demonstrated a band at 76 kDa in ventricular tissue using a polyclonal anti-Kv4.3 primary antibody (Alomone) but showed only a small section of membrane with no molecular weight markers although they did state that the band was not detected when the antibody was pre-incubated with antigen (109). A further study using a different primary

antibody (Chemicon), detected Kv4.3 at 75 kDa in human ventricular tissue but at a slightly lower molecular weight (70kDa) in the canine tissue. Interestingly, a study in rabbits, detected Kv4.3 at two molecular weights 78 and 68 kDa when using either the Chemicon primary antibody or a custom made antibody specific for the long splice variant Kv4.3 (138). The specificity of the Neuromab and Alomone primary antibodies is not known.

All the studies described above detected Kv4.3 at a slightly higher molecular weight than reported here using a monoclonal primary antibody. There are several possible explanations for this. Firstly, the weight of any band detected on a Western blot is determined by comparison with molecular weight markers. Small variations in the weights of different types of markers may exist and variations in the type of gel, buffers, and electrophoresis protocol may also influence how both the markers and samples migrate through a gel. When three other molecular markers were compared, the weight of this band was found to be 62kDa (Amersham ECL marker, RPN2107), 67 kDa (Sigma, M0671) and 80 kDa (Pierce Blue Ranger, 26651), results not shown (Julie Russell, personal communication). Secondly, different antibodies detect different epitopes of Kv4.3. If several “variants” of Kv4.3 of different molecular weight can exist, as suggested by some of these studies and indeed my own work, then different antibodies may recognise different variants of Kv4.3. At least two of the studies support the possibility that the band detected just above 40 kDa with the monoclonal primary antibody may also be Kv4.3. The reported molecular weight of Kv4.3 can therefore only be used as a guide to identifying the protein on a Western blot and evaluation of the whole membrane along with controls is important.

When using the polyclonal anti-Kv4.3 antibody (Alomone) in the initial experiments outline in this chapter, two bands were detected relatively near to the molecular weight of Kv4.3 as reported by other studies using this antibody. In figure 3-11A there is a faint band just above 60 kDa. This band was not clearly visible when either high concentrations of the primary antibody or a more sensitive detection system were used as shown in figure 3-12. The band was not clearly present in the human atrial sample that was compared correspond the animal brain positive controls in figure 3-13. The polyclonal antibody also detected a band at just above 80 kDa, however, this band also did not correspond to any bands detected in animal brain tissue. Neither band disappeared with when the primary antibody was pre-incubated with antigen as shown in figure 3-11B. It may be that the ratio of antigen-antibody was too low and there was insufficient antigen to bind all the antibody although this ratio of antigen:antibody did seem to prevent binding of the primary antibody

to animal brain tissue. Another possibility is that the antigenic peptide only bound a subpopulation of the polyclonal antibody leaving the remaining subpopulations, which recognised different epitopes of Kv4.3, able to bind to the human protein. This lack of specificity for just one epitope of an antigen is the hallmark of a polyclonal antibody. This means this type of antibody can detect the many possible variants of this protein which may exist and can be separated by gel electrophoresis. It is possible, therefore, that both the bands at 65 kDa and 80 kDa detected with the polyclonal antibody could both be variants of Kv4.3, however, the difficulty in confirming the nature of these bands led to this antibody being abandoned in favour of the monoclonal primary (Neuromab).

### **3.5.3 The role of normalisation in analysis of Western Blots and quantitative RT-PCR.**

In both Western blot analysis and quantitative RT-PCR, the expression of the ion channel subunits was normalised to the expression of GAPDH. In the Western Blots this is meant to correct for any variation in the amount of total protein loaded into different wells of the gel from different tissue samples. This may arise from inaccurate assessment of the total protein content of the tissue samples or pipetting errors in making the sample dilutions or in actually loading the gels. Normalising to GAPDH in this way is only valid if the expression of this protein does not vary between the tissues from the non  $\beta$ -blocked and  $\beta$ -blocked patients. This was shown to be the case. The mRNA expression of GAPDH was also shown to be similar between these groups although this was measured in tissue from different patients.

In the quantitative real time RT-PCR experiments two types of normalisation were used. Firstly, the  $C_t$  values for each primer product were normalised to one sample to correct for any variations in the efficiencies of the reaction between the different tissue samples or pipetting variations in distributing the master mix between samples. Secondly, each primer product was normalised to the mean of two “normalisation markers” of total cellular content from the same sample to account for any differences in the amount of RNA used at the start of the RT-PCR reaction. RT-PCR is an extremely sensitive technique that can detect very small differences in gene expression therefore any variables in the expression of the “normalising marker” can have a much bigger impact than it might in Western Blotting. The expression of so called reference or housekeeper genes like GAPDH are not always stable and can be influenced by a number of factors including heart failure which could potentially skew any data normalised to this gene alone (196). Another common

method of normalisation is to normalise to total RNA, in which usually a marker of rRNA, either 18S or 28S, is used. This is not without its problems as it cannot control for any errors introduced at the RT step of the PCR reaction and also assumes the rRNA:mRNA is the same for all samples. By normalising to the mean expression of 28S and GAPDH there is less chance of a systematic bias but it cannot remove this possibility completely.

In this study the expression of neither 28S nor GAPDH was significantly different between the tissue samples from non  $\beta$ -blocked or  $\beta$ -blocked patients. There was however, greater variability in the expression of 28S when all eight of the non  $\beta$ -blocked tissue samples were analysed. The two tissue samples responsible for this were samples 1 and 6 which had lower and higher amounts of 28S product respectively than the other samples from the non  $\beta$ -blocked patients. In order to accurately compare the end products of the PCR reactions equal amounts of cDNA from each sample should have been used at the start of the PCR reaction. For all the primer products, least product was consistently found in sample 1 and most in sample 6. This suggests the concentrations of cDNA in the stock solutions of these samples were different to that of the other tissue samples although a genuine difference in the amount of 28S relative to other the primer products in these samples cannot be completely excluded. An error could have occurred at a number of stages. It was known that a lower concentration of RNA was obtained from sample 1 as some of this sample was accidentally discarded during the RNA isolation step. It is possible, therefore, that the measurement of RNA concentration in this sample was less accurate potentially affecting the subsequent dilutions of RNA and cDNA. For sample 6, the results of both the spectrophotometry and gel analysis of RNA concentration were consistent making it more likely that an error may have occurred in either the calculation or pipetting steps involved in making the RNA and/or cDNA dilutions. For these reasons samples 1 and 6 were excluded from all analyses.

### **3.5.4 What do mRNA and protein expression actually tell us about functional ion channels?**

In this study both Kv4.3 mRNA and protein expression were measured whereas only mRNA was measured for Kv4.3 accessory subunits and other ion channels. By measuring mRNA levels for different ion channel subunits it is possible to compare the levels of gene expression of these subunits in different tissue samples. Increased mRNA should indicate increased transcription of the corresponding gene and would suggest increased translation resulting in increased protein levels. However, this is not necessarily the case. While

translation of mRNA generally occurs at a constant rate, considerable processing of mRNA occurs. This can result in different splice variants of a protein which may vary considerably in structure and function. Alternations in mRNA levels do not just indicate altered gene transcription but may also reflect variations in the stability of the mRNA. Increased mRNA degradation under the influence of cAMP has been shown to result in decreased expression of the ion channel protein Kv1.1 in a cell line (197). Two different mRNA transcripts with different stabilities have also been detected for another ion channel Kv1.4 (197).

Changes in mRNA expression are not the only way in which protein expression can change. Proteins undergo further processing including structural modifications that may include folding, glycosylation, phosphorylation, and association with other proteins including accessory proteins to form a functional ion channel. Any or all of these steps may be necessary to produce not only a functional protein but also to prevent protein degradation. While some of the accessory proteins measured in this study can alter the functional properties of Kv4.3 some, in particular KChAP, can also modify trafficking of Kv4.3 and therefore modify the expression of expression of Kv4.3 at the cell membrane. It should be remembered that simply measuring the amount of Kv4.3 in a cell does not necessarily provide information on whether that protein is functional.

This study shows that chronic  $\beta$ -blockade does not affect the expression of Kv4.3 mRNA or protein but what it cannot do is show whether the Kv4.3 expressed in the tissue from each group of patients is functionally identical. It should also be remembered that the mRNA and protein for Kv4.3 were not measured in tissue from the same patients due to the different requirements for storage and processing of the atrial tissue. While the characteristics of the two patients groups are similar in both the protein and mRNA experiments, they are not identical and various patient characteristics including sex, age, drugs, heart failure and myocardial ischaemia have been shown to affect ion channel expression. It is possible that small variations in the patient characteristics both between the non  $\beta$ -blocked and  $\beta$ -blocked groups and also between the protein and mRNA experiments may mask any influence of chronic  $\beta$ -blockade on ion channel expression.

This study also shows no change in the mRNA expression of various Kv4.3 related accessory subunits and several other ion channel pore forming subunits. As outlined above this does not necessarily mean chronic  $\beta$ -blockade does not affect protein expression of these subunits. There was a significant difference in mRNA expression of Kir2.1 with higher expression in the tissue from  $\beta$ -blocked patients compared to non  $\beta$ -blocked

patients. This could suggest chronic  $\beta$ -blockade may increase Kir2.1 gene expression or change the stability of the mRNA. It does not necessarily mean that there is increased functional Kir2.1 protein expression. There are several instances of changes in ion channel mRNA expression that have not been accompanied by changes in protein expression (111;198).

### **3.5.5 Can the adrenergic system influence ion channel expression?**

There is very little evidence looking at the effects of  $\beta$ -blockers or the adrenergic system in general, on ion channel expression. To my knowledge the only direct evidence that the adrenergic system may play a role in the regulation of potassium ion channel expression is from a study in adrenalectomised and catecholamine-depleted rats in which there is a decrease in Kv4.2 and 4.3 mRNA (58). This is clearly a different scenario than that of chronic treatment of patients with  $\beta$ -blockers and it is perhaps not surprising, that the results of this study do not support my findings. There is some evidence to suggest  $\beta$ -blockers can modify the expression of calcium handling proteins. The treatment of heart failure patients with  $\beta$ -blockers has been shown to increase the expression of sarcoplasmic-reticulum calcium ATPase (SERCA) and phospholamban (199;200). One of these studies also looked at NCX expression and found it unchanged which is in keeping with the results of this study although clearly the patient populations are different (199). There is also evidence to suggest  $\beta$ -adrenergic stimulation can increase the expression of Cav1.2 in cultured cardiac myocytes and this can be prevented by use of a  $\beta$ -blocker (201;202). It is difficult, however, to make any direct comparisons between these findings and the lack of any change in Cav1.2 mRNA expression associated with chronic  $\beta$ -blockade.

## **CHAPTER 4**

### **GENERAL DISCUSSION**

## **4.1 Electrophysiological and molecular effects of chronic $\beta$ -blockade on human atrial potassium currents**

In this work, the electrophysiological and molecular consequences of chronic  $\beta$ -adrenoceptor antagonist therapy on potassium currents in human atrial tissue were examined. Chronic treatment of patients with  $\beta$ -blockers was found to be associated with a reduction in  $I_{TO}$  current density in isolated atrial myocytes, but  $I_{KSUS}$  density remained unchanged. A reduction in  $I_{K1}$  current density was also demonstrated but only at -120 mV and the physiological significance of this change is likely to be minimal. The reduction in  $I_{TO}$  density was not due to any changes in its voltage dependency and was not accompanied by any change in the time dependent inactivation of the current. This reduction may contribute to the prolongation of the human atrial action potential duration seen in patients chronically treated with  $\beta$ -blockers. The preservation of the  $I_{TO}$  reduction even at rapid stimulation rates may be an important contributing factor to the ability of  $\beta$ -blockers to prevent AF. The mechanism underlying the reduction in  $I_{TO}$  current density associated with chronic  $\beta$ -blockade remains unclear. Unlike other examples of ion current remodelling, in this case, the reduction in  $I_{TO}$  was not due to a reduction in Kv4.3 protein or mRNA, nor was it due to changes in expression of mRNA encoding accessory proteins known to modify Kv4.3 expression and/or function.

## **4.2 Do ion current changes always mirror changes in ion channel expression?**

Remodelling of ion currents associated with altered ion channel expression is described in a number of different cardiac pathologies including AF, myocardial infarction, hypertrophy and heart failure (97;99;203). However, it does not necessarily follow that changes in ion currents always reflect a change in expression of ion channel components. Not all studies of these cardiac diseases have demonstrated remodelling of ion channels. Some studies of AF remodelling have not consistently demonstrated changes in  $I_{KUR}$  current and ion channel expression (2;12;111;112) while others do not report changes in the expression of the main  $I_{CaL}$  pore-forming subunit (204;205), despite evidence indicating  $I_{CaL}$  remodelling (2;9). In heart failure, remodelling of  $I_{K1}$  does appear to occur but reports of corresponding remodelling of  $I_{K1}$  ion channel expression are variable (115;137;138;203;203). Some studies have looked only at ion channel expression and therefore it is not clear whether the lack of remodelling of ion channels is accompanied by alterations in ion currents. There

are often many differences between studies of electrophysiological remodelling in cardiac disease including the type and species of cardiac myocytes studied, the pathological process underlying the cardiac disease along with methodological differences in experimental protocols used to study ion currents and ion channel expression. It can be argued that these reasons may account for any discrepancies in ion current or channel remodelling between studies. In general, however, most studies of electrophysiological remodelling in cardiac disease do support ion current remodelling as a result of altered ion channel expression. In particular, changes in either pore forming or accessory subunit expression are consistently described in situations where there is remodelling of  $I_{TO}$ .

No other studies have looked at  $\beta$ -blocker induced ion current remodelling but at least one study has shown involvement of the sympathetic nervous system or endogenous catecholamines in potassium current and channel remodelling. This study suggested reduced expression of Kv4.3 and 4.2 was the underlying mechanism responsible for the reduction in  $I_{TO}$  current density in this setting (58).

### **4.3 What is the mechanism underlying $\beta$ -blocker induced $I_{TO}$ reduction?**

There are several possible explanations for the reduction in  $I_{TO}$  current density seen in the cells from patients chronically treated with  $\beta$ -blockers. Direct channel block by the drug is one possible mechanism although, as discussed in chapter 2, it seems unlikely that drug is still present and actively blocking channels after isolation of the cells from atrial appendage tissue. Testing the acute effects of  $\beta$ -blocker application on isolated atrial myocytes from non  $\beta$ -blocked patients may give some idea of whether acute channel block is possible however, this would not be representative of the situation of a chronically treated patient. As discussed in chapter 3, another possibility is that there is altered accessory subunit expression at a protein level reflecting changes in translation rather than gene transcription. There are also a number of ways in which the function of either the pore-forming or accessory proteins could be modified within the cell without altering their level of expression.

Direct binding of a ligand, ion or other protein to an ion channel either on the intracellular or extracellular side may directly influence the function and activity of the channel. Some potassium channels are modulated by direct ligand interaction eg  $I_{KATP}$  and  $I_{KACH}$  which are non voltage dependent potassium currents that can contribute to repolarisation. The former

is inhibited by the binding of intracellular ATP while the latter is activated by acetylcholine binding to coupled G proteins. However, there is no real evidence to support the role of a binding ligand as necessary for the function of Kv4.3 distinct from its accessory proteins.  $I_{TO1}$ , as studied in this work, is a calcium independent current and therefore not directly modulated by the binding of calcium ions as are some channels particularly in non excitable cells. However, it is possible that calcium ions may influence  $I_{TO}$  by binding to accessory proteins like KChIP and frequenin which have calcium binding motifs (96). The effects of calcium on the function of these accessory proteins and the resultant effect on  $I_{TO}$  are unclear although the ability of frequenin to increase  $I_{TO}$  density appears, in expression systems, to be calcium dependent (206).

Other common mechanisms by which the function of proteins, including ion channel proteins, can be altered or regulated are through changes in pH, intracellular redox state and by post-translation modification. A reduction in  $I_{TO}$  density has been shown in animal ventricular myocytes in association with inhibition of major redox pathways which correlated with decreased Kv4.2 mRNA expression (207). Exposure to TNF $\alpha$  has also been shown to reduce  $I_{TO}$  via down-regulation of Kv4.2 expression. This effect was thought to be mediated via the induction of inducible nitric oxide synthase and the generation of reactive oxidant species (208). The generation of reactive oxidant species is a common feature of many pathological disease states including myocardial ischaemia, infarction and heart failure (209) however the incidence of these diseases in this study was similar between the  $\beta$ -blocked and non  $\beta$ -blocked patient groups. It is possible that the levels of circulating free catecholamines may have been affected by the chronic use of  $\beta$ -blockers and excess catecholamines have been shown to undergo auto-oxidation to produce free radicals (209). However, it is unlikely an altered intracellular redox state is the underlying mechanism accounting for the chronic  $\beta$ -blocker induced  $I_{TO}$  reduction since modulation of  $I_{TO}$  via oxidant species seems to involve altered expression of ion channel genes which was not found to be the case in this study.

#### **4.3.1 Post-translational modification**

Common mechanisms of post-translational modification of proteins include palmitoylation (attachment of fatty acids to cysteine residues of a protein), glycosylation and phosphorylation. These processes can help determine protein folding, transport, localisation and turnover at the cell membrane and therefore may directly affect the function of pore-forming and or accessory proteins. Post-translation modification of ion channel proteins may be important in determining their localisation to lipid rafts or

microdomains within the cell membrane where they can cluster and interact with other cell membrane-bound proteins, receptors, signalling molecules and intracellular anchoring proteins (210). Post-translational modification of Kv4.3 has not been studied in great detail. Palmitoylation of KChIP has been reported and may be an important factor in determining localisation of KChIP:Kv4.3 complexes to the cell membrane (96;211). There is not much evidence to support an important role for glycosylation in modifying Kv4.3. Kv4.x channels do not appear to have the structural motifs for attachments of N-linked oligosaccharides and there are no known structural motifs for O-linked glycosylation. However, one study has suggested that the removal of a negatively charged sugar residue from ventricular myocytes results in a reduction in  $I_{TO}$  (96).

Post translational modification of Kv4.3 by the addition of sugar or fatty acid residues could significantly affect its molecular weight and therefore affect detection by techniques like Western blotting. If chronic  $\beta$ -blockade altered the degree of post-translational modification of Kv4.3 this would not necessarily have been detected by experiments performed in this study. Further experiments perhaps designed to look at all the bands detected by the anti-Kv4.3 antibodies and or the presence of additional structural elements within the bands detected could be considered in addition to looking at the expression of accessory proteins. Studies could also be performed to look for possible differences in the location of Kv4.3 protein within cells from  $\beta$ -blocked and non  $\beta$ -blocked patients perhaps using confocal microscopy of cells stained with fluorescent labelled antibodies. This could help determine both the extent of cell surface expression of the Kv4.3 in addition to its co-localisation with other accessory proteins, and perhaps  $\beta$ -adrenoceptors.

#### **4.3.1.1 Phosphorylation**

The most common and widely studied mechanism for regulating protein function is that of phosphorylation. The addition or removal of phosphate from amino-acids tyrosine, serine and threonine are performed by kinase and phosphatase enzymes respectively. There is considerable evidence indicating ion channel activity can be modulated by protein kinases and phosphatases involving either (de)phosphorylation of the channel itself or of second messenger systems involved in regulating channel function. Altered phosphatase activity has been proposed as an alternative mechanism to ion channel remodelling to account for  $I_{CaL}$  remodelling in AF(212). Phosphorylation also seems to be an important regulatory mechanism of  $I_{TO}$ . The long splice variant of human Kv4.3 contains an amino acid sequence suitable for interaction and phosphorylation by protein tyrosine kinase C (PKC) (191) and activation of PKC has been shown to reduce the current density when this splice

variant was expressed in a cell line (154). Both Kv4.2 and Kv4.3 have sites for interaction with other protein kinases and there is experimental evidence that interaction with these enzymes can also have functional effects on  $I_{TO}$ . Activation of protein kinase A (PKA) has also been shown to reduce  $I_{TO}$  by affecting Kv4.2 channel opening in neurons and it is thought this effect is mediated via other protein kinases belonging to the ERK/MAPK (mitogen activated protein kinase) signalling cascade rather than via direct action of PKA on the ion channel. Modulation of  $I_{TO}$  by Kv4.2 phosphorylation via this pathway is dependent on the interaction of Kv4.2 with KCHIP subunits (213).

The calcium-calmodulin dependent protein kinase type II (CaMKII) is a calcium activated kinase that is highly expressed in heart tissue and plays an important regulatory role in intracellular calcium handling and excitation contraction coupling (214). CaMKII has also been shown to be an important modulator of ion channels (215). CaMKII can alter inactivation of  $I_{TO}$  and inhibiting this enzyme has been shown to increase the rate of  $I_{TO}$  inactivation in both cell lines and human atrial myocytes (216;217). Increasing the rate of  $I_{TO}$  inactivation would reduce the amount of current available for repolarisation and potentially prolong APD. However, in this work no change in  $I_{TO}$  inactivation was demonstrated. In contrast, another study in rat myocytes showed increased  $I_{TO}$  density associated with chronic CaMKII inhibition which might suggest CaMKII activation could reduce  $I_{TO}$ . (218). That study did not examine other changes in current characteristics but did note that the change in  $I_{TO}$  was not associated with any significant increase in ion channel associated genes or proteins. The increase in  $I_{TO}$  resulted in net shortening of APD despite the increase in  $I_{CaL}$  that also occurred.

While activation of protein kinases has been shown to be important in the regulation of gene expression, including recently KCHIP2, (219) it is a distinct possibility that direct phosphorylation of either Kv4.3 or a related accessory protein by these enzymes could underlie the reduction of  $I_{TO}$  in this study. The detection of phosphate residues within Kv4.3 bands detected by Western blotting may be possible. Antibodies to phosphorylated Kv4.2 have been used in brain tissue to look for distribution of phosphorylated Kv4.2 and it may well be feasible to use similar antibodies for Kv4.3 to look either at sectioned atrial appendage tissue or isolated cells. However, if phosphorylation of Kv4.3 or its accessory proteins is the mechanism by which  $I_{TO}$  is reduced in this study how does this link with chronic  $\beta$ -blockade?

#### 4.3.1.2 Phosphorylation and $\beta$ -adrenoceptors

There are three types of  $\beta$ -adrenoceptors ( $\beta$ -ARs) with  $\beta$ -AR<sub>1</sub> and  $\beta$ -AR<sub>2</sub> being the predominant subtypes expressed in the human heart. The ratio of  $\beta$ -AR<sub>1</sub>: $\beta$ -AR<sub>2</sub> in human atrial tissue is approximately 70:30 (220). The  $\beta$ -ARs are seven transmembrane spanning G-protein coupled receptors. Stimulation of these receptors leads to activation of stimulatory G-proteins resulting in production of cyclic adenosine 3'5' monophosphate (cAMP) (221). cAMP-dependent PKA then phosphorylates a variety of downstream, target proteins that can affect myocyte excitation and contraction. However, the signalling mechanisms resulting from activation of  $\beta$ -ARs are more complex than this simple linear signalling pathway.  $\beta$ -ARs can associate with multiple G-proteins and/or other signalling pathways particularly when the receptors are chronically activated. Chronic activation of  $\beta$ -AR<sub>1</sub> results in desensitisation of cAMP-PKA signalling and activation of CaMKII. In contrast, chronic stimulation of  $\beta$ -AR<sub>2</sub> results in a cAMP-PKA dependent switch from stimulatory to inhibitory G-protein coupling which can result in activation of a phosphoinositide 3-kinase (PI3K) signalling pathway, the ERK branch of the MAPK pathway and can inhibit PKA mediated phosphorylation. In contrast to  $\beta$ -AR signalling, agonist activation of  $\alpha$ -adrenoceptors ( $\alpha$ -ARs) results in the production of inositol triphosphate and activation of PKC (221).

In chronically  $\beta$ -blocked patients treated with  $\beta_1$  selective blockers there will be residual activation of  $\beta$ -AR<sub>2</sub> receptors and  $\alpha$ -ARs by endogenous catecholamines. This potentially will result in activation of PKC and ERK (although not via PKA activation) via chronic activation of these receptors. This could therefore result in a reduction in  $I_{TO}$  in this patient group. However, in the non  $\beta$ -blocked patients this reduction in  $I_{TO}$  might be expected to be enhanced by CaMKII activation via chronic  $\beta$ -AR<sub>1</sub> stimulation although, to my knowledge, there is no direct evidence that CaMKII activation would have this effect.

The signalling pathways involved in  $\beta$ -AR signalling are extremely complex and there is interaction at several levels between different pathways from both the same and different receptor subtypes. Clearly there is scope for different signalling pathways to be activated in both acute and chronic stimulation and these pathways have the potential to result in the direct phosphorylation of Kv4.3, and possibly other accessory proteins which can affect  $I_{TO}$ . These processes may be further complicated by the possible downregulation of  $\beta$ -AR expression as a consequence of chronic exposure to catecholamines in cardiac disease (220). Linking the reduction in  $I_{TO}$  seen in the cells from chronically  $\beta$ -blocked patients in

this study to a specific and single signalling pathways is difficult and probably an over simplification.

### 4.3.2 $\beta$ -adrenoceptors, $I_{TO}$ and calcium

The reduction in  $I_{TO}$  demonstrated in this work may well be the end result of numerous interacting factors within the cell which may affect protein trafficking, localisation on the cell membrane, phosphorylation and could still reflect changes in the expression of accessory genes which have yet to be discovered. It is likely however that, regardless of the mechanism, there is a strong link between the regulation of  $I_{TO}$  and calcium handling within the cell. A reduction in  $I_{TO}$  would be expected to increase the net influx of calcium ions during an action potential due to prolonged activation of  $I_{CaL}$ . This will then have knock on effects on intracellular calcium handling including activation of calcium dependent enzymes like CaMKII which, in addition to helping regulate  $I_{TO}$ , also modulates calcium release and re-uptake from the sarcoplasmic reticulum. This in turn helps determine the activity of the sodium calcium exchanger with the resulting current contributing directly to terminal repolarisation and therefore APD.  $\beta$ -ARs can potentially interact with this chain at a number of points. While they may directly affect  $I_{TO}$  as already discussed it has been long recognised that they play a crucial role in modulating intracellular calcium. This occurs in a number of ways most classically via cAMP-PKA mediated phosphorylation of the L-type calcium channel resulting in increased  $Ca^{2+}$  entry. Although  $I_{CaL}$  current density has been shown not to change in the setting of chronic  $\beta$ -blockade (29;151)  $\beta$ -AR signalling does affect both calcium related enzymes and the expression of calcium handling proteins like SERCA (199). What comes first,  $\beta$ -AR signalling or its block, changes in intracellular calcium or  $I_{TO}$  is unclear and very difficult to dissect in a human model.

## 4.4 A clinical perspective

The mechanism of action of  $I_{TO}$  reduction associated with chronic  $\beta$ -blockade may remain unclear but this does not detract from the clinical usefulness of this class of drug. Another question that remains unanswered is to what extent the electrophysiological changes demonstrated in this work explain the anti-arrhythmic action of  $\beta$ -blockers in preventing AF and how might this be exploited?

This work has shown that chronic  $\beta$ -blockade can reduce  $I_{TO}$  over a range of stimulation rates including those equivalent to the rapid atrial rates achieved in atrial fibrillation. This occurs both at steady state in the rate dependency experiments outlined in chapter 2 but also following a post rest current as demonstrated during the reactivation experiments. If this  $I_{TO}$  reduction results in prolongation of the atrial action potential and ERP at all rates, it would result in an increase in the minimal wavelength for re-entry and should be anti-arrhythmic. Potentially this could help prevent persistent AF from occurring secondary to either short bursts of paroxysmal AF or following pulmonary vein ectopics. This may help to explain the benefits of  $\beta$ -blockers in preventing recurrence or initiation of AF.

The potential anti-arrhythmic effects of  $\beta$ -blocker induced  $I_{TO}$  reduction and APD prolongation initially seem to be at odds with the pro-arrhythmic, electrophysiological remodelling that occurs in AF where a reduction in  $I_{TO}$  is associated with shortening of the APD. The key lies in the changes that occur to other ion currents in AF, in particular, the reduction in  $I_{CaL}$  and increase in  $I_{K1}$  (2;9) which have not been convincingly demonstrated in the setting of chronic  $\beta$ -blockade. This study has not examined the effects of chronic  $\beta$ -blockade on ion currents or indeed action potentials from patients in AF. It would be interesting to see whether  $\beta$ -blockers counteract the electrophysiological remodelling of AF in any way. This might be over optimistic given that the clinical efficacy of  $\beta$ -blockers is to prevent AF or its recurrence rather than cardioverting persistent or permanent AF (19).

Another aspect to consider is that APD prolongation is not always anti-arrhythmic. APD prolongation is seen in both heart failure and long QT syndromes which are associated with increased risk of ventricular (and sometimes atrial) arrhythmias. APD prolongation can result in early after-depolarisations which can produce premature impulses increasing the risk of developing re-entrant arrhythmias.

It is likely that  $I_{TO}$  reduction and APD prolongation are not the only anti-arrhythmic mechanisms of  $\beta$ -blockers. By blocking the actions of endogenous catecholamines on  $\beta$ -adrenoceptors,  $\beta$ -blockers can prevent their potentially pro-arrhythmic actions including enhanced automaticity, shortening of the action potential, increased heterogeneity of repolarisation, calcium overload, cardiac cell death, fibrosis and ischaemia (222). The contribution of  $\beta$ -blocker induced APD prolongation to the prevention of AF is therefore likely to depend on the individual patient, their clinical condition and risk factors for developing AF. This perhaps explains why pre-operative changes in electrophysiology in

$\beta$ -blocked patients are not associated with a reduction in the incidence of AF following cardiac surgery despite  $\beta$ -blockers being protective against AF in this setting (151). High levels of endogenous catecholamines due to the stress of surgery, acute cardiac ischaemia and the use of inotropic drugs are likely to be the major risk factors for post-operative AF and probably outweigh any potential benefit from pre-operative APD prolongation. It should also be remembered that  $\beta$ -blockers only have a modest anti-arrhythmic effect in preventing AF and so  $I_{TO}$  reduction and APD prolongation must have, at best, a modest role to play in the management of AF. However, it remains important to establish the long term electrophysiological consequences of such a commonly administered drug.

I suspect that exploitation of  $I_{TO}$  reduction as an anti-arrhythmic treatment for AF is therefore a long way from becoming reality. Its anti-arrhythmic contribution in a real world setting is uncertain. It is far from clear whether  $I_{TO}$  reduction is indeed the crucial step in the interaction between chronic  $\beta$ -blockade and APD prolongation. It is possible that it simply reflects or is secondary to, yet unrecognised changes in other currents or perhaps calcium handling. Atrial myocytes do not exist in isolation out with an electrophysiology experiment and the net effects of both  $I_{TO}$  reduction and chronic  $\beta$ -blockade on whole chamber and indeed whole hearts are unknown. However, the burden of AF to both patients and doctors is significant and is set to increase in the future and only by increasing our understanding of both the mechanisms of this arrhythmia and the actions of anti-arrhythmic drugs can we hope to impact on this.

## REFERENCE LIST

- (1) Heart Disease. A Textbook of Cardiovascular Medicine. In: Braunwald E, editor. 1997.
- (2) Workman AJ, Kane KA, Rankin AC. The contribution of ionic currents to changes in refractoriness of human atrial myocytes associated with chronic atrial fibrillation. *Cardiovasc Res* 2001; 52:226-235.
- (3) Fuster V, Ryden LE, Cannom DS, Crijns HJ, Curtis AB, Ellenbogen KA et al. ACC/AHA/ESC 2006 Guidelines for the Management of Patients with Atrial Fibrillation: a report of the American College of Cardiology/American Heart Association Task Force on Practice Guidelines and the European Society of Cardiology Committee for Practice Guidelines (Writing Committee to Revise the 2001 Guidelines for the Management of Patients With Atrial Fibrillation): developed in collaboration with the European Heart Rhythm Association and the Heart Rhythm Society. *Circulation* 2006; 114(7):e257-e354.
- (4) Nattel S. New ideas about atrial fibrillation 50 years on. *Nature* 2002; 415(6868):219-226.
- (5) Nattel S, Li D, Yue L. Basic mechanisms of atrial fibrillation-very new insights into very old ideas. *Ann Rev Physiol* 2000; 62:51-77.
- (6) Waldo AL. Mechanisms of atrial fibrillation. *J Cardiovasc Electrophysiol* 2003; 14(12 Suppl):S267-S274.
- (7) Wijffels MCEF, Kirchhof CJHJ, Dorland R, Allessie MA. Atrial fibrillation begets atrial fibrillation. A study in awake chronically instrumented goats. *Circulation* 1995; 92:1954-1968.
- (8) Brundel BJ, Henning RH, Kampinga HH, Van Gelder IC, Crijns HJ. Molecular mechanisms of remodeling in human atrial fibrillation. *Cardiovasc Res* 2002 May ;54 (2):315 -24 54:315-324.
- (9) Bosch RF, Zeng X, Grammer JB, Popovic K, Mewis C, Kühlkamp V. Ionic mechanisms of electrical remodeling in human atrial fibrillation. *Cardiovasc Res* 1999; 44:121-131.

- (10) Van Wagoner DR, Pond AL, Lamorgese M, Rossie SS, McCarthy PM, Nerbonne JM. Atrial L-type Ca<sup>2+</sup> currents and human atrial fibrillation. *Circ Res* 1999; 85:428-436.
- (11) Brandt MC, Priebe L, Bohle T, Sudkamp M, Beuckelmann DJ. The ultrarapid and the transient outward K<sup>+</sup> current in human atrial fibrillation. Their possible role in postoperative atrial fibrillation. *J Mol Cell Cardiol* 2000; 32:1885-1896.
- (12) Van Wagoner DR, Pond AL, McCarthy PM, Trimmer JS, Nerbonne JM. Outward K<sup>+</sup> current densities and Kv1.5 expression are reduced in chronic human atrial fibrillation. *Circ Res* 1997; 80:772-781.
- (13) Dobrev D, Graf E, Wettwer E, Himmel HM, Hala O, Doerfel C et al. Molecular basis of downregulation of G-protein-coupled inward rectifying K<sup>+</sup> current (IK,ACh) in chronic human atrial fibrillation: decrease in GIRK4 mRNA correlates with reduced IK,ACh and muscarinic receptor-mediated shortening of action potentials. *Circulation* 2001; 104:2551-2557.
- (14) Van der Velden HM, van Kempen MJ, Wijffels MC, van Zijverden M, Groenewegen WA, Allessie MA et al. Altered pattern of connexin40 distribution in persistent atrial fibrillation in the goat [see comments]. *J Cardiovasc Electrophysiol* 1998; 9:596-607.
- (15) Polontchouk L, Haefliger JA, Ebelt B, Schaefer T, Stuhlmann D, Mehlhorn U et al. Effects of chronic atrial fibrillation on gap junction distribution in human and rat atria. *J Am Coll Cardiol* 2001; 38(3):883-891.
- (16) Bosch RF, Nattel S. Cellular electrophysiology of atrial fibrillation. *Cardiovasc Res* 2002; 54:259-269.
- (17) National Institute for Health and Clinical Excellence (NICE). NICE clinical guideline 36. Atrial Fibrillation. National clinical guideline for management in primary and secondary care. June 2006
- (18) Van Gelder IC, Hagens VE, Bosker HA, Kingma JH, Kamp O, Kingma T et al. A comparison of rate control and rhythm control in patients with recurrent persistent atrial fibrillation. *N Engl J Med* 2002; 347(23):1834-1840.

- (19) Gronefeld GC, Hohnloser SH. b-blocker therapy in atrial fibrillation. *Pacing Clin Electrophysiol* 2003; 26:1607-1612.
- (20) Kuhlkamp V, Schirdewan A, Stangl K, Homberg M, Ploch M, Beck OA. Use of metoprolol CR/XL to maintain sinus rhythm after conversion from persistent atrial fibrillation: a randomized, double-blind, placebo-controlled study. *J Am Coll Cardiol* 2000; 36:139-146.
- (21) Plewan A, Lehmann G, Ndrepepa G, Schreieck J, Alt EU, Schomig A et al. Maintenance of sinus rhythm after electrical cardioversion of persistent atrial fibrillation; sotalol vs bisoprolol. *Eur Heart J* 2001; 22:1504-1510.
- (22) Steeds RP, Birchall AS, Smith M, Channer KS. An open label, randomised, crossover study comparing sotalol and atenolol in the treatment of symptomatic paroxysmal atrial fibrillation. *Heart* 1999; 82:170-175.
- (23) Crystal E, Connolly SJ, Sleik K, Ginger TJ, Yusuf S. Interventions on prevention of postoperative atrial fibrillation in patients undergoing heart surgery: a meta-analysis. *Circulation* 2002; 106:75-80.
- (24) Crijns HJ, Tjeerdsma G, De Kam PJ, Boomsma F, Van Gelder IC, Van Den Berg MP et al. Prognostic value of the presence and development of atrial fibrillation in patients with advanced chronic heart failure. *Eur Heart J* 2000; 21(15):1238-1245.
- (25) McMurray J, Kober L, Robertson M, Dargie H, Colucci W, Lopez-Sendon J et al. Antiarrhythmic effect of carvedilol after acute myocardial infarction: results of the Carvedilol Post-Infarct Survival Control in Left Ventricular Dysfunction (CAPRICORN) trial. *J Am Coll Cardiol* 2005; 45(4):525-530.
- (26) Van Veldhuisen DJ, Aass H, El Allaf D, Dunselman PH, Gullestad L, Halinen M et al. Presence and development of atrial fibrillation in chronic heart failure. Experiences from the MERIT-HF Study. *Eur J Heart Fail* 2006; 8(5):539-546.
- (27) Singh BN. Beta-Adrenergic blockers as antiarrhythmic and antifibrillatory compounds: an overview. *J Cardiovasc Pharmacol Ther* 2005; 10 Suppl 1:S3-S14.
- (28) Raine AE, Vaughan Williams EM. Adaptational responses to prolonged beta-adrenoceptor blockade in adult rabbits. *Br J Pharmacol* 1980; 70:205-218.

(29) Workman AJ, Kane KA, Russell JA, Norrie J, Rankin AC. Chronic beta-adrenoceptor blockade and human atrial cell electrophysiology: evidence of pharmacological remodelling. *Cardiovasc Res* 2003; 58:518-525.

(30) Pau D, Workman AJ, Kane KA, Rankin AC. Electrophysiological effects of 5-hydroxytryptamine on isolated human atrial myocytes, and the influence of chronic beta-adrenoceptor blockade. *Br J Pharmacol* 2003; 140:1434-1441.

(31) Kenyon JL, Gibbons WR. 4-Aminopyridine and the early outward current of sheep cardiac Purkinje fibers. *J Gen Physiol* 1979; 73(2):139-157.

(32) Coraboeuf E, Carmeliet E. Existence of two transient outward currents in sheep cardiac Purkinje fibers. *Pflugers Arch* 1982; 392(4):352-359.

(33) Tamargo J, Caballero R, Gomez R, Valenzuela C, Delpon E. Pharmacology of cardiac potassium channels. *Cardiovasc Res* 2004; 62:9-33.

(34) Escande D, Coulombe A, Faivre JF, Coraboeuf E. Two types of transient outward currents in adult human atrial cells. *Am J Physiol* 1987; 252:H142-H148.

(35) Amos GJ, Wettwer E, Metzger F, Li Q, Himmel HM, Ravens U. Differences between outward currents of human atrial and subepicardial ventricular myocytes. *J Physiol* 1996; 491:31-50.

(36) Firek L, Giles WR. Outward currents underlying repolarization in human atrial myocytes. *Cardiovasc Res* 1995; 30(1):31-38.

(37) Wettwer E, Ravens U. Recording cardiac potassium currents with whole-cell voltage clamp technique. In: Dhein S, Wilhelm F, Delmar M, editors. *Practical Methods in Cardiovascular Research*. Springer, 2005.

(38) Fermini B, Wang Z, Duan D, Nattel S. Differences in rate dependence of transient outward current in rabbit and human atrium. *Am J Physiol* 1992; 263:H1747-H1754.

(39) Shibata EF, Drury T, Refsum H, Aldrete V, Giles W. Contributions of a transient outward current to repolarization in human atrium. *Am J Physiol* 1989; 257:H1773-H1781.

- (40) Wettwer E, Amos GJ, Posival H, Ravens U. Transient outward current in human ventricular myocytes of subepicardial and subendocardial origin. *Circ Res* 1994; 75(3):473-482.
- (41) Nabauer M, Beuckelmann DJ, Uberfuhr P, Steinbeck G. Regional differences in current density and rate-dependent properties of the transient outward current in subepicardial and subendocardial myocytes of human left ventricle. *Circulation* 1996; 93(1):168-177.
- (42) Varro A, Nanasi PP, Lathrop DA. Potassium currents in isolated human atrial and ventricular cardiocytes. *Acta Physiol Scand* 1993; 149(2):133-142.
- (43) Escande D, Loisanche D, Planche C, Coraboeuf E. Age-related changes of action potential plateau shape in isolated human atrial fibers. *Am J Physiol* 1985; 249(4 Pt 2):H843-H850.
- (44) Beuckelmann DJ, Nabauer M, Erdmann E. Alterations of K<sup>+</sup> currents in isolated human ventricular myocytes from patients with terminal heart failure. *Circ Res* 1993; 73:379-385.
- (45) Wang Z, Pelletier LC, Talajic M, Nattel S. Effects of flecainide and quinidine on human atrial action- potentials - role of rate-dependence and comparison with guinea- pig, rabbit, and dog-tissues. *Circulation* 1990; 82:274-283.
- (46) Swartz KJ. Tarantula toxins interacting with voltage sensors in potassium channels. *Toxicon* 2006.
- (47) Sanguinetti MC, Johnson JH, Hammerland LG, Kelbaugh PR, Volkmann RA, Saccomano NA et al. Heteropodatoxins: peptides isolated from spider venom that block Kv4.2 potassium channels. *Mol Pharmacol* 1997; 51(3):491-498.
- (48) Diochot S, Drici M-D, Moinier D, Fink M, Lazdunski M. Effects of phrixotoxins on the Kv4 family of potassium channels and implications for the role of Ito1 in cardiac electrogenesis. *Br J Pharmacol* 1999; 126:251-263.
- (49) Priebe L, Beuckelmann DJ. Simulation study of cellular electric properties in heart failure. *Circ Res* 1998; 82(11):1206-1223.

(50) Greenstein JL, Wu R, Po S, Tomaselli GF, Winslow RL. Role of the calcium-independent transient outward current Ito1 in shaping action potential morphology and duration. *Circ Res* 2000; 87:1026-1033.

(51) Dobrev D, Ravens U. Remodeling of cardiomyocyte ion channels in human atrial fibrillation. *Basic Res Cardiol* 2003; 98:137-148.

(52) Yue L, Feng J, Gaspo R, Li GR, Wang Z, Nattel S. Ionic remodeling underlying action potential changes in a canine model of atrial fibrillation. *Circ Res* 1997; 81:512-525.

(53) Cha TJ, Ehrlich JR, Zhang L, Nattel S. Atrial ionic remodeling induced by atrial tachycardia in the presence of congestive heart failure. *Circulation* 2004; 110(12):1520-1526.

(54) Zhang H, Garratt CJ, Zhu J, Holden AV. Role of up-regulation of IK1 in action potential shortening associated with atrial fibrillation in humans. *Cardiovasc Res* 2005; 66(3):493-502.

(55) Schreieck J, Wang Y, Overbeck M, Schomig A, Schmitt C. Altered transient outward current in human atrial myocytes of patients with reduced left ventricular function. *J Cardiovasc Electrophysiol* 2000; 11:180-192.

(56) Deng C, Yu X, Kuang S, Zhang W, Zhou Z, Zhang K et al. Effects of carvedilol on transient outward and ultra-rapid delayed rectifier potassium currents in human atrial myocytes. *Life Sci* 2007; 80(7):665-671.

(57) Plank DM, Yatani A, Ritsu H, Witt S, Glascock B, Lalli MJ et al. Calcium dynamics in the failing heart: restoration by beta-adrenergic receptor blockade. *Am J Physiol Heart Circ Physiol* 2003; 285(1):H305-H315.

(58) Bru-Mercier G, Deroubaix E, Capuano V, Ruchon Y, Rucker-Martin C, Coulombe A et al. Expression of heart K<sup>+</sup> channels in adrenalectomized and catecholamine-depleted reserpine-treated rats. *J Mol Cell Cardiol* 2003; 35:153-163.

(59) Van der Heyden MA, Wijnhoven TJ, Opthof T. Molecular aspects of adrenergic modulation of the transient outward current. *Cardiovasc Res* 2006; 71(3):430-442.

- (60) Pacioretty LM, Gilmour RF. Restoration of transient outward current by norepinephrine in cultured canine cardiac myocytes. *Am J Physiol* 1998; 275:H1599-H1605.
- (61) Meszaros J, Ryder KO, Hart G. Transient outward current in catecholamine-induced cardiac hypertrophy in the rat. *Am J Physiol* 1996; 271:H2360-H2367.
- (62) Lopatin AN, Nichols CG. Inward rectifiers in the heart: an update on I(K1). *J Mol Cell Cardiol* 2001; 33(4):625-638.
- (63) Ravens U, Wettwer E. Electrophysiological aspects of changes in heart rate. *Basic Res Cardiol* 1998; 93; Suppl. 1:60-65.
- (64) Dhamoon AS, Jalife J. The inward rectifier current (IK1) controls cardiac excitability and is involved in arrhythmogenesis. *Heart Rhythm* 2005; 2(3):316-324.
- (65) Lopatin AN, Makhina EN, Nichols CG. Potassium channel block by cytoplasmic polyamines as the mechanism of intrinsic rectification. *Nature* 1994; 372(6504):366-369.
- (66) Ficker E, Taglialatela M, Wible BA, Henley CM, Brown AM. Spermine and spermidine as gating molecules for inward rectifier K<sup>+</sup> channels. *Science* 1994; 266(5187):1068-1072.
- (67) Shyng SL, Sha Q, Ferrigni T, Lopatin AN, Nichols CG. Depletion of intracellular polyamines relieves inward rectification of potassium channels. *Proc Natl Acad Sci U S A* 1996; 93(21):12014-12019.
- (68) Schram G, Pourrier M, Wang Z, White M, Nattel S. Barium block of Kir2 and human cardiac inward rectifier currents: evidence for subunit-heteromeric contribution to native currents. *Cardiovasc Res* 2003; 59:328-338.
- (69) Ferreira G, Yi J, Rios E, Shirokov R. Ion-dependent inactivation of barium current through L-type calcium channels. *J Gen Physiol* 1997; 109(4):449-461.
- (70) Dobrev D, Wettwer E, Kortner A, Knaut M, Schuler S, Ravens U. Human inward rectifier potassium channels in chronic and postoperative atrial fibrillation. *Cardiovasc Res* 2002; 54:397-404.

(71) Samie FH, Berenfeld O, Anumonwo J, Mironov SF, Udassi S, Beaumont J et al. Rectification of the background potassium current: a determinant of rotor dynamics in ventricular fibrillation. *Circ Res* 2001; 89(12):1216-1223.

(72) Warren M, Guha PK, Berenfeld O, Zaitsev A, Anumonwo JM, Dhamoon AS et al. Blockade of the inward rectifying potassium current terminates ventricular fibrillation in the guinea pig heart. *J Cardiovasc Electrophysiol* 2003; 14(6):621-631.

(73) Rees SA, Curtis MJ. Specific IK1 blockade: a new antiarrhythmic mechanism? Effect of RP58866 on ventricular arrhythmias in rat, rabbit, and primate. *Circulation* 1993; 87(6):1979-1989.

(74) Pinto JMB, Boyden PA. Electrical remodeling in ischemia and infarction. *Cardiovasc Res* 1999; 42:284-297.

(75) Brooksby P, Levi AJ, Jones JV. The electrophysiological characteristics of hypertrophied ventricular myocytes from the spontaneously hypertensive rat. *J Hypertens* 1993; 11(6):611-622.

(76) Fauconnier J, Lacampagne A, Rauzier JM, Vassort G, Richard S. Ca<sup>2+</sup>-dependent reduction of IK1 in rat ventricular cells: a novel paradigm for arrhythmia in heart failure? *Cardiovasc Res* 2005; 68(2):204-212.

(77) Kaab S, Nuss HB, Chiamvimonvat N, O'Rourke B, Pak PH, Kass DA et al. Ionic mechanism of action potential prolongation in ventricular myocytes from dogs with pacing-induced heart failure. *Circ Res* 1996; 78:262-273.

(78) Tsuji Y, Opthof T, Kamiya K, Yasui K, Liu W, Lu Z et al. Pacing-induced heart failure causes a reduction of delayed rectifier potassium currents along with decreases in calcium and transient outward currents in rabbit ventricle. *Cardiovasc Res* 2000; 48(2):300-309.

(79) Tomaselli GF, Marbán E. Electrophysiological remodeling in hypertrophy and heart failure. *Cardiovasc Res* 1999; 42:270-283.

(80) Koumi S, Sato R, Nagasawa K, Hayakawa H. Activation of inwardly rectifying potassium channels by muscarinic receptor-linked G protein in isolated human ventricular myocytes. *Journal Of Membrane Biology* 1997; 157:71-81.

- (81) Cheng J, Niwa R, Kamiya K, Toyama J, Kodama I. Carvedilol blocks the repolarizing K<sup>+</sup> currents and the L-type Ca<sup>2+</sup> current in rabbit ventricular myocytes. *Eur J Pharmacol* 1999; 376(1-2):189-201.
- (82) Kikuta J, Ishii M, Kishimoto K, Kurachi Y. Carvedilol blocks cardiac K<sub>ATP</sub> and K<sub>G</sub> but not I<sub>K1</sub> channels by acting at the bundle-crossing regions. *Eur J Pharmacol* 2006; 529(1-3):47-54.
- (83) Takagi S, Kihara Y, Mitsuiye T, Wang Z, Sasayama S. Effects of tilisolol, a nonselective beta-adrenergic blocker, on the membrane currents of isolated guinea pig ventricular myocytes. *J Cardiovasc Pharmacol* 1997; 29(5):593-598.
- (84) Zhang LM, Wang Z, Nattel S. Effects of sustained  $\beta$ -adrenergic stimulation on ionic currents of cultured adult guinea pig cardiomyocytes. *Am J Physiol* 2002; 282:H880-H889.
- (85) Liu QY, Rosen MR, McKinnon D, Robinson RB. Sympathetic innervation modulates repolarizing K<sup>+</sup> currents in rat epicardial myocytes. *Am J Physiol* 1998; 274:H915-H922.
- (86) Tseng GN. I(Kr): the hERG channel. *J Mol Cell Cardiol* 2001; 33(5):835-849.
- (87) Wang Z, Fermini B, Nattel S. Delayed rectifier outward current and repolarization in human atrial myocytes. *Circ Res* 1993; 73:276-285.
- (88) Li GR, Feng J, Yue L, Carrier M, Nattel S. Evidence for two components of delayed rectifier K<sup>+</sup> current in human ventricular myocytes. *Circ Res* 1996; 78(4):689-696.
- (89) Wang Z, Fermini B, Nattel S. Rapid and slow components of delayed rectifier current in human atrial myocytes. *Cardiovasc Res* 1994; 28:1540-1546.
- (90) Wang Z, Fermini B, Nattel S. Sustained depolarisation-induced outward current in human atrial myocytes. Evidence for a novel delayed rectifier K<sup>+</sup> current similar to Kv1.5 cloned channel currents. *Circ Res* 1993; 73:1061-1076.
- (91) Nattel S, Matthews C, De Blasio E, Han W, Li D, Yue L. Dose-dependence of 4-aminopyridine plasma concentrations and electrophysiological effects in dogs : potential relevance to ionic mechanisms in vivo. *Circulation* 2000; 101(10):1179-1184.

(92) Wettwer E, Hala O, Christ T, Heubach JF, Dobrev D, Knaut M et al. Role of  $I_{Kur}$  in controlling action potential shape and contractility in the human atrium: influence of chronic atrial fibrillation. *Circulation* 2004; 110(16):2299-2306.

(93) Xu ZX, Jin MW. Characterization of transient outward  $K^+$  current and ultra-rapid delayed rectifier  $K^+$  current in isolated human atrial myocytes from patients with congestive heart failure. *Acta Pharmacol Sin* 2002; 23(2):110-116.

(94) Nattel S, Yue L, Wang Z. Cardiac ultrarapid delayed rectifiers: a novel potassium current family of functional similarity and molecular diversity. *Cell Physiol Biochem* 1999; 9(4-5):217-226.

(95) Feng J, Wang Z, Li GR, Nattel S. Effects of class III antiarrhythmic drugs on transient outward and ultra-rapid delayed rectifier currents in human atrial myocytes. *J Pharmacol Exp Ther* 1997; 281(1):384-392.

(96) Birnbaum SG, Varga AW, Yuan LL, Anderson AE, Sweatt JD, Schrader LA. Structure and function of Kv4-family transient potassium channels. *Physiol Rev* 2004; 84(3):803-833.

(97) Nerbonne JM, Kass RS. Molecular physiology of cardiac repolarization. *Physiol Rev* 2005; 85(4):1205-1253.

(98) Snyders DJ. Structure and function of cardiac potassium channels. *Cardiovasc Res* 1999; 42(2):377-390.

(99) Oudit GY, Kassiri Z, Sah R, Ramirez RJ, Zobel C, Backx PH. The molecular physiology of the cardiac transient outward potassium current ( $I_{to}$ ) in normal and diseased myocardium. *J Mol Cell Cardiol* 2001; 33:851-872.

(100) Fiset C, Clark RB, Shimoni Y, Giles WR. Shal-type channels contribute to the  $Ca^{2+}$ -independent transient outward  $K^+$  current in rat ventricle. *J Physiol* 1997; 500 ( Pt 1):51-64.

(101) Bou-Abboud E, Nerbonne JM. Molecular correlates of the calcium-independent, depolarization-activated  $K^+$  currents in rat atrial myocytes. *J Physiol* 1999; 517 ( Pt 2):407-420.

- (102) Barry DM, Xu H, Schuessler RB, Nerbonne JM. Functional knockout of the transient outward current, long-QT syndrome, and cardiac remodeling in mice expressing a dominant-negative Kv4 alpha subunit. *Circ Res* 1998; 83(5):560-567.
- (103) Dixon JE, McKinnon D. Quantitative analysis of potassium channel mRNA expression in atrial and ventricular muscle of rats. *Circ Res* 1994; 75(2):252-260.
- (104) Wang Z, Feng J, Shi H, Pond A, Nerbonne JM, Nattel S. Potential molecular basis of different physiological properties of the transient outward K<sup>+</sup> current in rabbit and human atrial myocytes. *Circ Res* 1999; 84:551-561.
- (105) Dilks D, Ling HP, Cockett M, Sokol P, Numann R. Cloning and expression of the human kv4.3 potassium channel. *J Neurophysiol* 1999; 81(4):1974-1977.
- (106) Bertaso F, Sharpe CC, Hendry BM, James AF. Expression of voltage-gated K<sup>+</sup> channels in human atrium. *Basic Res Cardiol* 2002; 97(6):424-433.
- (107) Nerbonne JM. Molecular basis of functional voltage-gated K<sup>+</sup> channel diversity in the mammalian myocardium. *J Physiol* 2000; 525:285-298.
- (108) Zicha S, Xiao L, Stafford S, Cha TJ, Han W, Varro A et al. Transmural expression of transient outward potassium current subunits in normal and failing canine and human hearts. *J Physiol* 2004; 561(Pt 3):735-748.
- (109) Szabo G, Szentandrassy N, Biro T, Toth BI, Czifra G, Magyar J et al. Asymmetrical distribution of ion channels in canine and human left-ventricular wall: epicardium versus midmyocardium. *Pflugers Arch* 2005; 450(5):307-316.
- (110) Rosati B, Pan Z, Lypen S, Wang HS, Cohen I, Dixon JE et al. Regulation of KChIP2 potassium channel beta subunit gene expression underlies the gradient of transient outward current in canine and human ventricle. *J Physiol* 2001 May 15 ;533 (Pt 1 ):119 -25  
533:119-125.
- (111) Brundel BJ, Van Gelder IC, Henning RH, Tuinenburg AE, Wietses M, Grandjean JG et al. Alterations in potassium channel gene expression in atria of patients with persistent and paroxysmal atrial fibrillation: differential regulation of protein and mRNA levels for K<sup>+</sup> channels. *J Am Coll Cardiol* 2001; 37(3):926-932.

(112) Grammer JB, Bosch RF, Kuhlkamp V, Seipel L. Molecular remodeling of Kv4.3 potassium channels in human atrial fibrillation. *J Cardiovasc Electrophysiol* 2000; 11:626-633.

(113) Yamashita T, Murakawa Y, Hayami N, Fukui E, Kasaoka Y, Inoue M et al. Short-term effects of rapid pacing on mRNA level of voltage-dependent K<sup>+</sup> channels in rat atrium: electrical remodeling in paroxysmal atrial tachycardia. *Circulation* 2000; 101(16):2007-2014.

(114) Tsuji Y, Zicha S, Qi XY, Kodama I, Nattel S. Potassium channel subunit remodeling in rabbits exposed to long-term bradycardia or tachycardia: discrete arrhythmogenic consequences related to differential delayed-rectifier changes. *Circulation* 2006; 113(3):345-355.

(115) Kaab S, Dixon J, Duc J, Ashen D, Nabauer M, Beuckelmann DJ et al. Molecular basis of transient outward potassium current downregulation in human heart failure: a decrease in Kv4.3 mRNA correlates with a reduction in current density. *Circulation* 1998; 98:1383-1393.

(116) Radicke S, Cotella D, Graf EM, Banse U, Jost N, Varro A et al. Functional modulation of the transient outward current I<sub>to</sub> by KCNE beta-subunits and regional distribution in human non-failing and failing hearts. *Cardiovasc Res* 2006; 71(4):695-703.

(117) Decher N, Uyguner O, Scherer CR, Karaman B, Yuksel-Apak M, Busch AE et al. hKChIP2 is a functional modifier of hKv4.3 potassium channels: cloning and expression of a short hKChIP2 splice variant. *Cardiovasc Res* 2001; 52:255-264.

(118) An WF, Bowlby MR, Betty M, Cao J, Ling H-P, Mendoza G et al. Modulation of A-type potassium channels by a family of calcium sensors. *Nature* 2000; 403:553-556.

(119) Kuo HC, Cheng CF, Clark RB, Lin JJ, Lin JL, Hoshijima M et al. A defect in the Kv channel-interacting protein 2 (KChIP2) gene leads to a complete loss of I<sub>to</sub> and confers susceptibility to ventricular tachycardia. *Cell* 2001; 107(6):801-813.

(120) Rosati B, Grau F, Rodriguez S, Li H, Nerbonne JM, McKinnon D. Concordant expression of KChIP2 mRNA, protein and transient outward current throughout the canine ventricle. *J Physiol* 2003; 548:815-822.

(121) Deschenes I, DiSilvestre D, Juang GJ, Wu RC, An WF, Tomaselli GF. Regulation of Kv4.3 current by KChIP2 splice variants: a component of native cardiac I(to)? *Circulation* 2002 Jul 23 ;106 (4 ):423 -9 106:423-429.

(122) Gaborit N, Steenman M, Lamirault G, Le Meur N, Le Bouter S, Lande G et al. Human atrial ion channel and transporter subunit gene-expression remodeling associated with valvular heart disease and atrial fibrillation. *Circulation* 2005; 112(4):471-481.

(123) Apkon M, Nerbonne JM. Characterization of two distinct depolarization-activated K<sup>+</sup> currents in isolated adult rat ventricular myocytes. *J Gen Physiol* 1991; 97(5):973-1011.

(124) England SK, Uebele VN, Shear H, Kodali J, Bennett PB, Tamkun MM. Characterization of a voltage-gated K<sup>+</sup> channel beta subunit expressed in human heart. *Proc Natl Acad Sci U S A* 1995; 92(14):6309-6313.

(125) England SK, Uebele VN, Kodali J, Bennett PB, Tamkun MM. A novel K<sup>+</sup> channel beta-subunit (hKv beta 1.3) is produced via alternative mRNA splicing. *J Biol Chem* 1995; 270(48):28531-28534.

(126) Yang E-K, Alvira MR, Levitan ES, Takimoto K. Kvb subunits increase expression of Kv4.3 channels by interacting with their C termini. *J Biol Chem* 2001; 276:4839-4844.

(127) Deschenes I, Tomaselli GF. Modulation of Kv4.3 current by accessory subunits. *FEBS Lett* 2002 Sep 25 ;528 (1 -3 ):183 -8 528:183-188.

(128) Wible BA, Yang Q, Kuryshev YA, Accili EA, Brown AM. Cloning and expression of a novel K<sup>+</sup> channel regulatory protein, KChAP. *J Biol Chem* 1998; 273(19):11745-11751.

(129) Kuryshev YA, Wible BA, Gudz TI, Ramirez AN, Brown AM. KChAP/Kvbeta1.2 interactions and their effects on cardiac Kv channel expression. *Am J Physiol Cell Physiol* 2001; 281(1):C290-C299.

(130) Pourrier M, Schram G, Nattel S. Properties, expression and potential roles of cardiac K<sup>+</sup> channel accessory subunits: MinK, MiRPs, KChIP, and KChAP. *J Membrane Biol* 2003; 194:141-152.

- (131) Li Y, Um SY, McDonald TV. Voltage-gated potassium channels: regulation by accessory subunits. *Neuroscientist* 2006; 12(3):199-210.
- (132) Guo W, Malin SA, Johns DC, Jeromin A, Nerbonne JM. Modulation of Kv4-encoded K(+) currents in the mammalian myocardium by neuronal calcium sensor-1. *J Biol Chem* 2002; 277(29):26436-26443.
- (133) Chen C, Yu L, Zhang P, Jiang J, Zhang Y, Chen X et al. Human neuronal calcium sensor-1 shows the highest expression level in cerebral cortex. *Neurosci Lett* 2002; 319(2):67-70.
- (134) Radicke S, Cotella D, Graf EM, Ravens U, Wettwer E. Expression and function of dipeptidyl-aminopeptidase-like protein 6 as a putative beta-subunit of human cardiac transient outward current encoded by Kv4.3. *J Physiol* 2005; 565(Pt 3):751-756.
- (135) Nadal MS, Ozaita A, Amarillo Y, Vega-Saenz dM, Ma Y, Mo W et al. The CD26-related dipeptidyl aminopeptidase-like protein DPPX is a critical component of neuronal A-type K<sup>+</sup> channels. *Neuron* 2003; 37(3):449-461.
- (136) Nakamura TY, Artman M, Rudy B, Coetzee WA. Inhibition of rat ventricular IK1 with antisense oligonucleotides targeted to Kir2.1 mRNA. *Am J Physiol* 1998; 274(3 Pt 2):H892-H900.
- (137) Wang Z, Yue L, White M, Pelletier G, Nattel S. Differential distribution of inward rectifier potassium channel transcripts in human atrium versus ventricle. *Circulation* 1998; 98:2422-2428.
- (138) Rose J, Armoundas AA, Tian Y, DiSilvestre D, Burysek M, Halperin V et al. Molecular correlates of altered expression of potassium currents in failing rabbit myocardium. *Am J Physiol Heart Circ Physiol* 2005; 288(5):H2077-H2087.
- (139) Lesage F, Guillemare E, Fink M, Duprat F, Lazdunski M, Romey G et al. TWIK-1, a ubiquitous human weakly inward rectifying K<sup>+</sup> channel with a novel structure. *EMBO J* 1996; 15:1004-1011.
- (140) Feng J, Wible B, Li GR, Wang Z, Nattel S. Antisense oligodeoxynucleotides directed against Kv1.5 mRNA specifically inhibit ultrarapid delayed rectifier K<sup>+</sup> current in cultured adult human atrial myocytes. *Circ Res* 1997; 80:572-579.

- (141) Lai LP, Su MJ, Lin JL, Lin FY, Tsai CH, Chen YS et al. Changes in the mRNA levels of delayed rectifier potassium channels in human atrial fibrillation. *Cardiology* 1999; 92:248-255.
- (142) Olson TM, Alekseev AE, Liu XK, Park S, Zingman LV, Bienengraeber M et al. Kv1.5 channelopathy due to KCNA5 loss-of-function mutation causes human atrial fibrillation. *Hum Mol Genet* 2006; 15(14):2185-2191.
- (143) Lai LP, Su MJ, Lin JL, Lin FY, Tsai CH, Chen YS et al. Down-regulation of L-type calcium channel and sarcoplasmic reticular Ca<sup>2+</sup>-ATPase mRNA in human atrial fibrillation without significant change in the mRNA of ryanodine receptor, calsequestrin and phospholamban: an insight into the mechanism of atrial electrical remodeling. *J Am Coll Cardiol* 1999; 33(5):1231-1237.
- (144) Wiesfeld AC, Hemels ME, Van Tintelen JP, Van Den Berg MP, Van Veldhuisen DJ, Van Gelder IC. Genetic aspects of atrial fibrillation. *Cardiovasc Res* 2005; 67(3):414-418.
- (145) Sakmann B, Neher E. Patch clamp techniques for studying ionic channels in excitable membranes. *Annu Rev Physiol* 1984; 46:455-472.
- (146) World Medical Association Declaration of Helsinki. Recommendations guiding physicians in biomedical research involving human subjects. *Cardiovasc Res* 1997; 35:2-3.
- (147) Escande D, Coulombe A, Faivre JF, Deroubaix E, Coraboeuf E. Two types of transient outward currents in adult human atrial cells. *Am J Physiol* 1987; 252(1 Pt 2):H142-H148.
- (148) Harding SE, Jones SM, O'Gara P, Vescovo G, Poole-Wilson PA. Reduced beta-agonist sensitivity in single atrial cells from failing human hearts. *Am J Physiol* 1990; 259(4 Pt 2):H1009-H1014.
- (149) Bustamante JO, Watanabe T, Murphy DA, McDonald TF. Isolation of single atrial and ventricular cells from the human heart. *Can Med Assoc J* 1982; 126:791-793.
- (150) Barry PH, Lynch JW. Liquid junction potentials and small-cell effects in patch-clamp analysis. *Journal Of Membrane Biology* 1991; 121:101-117.

(151) Workman AJ, Pau D, Redpath CJ, Marshall GE, Russell JA, Kane KA et al. Post-operative atrial fibrillation is influenced by beta-blocker therapy but not by pre-operative atrial cellular electrophysiology. *J Cardiovasc Electrophysiol* 2006; 17(11):1230-1238.

(152) Raine AEG, Vaughan Williams EM. Adaptation to prolonged b-blockade of rabbit atrial, Purkinje, and ventricular potentials, and of papillary muscle contraction. Time-course of development of and recovery from adaptation. *Circ Res* 1981; 48:804-812.

(153) Bru-Mercier G, Deroubaix E, Rousseau D, Coulombe A, Renaud J-F. Depressed transient outward potassium current density in catecholamine-depleted rat ventricular myocytes. *Am J Physiol* 2002; 282:H1237-H1247.

(154) Po SS, Wu RC, Juang GJ, Kong W, Tomaselli GF. Mechanism of alpha-adrenergic regulation of expressed hKv4.3 currents. *Am J Physiol Heart Circ Physiol* 2001; 281(6):H2518-H2527.

(155) Gallego M, Casis O. Regulation of cardiac transient outward potassium current by norepinephrine in normal and diabetic rats. *Diabetes Metab Res Rev* 2001; 17(4):304-309.

(156) Michel MC, Pingsmann A, Beckeringh JJ, Zerkowski HR, Doetsch N, Brodde OE. Selective regulation of beta 1- and beta 2-adrenoceptors in the human heart by chronic beta-adrenoceptor antagonist treatment. *Br J Pharmacol* 1988; 94:685-692.

(157) Hall JA, Petch MC, Brown MJ. In vivo demonstration of cardiac beta 2-adrenoceptor sensitization by beta 1-antagonist treatment. *Circ Res* 1991; 69:959-964.

(158) Edvardsson N, Olsson SB. Effects of acute and chronic beta-receptor blockade on ventricular repolarisation in man. *Br Heart J* 1981; 45:628-636.

(159) Robinson C, Birkhead J, Crook B, Jennings K, Jewitt D. Clinical electrophysiological effects of atenolol--a new cardioselective beta-blocking agent. *Br Heart J* 1978; 40(1):14-21.

(160) Clementy J, Samoyeau R, Coste P, Bricaud H. Study of the electrophysiological properties of intravenous bisoprolol in patients with and without coronary artery disease by programmed stimulation. *J Cardiovasc Pharmacol* 1990; 16 Suppl 5:S169-S174.

(161) Creamer JE, Nathan AW, Shennan A, Camm AJ. Acute and chronic effects of sotalol and propranolol on ventricular repolarization using constant-rate pacing. *Am J Cardiol* 1986; 57:1092-1096.

(162) Duff HJ, Roden DM, Brorson L, Wood AJJ, Dawson AK, Primm RK et al. Electrophysiologic actions of high plasma concentrations of propranolol in human subjects. *J Am Coll Cardiol* 1983; 2:1134-1140.

(163) Janse MJ. Electrophysiological changes in heart failure and their relationship to arrhythmogenesis. *Cardiovasc Res* 2004; 61(2):208-217.

(164) Wang Y, Xu H, Kumar R, Tipparaju SM, Wagner MB, Joyner RW. Differences in transient outward current properties between neonatal and adult human atrial myocytes. *J Mol Cell Cardiol* 2003 Sep;35 (9 ):1083 -92 35:1083-1092.

(165) Wang L, Duff HJ. Developmental changes in transient outward current in mouse ventricle. *Circ Res* 1997; 81(1):120-127.

(166) Crumb WJ, Jr., Pigott JD, Clarkson CW. Comparison of Ito in young and adult human atrial myocytes: evidence for developmental changes. *Am J Physiol* 1995; 268(3 Pt 2):H1335-H1342.

(167) Cerbai E, Crucitti A, Sartiani L, De Paoli P, Pino R, Rodriguez ML et al. Long-term treatment of spontaneously hypertensive rats with losartan and electrophysiological remodeling of cardiac myocytes. *Cardiovasc Res* 2000 Jan 14 ;45 (2 ):388 -96 45(2):388-396.

(168) Le Grand BL, Hatem S, Deroubaix E, Couetil JP, Coraboeuf E. Depressed transient outward and calcium currents in dilated human atria. *Cardiovasc Res* 1994; 28:548-556.

(169) Verkerk AO, Wilders R, Veldkamp MW, de Geringel W, Kirkels JH, Tan HL. Gender disparities in cardiac cellular electrophysiology and arrhythmia susceptibility in human failing ventricular myocytes. *Int Heart J* 2005; 46(6):1105-1118.

(170) Gao Z, Lau CP, Chiu SW, Li GR. Inhibition of ultra-rapid delayed rectifier K<sup>+</sup> current by verapamil in human atrial myocytes. *J Mol Cell Cardiol* 2004; 36(2):257-263.

(171) Patti G, Chello M, Candura D, Pasceri V, D'Ambrosio A, Covino E et al. Randomized trial of atorvastatin for reduction of postoperative atrial fibrillation in patients undergoing cardiac surgery: results of the ARMYDA-3 (Atorvastatin for Reduction of MYocardial Dysrhythmia After cardiac surgery) study. *Circulation* 2006; 114(14):1455-1461.

(172) Boos CJ, Anderson RA, Lip GY. Is atrial fibrillation an inflammatory disorder? *Eur Heart J* 2006; 27(2):136-149.

(173) Li GR, Feng J, Wang Z, Fermini B, Nattel S. Adrenergic modulation of ultrarapid delayed rectifier K<sup>+</sup> current in human atrial myocytes. *Circ Res* 1996; 78(5):903-915.

(174) Feng J, Xu D, Wang Z., Nattel S. Ultrarapid delayed rectifier current inactivation in human atrial myocytes: properties and consequences. *Am J Physiol* 1998; 275(5 Pt 2):H1717-H1725.

(175) Koumi S, Backer CL, Arentzen CE, Sato R. beta-Adrenergic modulation of the inwardly rectifying potassium channel in isolated human ventricular myocytes. Alteration in channel response to beta-adrenergic stimulation in failing human hearts. *J Clin Invest* 1995; 96(6):2870-2881.

(176) Domenighetti AA, Boixel C, Cefai D, Abriel H, Pedrazzini T. Chronic angiotensin II stimulation in the heart produces an acquired long QT syndrome associated with IK1 potassium current downregulation. *J Mol Cell Cardiol* 2007; 42(1):63-70.

(177) Nabauer M, Beuckelmann DJ, Uberfuhr P, Steinbeck G. Regional differences in current-density and rate-dependent properties of the transient outward current in subepicardial and subendocardial myocytes of human left-ventricle. *Circulation* 1996; 93:168-177.

(178) Yamashita T, Nakajima T, Hazama H, Hamada E, Murakawa Y, Sawada K et al. Regional differences in transient outward current density and inhomogeneities of repolarization in rabbit right atrium. *Circulation* 1995; 92(10):3061-3069.

(179) Yue L, Feng J, Li GR, Nattel S. Transient outward and delayed rectifier currents in canine atrium: properties and role of isolation methods. *Am J Physiol* 1996; 270:H2157-H2168.

- (180) Agus ZS, Dukes ID, Morad M. Divalent cations modulate the transient outward current in rat ventricular myocytes. *Am J Physiol* 1991; 261(2 Pt 1):C310-C318.
- (181) Nabauer M, Beuckelmann DJ, Erdmann E. Characteristics of transient outward current in human ventricular myocytes from patients with terminal heart failure. *Circ Res* 1993; 73(2):386-394.
- (182) Sun X, Wang HS. Role of the transient outward current (Ito) in shaping canine ventricular action potential--a dynamic clamp study. *J Physiol* 2005; 564(Pt 2):411-419.
- (183) Philipson KD, Nicoll DA. Sodium-calcium exchange: a molecular perspective. *Annu Rev Physiol* 2000; 62:111-133.
- (184) Dvorak Z, Pascussi JM, Modriansky M. Approaches to messenger RNA detection - comparison of methods. *Biomed Pap Med Fac Univ Palacky Olomouc Czech Repub* 2003; 147(2):131-135.
- (185) Saiki RK, Gelfand DH, Stoffel S, Scharf SJ, Higuchi R, Horn GT et al. Primer-directed enzymatic amplification of DNA with a thermostable DNA polymerase. *Science* 1988; 239(4839):487-491.
- (186) Nolan T, Hands RE, Bustin SA. Quantification of mRNA using real-time RT-PCR. *Nat Protoc* 2006; 1(3):1559-1582.
- (187) Kurien BT, Scofield RH. Western blotting. *Methods* 2006; 38(4):283-293.
- (188) *Practical Methods in Cardiovascular Research*. Springer, 2005.
- (189) *Gel electrophoresis of proteins*. Oxford, 1998.
- (190) Towbin H, Staehelin T, Gordon J. Electrophoretic transfer of proteins from polyacrylamide gels to nitrocellulose sheets: procedure and some applications. *Proc Natl Acad Sci U S A* 1979; 76(9):4350-4354.
- (191) Kong W, Po S, Yamagishi T, Ashen MD, Stetten G, Tomaselli GF. Isolation and characterization of the human gene encoding Ito: further diversity by alternative mRNA splicing. *Am J Physiol* 1998; 275:H1963-H1970.

(192) Ordog B, Brutyo E, Puskas LG, Papp JG, Varro A, Szabad J et al. Gene expression profiling of human cardiac potassium and sodium channels. *Int J Cardiol* 2006; 111(3):386-393.

(193) Burgoyne RD, Weiss JL. The neuronal calcium sensor family of Ca<sup>2+</sup>-binding proteins. *Biochem J* 2001; 353(Pt 1):1-12.

(194) Majumder K, De Biasi M, Wang Z, Wible BA. Molecular cloning and functional expression of a novel potassium channel beta-subunit from human atrium. *FEBS Lett* 1995; 361:13-16.

(195) Wang Y, Xu H, Kumar R, Tipparaju SM, Wagner MB, Joyner RW. Differences in transient outward current properties between neonatal and adult human atrial myocytes. *J Mol Cell Cardiol* 2003; 35(9):1083-1092.

(196) Brattelid T, Tveit K, Birkeland JA, Sjaastad I, Qvigstad E, Krobert KA et al. Expression of mRNA encoding G protein-coupled receptors involved in congestive heart failure : A quantitative RT-PCR study and the question of normalisation. *Basic Res Cardiol* 2007; 102(3):198-208.

(197) Roden DM, Kupersmidt S. From genes to channels: normal mechanisms. *Cardiovasc Res* 1999; 42:318-326.

(198) Brundel BJM, Van Gelder IC, Henning RH, Tieleman RG, Tuinenburg AE, Wietses M et al. Ion channel remodeling is related to intraoperative atrial effective refractory periods in patients with paroxysmal and persistent atrial fibrillation. *Circulation* 2001; 103:684-690.

(199) Yasumura Y, Takemura K, Sakamoto A, Kitakaze M, Miyatake K. Changes in myocardial gene expression associated with beta-blocker therapy in patients with chronic heart failure. *J Card Fail* 2003; 9(6):469-474.

(200) Lowes BD, Gilbert EM, Abraham WT, Minobe WA, Larrabee P, Ferguson D et al. Myocardial gene expression in dilated cardiomyopathy treated with beta-blocking agents. *N Engl J Med* 2002; 346(18):1357-1365.

(201) Fan IQ, Chen B, Marsh JD. Transcriptional regulation of L-type calcium channel expression in cardiac myocytes. *J Mol Cell Cardiol* 2000; 32(10):1841-1849.

(202) Akuzawa-Tateyama M, Tateyama M, Ochi R. Sustained beta-adrenergic stimulation increased L-type  $\text{Ca}^{2+}$  channel expression in cultured quiescent ventricular myocytes. *J Physiol Sci* 2006; 56(2):165-172.

(203) Nattel S, Maguy A, Le Bouter S, Yeh YH. Arrhythmogenic ion-channel remodeling in the heart: heart failure, myocardial infarction, and atrial fibrillation. *Physiol Rev* 2007; 87(2):425-456.

(204) Grammer JB, Zeng X, Bosch RF, Kuhlkamp V. Atrial L-type  $\text{Ca}^{2+}$ -channel, beta-adrenoreceptor, and 5-hydroxytryptamine type 4 receptor mRNAs in human atrial fibrillation. *Basic Res Cardiol* 2001 Feb; 96 (1 ):82 -90 96:82-90.

(205) Schotten U, Haase H, Frechen D, Greiser M, Stellbrink C, Vazquez-Jimenez JF et al. The L-type  $\text{Ca}^{2+}$ -channel subunits  $\alpha_1\text{C}$  and  $\beta_2$  are not downregulated in atrial myocardium of patients with chronic atrial fibrillation. *J Mol Cell Cardiol* 2003; 35(5):437-443.

(206) Nakamura TY, Pountney DJ, Ozaita A, Nandi S, Ueda S, Rudy B et al. A role for frequenin, a  $\text{Ca}^{2+}$ -binding protein, as a regulator of  $\text{Kv}4$   $\text{K}^{+}$ -currents. *Proc Natl Acad Sci USA* 2001; 98:12808-12813.

(207) Li X, Li S, Xu Z, Lou MF, Anding P, Liu D et al. Redox control of  $\text{K}^{+}$  channel remodeling in rat ventricle. *J Mol Cell Cardiol* 2006; 40(3):339-349.

(208) Fernandez-Velasco M, Ruiz-Hurtado G, Hurtado O, Moro MA, Delgado C. TNF- $\alpha$  downregulates transient outward potassium current in rat ventricular myocytes through iNOS overexpression and oxidant species generation. *Am J Physiol Heart Circ Physiol* 2007; 293(1):H238-H245.

(209) Singal PK, Khaper N, Palace V, Kumar D. The role of oxidative stress in the genesis of heart disease. *Cardiovasc Res* 1998; 40(3):426-432.

(210) Maguy A, Hebert TE, Nattel S. Involvement of lipid rafts and caveolae in cardiac ion channel function. *Cardiovasc Res* 2006; 69(4):798-807.

(211) Takimoto K, Yang EK, Conforti L. Palmitoylation of KChIP splicing variants is required for efficient cell surface expression of  $\text{Kv}4.3$  channels. *J Biol Chem* 2002; 277(30):26904-26911.

(212) Christ T, Boknik P, Wohrl S, Wettwer E, Graf EM, Bosch RF et al. L-type Ca<sup>2+</sup> current downregulation in chronic human atrial fibrillation is associated with increased activity of protein phosphatases. *Circulation* 2004; 110(17):2651-2657.

(213) Schrader LA, Birnbaum SG, Nadin BM, Ren Y, Bui D, Anderson AE et al. ERK/MAPK regulates the Kv4.2 potassium channel by direct phosphorylation of the pore-forming subunit. *Am J Physiol Cell Physiol* 2006; 290(3):C852-C861.

(214) Maier LS, Bers DM. Role of Ca<sup>2+</sup>/calmodulin-dependent protein kinase (CaMK) in excitation-contraction coupling in the heart. *Cardiovasc Res* 2007; 73(4):631-640.

(215) Pitt GS. Calmodulin and CaMKII as molecular switches for cardiac ion channels. *Cardiovasc Res* 2007; 73(4):641-647.

(216) Sergeant GP, Ohya S, Reihill JA, Perrino BA, Amberg GC, Imaizumi Y et al. Regulation of Kv4.3 currents by Ca<sup>2+</sup>/calmodulin-dependent protein kinase II. *Am J Physiol Cell Physiol* 2005; 288(2):C304-C313.

(217) Tessier S., Karczewski P., Krause E.G, Pansard Y., Acar C., Lang-Lazdunski M. et al. Regulation of the transient outward K<sup>+</sup> current by Ca<sup>2+</sup>/calmodulin-dependent protein kinases II in human atrial myocytes. *Circ Res* 1999; 85:810-819.

(218) Li J, Marionneau C, Zhang R, Shah V, Hell JW, Nerbonne JM et al. Calmodulin kinase II inhibition shortens action potential duration by upregulation of K<sup>+</sup> currents. *Circ Res* 2006; 99(10):1092-1099.

(219) Jia Y, Takimoto K. Mitogen-activated protein kinases control cardiac KCHIP2 gene expression. *Circ Res* 2006; 98(3):386-393.

(220) Wallukat G. The beta-adrenergic receptors. *Herz* 2002; 27(7):683-690.

(221) Xiao RP, Zhu W, Zheng M, Cao C, Zhang Y, Lakatta EG et al. Subtype-specific alpha1- and beta-adrenoceptor signaling in the heart. *Trends Pharmacol Sci* 2006; 27(6):330-337.

(222) Dorian P. Antiarrhythmic action of beta-blockers: potential mechanisms. *J Cardiovasc Pharmacol Ther* 2005; 10 Suppl 1:S15-S22.







